

Beaufort Sea Coastal Sediment Study

Numerical Estimation of Sediment Transport and Nearshore Profile Adjustment

Part I - Text



July 1985
Keith Philpott Consulting Limited

Department of Indian and Northern Affairs
and
The Geological Survey of Canada,
Department of Energy, Mines, and Resources, Canada

Final Report

BEAUFORT SEA COASTAL SEDIMENT STUDY

PART 1 - TEXT

Numerical Estimation of Sediment Transport and
Nearshore Profile Adjustment at Coastal Sites in
the Canadian Beaufort Sea - Part of the Northern
Oil and Gas Action Plan (NOGAP)

B.M. Pinchin, R.B. Nairn, and K.L. Philpott

Keith Philpott Consulting Limited

P.O. Box 938
Thornhill, Ontario
L3T 4A5

Phone: (416) 889-1976
Telex: 06-986766 TOR

ABSTRACT

This report responds to a need for better data on coastal processes in the Canadian Beaufort Sea required by Government and by the Oil and Gas Industry for the siting and design of new shore-base facilities. Numerical estimates of alongshore sediment transport and nearshore profile adjustments are developed for the following sites: Atkinson Point, N.W.T.; Kay Point, Yukon; King Point, Yukon; North Head, N.W.T.; Stokes Point, Yukon; and Tuktoyaktuk, N.W.T. The influence of storm surges of coastal processes is also investigated. The evolution on the shoreline at King Point under existing conditions and with a total littoral barrier structure has been modelled. Offshore and nearshore wave climates have been computed for seven sites; the six mentioned plus Pauline Cove on Herschel Island. They are based on new fourteen-year parametric hindcasts. The inshore wave climates were computed using two-dimensional spectral transfer techniques with allowance for shallow water equilibrium spectral forms. The report is in two Parts: Part I comprises the full text with summaries of results; Part II comprises seven complete data packages, one for each of the sites considered.

Table of Contents

List of Figures

List of Tables

1. Introduction

- 1.1 Purpose 1-1
 - 1.1.1 Readership 1-4
- 1.2 Acknowledgements 1-6
- 1.3 Arrangement of Report 1-7
- 1.4 Scope of Work 1-8
 - 1.4.1 Part I 1-8
 - 1.4.2 Part II 1-10
- 1.5 Summary of Numerical Work 1-11
 - 1.5.1 Computation of Inshore Wave Climates 1-11
 - 1.5.2 Surge Sensitivity Analysis 1-13
 - 1.5.3 Alongshore Sediment Transport Estimates 1-15
 - 1.5.4 Nearshore Profile Adjustments 1-16
 - 1.5.5 Evaluation of the Effect of a Coastal Structure at King Point 1-17

2 Data Sources and Review of Previous Work

2.0 Introduction 2-1

2.1 Environmental Data

- 2.1.1 Previous Reports 2-2
- 2.1.2 Water Level Records 2-3
- 2.1.3 Wind Records 2-5
- 2.1.4 Wave Data 2-7
- 2.1.5 Other Environmental Data 2-8

2.2 Surveys & Graphics

- 2.2.1 Ice Charts 2-9
- 2.2.2 Hydrographic Charts and Fields Sheets 2-9
- 2.2.3 Air Photos and Other Site Graphics 2-11

2.3 The Arctic Coastal Environment

- 2.3.1 Arctic Coastal Processes 2-20
- 2.3.2 Coastal Profiles & Sediment Texture Data 2-25
- 2.3.3 Previous Site Specific Studies of Coastal Process 2-28

2.3.4	Site Descriptions	
	- Atkinson Point	2-31
	- Kay Point	2-32
	- King Point	2-32
	- North Head	2-33
	- Pauline Cove	2-34
	- Stokes Point	2-34
	- Tuktoyaktuk	2-35
3.	Synthesis of Environmental Data - Wind-Wave Hindcasts	
3.1	Summary of Wave Hindcasting Work	3-1
3.2	Parametric Hindcasting by the Effective Wave Procedure	
3.2.1	Input Data for the Parametric Models	3-3
3.2.2	The Effective Wave	3-4
3.2.3	The Generated Wave & Wave Generation Sequences	3-5
3.2.4	The Decayed Wave and Decay Sequences	3-6
3.2.5	Parametric Models Applied	3-8
3.3	Modifications to Hindcasting Procedure for Use in the Beaufort Sea	3-9
3.3.1	Time-varying fetches	3-9
3.3.2	Deep and Shallow Fetch Sectors	3-10
3.3.3	Frictional Hindcast Model	3-10
3.4	Input Data for the PHEW Procedure	
3.4.1	Wind Data	3-12
3.4.2	Fetch Definitions	3-13
3.5	Calibration of the PHEW Procedure	3-15
3.6	Fourteen Year Hindcasts	3-24
3.6.1	Common Fetches	3-25
3.6.2	Hindcasting at North Head	3-29
3.6.3	Hindcasting at Tuktoyaktuk	3-34
3.6.4	Wave Statistics Plots and Tables	3-38
4	Nearshore Wave Transformation	
4.1	Wave Refraction Analysis and Spectral Transfer	4-1
4.1.1	Outline of Procedure	4-1
4.1.2	Wave Ray Tracking	4-2
4.1.3	Preparation of Grids	4-3
4.1.4	Forward and Back-tracked Refraction Diagrams	4-5
4.1.5	Wave Spectrum Transfer	4-10
4.1.6	The Deep Water Spectrum Model	4-11
4.1.7	The Conservative Inshore Directional Model	4-12
4.1.8	The Inshore Wave Height Factor	4-14
4.1.9	Shallow Water Saturated Spectrum	4-15
4.1.10	Computed Nearshore Wave Conditions	4-17

4.2	Inshore Wave Statistics	4-19
4.3	Wave Transformations at North Head	4-19
4.4	Wave Transformations at Tuktoyaktuk	4-23
5	Surge Sensitivity Analysis	
5.1	Objective	5-1
5.2	Effects of a Surge on the Numerical Models	5-1
	5.2.1 The Wave Hindcast and Nearshore Transformation	5-1
	5.2.2 Alongshore Sediment Transport Package	5-7
	5.2.3 Nearshore Profile Adjustments	5-7
5.3	Surges in the Beaufort Sea	5-8
5.4	Description of the Storm Event Used in the Sensitivity Analysis	5-13
5.5	Results & Comments	5-14
	5.5.1 Alongshore Sediment Transport	5-16
5.6	Implications of Surge Sensitivity Analysis.	5-18
6	Littoral Transport Estimation	
6.1	Outline of Method	6-1
6.2	Alongshore Sediment Transport Package	6-2
	6.2.1 Bulk Energy Models	6-2
	6.2.2 Detailed Predictors	6-4
	6.2.2.1 Bijker Related Models	6-5
	6.2.2.2 Adapted Ackers & White Models	6-7
	6.2.3. Alongshore Current Model	6-9
6.3	Application of the Alongshore Sediment Transport Model	6-14
	6.3.1 Optional Modes of Operation	6-14
	6.3.2 Input Data	6-15
6.4	Sediment Transport Results	6-18
	6.4.1 Form of Results	6-18
	6.4.2 Summary of Results	6-21
	6.4.3 Selection of Valid Models	6-21
	6.4.4 Evaluation of Sediment Transport Models and Possible Sources of Error	6-28

	Nearshore Profile Adjustment	
7.1	Introduction	7-1
7.2	Theoretical Background	7-2
7.3	Outline of Method	7-4
	7.3.1 Calibration	7-4
	7.3.2 Storm Surge Analysis	7-7
7.4	Application	7-7
	7.4.1 Operational modes	7-7
	7.4.2 Input Data	7-8
7.5	Form of Results	7-11
7.6	Discussion of Results	7-11
	7.6.1 Atkinson Point	7-11
	7.6.2 Kay Point	7-16
	7.6.3 King Point	7-21
	7.6.4 Stokes Point	7-26
	7.6.5 Tuktoyaktuk	7-26
8	Beach Plan Evolution	
8.1	Introduction	8-1
8.2	Description of the Model	
	8.2.1 Theoretical Background	8-2
	8.2.2 Input Data & Operation	8-6
8.3	Potential and Actual Transport Rates	8-10
8.4	Form of Results	8-12
8.5	Discussion of Results	8-13
8.6	Feasibility of Fish Migration Passages	8-16
9	Discussion of Methodology and Results	
9.1	Overview of Methodology	9-1
9.2	Wave Hindcasting	9-2
9.3	Nearshore Wave Transformation	9-3
9.4	Alongshore Sediment Transport Models	9-4
	9.4.1 Bulk Energy Predictors	9-6
	9.4.2 Detailed Predictors	9-7
9.5	Nearshore Profile Adjustment with SEGAR	9-9

9.6	Beach Plan Evolution Modelling	9-13
9.7	Evaluation of Results by Site	9-13
	9.7.1 Atkinson Point	9-14
	9.7.2 Kay Point	9-17
	9.7.3 King Point	9-18
	9.7.4 North Head	9-20
	9.7.5 Pauline Cove	9-21
	9.7.6 Stokes Point	9-21
	9.7.7 Tuktoyaktuk	9-22

10 Conclusions

10.1	Data	10-1
	10.1.1 Wind Records	10-1
	10.1.2 Water Level Records	10-2
	10.1.3 Wave Measurements	10-2
	10.1.4 Geomorphology and Sediment Texture	10-4
10.2	Nearshore Wave Climates - Wave Hindcasting and Wave Transformation	10-5
10.3	Effects of Surges on Coastal Processes	10-8
10.4	Numerical Estimates of Alongshore Sediment Transport	10-9
10.5	Nearshore Profile Adjustments	10-12
10.6	Application of the Beach Plan Model at King Point	10-14

References

Appendix A

Wave hindcast calibration plots - Figures A1 to A42

Appendix B

Copy of Swart, D.H. 1976 Predictive equations regarding coastal transport. 15th Coastal Engineering Conference. A.S.C.E., Hawaii.

List of Figures	Page
1.1 Study Area	1-3
2.1 Atkinson Point Site Plan	2-13
2.2 Kay Point Site Plan	2-14
2.3 King Point Site Plan	2-15
2.4 North Head Site Plan	2-16
2.5 Pauline Cove Site Plan	2-17
2.6 Stokes Point Site Plan	2-18
2.7 Tuktoyaktuk Site Plan	2-19
3.1 Overwater to Overland Wind Speed Ratio	3-14
3.2 Comparison of Measured Wave Data August 1977 and September 1977	3-17
3.3 Comparison of Measured Wave Data August 1976 and September 1976	3-18
3.4 Comparison of Measured Wave Data October 1976	3-19
3.5 Deep Water Fetch Sites for Pauline Cove, Stokes Point, Kay Point and King Point	3-26
3.6 Deep Water Fetch Site for North Head and Tuktoyaktuk	3-27
3.7 Deep Water Fetch Site for Atkinson Point	3-28
3.8 Pauline Cove: Local Hindcast Fetch Sectors	3-30
3.9 Stokes Point: Local Hindcast Fetch Sectors	3-31
3.10 Kay Point: Local Hindcast Fetch Sectors	3-32
3.11 King Point: Local Hindcast Fetch Sectors	3-33
3.12 North Head: Local Hindcast Fetch Sectors	3-35
3.13 Tuktoyaktuk: Local Hindcast Fetch Sectors	3-36

3.14	King Point: Scatter Diagram for Deep Water Wave Data 1970-1983	3-39
3.16	King Point: Weibull Long Term Distribution Wave Heights	3-43
3.17	King Point: Deep Water Wave Energy Distribution 1970-1983	3-47
3.18	King Point: Deep Water Wave Height Exceedance 1970-1983	3-49
3.19	King Point: Deep Water Wave Height Period Exceedance 1970-1983	3-49
3.20	King Point: Deep Water Wave Period Occurrence 1970-1983	3-50
3.21	King Point: Deep Water Wave Height Persistence Favourable and Unfavourable Spells	3-51
4.1	King Point: Forward-Track Ray Diagram	4-6
4.2	King Point: Backward-Track Ray Diagram	4-9
4.3	Dimensionless Function	4-16
4.4	King Point: Wave Spectrum Transformation Results for Node Number 01	4-18
4.5	North Head Backward-Track Ray Diagram	4-21
4.6	North Head Wave Spectrum Transformation Results for Node Number 01	4-22
4.7	Tuktoyaktuk Backward-Track Ray Diagram	4-24
4.8	Tuktoyaktuk Nodal Dimensions and Mesh Size of Refraction Model Grids	4-25
5.1	King Point: Comparison of Spectral Transfer Results at Different Water Levels (T=10.0s)	5-3
5.2	King Point: Comparison of Spectral Transfer Results at Different Water Levels (T=7.9s)	5-4
5.3	King Point: Comparison of Spectral Transfer Results at Different Water Levels (T=5.0s)	5-5

5.4	King Point: Comparison of Spectral Transfer Results at Different Water Levels (T=3.2s)	5-6
5.5	Periods of Tide Gauge Operation and Surge Occurrences at Tuktoyaktuk	5-9
5.6	Periods of Temporary Tide Gauge Operation in the Beaufort Sea	5-10
5.7	Approximate Return Periods of Extreme Storm Water Levels at Tuktoyaktuk	5-12
5.8	Two-Day Storm Surge Used for Sensitivity Analysis at King Point	5-15
6.1	King Point: Profiles Used in Sediment Transport Predictions	6-17
6.2	Atkinson Point: Best Estimates of Net Potential Sediment Transport Rates	6-23
6.3	Kay Point: Best Estimates of Net Potential Sediment Transport Rates	6-23
6.4	King Point: Best Estimates of Net Potential Sediment Transport Rates	6-24
6.5	North Head: Best Estimates of Net Potential Sediment Transport Rates	6-24
6.6	Stokes Point: Best Estimates of Net Potential Sediment Transport Rates	6-25
6.7	Tuktoyaktuk: Best Estimates of Net Potential Sediment Transport Rates	6-25
7.1	Initial Profiles for the Nearshore Profile Adjustment Analysis	7-9
7.2 to 7.5	Atkinson Point Calibration Runs for Profile Adjustment	7-12
7.6	Kay Point Calibration Run for Profile Adjustment	7-17
7.7 to 7.9	Kay Point Storm Runs for Profile Adjustment	7-18
7.10	King Point Calibration Run for Profile Adjustment	7-22

7.11 to 7.13 King Point Storm Runs for Profile Adjustment	7-23
7.14 Stokes Point Calibration Run for Profile Adjustment	7-27
7.15 Stokes Point Storm Run for Profile Adjustment	7-28
7.16 Tuktoyaktuk Calibration Run for Profile Adjustment	7-29
8.1 Reference Diagram for Beach Evolution Models	8-3
8.2 Baseline Location for Beach Plan Evolution Model (King Point)	8-5
8.3 Forward Tracking at King Point	8-9
8.4 Beach Plan Shape Evolution Without a Structure at King Point 1970-1983	8-14
8.5 Beach Plan Shape Evolution With a Structure at King Point 1970-1983	8-15
9.1 Coastal Processes at King Point	9-16

List of Tables	Page
2.1 Wind Data Records	2-6
2.2 Ice Charts	2-10
2.3 Hydrographic Charts	2-10
2.4 Hydrographic Field Sheets	2-12
2.5 Data Base for Coastal Profiles and Sediment Texture	2-27
3.1 Comparison of Offshore and Tuktoyaktuk Winds in the summer of 1982	3-14
3.2 MEDS Wave Recording Stations	3-16
3.3 MEDS Station 191 List of Month-Long Calibration Tests Comparing Hindcast with Measured Wave Heights and Periods	3-21
3.4 MEDS Stations 25 and 50 List of Month-Long Calibration Tests Comparing Hindcast with Measured Wave Heights and Periods	3-22
3.5 Weibull Probability Analysis - King Point	3-41
3.6 Least Squares Fit on LogLog $[1/(1-P)]$ - King Point	3-41
3.7 Least Squares Curve Fit on Reduced Data - King Point	3-43
3.8 Predicted Wave Heights for Given Return Periods - King Point	3-43
3.9 Percentage Wave Power Distribution - King Point	3-46
3.10 All Directions Wave Table - King Point	3-53
5.1 Surge Factors at the Study Sites	5-14
5.2 Two-Day Surge Net Sediment Transport Results at King Point (Node 1)	5-14
6.1 The Sediment Transport Models - References and General Classification	6-3
6.2 King Point Input for the Sediment Transport Package (SEDX)	6-16
6.3 King Point SEDX Results (I) - Node 1	6-19
6.4 King Point SEDX Results (II) - Node 1	6-20

6.5 Summary of Sediment Transport Results and Best Estimates- All Sites	6-22
7.1 Maximum Wave Condition During Simulated Storm Surges for SEGAR Runs	7-10
8.1 Application of the Beach Plan Model at King Point, Operating Conditions for Final Run Without a Structure	8-7
8.2 Application of the Beach Plan Model at King Point, Operating Conditions for Final Run With a Structure	8-8
9.1 Beach Profile Heights & Estimated Surge Heights Beach Profile Calibration Sites	9-12

BEAUFORT SEA COASTAL SEDIMENT STUDY

Numerical estimation of sediment transport and nearshore profile adjustments at coastal sites in the Canadian Beaufort Sea -
Part of the Northern Oil and Gas Action Plan (NOGAP)

SECTION 1 INTRODUCTION

1.1 Purpose

This addresses the need for better data on coastal processes in the Canadian Beaufort Sea. Data and information are required by Government and by the Oil and Gas Industry for the siting and design of shore-base facilities. For this, one of the most urgent requirements is for a better understanding of the magnitudes and variations of the following:

- inshore wave climates;
- influence of surges on coastal processes;
- alongshore sediment transport rates;
- nearshore coastal profile adjustments;
- impact of a typical structure on coastal processes.

The purpose of this study was to apply advanced numerical estimation techniques to each of the above-mentioned phenomena at one or more of seven designated sites:

1. Atkinson Point, N.W.T.
2. Kay Point, Yukon
3. King Point, Yukon,
4. North Head, N.W.T
5. Pauline Cove, (Herschel Island), Yukon
6. Stokes Point, Yukon
7. Tuktoyaktuk, N.W.T

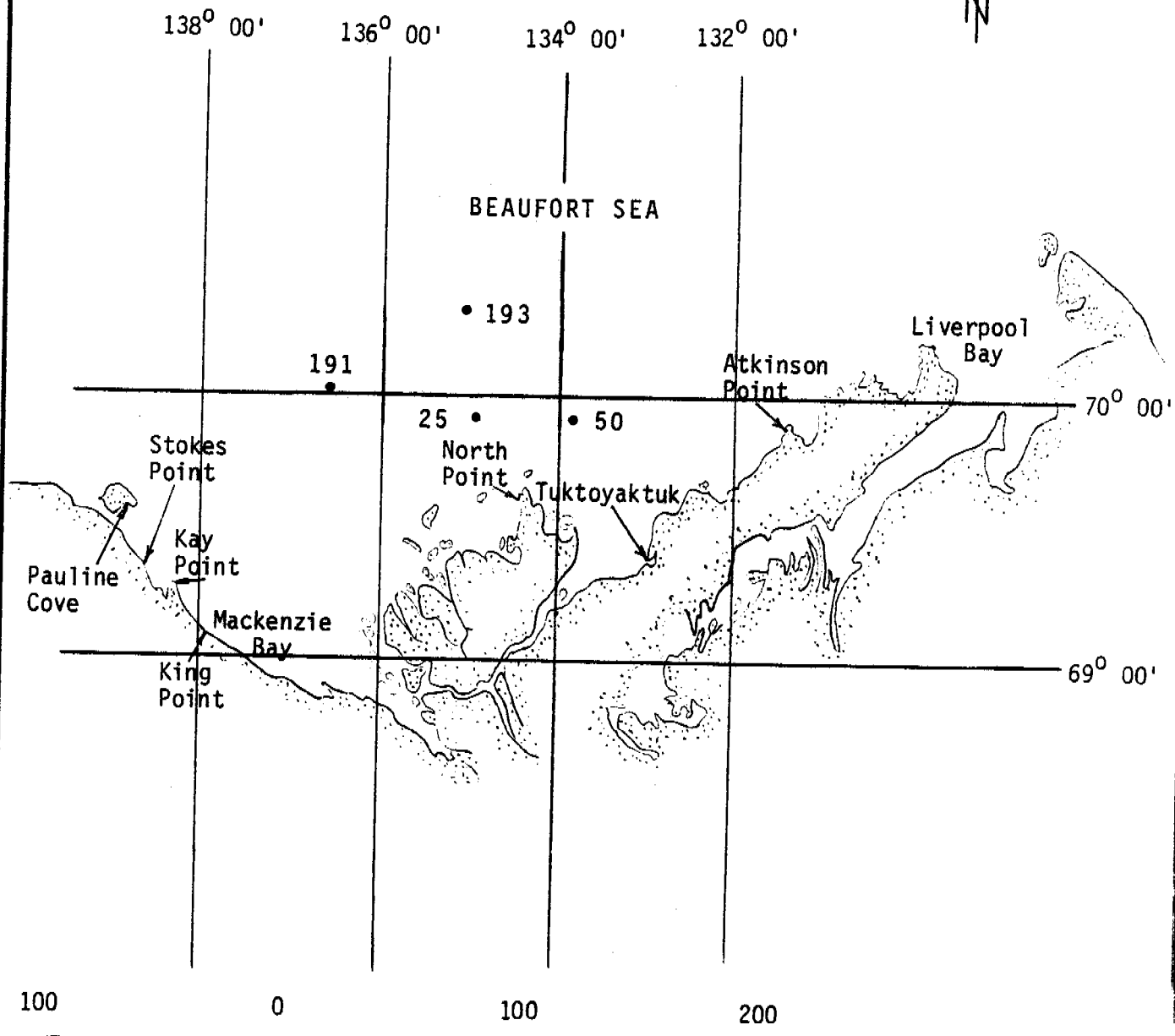
The site locations are shown in Figure 1.1.

King Point was to be regarded as a key location, being considered the most likely site for the next new shore-base facility. For this reason it was selected for study of the impact of a structure and generally to be treated preferentially in the course of the work.

FIGURE 1.1

KEY

• MEDS Wave Measurement Station



100 0 100 200

————— X 1000 Metres

<p>BEAUFORT SEA COASTAL SEDIMENT STUDY</p> <p>Study Area</p>	Date: 8 Mar 85
	Scales as shown
	Checked by:
	Keith Philpott Consulting Limited

1.1.1 Readership

The intention of this study was to generate data of direct value to those in Government and Industry responsible for detailed planning of shore-base facilities, pipeline shore crossings and the like.

To the extent that it has produced acceptable data, it can be so used. In this respect the wave climate data will be of value where it fills gaps in the available data base.

The inshore wave climate data is of special value, not only because it fills gaps but because it corrects some significant errors that have characterized most previous work due to the over-simple methods used, and in particular their neglect of the shallow water spectral saturation effect.

The alongshore sediment transport computations and coastal profile adjustment data to a large extent fill a gap and should also provide better estimates for several places that have been studied previously.

For coastal research workers the report will be of interest as a demonstration of the application of state of the art coastal process software to the complex arctic coastal environment. It shows, on one hand, the strength and



versatility of the wave analysis techniques, and on the other hand, the need for further research and development of the coastal sediment transport models. Some steps in this direction will be implemented in the immediate future; others will require a major new research effort.

Finally, it is probable that one of the major benefits of this work has been to highlight the inadequacies of the available field data base and to point to the urgent need to rectify the deficiencies before coastal development actually takes place.

1.2 Acknowledgements

The work reported here was carried out under contract to the Department of Indian Affairs and Northern Development and the Geological Survey of Canada, Department of Energy, Mines, and Resources. It forms part of the Northern Oil and Gas Action Plan NOGAP. In this connection, the advice and support of Scientific Authorities Dr. D.M. Barnett of DIAND and Dr. D.L. Forbes of EMR is gratefully acknowledged.

The specialist information and comment provided by outside consultants Dr. John Harper of Dobrocky Seatech and Dr. Ken Croasdale of Croasdale Associates has made a significant contribution to the work. We also thank J.L. Lussenburg, Gulf Canada Resources, for information and for agreeing to review this report.

In-house contributions of technologists Ed Caverly and Marilyn Haines to all phases of the work and of secretary Billie Oxley who performed the word processing, are acknowledged with special thanks.

Last but not least we acknowledge our continuing debt to Dr. Chris Fleming, now with Halcrow, U.K., for his contribution to the numerical modelling and for his valuable advice in review of this report, and to Dr. Harry Swart who developed the sediment transport models SEDX and SEGAR.

1.3 Arrangement of the Report

The report is arranged in two parts:

Part I Main Text describing:

Input data and Information

Methodologies

Summaries of Results

Discussion

Conclusions

Recommendations

Appendices

Part II Complete Data Compilations for each site:

Site Descriptions

Wave Climate Statistics

Coastal Process Data

1.4 Scope of the Report

1.4.1 Part 1

Numerical estimates of annual alongshore sediment transport and nearshore profile adjustments under storm action are developed for six coastal sites in the Canadian Beaufort Sea. The six sites are near Atkinson Point, Kay Point, King Point, North Head, Stokes Point, and Tuktoyaktuk.

The influence of storm surges on alongshore sediment transport and nearshore profile adjustment was also investigated at the same sites.

The evolution of the shoreline near King Point has been investigated under existing conditions and as it would be with a total littoral barrier structure in place.

Offshore wave climates were computed for the six sites mentioned plus another near Pauline Cove on Herschel Island. They are based on new fourteen-year parametric wave hindcasts.

Two-dimensional, directional spectral transfer techniques with allowance for shallow water equilibrium spectral forms were used to obtain the inshore wave climates from the hindcast results.

The sequence of presentation of the work is as follows:

1. Data and Literature Searches. (Section 2)
2. Computation of inshore wave climate.
(Sections 3 and 4)
3. Investigation of the sensitivity of coastal processes to storm surge action. (Section 5)
4. Estimation of alongshore sediment transport rates.
(Section 6)
5. Estimation of coastal profile adjustments under different patterns of wave attack. (Section 7)
6. Evaluation of the effect of a coastal structure at the King Point site. (Section 8)

Part I the Report concludes with discussion of methods and results (Section 9), Conclusions (Section 10), and Recommendations (Section 11).

1.4.2 Part II

Part II of the Report contains an outline of methodology and seven complete sets of numerical results for each of the sites in alphabetical order. Each data set is separately paginated. For each site information is presented in the following sequence, (according to availability):

- Description of Site and Site Plan
- Deepwater/Offshore Wave Statistics
- Nearshore Wave Transformation Analysis
- Inshore Wave Statistics (King Point only)
- Alongshore Sediment Transport Rates (excludes Pauline Cove)
- Nearshore Profile Adjustment Results (excludes Pauline Cove and North Head)
- Beach Plan Evolution (King Point only)

1.5 Summary of Numerical Work

This summary of the numerical work is intended as a preview of the report proper. It is in the sequence indicated in 1.4.1 - Scope of Part I.

1.5.1 Computation of Inshore Wave Climates

Inshore wave climates were computed for fourteen years for two "nodes" at each of the seven sites. The nodes were located just beyond the breaker zone, typically around the four-metre contour. The work was done in two interactive phases:

- 1, computation of offshore wave climates using wind-wave hindcasting (See Section 3), and
- 2, conversion to inshore climate with computed nearshore wave transformation functions using the spectral transfer technique. (See Section 4).

The procedure used to predict the offshore wave climates used in this study, parametric hindcasting of effective waves (PHEW), provides a flexible vehicle for calibration purposes with good definition of wave directions. However, in the absence of directional wave measurements, the hindcasting procedure had to be calibrated and verified using four sets of non-directional wave measurements.

A wind data set for use in the hindcasts had to be synthesized by selectively merging three sets of wind records from Tuktoyaktuk (1970-1983).

The two-dimensional directional spectral transfer technique (SPECTRANS) used for computing wave refraction is based on linear wave-ray backtracking and deepwater JONSWAP spectra. A shallow water spectral saturation criterion was also incorporated.

The method provides accurate unambiguous definition of inshore wave conditions for virtually any combination of bathymetry and sheltering conditions. It would appear from the results obtained here, that most previous studies have significantly overestimated the severity of inshore wave climates.

This project has provided a useful opportunity for the implementation of some improved procedures for parametric wave hindcasting and nearshore wave transformation at the seven sites. These include procedures to accommodate:

- Time-varying fetch lengths due to changing ice edge
- Effective depth of fetches varying with time and direction
- Simultaneous wave generation in deep and shallow fetches
- Shore parallel and offshore wind effects
- Complex sheltering due to adjacent coastal forms
- Wave height reduction due to spectral saturation

Both offshore and inshore wave climate data were computed for the seven sites. The inshore wave climate results were used as primary input data for coastal sediment transport models.

Offshore wave climate statistics for all sites are presented in Part II of this report. Inshore wave statistics are also presented for King Point only.

1.5.2 Sensitivity to Surges

1) The effects of storm surge events on estimates of alongshore sediment transport and nearshore profile adjustment were extensively investigated. The objective was to determine

the extent to which storm surge events contribute to coastal change and to determine how to incorporate these effects in subsequent sediment transport computations.

2) Typical "large" and "average" surge events were defined for each site using the results of previous studies. These surges were then applied to the alongshore sediment transport computation system SEDX and to the profile adjustment model SEGAR.

3) It was found that water level changes due to surges may either increase or decrease the alongshore transport rates depending on local conditions but that the effect on average rates would not exceed 10% for the sites examined. This is negligible considering the level of accuracy attainable by current alongshore sediment transport estimation methods.

Surges have a much greater effect on nearshore profile adjustments and the reports of surge effects must therefore be attributed more to this cause. This is apparent in the results described in Section 7. However, the most spectacular reports of major coastal retreats in the Beaufort Sea include effects of ground ice melting which were not accounted for in the nearshore profile adjustment model SEGAR.

1.5.3 Alongshore Sediment Transport Estimates

The alongshore sediment transport estimates were carried out using a modelling system which incorporates twelve different state of the art predictor models. Three were simple non-detailed bulk energy models including the original CERC formula. The remaining nine models were detailed predictors which incorporate roughness estimators and an alongshore current model. All models draw from a common input data set.

These models had previously been found to give relatively consistent results on oceanic beach coasts but rather more scattered answers in less typical places such as Pointe Sapin, New Brunswick (Fleming, Philpott, and Pinchin, 1984). This project was therefore a valuable test of the limits of applicability of these models to non-typical site conditions involving such special features as exceptionally mild wave climates, transgressive barrier beaches, ice bonded sediments, cohesive coasts, fine grained sediments on steep slopes, and gravel beaches.

All of the detailed predictors gave more or less unstable results at some of the sites but the Nielsen et al., (1978) breaking wave model was judged better than the others overall. Stable, though not necessarily more accurate, results

were consistently obtained from two of the three bulk energy models, the CERC model itself and a recent development of it, Davies (1984).

"Best estimates" of alongshore sediment transport were obtained by averaging results of several models after eliminating those that yielded unrealistically high or low results. The selection of valid models varied from site to site. The wide scatter of results from detailed predictors underlines the need for further development and calibration of these models.

The results of the alongshore transport computations are summarized in Section 6 of Part I and complete results for all six sites are given in Part II.

1.5.4 Nearshore Profile Adjustments

The investigation of profile adjustment was performed with a numerical model based on onshore-offshore sediment transport theory developed by Swart (1974). The model computes changes in the position and shape of the nearshore profile resulting from wave attack at variable water levels.

Results from this model and similar models have been verified at several oceanic sites and in the laboratory. However, significant difficulty was encountered in applying the model at the study sites. At sites where the investigation provided reasonable results there was a definite trend for shoreline retreat to increase with increased water level. A complete presentation of the nearshore profile adjustment investigation is presented in Section 7.

1.5.5 Evaluation of the Effect of a Coastal Structure at King Point

As the "key site", King Point was selected for investigation of the effect of a hypothetical coastal structure. This was carried out assuming the construction of a jetty forming a total barrier to alongshore sediment transport.

The effects of the structure were investigated by successful adaptation of the existing beach plan evolution model BPLAN to the non-typical conditions at King Point. The model assumes a simple beach coast with unrestricted sand supply whereas the King Point coast includes eroding cohesive tundra bluffs, non-saturated alongshore transport rates, and a prograding barrier beach with overwashing.

The inshore wave data for the beach plan evolution model were derived from SPECTRANS for five nodes, with wave data utilized in chronological sequence. Additional nodes are interpolated. The wave data were applied to a "one-line" beach model using a bulk energy alongshore transport predictor. BPLAN was modified to account for the special characteristics of the site by introducing a spatially varied beach height adjustment factor. It was successfully calibrated with simple sediment budget data derived from bluff composition, bluff recession, and beach accretion data from the field.

Although this is a simple model, the incorporation of several data points to ensure a well defined shoreline, the evaluation of the effects of continuity among them, and the facility for calibration, all suggest that beach plan modelling provides a practical operational tool correlating shoreline change data with estimates of alongshore transport for the less typical coastline.

See Section 8 of this part of the report for further details and Part II for a complete compilation of results.

SECTION 2 DATA SOURCES AND REVIEW OF PREVIOUS WORK

2.0 Introduction

All sources of regional and site specific data and information used in this study are identified in this section. This includes meteorological and oceanographic, and geotechnical/geological data together with technical reports and published literature referred to for interpretive purposes or as sources of relevant information.

Basic environmental data and related studies are presented first, followed by site specific data related to coastal processes or morphology, and finally, brief descriptions of the seven sites are given. Here, and elsewhere in this report, the sites are introduced in alphabetical sequence by name.

In concluding this introduction it should also be mentioned that the data in the region are still relatively scarce, so that in a number of cases resort has been made to interpolation, extrapolation, and , in some instances, to inference where data actually are lacking.

2.1 Environmental Data

2.1.1 Previous Reports

A considerable number of studies have been made of environmental factors that could influence alongshore sediment transport and coastal profile adjustments on the shores of the Beaufort Sea. Most of these have appeared since 1974/75 when the "Beaufort Sea Project" was put in hand by the Government of Canada. For example, Lalonde and McCulloch (1975), on ratios of wind speed over water to that over land; Henry (1975), Henry and Heaps (1976) on storm surges.

At that time there was little field evidence on which to base conclusions. As field data became available further studies appeared: Baird and Hall (1980) produced hindcast wave estimates for several island sites. In 1981 Hodgins et al, and Hodgins and Dal-Santo produced studies of extreme water level and wave conditions obtaining results which were substantially more severe than Baird's. These were updated in later studies by Hodgins and Harry (1982) and MEP (1983) which led in turn to more moderate estimates of extreme storm conditions. More recently, Danard (1983); Danard and Grey (1984); and Niwinski and Hodgins (1984), have cooperated with Henry (1984) in a new study of extreme water level and wave conditions at Tuktoyaktuk.

Among the recurrent issues evident in these studies is the paucity of wind and water level records, from around and over the Beaufort Sea. Comparisons of wind over water with winds measured on land were made in several of the above studies and also Readshaw (1982 and 1983). Tuktoyaktuk wind records have commonly been used as a basis of comparison because they provide the longest relatively complete data set in the region.

Water level records are quite fragmentary with numerous gaps even in the Tuktoyaktuk records, which Henry 1975, 1984 has nonetheless used for calibration and verification of numerically computed positive surge results. Although the relative abundance of negative surges has been noticed (Henry and Heaps, 1976) and observers have commented on their probable effects (private communications, D.L. Forbes, J.R. Harper); they have not yet been studied in detail.

2.1.2 Water Level Records

Water level records are sparse. The only permanent gauge, the one at Tuktoyaktuk, has operated since 1961. Unfortunately, the record is marred by numerous gaps, some of several months duration. Elsewhere there are only temporary gauge records mostly of one or two months for one or more years. Where several years are available they are not necessarily consecutive; for example, at Atkinson Point, one of the better represented sites, one to two months of data are

available from 1971, 72, 74, 75, 81 and 82. Henry, (1984) provides a water level data coverage report which is reproduced in Figures 5.5 and 5.6 of this report.

Tide ranges throughout the area of interest are relatively small, about 0.3 m for average tides and 0.8 m for large tides. The mean water level relative to tidal datum has been taken as 0.5 m for all sites examined in this study.

For the purposes of this study the primary interest in water levels concerns the effects of surges on coastal processes. Henry (1984) has provided an overview of positive surges recorded or observed at Tuktoyaktuk, which is illustrated in Figure 5.5 of this report. It shows that five large storm surges exceeding 1.5 m occurred in the 23 years from 1961 to 1983. The most recent of these occurred in 1972. Only two of the five were recorded. Also twenty-one smaller surges less than 1.5 m were recorded in the same period. There may well have been at least four or five other small surges that went unrecorded. Only four surges were recorded in the ten years 1974-1983. Almost all surges occur in three open water months: July, August, September.

The 1:100 year storm surge at Tuktoyaktuk was estimated to be 3.3 m by Henry and Heaps (1976). Kolberg and Shah (1976) obtained the same value in an independent study. Also, Henry and Heaps using a numerical storm surge model have provided storm surge distribution

maps from which storm surge heights at Tuktoyaktuk can be related to probable surge heights at the other six sites. It is based on a typical north-westerly storm. See Section 5.

Using Figure 5.5 (from Henry, 1984) as a guide, complete sets of Tuktoyaktuk water level records were obtained from MEDS for all months in which storm surges were recorded.

2.1.3 Wind Records

Wind data is used for wave hindcasting. It had been decided to extend the wave hindcast over the longest possible period for which suitable wind records existed. Tuktoyaktuk, for which records extend back to 1970, was the only feasible source. Wind data on magnetic tape was obtained from the Atmospheric Environment Service of Environment Canada.

The standard information required for the wind-wave hindcast model (PHEW) is one- or three-hourly wind speed data measured to the nearest ten degrees. However a complete and continuous data set meeting the above requirements did not exist. Instead, three heterogeneous sets of data had to be merged to form a usable data set. See Table 2.1. The measurements were taken at two stations, Tuktoyaktuk and Tuktoyaktuk A, which are in close proximity to each other. At Tuktoyaktuk wind speeds and 36 point direction measurements were taken 4 times a day. At Tuktoyaktuk A measured

Table 2.1

Wind Data Records

Tuktoyaktuk, N.W.T. Source: A.E.S. Jan. 1970 to Dec. 1983.

Directions: sixteen directions from Jan. 1970 to Dec. 1970 and thirty-six directions from Jan. 1971 to Dec. 1983. Wind speeds: km/hr. Wind data every sixth hour. Magnetic Tape No. C21056.

Tuktoyaktuk "A", N.W.T. Source: A.E.S. April 1970 to Dec. 1983.

Directions: sixteen directions from April 1970 to Sept. 1970 and thirty-six directions from Feb. 1971 to Dec. 1983. Wind speeds: km/hr. Wind data hourly but not for 24 hours each day. Magnetic Tape No. C21056.

Tuktoyaktuk "A", N.W.T. Source: A.E.S. April 1970 to Sept.

1983. Directions: eight directions. Wind speeds: km/hr. Wind mileage averaged hourly. Magnetic Tape No. C20977

wind speeds and 36 point direction measurements were recorded on an hourly basis but not for 24 hours each day; they were available for varying time intervals during the day. Finally, the third data set consisted of measurements from a mileage type anemometer located at Tuktoyaktuk A. An average wind speed for each hour of the day at 8 compass points was given, derived from the measurements. The other two data sets provide instantaneous velocities. Details of the procedure by which these data sets were merged and edited are outlined in Section 3.

2.1.4 Wave data

Wave records were required in this study for the purpose of calibrating the wave hindcasting procedure. Directional measurements are very desirable but none were available. However, non-directional data are available from Marine Environment Data Service, Fisheries and Oceans Canada. The output comprises significant wave height and peak period plus spectral density data at 3 hourly intervals.

Although non-directional accelerometer wave gauges have been deployed at numerous sites in the Canadian Beaufort Sea, since 1975 all records are of short duration and most are incomplete. It was therefore not possible to obtain six months of records at one site as had been proposed. After reviewing seventeen possible wave records,

it was eventually decided to calibrate the wave hindcast for two offshore island wave recorder sites, Pullen NE (MEDS Station 50) and Gulf #2 (MEDS Station 191) with records aggregating less than five months. These stations were more or less centrally located in the area offshore from the seven coastal sites. Two other nearby simultaneous sets of wave data were also used for verification (MEDS Stations 25 and 193). See section 3.5 and Table 3.2 for details.

It was subsequently concluded that it would have been of considerable value to have used wave records from one of the shallower and confined water areas represented in the study such as Kugmallit Bay or near Stokes Point. However, no suitable shallow water records yet exist.

2.1.5 Other Environmental Data

Several other parameters of secondary importance to this study have been examined and referred to in this study. These include currents, water temperature and radiation. The main sources of information on these secondary parameters have been data syntheses such as the Beaufort Sea E.I.S. In addition, sea ice data in the form of ice charts has been analyzed in detail. (See 2.2.1).

The main source of information on these secondary parameters has been data syntheses such as the Beaufort Sea E.I.S.

2.2 Surveys Graphics

2.2.1 Ice Charts

Because wave generating fetches in the Beaufort Sea are largely bounded by the constantly changing edge of the ice, it was considered necessary to introduce a time varying-fetch into the wave hindcasting procedure.

Data to define the ice limited fetches was obtained from weekly ice charts which are available since before 1970, the starting year for the wave hindcast. Nearly 400 charts were obtained from the Ice Centre, Atmospheric Environment Service, Environment Canada. They were at three different scales and more than one method of describing ice coverage had been used over the period of the charts. See Table 2.2 for further detail.

2.2.2 Hydrographic Charts and Field Sheets

Published hydrographic charts have been used for general reference purposes (Table 2.3). However, for detailed analysis of bathymetric data, in particular for the preparation of wave refraction grids, hydrographic field sheets in U.T.M. coordinates have been used. Prints were supplied by the Canadian Hydrographic Data Centre, Fisheries and Oceans, Canada.

Table 2.2

Ice Charts

Atmospheric Environment Service

Ice Centre, Environment Canada.

Weekly ice charts were obtained for open water season (which is generally from June until mid-October) for the period 1970 to 1983.

Period:	Scale:
May 21, 1970 to Oct. 29, 1975	1:8,790,000
June 20, 1975 to April 20, 1982	1:4,900,000
May 15, 1982	1:16,000,000
June 22, 1982 to Dec. 8, 1983	1:4,900,000

Table 2.3

Hydrographic Charts

Canadian Hydrographic Service

Name	Scale	Title	Date
7650	1:500,000	Barter Island to Toker Point	1974
7651	1:500,000	Toker Point to Cape Lyon and Cape Kellet	1974
7604	1:500,000	Pelly Island to Toker Point including Kugmallit Bay	1972
7625	1:15,000	Tuktoyaktuk and Approaches	1975
7603	1:60,000	Herschel Island to Kay Point	1984
7601	1:150,000	Siku Point to Kay Point	1975

Twenty-three field sheets were utilized as listed in Table 2.4. Variations in scale from 1:6,000 near Tuktoyaktuk, to 1:100,000 created matching problems, as did the fact that a U.T.M. zone boundary passes through some of the grids. The age range of the surveys, 1956-1983, was not in itself a problem.

2.2.3 Air Photos and Other Site Graphics

At least two airphotos were provided for each site. These were used to assist in understanding the morphological character of each location. Except in the case of the barrier beach at King Point, they were not used to assess coastal changes.

A detailed oral and visual presentation of tundra cliff morphology and degradation processes near King Point was provided by David Harry, GSC. A collection of photos from the King Point area was provided late in the study by W. Field, Fisheries and Oceans, who has also given detailed descriptions of the King Point barrier.

Site locations are shown in Figure 1.1, and plans of the seven sites are shown in Figures 2.1 to 2.7 in alphabetical order. The nodes which appear in these figures mark the locations for which nearshore wave climate data and sediment transport data were developed. (See section 4 et seq.)

Table 2.4
Hydrographic Field Sheets
Canadian Hydrographic Service

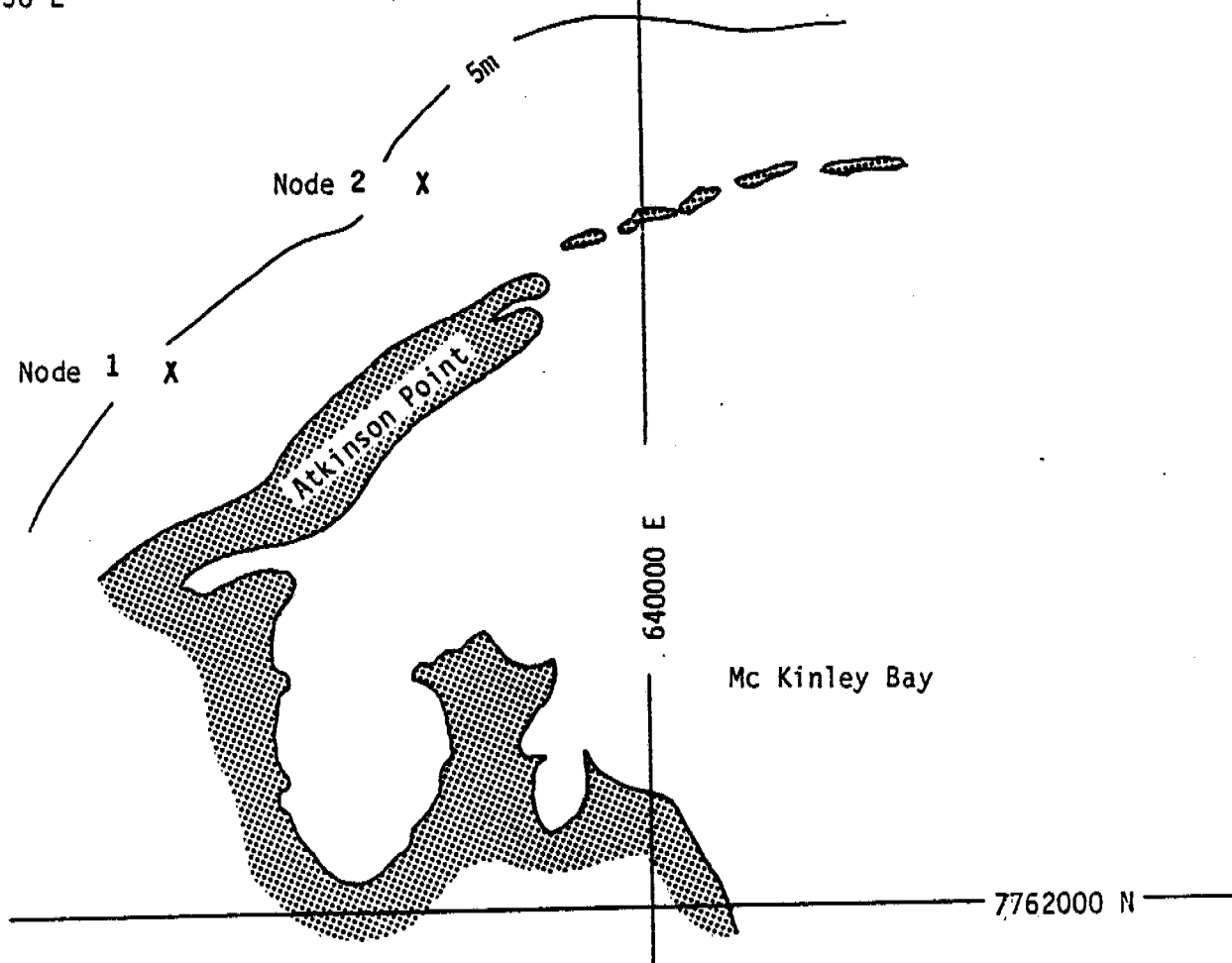
F.S. No.	Location	Year	Scale
F.S. 2651	Tuktoyaktuk Harbour	1956	1:6,000
F.S. 2651	Approaches to Tuktoyaktuk Harbour	1956	1:24,000
F.S. 3588	Herschel Island & Mackenzie Bay	1969	1:50,000
F.S. 3589	Herschel Island & Mackenzie Bay	1969	1:50,000
F.S. 3590	Beaufort Sea Sheet #1	1969	1:100,000
F.S. 3591	Beaufort Sea Sheet #2	1970	1:100,000
F.S. 10018	Trent Bay	1963	1:12,000
F.S. 10026	Toker Point to Hutchison Bay	1964	1:50,000
W.A. 10028	Atkinson Point to Novorak Point	1979	1:50,000
W.A. 10037	Kugmallit Bay	1964	1:75,000
F.S. 10045	White Summit	1964	1:50,000
F.S. 10059	Hutchison Bay	1967	1:50,000
W.A. 10070	Herschel Island to Kay Point	1970	1:50,000
W.A. 10071	Western Arctic Mackenzie Bay	1970	1:50,000
F.S. 10072	Mackenzie Bay	1970	1:50,000
W.A. 10073	Mackenzie Bay (Northern Part)	1970	1:50,000
W.A. 10085	Beaufort Sea Sheet #1	1971	1:100,000
W.A. 10086	Beaufort Sea Sheet #2	1971	1:100,000
W.A. 10087	Beaufort Sea Sheet #3	1971	1:100,000
W.A. 10093	Beaufort Sea Sheet #3	1972	1:100,000
F.S. 10101	Mackenzie Bay	1974	1:50,000
W.A. 10128	Approaches to Tuktoyaktuk Harbour	1979	1:40,000
F.S. 10189	Herschel Island, Yukon Coast	1983	1:100,000

Node 1

7766900 N
638475 E

Node 2

7765650 N
636750 E



Universal Transverse Mercator Projection
Zone 8



Scale
in
Metres

BEAUFORT SEA COASTAL SEDIMENT STUDY

Atkinson Point: Site Plan Showing Nodes

Date: 2 May 85

Scales as shown

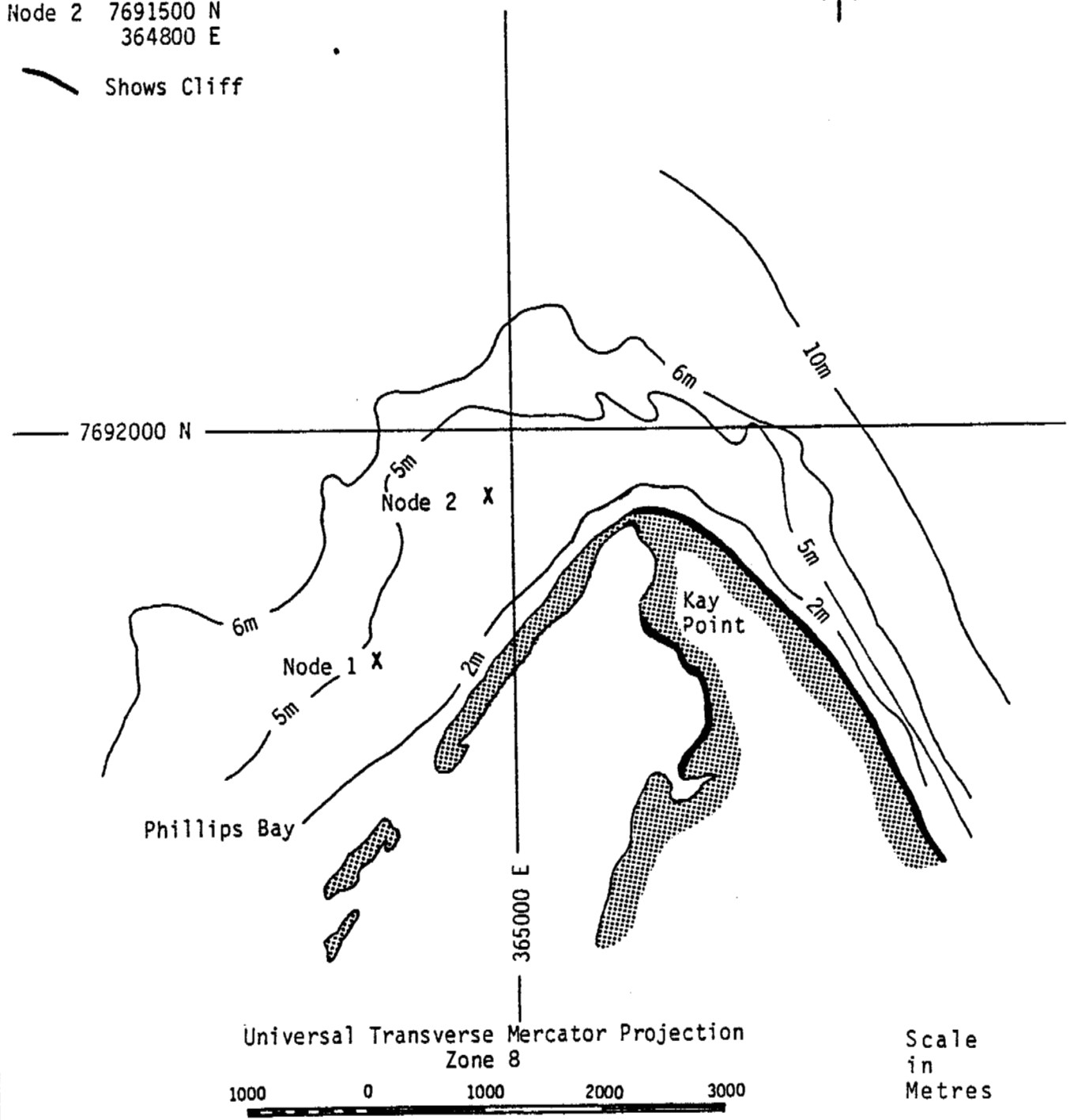
Checked by:

Keith Philpott
Consulting Limited

Node 1 7690100 N
363850 E

Node 2 7691500 N
364800 E

Shows Cliff



BEAUFORT SEA COASTAL SEDIMENT STUDY

Kay Point: Site Plan Showing Nodes

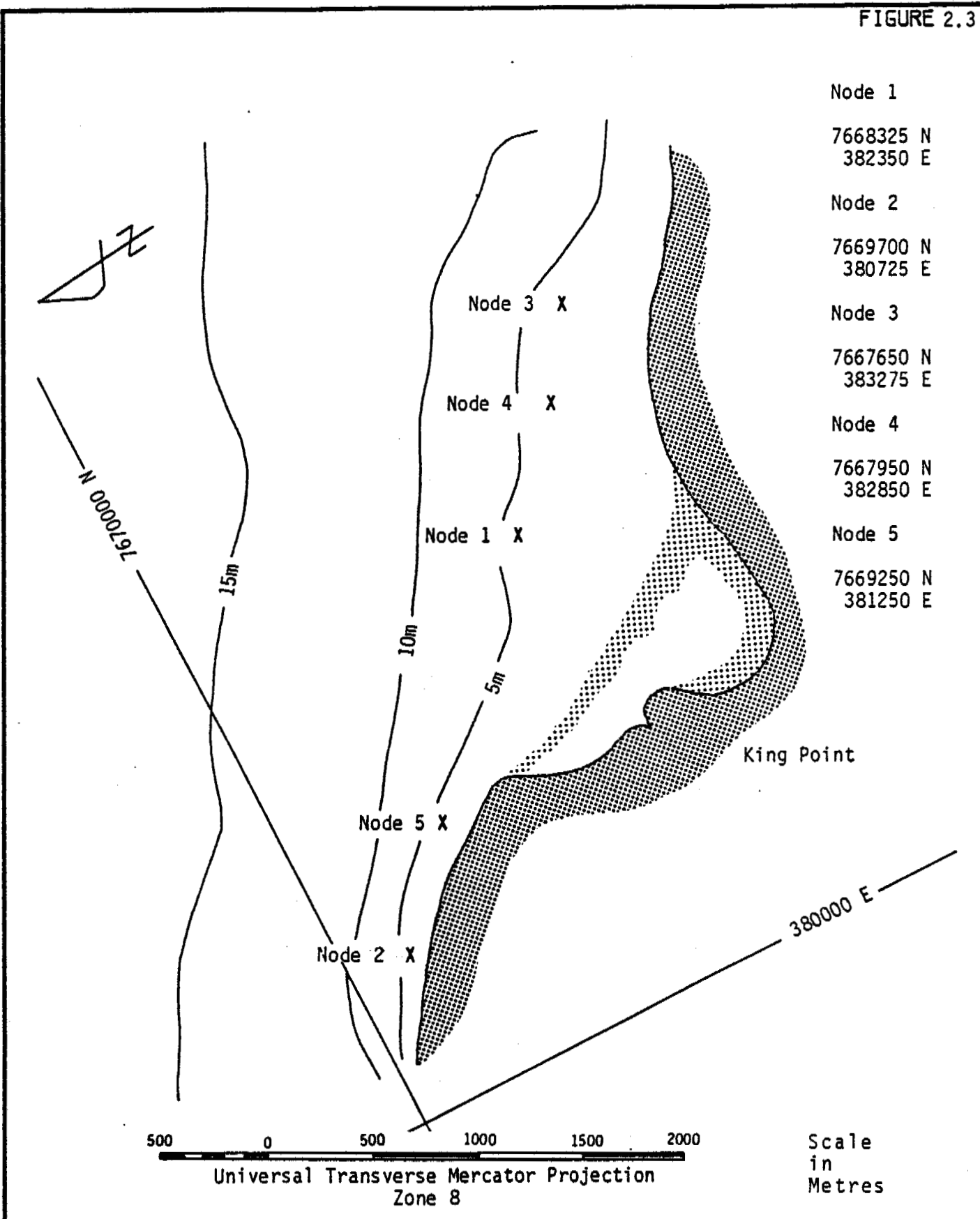
Date: 2 May 85

Scales as shown

Checked by:

Keith Philpott
Consulting Limited

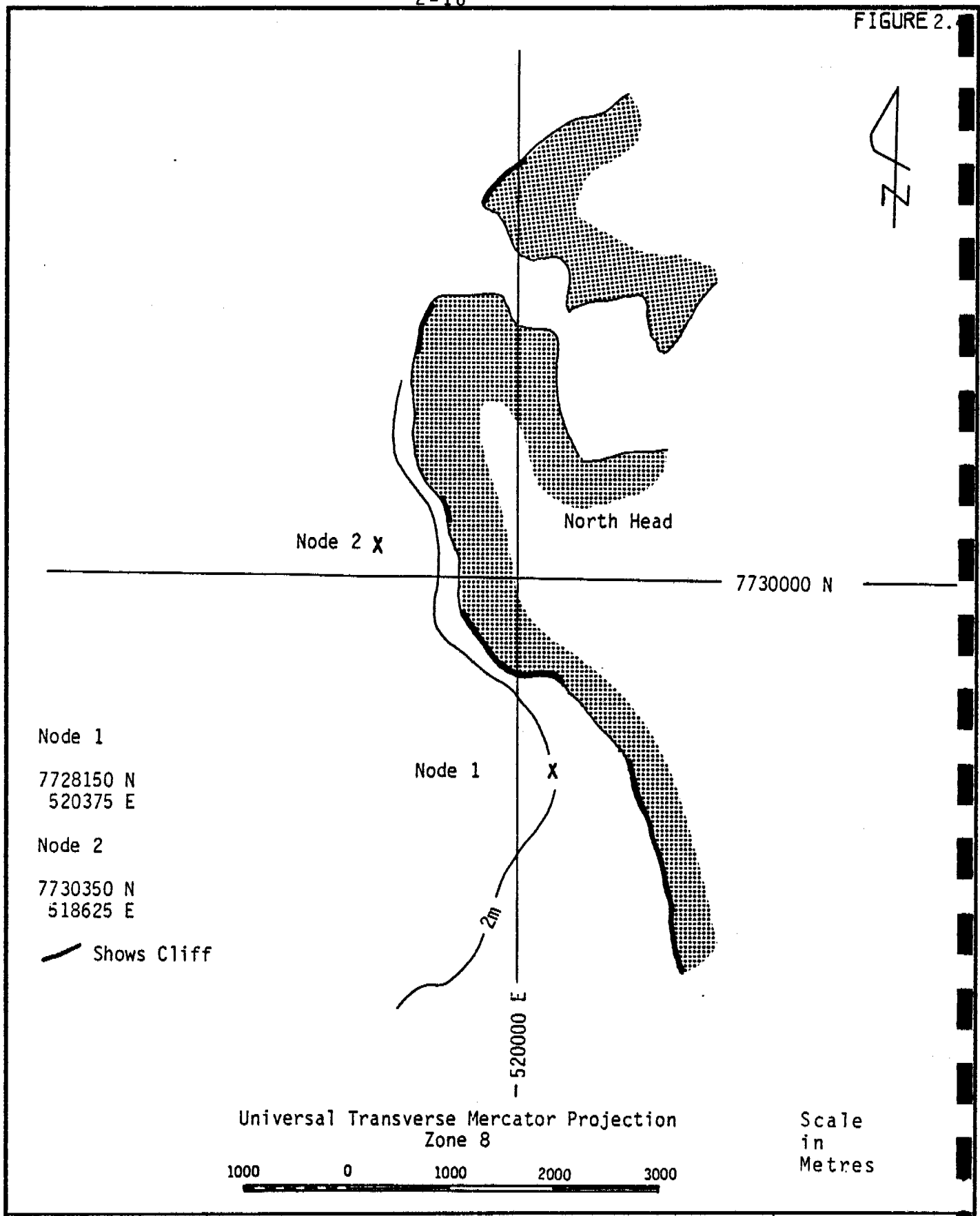
FIGURE 2.3



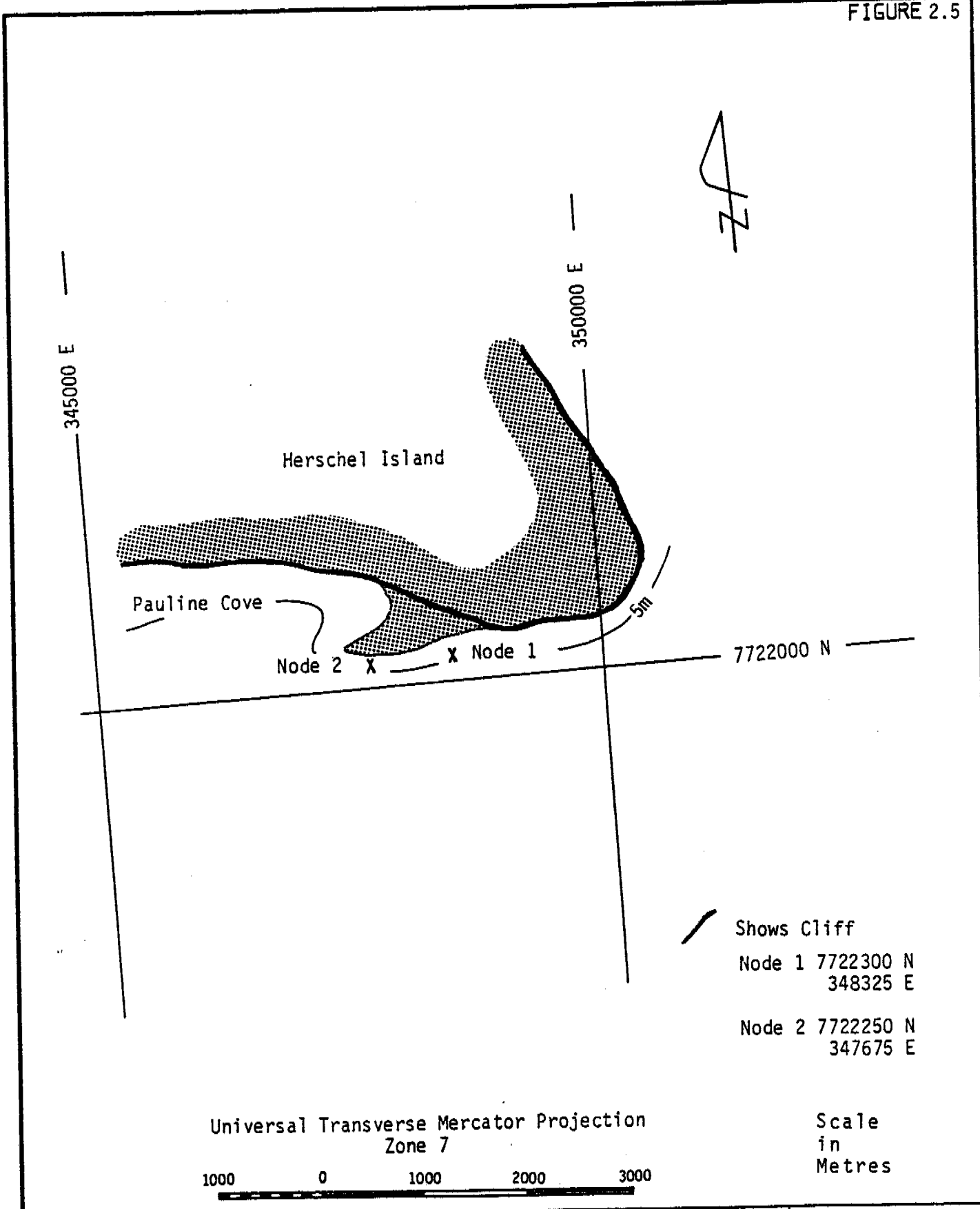
BEAUFORT SEA COASTAL SEDIMENT STUDY

King Point: Site Plan Showing Nodes

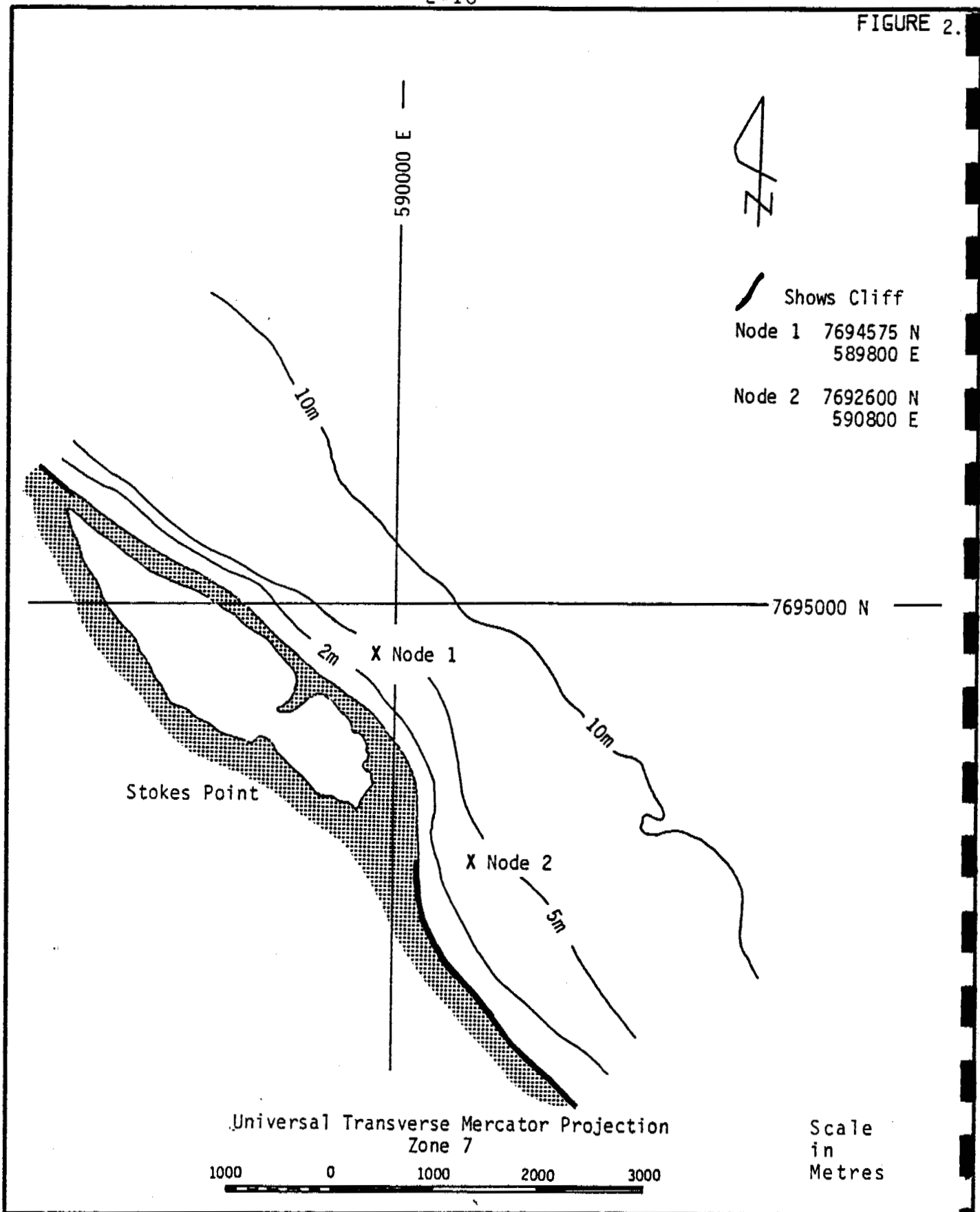
Date: 2 May 85
 Scales as shown
 Checked by:
 Keith Philpott
 Consulting Limited



BEAUFORT SEA COASTAL SEDIMENT STUDY	Date: 2 May 85
	Scales as shown
North Head: Site Plan Showing Nodes	Checked by:
	Keith Philpott
	Consulting Limited



BEAUFORT SEA COASTAL SEDIMENT STUDY	Date: 2 May 85
	Scales as shown
Pauline Cove: Site Plan Showing Nodes	Checked by:
	Keith Philippott Consulting Limited

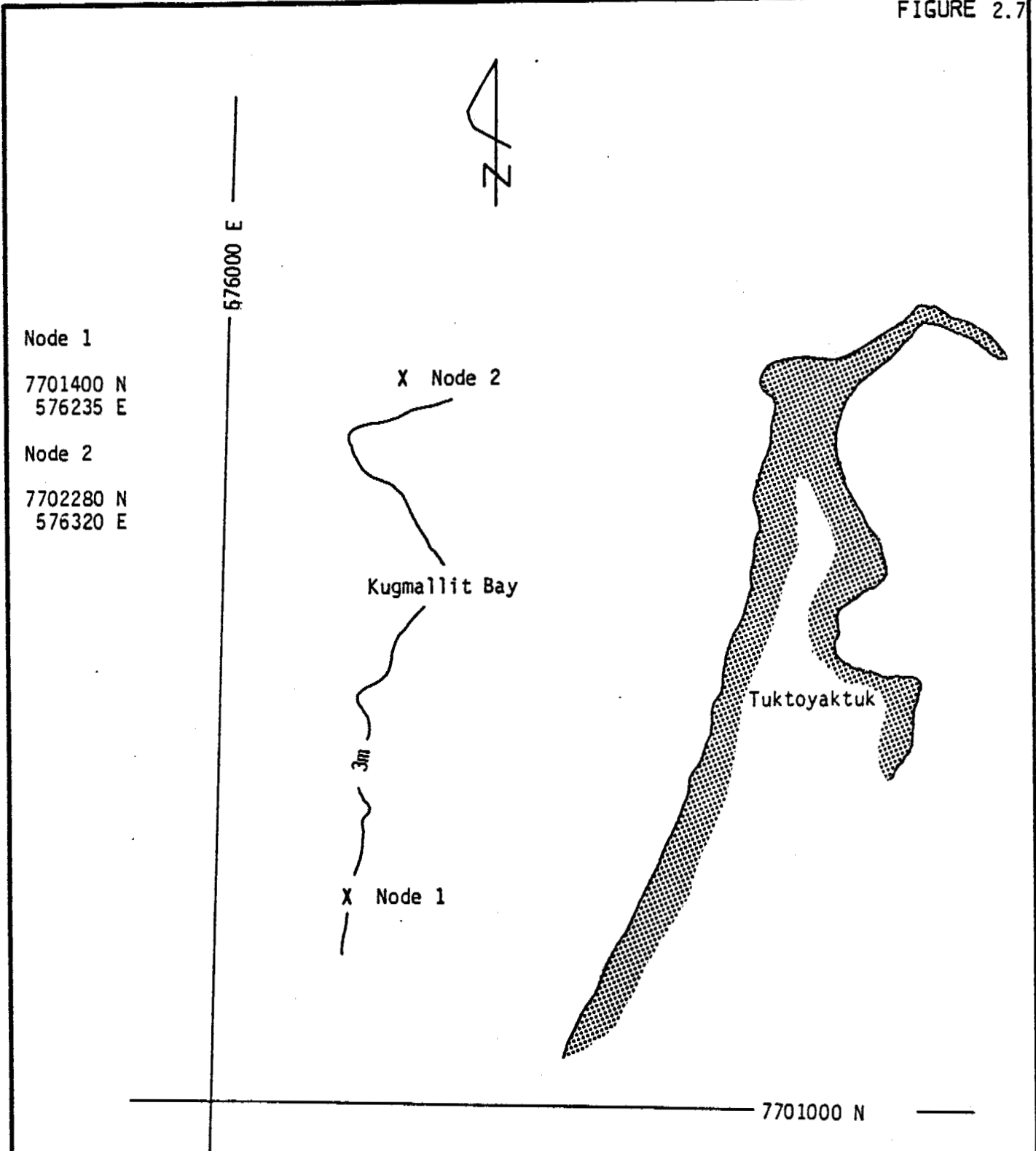


Universal Transverse Mercator Projection
Zone 7

1000 0 1000 2000 3000

Scale
in
Metres

BEAUFORT SEA COASTAL SEDIMENT STUDY	Date: 2 May 85
	Scales as shown
Stokes Point: Site Plan Showing Nodes	Checked by:
	Keith Philpott
	Consulting Limited



Universal Transverse Mercator Projection
Zone 8



Scale
in
Metres

BEAUFORT SEA COASTAL SEDIMENT STUDY	Date: 2 May 85
	Scales as shown
Tuktoyaktuk: Site Plan Showing Nodes	Checked by:
	Keith Philpott Consulting Limited

2.3 The Arctic Coastal Environment

2.3.1 Arctic Coastal Processes

There is a growing literature on the special characteristics of arctic coastal processes. These studies were effectively summarized by Owens and Harper (1983). They briefly describe how sea ice, shore zone ice and terrestrial ice all affect coastal processes. Although this is not the place for an indepth review of the subject, it is necessary to indicate the more important ways that arctic coasts differ from the sandy beach coasts assumed in the derivation of virtually all of the sediment transport models utilized in this study.

First, for purposes of comparison, there are four fundamental assumptions on which the coastal process models used in this study are implicitly based.

1. Coastal processes are wholly mechanical.
2. They are controlled by the unrestricted effect of wave energy, modulated to a limited extent by variations in water level.

3. The solid phase of the coastal interface consists entirely of a permeable assemblage of mobile cohesionless particles.
4. The extent and thickness of the non-cohesive material is great enough to ensure that wave-particle interaction cannot be affected in any way by an impermeable surface or bonded material such as rock, clay, ice, or ice-bonded sediment.

The basic ways in which an arctic coast differs from a typical beach are:

1. Arctic coastal processes are influenced by thermal effects as well as mechanical effects.
2. The solid phase of an arctic coast can include varying proportions, and patterns of occurrence of ice and/or ice bonded sediment which may interfere with wave action and/or particle motion.

Where erosion of a given volume of material from an ice-rich coast takes place, the yield of sediment released into the littoral zone is less than in the case of a sandy beach coast. This could have the effect of increasing the rate of recession or reducing the rate of accretion, if the supply of sediment, and hence the actual alongshore sediment transport rate, is less than the potential rate as determined by wave action. This is similar to the situation that occurs in the case of cohesive coasts where only a fraction of the

eroded material remains in the littoral zone and the supply of cohesionless material is less than the alongshore transporting capacity of the waves (Philpott, 1984). A practical problem in both cases is that available models can only compute potential rates and hence, other things being equal, will tend to overestimate alongshore transport rates. This also means that there is no longer the direct connection between alongshore transport and shoreline recession on which beach-coast theory is built.

Typical arctic coastal processes which may accelerate coastal change include seabed ice scour, ice-override of the coastal zone, ground ice melt and ground ice slump. Processes which may retard coastal change include formation of protective ice ridges, ice foot, and ice bonding of beach material. In each case, the variations in rates of coastal change in an arctic environment are to be understood as being relative to rates of change of a classical sandy beach coast exposed to the same wave action.

This discussion is concluded with a brief assessment of probable influence of each of the above-mentioned thermal phenomena and their likely effect on the model results.

Sea bed ice scour in the littoral zone may cause deformations of the nearshore profile (W. Field, private communication), but these are quickly erased by wave action with little or no lasting effect.

Ice override has received a lot of attention because of its potentially disastrous consequences. See, for example; Croasdale (1978), Harper and Owens (1981) and, Harper (1983). However, the frequency of occurrence is very low and not likely to have seriously affected any of the seven sites since 1970, the starting year of our model simulations.

Melting of ground ice and consequent slumping are the principal factors leading to the high recession rates observed along arctic shorelines where bluffs are present (Harper 1978). This has probably affected several of the sites, such as Pauline Cove, King Point, North Head and in particular, Tuktoyaktuk. These phenomena are not reproduced in the sediment transport and profile adjustment models although they can be allowed for in the beach plan evolution model (See Section 8).

Melting ground ice also affects beaches creating furrowed profiles where melting has occurred. However, such profile deformations are quickly erased by wave action and appear to have no lasting effect on coastal change. The same appears to be generally true of beach deformations due to ice-push and ice-thrust.

Ice masses tend to build up along coastlines in the form of ice foot and ice ridges. Opinions seem to differ on their protective effect. Where such ice formations persist after the adjacent floe ice has melted, they provide protection, as mentioned by McDonald and Lewis (1973). However, Forbes (private communication) has suggested that the persistence of these shore fast ice forms is not generally an important factor, since most of this ice has melted by the time the ice edge has retreated far enough to allow moderate seas to be generated.

Ice bonding of beach material will have some effect, but due to the rapid intrusion of salt water into the beach face in the spring, the rate and extent of melting of interstitial ice is quite rapid. (Owens and Harper, 1977; Harper et al 1978.) However, Harper also concludes that "the normal thaw of ice bonded material in the beach limits the depth of which littoral sediments can be distributed". Supporting this: a typical thaw depth is in the order of one to one and a half metres, while coastal profile changes during major storms may exceed two metres vertically and five metres horizontally.

2.3.2 Beach profiles & Sediment Texture Data

Beach and nearshore bottom profiles are used along with bottom sediment texture data in the computation of alongshore sediment transport rates using detailed predictors (models in which the distribution of alongshore transport is computed from computed roughness and computed alongshore current distribution).

Profile and sediment texture data proved to be somewhat hard to come by, and at one site - Pauline Cove - unavailable. At the other six sites, a variety of sources was tapped yielding usable data in variable amounts and qualities. Sources and amounts of data are summarized in Table 2.5 which is supplemented by the following comments.

Not surprisingly, Tuktoyaktuk data was most prolific. Numerous nearshore profiles had been measured, forty-four boreholes were sunk and numerous sediment samples collected and analyzed by Kolberg and Shah (1976). These were supplemented by some data from 1984 obtained by an A.G.C. (Atlantic Geoscience Centre) field team.

Stokes Point had also been relatively well investigated for Gulf Canada Resources in 1982 by Hardy Associates as well as by Readshaw (1983). Again additional information was also available from A.G.C.

The other sites were generally less well supplied with data. Virtually, no direct evidence from North Head other than descriptions (Forbes, private communication) and the upper sample results from two bore hole records. At King Point, also, it was necessary to rely on descriptive material (C.P. Lewis, W. Field) supplemented by sample analyses and a sounding survey from Peter Kiewit and Sons Co. Ltd. From Kay Point there were two sets of profiles and seven sample analyses (Forbes and Frobels, 1985), part of a larger data base assembled by McDonald and Lewis (1973) and Lewis and Forbes (1975). From Atkinson Point there were again two profile data sets, but only one textural analysis result.

Table 2.5

Data base for Coastal Profiles
and Sediment Texture

Atkinson Point	4 nearshore profiles. 2 beach profiles. 1 foreshore sediment sample.	C.P. Lewis 1973 A.G.C. 1984 A.G.C. 1984
Kay Point	2 nearshore profiles. 2 beach profiles. 6 nearshore samples. 1 beach sample	A.G.C. 1984 A.G.C. 1984 A.G.C. 1984 A.G.C. 1984
King Point	1 beach profile with notes by B. McDonald nearshore profiles " " " 6 nearshore samples site descriptions	McDonald & Lewis 1973 D.C. McDonald 1972 C.H.S. F.S. Kiewit 1983 survey Kiewit 1983 W. Field 1984
North Head	profiles deduced sediment samples site description	C.H.S. F.S. A.G.C. boreholes D.L. Forbes
Pauline Cove	No usable data	
Stokes Point	2 nearshore profiles beach and nearshore profile 10 samples beach & nearshore 1 beach sample 2 nearshore samples	Hardy 1983 A.G.C. 1984 Hardy 1983 A.G.C. 1984 A.G.C. 1984
Tuktoyaktuk	Detailed survey 44 bore holes 2 beach profiles 2 nearshore profiles 2 nearshore sample	D.P.W. (Kolberg) 1976 D.P.W. (Kolberg) 1976 A.G.C. 1984 A.G.C. 1984 A.G.C. 1984

2.3.3 Previous Site Specific Studies of Coastal Processes

Detailed studies of coastal processes, including numerical estimates of alongshore sediment transport have been undertaken at four of the seven sites addressed in this study.

1) Atkinson Point:

A preliminary coastal engineering study was undertaken for Gulf Canada in connection with a possible supply base at McKinley Bay, Readshaw (1982). The study included a 10-year wave hindcast, forward-tracked wave refraction, and monthly alongshore sediment transport computations based on a modified CERC bulk model (Kamphuis and Readshaw, 1978). The average net alongshore transport was found to range from 29,000 to 38,000 m³/year, eastwards towards McKinley Bay. This study also suggests that the distal end of Atkinson Point had diminished in width from 1950 due to overwashing into the Bay.

2) Kay Point:

Coastal processes at Kay Point were examined by Forbes (1981) as part of a research project concerning the hydrology and sedimentology of the Babbage River Estuary. This investigation included day by day alongshore sediment transport estimates for two open water seasons, 1975 and 1976. Fetches were defined from

ice charts; winds were obtained from Kay Point (temporary anemometer). Forward tracked wave refraction was used, together with the conventional CERC bulk model. Rates obtained varied from 7000 to 21000 m³/year southwards towards the tip of the Kay Point spit.

3) Stokes Point:

Another coastal engineering study was carried out by Readshaw (1983) for Gulf Canada for another possible supply base marine facility at Stokes Point. The methodology was basically similar although in this case more detailed supporting work was performed to obtain the best wind data corrections and to calibrate the hindcast. The nearshore bathymetry appears to have created some problems and modified procedures using smoothed contours and applying plane beach refraction were apparently introduced to circumvent the problems. This was evidently a difficult site to deal with using conventional forward-tracked refraction because of the complex pattern of depth variation and the sheltering effects of Herschel Island and Kay Point. It is noted that Readshaw used monthly average ice edge data to define fetches at both Stokes Point and Atkinson Point, which would have affected the results.

The potential net annual alongshore sediment transport rates at Stokes Point were found by Readshaw to be suprisingly high, 140,000 m³/year to 560,000 m³/year for various points along

the shoreline and a second set of lower estimates in the range 30,000 m³/year to 120,000 m³/year were also provided by him. The latter set of estimates were obtained using a reduced coefficient in the CERC equation based on results published by Kamphuis and Readshaw (1978) for surf zones characterized by spilling breakers. However, in both cases the pattern of transport diverged from the point towards the east and west in a relatively symmetrical pattern. This pattern led to the suggestion that Stokes Point is a relict depositional structure now subject to relatively rapid erosion. However, this hypothesis is not in accord with geomorphological indications (McDonald and Lewis, 1973).

4) Tuktoyaktuk:

Tuktoyaktuk was studied by Kolberg and Shah (1976). This was an engineering study of shore erosion and protective measures. It included extensive profile measurements, geotechnical, sediment and permafrost studies as well as the estimation of alongshore sediment transport. It is the most detailed coastal investigation of Tuktoyaktuk that we are aware of. Coastal geomorphology and coastal recession rates, which were very high, were also examined. The net alongshore transport rate was estimated at about 31,000 m³/year, moving in a southerly direction. Their estimation method is not described in detail but it is known that they used forward-tracked refraction

diagrams and a CERC-type bulk model. Unfortunately frost table monitoring data is incomplete.

2.3.4 Site Descriptions

The following subsections provide brief descriptions of morphological characteristics of the coastal environments of each of the sites. These are based on several sources, including regional sediment studies such as Harper and Penland, 1982 and Fissel and Birch 1984, as well as more detailed studies like McDonald and Lewis, 1973, and the most recent studies: Forbes and Frobel, and Harper et al., both of 1985.

1) Atkinson Point

At Atkinson Point a 3 km long, low, wide, medium-fine sand spit extends towards the north-east across the western half of the mouth of McKinley Bay from an anchor point comprising a reach of receding low, sand rich cliffs. The distal end of the spit terminates in a wide, low sand bank which extends a further 3 km across the mouth of the Bay. See Figure 2.1.

Atkinson Point Beach differs from the other six sites of this study; it is all sand, whereas at each of the other sites there is either a significant proportion of gravel or coarser material or very fine material.

According to Forbes and Frobel, (1985) Atkinson Point has been stable for the last decade even though previous evidence including Readshaw, 1983, suggests a significant rate of transgression.

2) Kay Point

Kay Point is a narrow transgressive, gravel barrier which extends over 4 km southwards from the rapidly retreating cliffed headland to which it is anchored at its northern end. See Figure 2.2. The spit features a narrow relatively steep coarse grained beach face.

McDonald and Lewis 1973 mapped shore line changes from 1944 to 1970 using air photos. This suggested cliff recession rates of the order of two metres per year. The spit itself retreated one hundred metres and was breached, while the tip prograded by more than 600 m. Sand banks extend 1.5 to 2 km beyond the tip of the spit.

3) King Point

The King Point site includes a 50 m high ice-rich eroding cliff to the west of a lagoon with a barrier beach 2 km long. See Figure 2.3. Similar cliffs about 20 m high occur east of the lagoon. The lagoon was evidently formed by transgressive

breaching of a lake. Its depth was about 3 metres in the nineteen fifties. According to airphotos the barrier was complete in 1970, but 16 years earlier it appeared as a spit which extended from the west, about three quarters of the distance across the mouth of the lagoon from King Point. The net eastward transport required to produce this change was estimated 20,000 m³/annum (Gillie, private communication). The barrier beach consists of sand and gravel, its crest about 2.5 metres above sea level. Recession rates for the bluffs for 10 to 20 km west from King Point have been estimated at about one metre per year (McDonald and Lewis 1973). The western end of the barrier must have transgressed at a similar rate. The cliffs to the east, within about half a kilometre of the lagoon, were subject to higher recession rates, about 3 m/a and beyond that, further to the east, the rates were 1.5 - 2.5 m/a (McDonald and Lewis, 1973). Textural composition of the cliffs suggested that 5 - 10% of the material is coarse enough to remain in the littoral zone.

4) North Head

Very little direct evidence was available for this site other than some recent nearshore bore holes. (K. Moran, private communication). North Head is a low cliff, largely composed of ice-rich fine grained sediment, bordering very shallow water. See Figure 2.4. Indications are that beach slopes are gentle

although no profile data is available. There is some doubt that conventional sand-beach process models can be applied at this site. The extremity of North Head is known to be receding. From the geography of the area it is apparent that alongshore sediment transport must be southwards into a more sheltered area where accumulation must take place.

5) Pauline Cove

This site is located on the exposed south-facing headland outside the cove by which it is named. See Figure 2.5. There is no detailed documentary evidence, but it appears that there is a comparatively narrow coarse-grained beach at the foot of the cliff. (Forbes, private communication). Nearshore bathymetry was inferred from CHS field sheets. There was insufficient data to apply the sediment transport models at the Pauline Cove Site.

6) Stokes Point

Stokes Point is a beach ridge foreland complex about 5 km long and up to 700 m wide formed from sand and gravel. See Figure 2.6. The overall configuration, and in particular the ridge and swale formation of the eastern 2 km, indicate formation due to alongshore transport from the north west, with

progradation to the south east, [McDonald and Lewis (1973); Forbes, private communication]. Harper et al., 1985, report small rates of coastal change suggesting the morphology of Stokes Point is relatively stable. In contrast, Readshaw (1983) suggested that the entire foreland is undergoing rapid erosion, although, on the whole, that appears incorrect.

7) Tuktoyaktuk

The site at Tuktoyaktuk comprises the shore of a barrier which separates part of Tuktoyaktuk Harbour from Kugmallit Bay. The barrier is described as sandy gravel. (Forbes and Frobels, 1985). See Figure 2.7. A sparse, coarse-grained beach fronts low tundra cliffs, but there is a substantial deposit of sand close to the shoreline. High rates of recession have been reported. Kolberg and Shah, 1976; Forbes and Frobels, 1985; Harper et al., 1985. Because the area is well sheltered (and the recession rates are relatively high), it appears that thermal erosion may be important at this site.

SECTION 3 WAVE HINDCASTS AND COMPARISON WITH MEASUREMENTS

3.1 Summary of Wave Hindcasting Work

Month-long calibration wave hindcasts were performed at two Beaufort Sea wave recording stations for periods when wave measurements were available for comparison. Four parametric hindcast models were applied with various procedural options to determine the best fit with measurements by comparison of time series plots. Fourteen-year (1970-1983) hindcasts were then performed for the seven field sites using the preferred combination of options. The month-long calibration comparisons are shown in Appendix A as time series plots and the fourteen-year hindcast results are presented in the form of standard wave statistics plots and tables, in the appropriate sections of Part II of this report.

3.2 Parametric Hindcasting by the Effective Wave Procedure

The philosophy underlying the hindcasting procedure is that parametric models are approximations to two-dimensional spectral models. Hence, to optimize parametric model performance it is at first necessary to approach the two-dimensionality of the spectral models by eliminating the subdivision of the wave generation

process into predetermined sectors of fetch. When wind direction varies gradually but continuously, it is impossible to divide time into clearly defined sequences of wave generation and wave decay. Thus, generating and decaying wave trains are present, varying in height and period at all times and both must be considered.

The hindcasting procedure used is referred to as the Parametric Hindcasting of Effective Waves (PHEW). It will work with any parametric model which takes wind speed, wind duration, and fetch length as inputs. (Fleming, Philpott, and Pinchin, 1984).

The PHEW procedure permits fetches of arbitrary angular width and requires no fetch defining pre-processing of wind data. In effect, the hindcast proceeds hour by hour irrespective of fetch, with wave generation and decay sequences being defined by the occurrence of rapid changes in wind speed and direction, not by the crossing of fetch boundaries. Accurate definition of wave direction, the smoothing of directions, and the transitions from fetch to fetch are implicitly built into this procedure.

The result of each time-step of the hindcast calculation is an "effective" significant wave height, a peak period, and a direction defined to the nearest degree. The effective wave incorporates two components: a generated wave and a decayed wave. The resulting statistics can be accumulated by any chosen ranges of direction independent of the fetch sectors used in the calculations.

3.2.1 Input Data for the Parametric Models

The parametric hindcast models require wind speed, wind duration, and fetch length as input data. Wind data is input to the PHEW procedure as an equal increment time series of wind speed and direction. The PHEW procedure computes the wind speed and duration to be used in the parametric models by averaging the input wind speeds over an appropriate length of time. This method is described in Section 3.2.3.

Fetch length is defined as a function of azimuth from the hindcast site. The PHEW capabilities include the option of using either "straight fetches" or "effective fetches". Straight fetches are measured directly from ice charts or hydrographic charts and are subjectively chosen to represent an average fetch for the sector under consideration. Effective fetches are computed from the measured straight fetches by adapting the method presented in the Shore Protection Manual (CERC, 1977). With this method the fetch length of a sector is determined by summing and averaging the cosine components of fetch length from other sectors whose central radials are within 45 degrees (on either side) of the central radial of the fetch under consideration.

3.2.2 The Effective Wave

The effective wave condition predicted at any given time step is assumed to be composed of two components: a generated wave and a decayed wave. The generated wave will have been generated by the current wind field and the decayed wave by an earlier wind field.

Both components are defined by three parameters:

- a characteristic wave height;
- a characteristic wave period;
- the deep water back-azimuth direction.

The component wave with the greater height is referred to as the dominant wave. The effective wave is then defined as follows:

height = r.m.s. sum of generated and decayed wave heights
period = period of the dominant wave
direction = direction of the dominant wave.

Any waves less than 0.1 m in height are neglected as and when they arise in the computation. This means that effective waves up to 0.14 m in height may be neglected. The wave decay process is only applied to dominant waves.

3.2.3 The Generated Wave and Wave Generation Sequences

The characteristic parameters of the component generated wave, at any given time-step, are determined from the selected parametric hindcast model by the application of a wind speed and duration computed from the input wind data for the time-steps immediately preceding and including the given time-step. The PHEW procedure hindcasts the wave height produced by the average wind speed over a number of time-steps, that is the wind duration, for a series of wind durations ending at the given time-step and starting at progressively earlier time-steps. This is referred to as back-stepping.

At the end of a back-stepping sequence the largest wave height that was hindcast during the back-stepping is considered to be the generated wave height for the time-step under consideration. The wind speed that generated the wave was the average of the input data wind speeds over the duration of the generating process. The direction of the wave is taken as the mean of the wind directions over the generating sequence.

The hindcast wave computed at each back-step may have been either fetch limited or duration limited. The wind duration was equal to the time interval between time-steps multiplied by the number of back-steps being considered. The maximum fetch length was the fetch length in the direction of wave generation, that is the

mean of the wind directions. Each of the parametric hindcast models has its own criteria for determining whether a wave is fetch or duration limited.

The back-stepping process is terminated by one of two possible occurrences: a rapid change in wind direction, or having considered a fixed maximum duration. The latter proves necessary to guard against cases where the wind has been slowly varying over arbitrarily long durations. A rapid change in wind direction is considered to have occurred when the wind direction at the next back-step differs from the average wind direction (i.e. wave direction) of the immediately preceding sequence of back-steps by an amount exceeding a pre-set wave divergence angle. The wave divergence angle and the maximum allowable number of back-steps are options available to be set as desired in the PHEW procedure.

3.2.4 The Decayed Wave and Decay Sequences

A wave decay sequence is initiated under the PHEW procedure by one of two possible events.

1. When a calm is encountered after having completed all operations at a given time-step, (i.e., when the effective wave condition has been defined) and the next step forward is begun.

2. When, during back-stepping, a rapid change of wind direction is encountered, defined by exceeding the pre-set wave divergence angle.

In each case, the wave to be decayed is the dominant wave component immediately preceding the event. The period and direction of the decayed wave remain the same, while the decayed height H_d decreases with time t from its initial value H_D as follows:

$$H_d(t) = H_D(1 - t.C_g/F)^x \text{ for } H_d \geq 0.1 \text{ m} \quad (3.1)$$

If $H_d < 0.1 \text{ m}$, then it is assumed to be zero.

Where: H_D = dominant wave height preceding decay

H_d = decayed wave height

t = time from start of decay

C_g = group velocity associated with the
dominant wave period T_D

F = fetch length

x = wave decay exponent.

The wave decay exponent may have any positive value. Tests were made with $x = 1$, linear decay; $x = 2$, quadratic decay; and $x = \infty$, instantaneous decay ($H_d = 0$). Linear decay produced marginally better results and was therefore adopted.

In practice, the wave decay process will invariably be completed in substantially less than the maximum wave generation duration.

3.2.5 Parametric Models Applied

Four parametric wave hindcasting models have been investigated:

1. Darbyshire and Draper (Coastal Waters Version);
2. JONSWAP (parameterized version);
3. S.M.B. deep water (revised version by Bretschneider);
4. S.M.B. shallow water (revised version by Bretschneider).

The first method, based on Darbyshire and Draper (1963), has been formulated in parametric form (Carter, 1980). This is a purely empirical method based largely on data from the Irish Sea. The second method, JONSWAP (Hasselmann, 1974) is based on a semi-theoretical approach of wave spectrum development as a function of wind speed. The version used here for wave hindcasting has been parameterized to incorporate the usual hindcasting parameters of fetch and wind duration as well as wind speed (H.R.S., 1982). The third and fourth methods are based on the Sverdrup-Munk-Bretschneider (S.M.B.) deep water and shallow hindcasting equations as revised by

Bretschneider (1973). The shallow water version, which was used for fetches less than 20 m deep, provides for wave energy losses due to bottom effects. Details of the equations used in each of these models may be found in Fleming, Philpott, and Pinchin, (1984).

3.3 Modification to Hindcasting Procedure for Use in the Beaufort Sea

A number of modifications had to be made to the PHEW procedure to make it suitable for use in the Beaufort Sea. These changes were required because of the moving sea ice and large shallow areas near the hindcast site.

3.3.1 Time-Varying Fetches

In most cases fetches in the Beaufort Sea are limited by the extent of the sea ice. A routine was incorporated in the PHEW procedure for automatic variation of fetch lengths depending on the location of the sea ice. Fetch lengths can be input for any dates during a hindcast run, and fetch lengths are then linearly interpolated for each day. The PHEW procedure does not restrict the dates at which fetch lengths may be input.

3.3.2 Deep and Shallow Fetch Sectors

Because of the relatively large areas of shallow water in the Beaufort Sea, a capability for shallow water wave generation was introduced to the PHEW procedure. Any fetch sector can be designated as always being a "shallow water" fetch, as always being a "deep water" fetch, or as being either a shallow water or deep water fetch at any time, depending on the fetch length at that time. If the last option is chosen then the fetch length at which the fetch changed from shallow water to deep water has to be input. It was necessary to include this option because a fetch which may have predominantly deep water when the ice edge is far off the hindcast site could be predominantly shallow when the ice edge is close to the hindcast site.

If a fetch is designated as deep water then the parametric model that has been chosen for that hindcast run is used to predict the wave height and period. If, however, a fetch is designated as shallow water then the S.M.B. shallow water parametric hindcast model is used, irrespective of which parametric model has been selected for the hindcast run. (Although it was developed and used in this study, the need for this option is under review in the light of ongoing work on shallow water equilibrium forms).

3.3.3 Frictional Hindcast Model

The inclusion of shallow water fetches, as described in Section 3.3.2, was to cover the instances when a fetch sector could

be considered to have mostly deep or mostly shallow water. At Tuktoyaktuk, however, when the ice edge is well offshore there are, to the north, fetches which are deep offshore but shallow for a significant portion nearshore. The shallow portion of these fetches are long enough that the wave energy losses due to bottom action will have a significant effect.

The shallow water S.M.B. parametric hindcast model could not be used to hindcast waves for these fetches. Even though the model implicitly considers the effects of bottom action, it assumes that the bottom effects are present during the entire wave generation process. At Tuktoyaktuk, however, deep water waves are generated without the effects of bottom action, and are then subjected to this action as they propagate through Kugmallit Bay. This results in the wave heights being significantly reduced but the wave periods remaining essentially unchanged.

This problem was handled by providing a "frictional hindcast" option in the PHEW procedure. When this option is selected the PHEW procedure hindcasts the wave heights with the S.M.B. shallow water parametric model and the wave periods with the S.M.B. deep water parametric model.

3.4 Input Data for the PHEW Procedure

3.4.1 Wind Data

Wind data is not normally pre-processed with the PHEW procedure. However, a considerable amount of effort was required to repair and fill in missing data. Three sets of wind measurements from two Atmospheric Environment Service recording stations, Tuktoyaktuk and Tuktoyaktuk A, had to be selectively merged to obtain a sufficiently complete data set. The desired result was a record with directions to 10 degrees as well as average hourly wind speeds. However, in several areas of the record, instantaneous velocities had to be used and interpolation was sometimes required to fill data gaps up to a maximum of twelve hours.

The time increment for the hindcast was made equal to the wind sampling interval of one hour. Wind speeds less than a specified threshold were treated as calms that could trigger wave decay. The threshold wind speed used in this work was 1.0 m/s. Hindcasts were not performed when wind speeds, averaged over time, fell below the same threshold.

The overland wind speeds measured at Tuktoyaktuk were adjusted to account for differences in friction between the land and sea. Baird and Hall (1980) present an extensive review of wind ratio modifications used in previous hindcasts. They developed a wind speed transfer function as a function of overland speed by comparing

frequency of occurrence histograms between overland measurements at Tuktoyaktuk and overwater measurements at offshore islands Ukalerk and Kopanoar. The ratios derived by Baird and Hall were used in this study and are shown in Figure 3.1.

A more restricted study on winds in the area, which was only made available to the consultant at a late stage in this work, suggests that onshore overwater winds above 20 km/hour should be higher than proposed by Baird and Hall (Danard and Gray, 1984). In this study wind data measured at Tuktoyaktuk Airport was compared with wind measurements taken at offshore drilling rigs. See Table 3.1

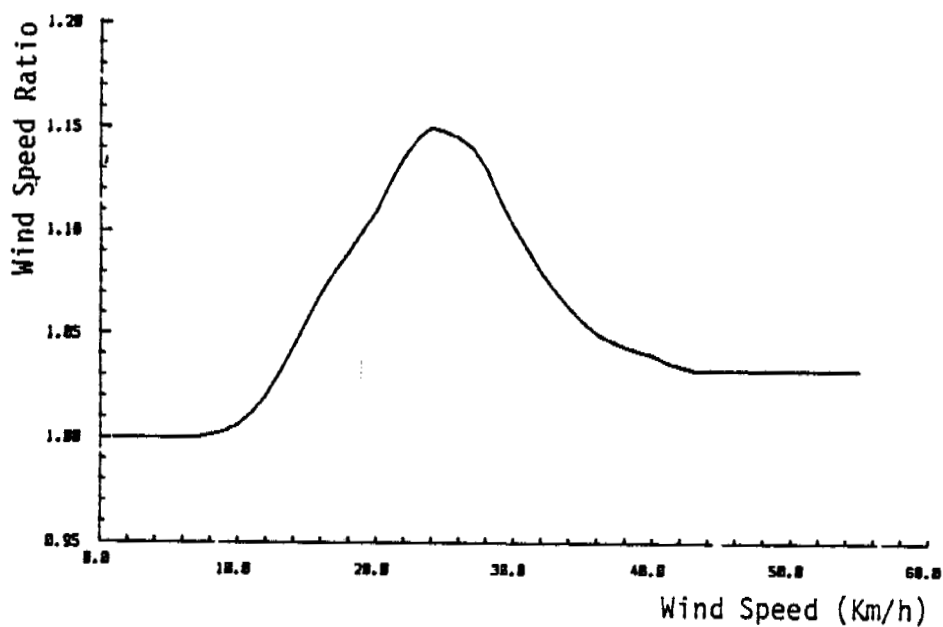
3.4.2 Fetch Definitions

The fetch lengths were taken from hydrographic charts for land restricted fetches and from ice charts for fetches which were restricted by ice. The ice charts show areas covered by ice with different regions categorized by the fraction of the water surface covered with ice floes. Ice charts are available on a weekly basis as described in Section 2.1.5. Ice limited fetch lengths were defined on a daily basis by interpolating between the weekly chart data.

Table 3.1 From Danard and Gray, 1984

Comparison of offshore and Tuktoyaktuk winds in the summer of 1982

Station	Lat.	Long.	Speed ratio	Angle diff. ()	Number of wind pairs
Tarsuit Island	69.8	136.2	1.28	0.1	367
McKinley Bay	69.9	131.2	1.01	0.9	117
Irkuluk B-35			1.16	-0.6	241
Nerlerk M-98	70.5	133.5	1.12	0.4	136
Orvilruk 0-3	70.3	136.5	1.18	-0.4	201
Kenalook J-94	70.7	134.0	1.19	-0.3	335
Kiggavik H-32			1.18	-0.5	244
Aiverk I-45			1.05	0.2	96
All stations			1.18	-0.1	1737



Overwater to Overland Wind Speed Ratio

FIGURE 3.1

The limit of the ice coverage was taken as the boundary of the 3/10 ice concentration region, that is to say concentrations up to 2/10 are included as part of the wave generating fetch. Fetch lengths less than 2 km were not considered.

3.5 Calibration of the PHEW Procedure

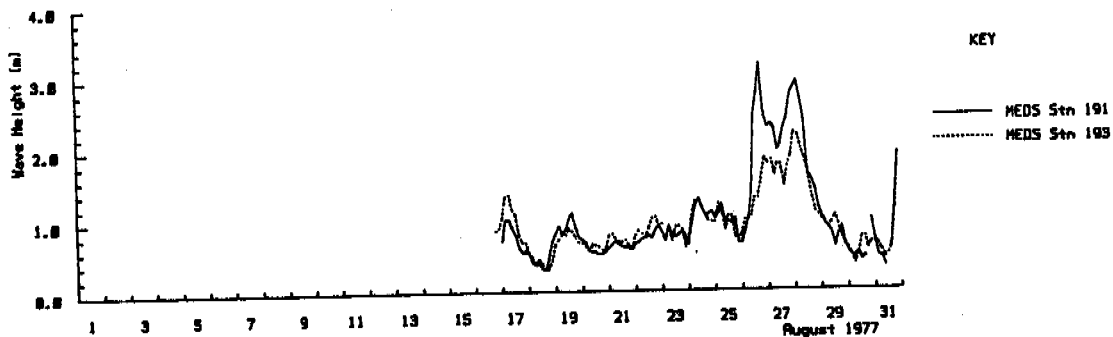
The basic method of calibrating the PHEW procedure is to perform hindcasts with a number of procedural options and to compare the results with measured wave data. The combination of options that gives the best results is then used for hindcasting. Although wave measurement gauges have been deployed at a number of sites in the Beaufort Sea all data sets are of a short record and most of these are incomplete. Problems in recording wave data are often encountered in the Beaufort Sea so it was decided that the measured wave data used for the calibration comparisons should be verified if at all possible.

Two main hindcast calibration stations were chosen, MEDS Station 191 and MEDS Station 50. These were verified by MEDS Stations 193 and 25 respectively. Table 3.2 gives a brief description of the stations, and Figures 3.2, 3.3, and 3.4 show the data comparison plots. The study area map, Figure 1.1, shows the locations.

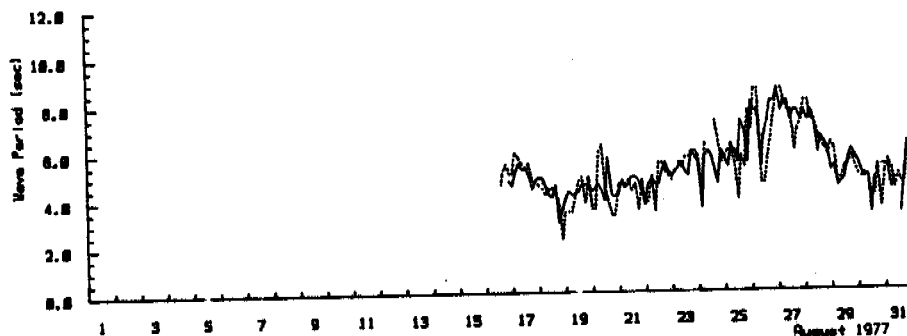
Table 3.2 MEDS Wave Recording Stations

MEDS Station	Latitude N	Longitude W	Depth(m)	Coverage
191	70°-08'-24"	136°-24'-48"	42.7	Aug. 16-Oct.11,'77
193	70°-23'-54"	135°-06'-00"	64.0	Aug. 7-Oct. 1,'77
50	69°-57'-05"	133°-50'-05"	15.0	Aug. 8-Oct. 8,'76
25	69°-58'-05"	134°-59'-00"	15.0	Aug. 8-Oct. 9,'76

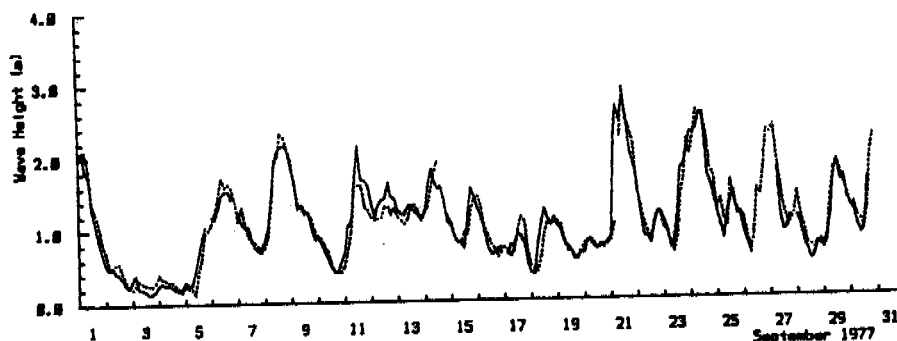
Examination of Figure 3.2 shows very good agreement between Stations 191 and 193 with the exception of the August 26 and 27 storm. It was concluded that Station 191 could be used for hindcast calibration. The agreement between Stations 25 and 50 is not as good, as can be seen from Figures 3.3 and 3.4. There appears to be a possible 48-hour time difference in the September 7-9 peaks of these two data sets. The two data sets are quite close during August, with the exception of the 14th, but not as good for September and October.



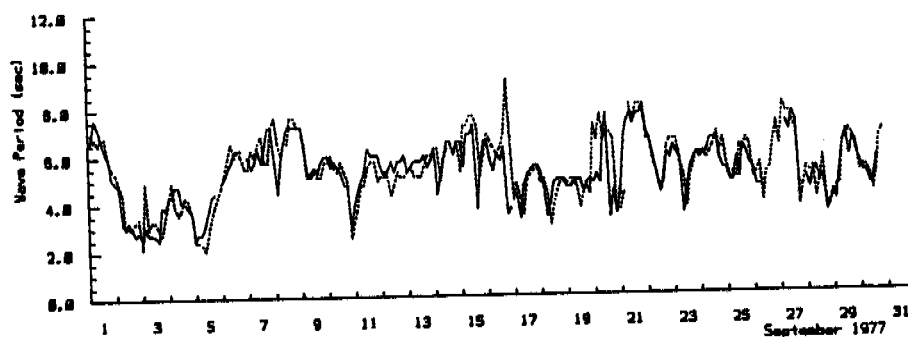
Significant Wave Height



Peak Wave Period



Significant Wave Height



Peak Wave Period

BEAUFORT SEA COASTAL SEDIMENT STUDY

Comparison of Measured Wave Data
August 1977 and September 1977

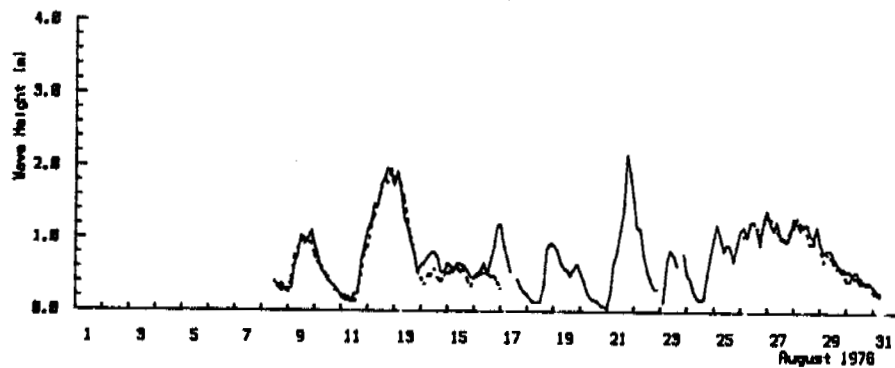
Date: 16 May 85

Scales as shown

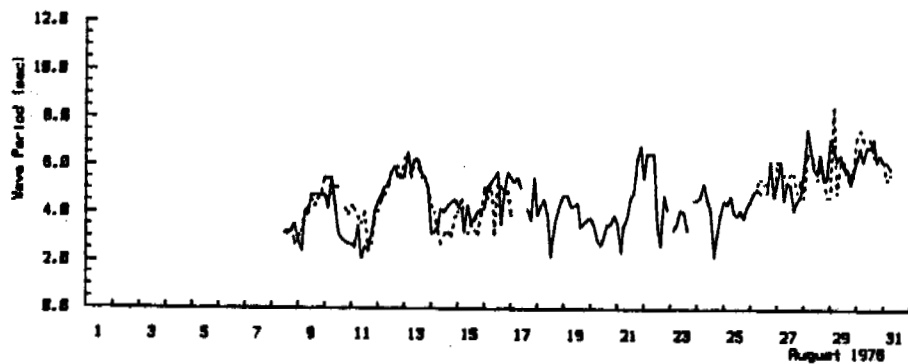
Checked by:

Keith Philpott
Consulting Limited

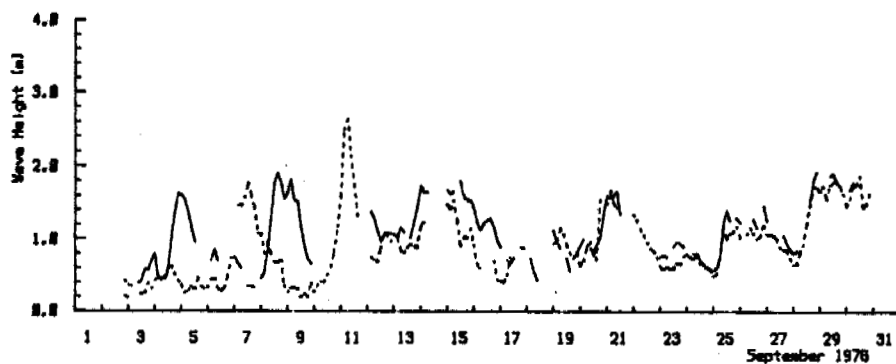
FIGURE 3.3



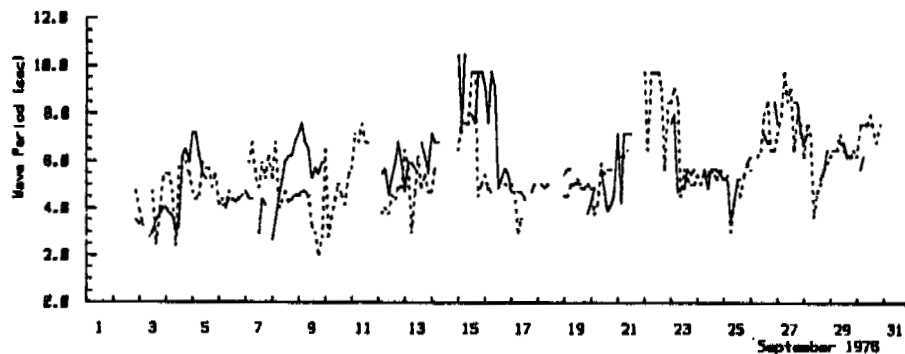
Significant Wave Height



Peak Wave Period



Significant Wave Height



Peak Wave Period

BEAUFORT SEA COASTAL SEDIMENT STUDY

Comparison of Measured Wave Data
August 1976 and September 1976

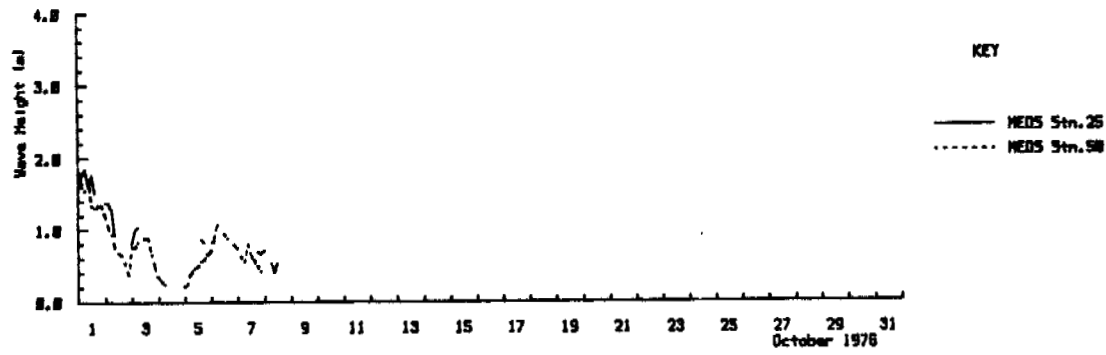
Date: 16 May 85

Scales as shown

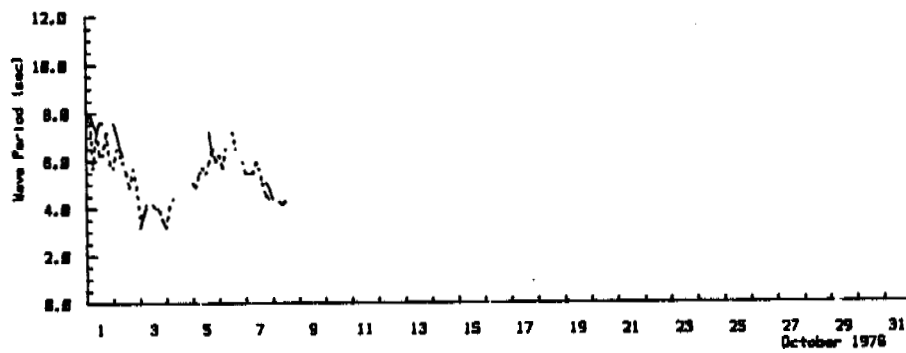
Checked by:

Keith Philpott
Consulting Limited

FIGURE 3.4



Significant Wave Height



Peak Wave Period

BEAUFORT SEA COASTAL SEDIMENT STUDY

Comparison of Measured Wave Data
 October 1976

Date: 16 May 85

Scales as shown

Checked by:

Keith Philpott
 Consulting Limited

It was concluded that Stations 25 and 50 could be used for hindcast calibration, but could not be considered to be as reliable as the data from Station 191. It was decided that the hindcast calibration would be first performed for Station 191. The resulting best estimates of procedural options would then be verified against Station 50 with the exception of August 17 to August 26, 1977. Station 25 would be used for this period.

A total of thirty-six month-long trial hindcasts were made for the months covered by the recorded data. The results are shown in Appendix A pages A1 to A24 and A28 to A39. The various combinations of models and input parameters are listed in Tables 3.3 and 3.4.

Table 3.3
MEDS Station 191

List of Month-Long Calibration Tests Comparing
Hindcast with Measured Wave Heights and Periods

Run	(2)	(3)	(4)	(5)	(6)	Appendix
1	SMB	(45)	straight	linear	4 days	A1 - A3
2	JONSWAP	(45)	straight	linear	4 days	A4 - A6
3	Draper	(45)	straight	linear	4 days	A7 - A9
4	SMB	(45)	straight	linear	2 days	A10 - A12
5	SMB	(45)	effective	linear	4 days	A13 - A15
6	SMB	(60)	straight	linear	4 days	A16 - A18
7	SMB	(60)	straight	total	4 days	A19 - A21
8	SMB	(60)	straight	quadratic	4 days	A22 - A24

- Notes: (1) a run was performed for each month Aug. - Oct.
- (2) Parametric Hindcast Models
 SMB = SMB (deep water version), Bretschneider (1973)
 Draper = Darbyshire and Draper (1963) parameterized
 by Carter
 JONSWAP = Hasselman (1974) parameterized by HRS (1982)
- (3) Wind Direction Divergence Angle 45, 60 degrees
- (4) straight = straight fetch as described in 3.2.1
 effective = effective fetch as described in 3.2.1
- (5) linear = linear decay as described in 3.2.4
 total = total decay as described in 3.2.4
 quadratic = quadratic decay as described in 3.2.4
- (6) Maximum Wave Generation Duration 2 or 4 days.

Table 3.4
MEDS Stations 25 and 50

List of Month-Long Calibration Tests Comparing
Hindcast with Measured Wave Heights and Periods

Run	(2)	(3)	(4)	(5)	(6)	Appendix
1	SMB	(45)	straight	linear	4 days	A28 - A30
3	Draper	(45)	straight	linear	4 days	A31 - A33
5	SMB	(45)	effective	linear	4 days	A34 - A36
6	SMB	(60)	straight	linear	4 days	A37 - A39

- Notes: (1) a run was performed for each month Aug. - Oct.
- (2) Parametric Hindcast Models
 SMB = SMB (deep water version), Bretschneider (1973)
 Draper = Darbyshire and Draper (1963) parameterized
 by Carter
 JONSWAP = Hasselman (1974) parameterized by HRS (1982)
- (3) Wind Direction Divergence Angle 45, 60 degrees
- (4) straight = straight fetch as described in 3.2.1
 effective = effective fetch as described in 3.2.1
- (5) linear = linear decay as described in 3.2.4
 total = total decay as described in 3.2.4
 quadratic = quadratic decay as described in 3.2.4
- (6) Maximum Wave Generation Duration 2 or 4 days.

The determination of the best combination of parametric model and other optional parameters, such as the wind divergence angles, is ultimately a matter of judgement. Although some aspects are easily recognized as being different, it is not always obvious that one trial hindcast is definitely better or worse than another.

It seems that the S.M.B. deep water model gives the best results overall (and Run 6 was judged the best hindcast), although the results from the Draper model are very close and even better in some instances especially when wave period is considered. The JONSWAP model had a tendency to considerably over-predict wave heights. In common with other hindcasting models, the estimates of wave height are significantly better than those of wave period. Longer swell-type waves are not described well.

In general, there was a tendency for the calibration and verification hindcasts to under-predict measured occurrences of large waves. One particular instance of this was on September 11th, 1976 at MEDS Station 50 when the measured wave height was 2.6 m (See Appendix A29). The wind speeds measured at Tuktoyaktuk for the same date are considerably less than would be required to produce such a wave. A detailed check showed that 2.6 m waves could not be hindcast even with an exaggerated land-sea wind speed ratio. It was also found that during periods of rapidly changing winds at Tuktoyaktuk, the calibration was poor. (This can be observed by comparing the measured wind profiles for Aug.-Oct. 1976 at

Tuktoyaktuk - Appendix A25-A27, to the calibration hindcasts for Station 191 - Appendix A16-A18; and measured wind profiles for Aug.-Oct. 1977 at Tuktoyaktuk - Appendix A40-A42, to the verification hindcasts for Stations 25 and 50 - Appendix A37-A39). Most of these problems are directly attributable to the remoteness of the wind measuring station from the wave measurement stations. In some cases rapid changes in the position of the ice edge would have contributed.

3.6 Fourteen-Year Hindcasts

Basis of Hindcasts

From available wind data and on the basis of calibration and verification test runs, the following conditions were established for the fourteen-year deep water wave hindcasts off the seven field investigation sites (Pauline Cove, Stokes Point, Kay Point, King Point, North Head, Tuktoyaktuk, and Atkinson Point).

-Hindcast model	SMB deep and shallow water versions
-Location of wind record	Tuktoyaktuk
-Years of wind record	1970-1983 incl.
-Maximum open water season	1 June - 1 November
-Wind direction increments	10 degrees
-Hindcast time-step	1 hour
-Minimum wind speed for hindcast	1.0 m/s
-Fetch sector maximum width at ice boundaries	20 degrees
-Maximum wave divergence angle	60 degrees
-Maximum duration of wind in one wave generation sequence	4 days
-Wave decay exponent	unity (linear decay)
-Wave decay time	duration of wave travel over fetch
-Fetch type	straight
-Model precision	
wave height	0.1 m
wave period	0.1 m
wave direction	1 degree

3.6.1 Common Fetches

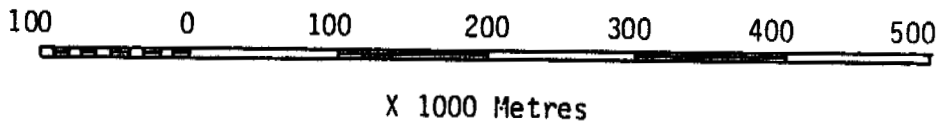
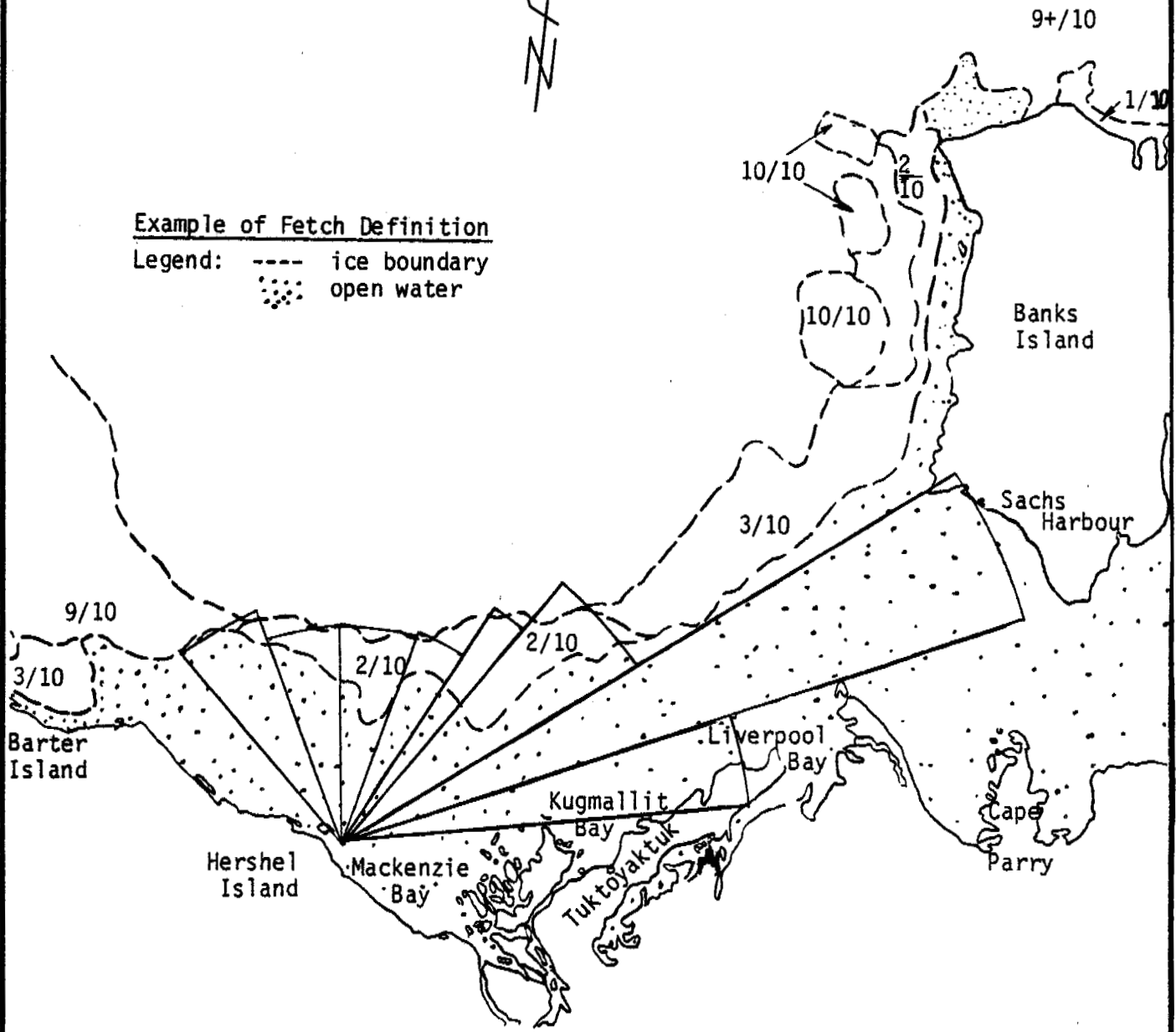
It had been originally anticipated that the seven study sites could be described by three sets of deep water fetch sectors. There was to be one set for the four westerly sites: Pauline Cove, Stokes Point, Kay Point, and King Point (see Figure 3.5), one set for North Head and Tuktoyaktuk (Figure 3.6), and one set for Atkinson Point (Figure 3.7). It was felt that the distances from the common fetch points to the study sites would be small compared with the distances from the fetch points to the edge of the ice, and since hindcasting is insensitive to fetch lengths that this approximation would be acceptable. Each of the seven study sites was to have its own local hindcast fetches which would usually be restricted by land rather than ice.

FIGURE
3.5



Example of Fetch Definition

Legend: --- ice boundary
 ···· open water



BEAUFORT SEA COASTAL SEDIMENT STUDY

Date: 20 Dec 84

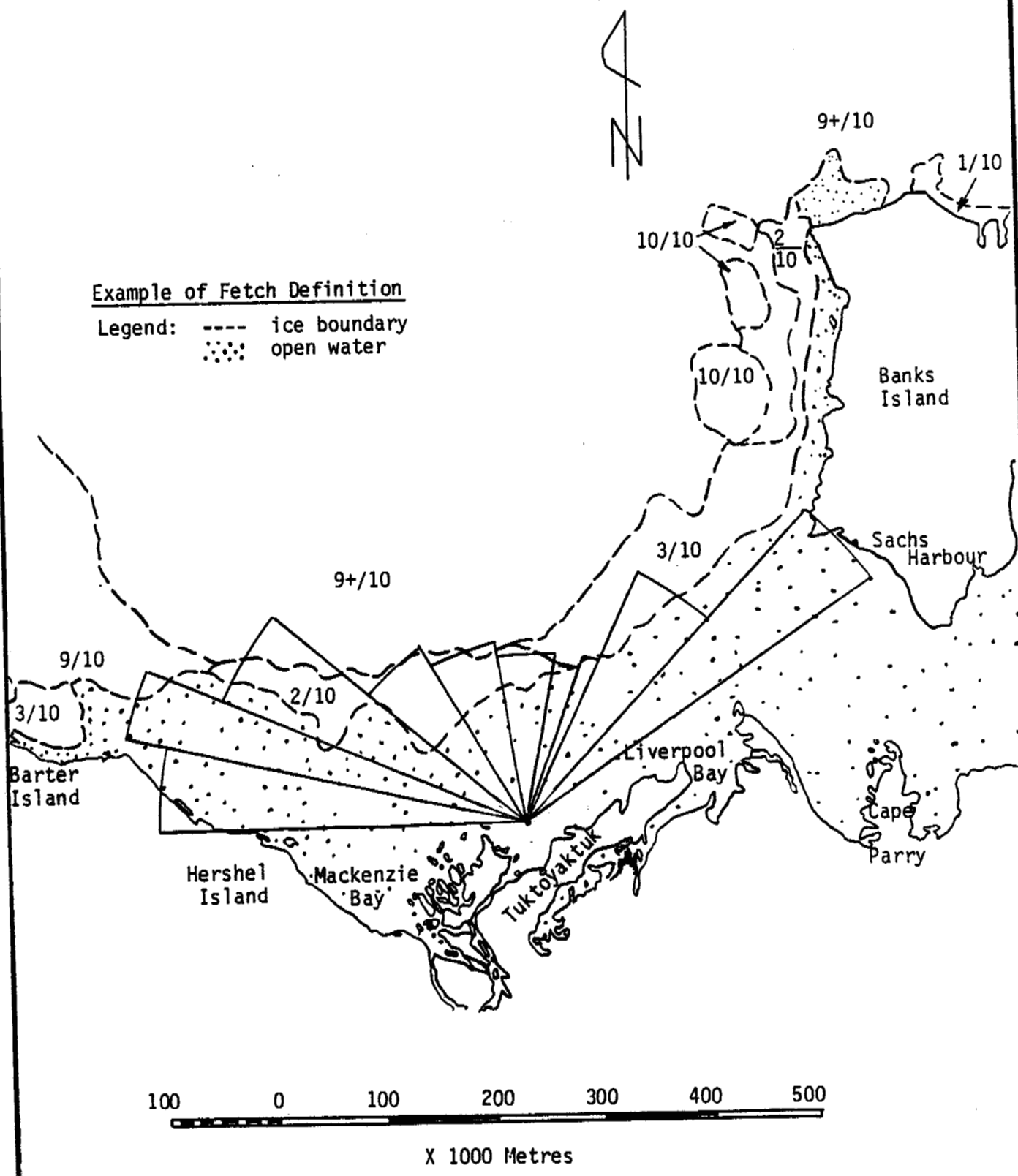
Scales as shown

Checked by:

Keith Philpott
 Consulting Limited

Deep Water Fetch Site For Pauline Cove, Stokes Point,
 Kay Point And King Point

FIGURE
3.6



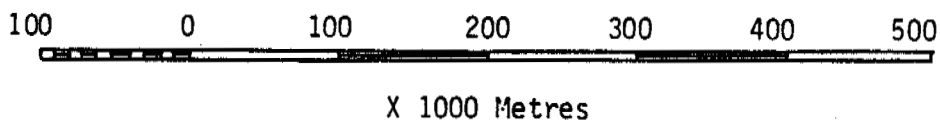
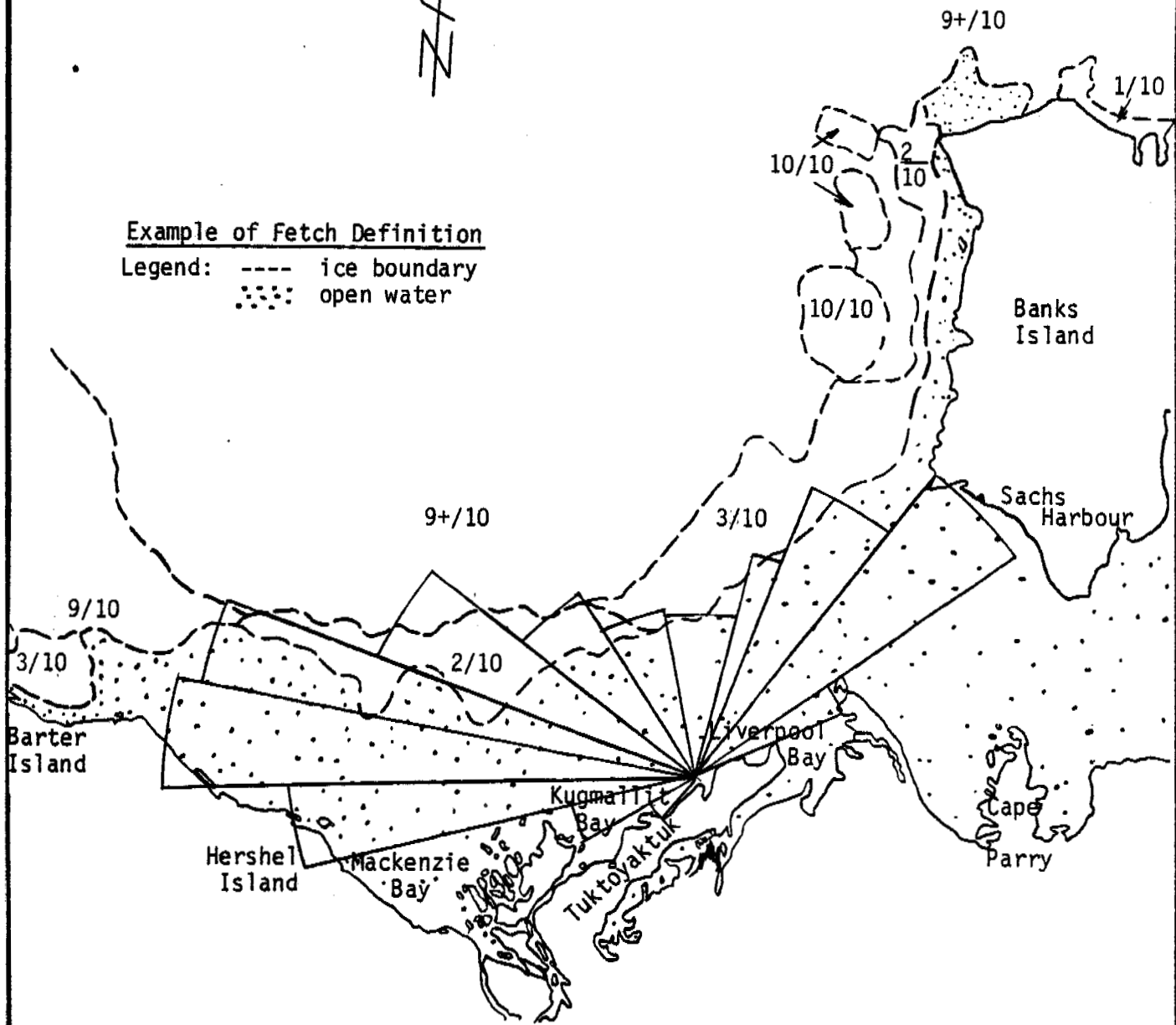
BEAUFORT SEA COASTAL SEDIMENT STUDY	Date: 28 Dec 84
	Scales as shown
Deep Water Fetch Site For North Head and Tukttoyaktuk	Checked by:
	Keith Philpott Consulting Limited

FIGURE
3.7



Example of Fetch Definition

Legend: ---- ice boundary
 open water



BEAUFORT SEA COASTAL SEDIMENT STUDY

Deep Water Fetch Site For Atkinson Point

Date: 28 Dec 84

Scales as shown

Checked by:

Keith Philpott
 Consulting Limited

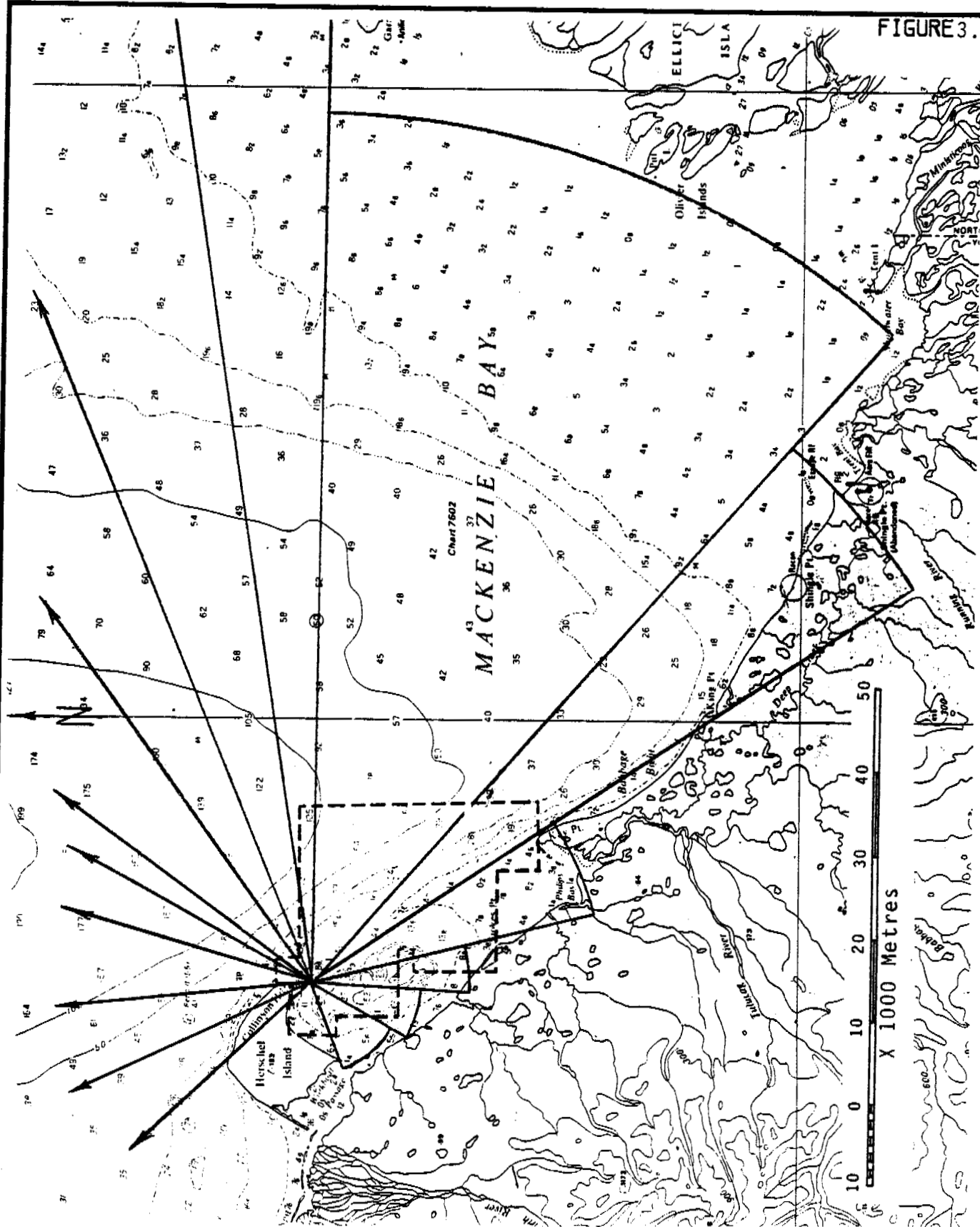
It was found, however, that the 3/10 ice edge was quite close to the study sites for significant durations and this caused the error in using common fetches to become significant. As a result, deep water fetch lengths were measured for all sites until the ice was approximately 150 km offshore. After this the common deep water fetches were again used. Figures 3.8 to 3.11 show the local fetch sectors as well as the outline of the refraction grids for the four western study sites. The fetches for Atkinson Point, as shown in Figure 3.7, remained unchanged. The fetch sectors which are shown with arrows are the deep water sectors that use a common hindcasting point when the ice is well offshore.

As fetches are defined by angular limits the gaps shown between some of the fetch sectors do not indicate areas where fetches have not been defined. These apparent gaps are a result of the need to measure fetch lengths to the proximity of the refraction grid boundaries rather than to a specific common point within the grids. The results of the hindcasts are presented in Part II as standard wave statistics plots and tables as described in section 3.6.4.

3.6.2 Hindcasting at North Head

The spectral transformation wave refraction analysis results for North Head (as described in section 4 and presented in Part II) showed that it was possible for deep water waves with a

FIGURE 3.8



BEAUFORT SEA COASTAL SEDIMENT STUDY

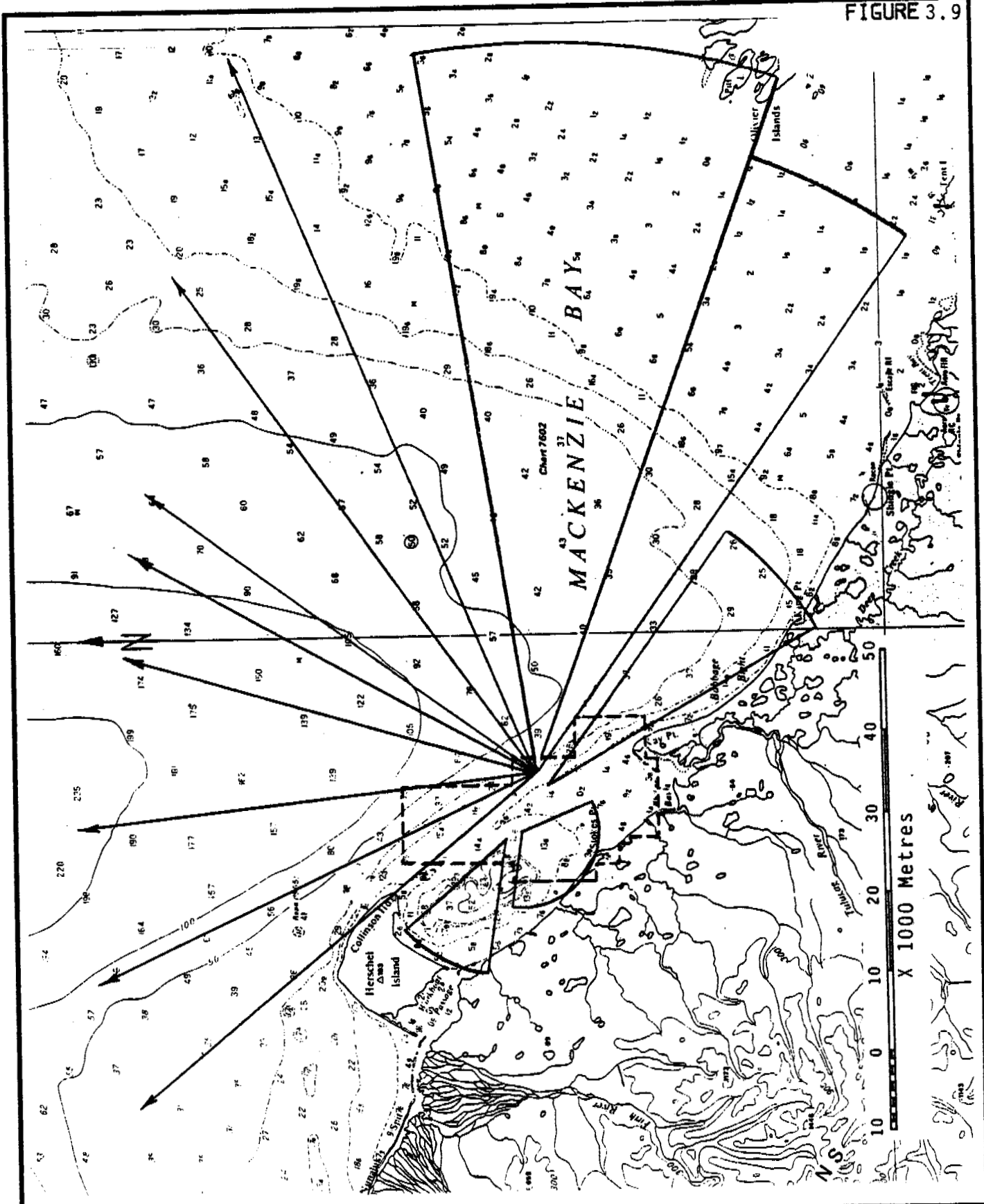
Pauline Cove: Local Hindcast Fetch Sectors

Date: 21 Mar 85

Checked by:

Keith Philpott

Consulting Limited

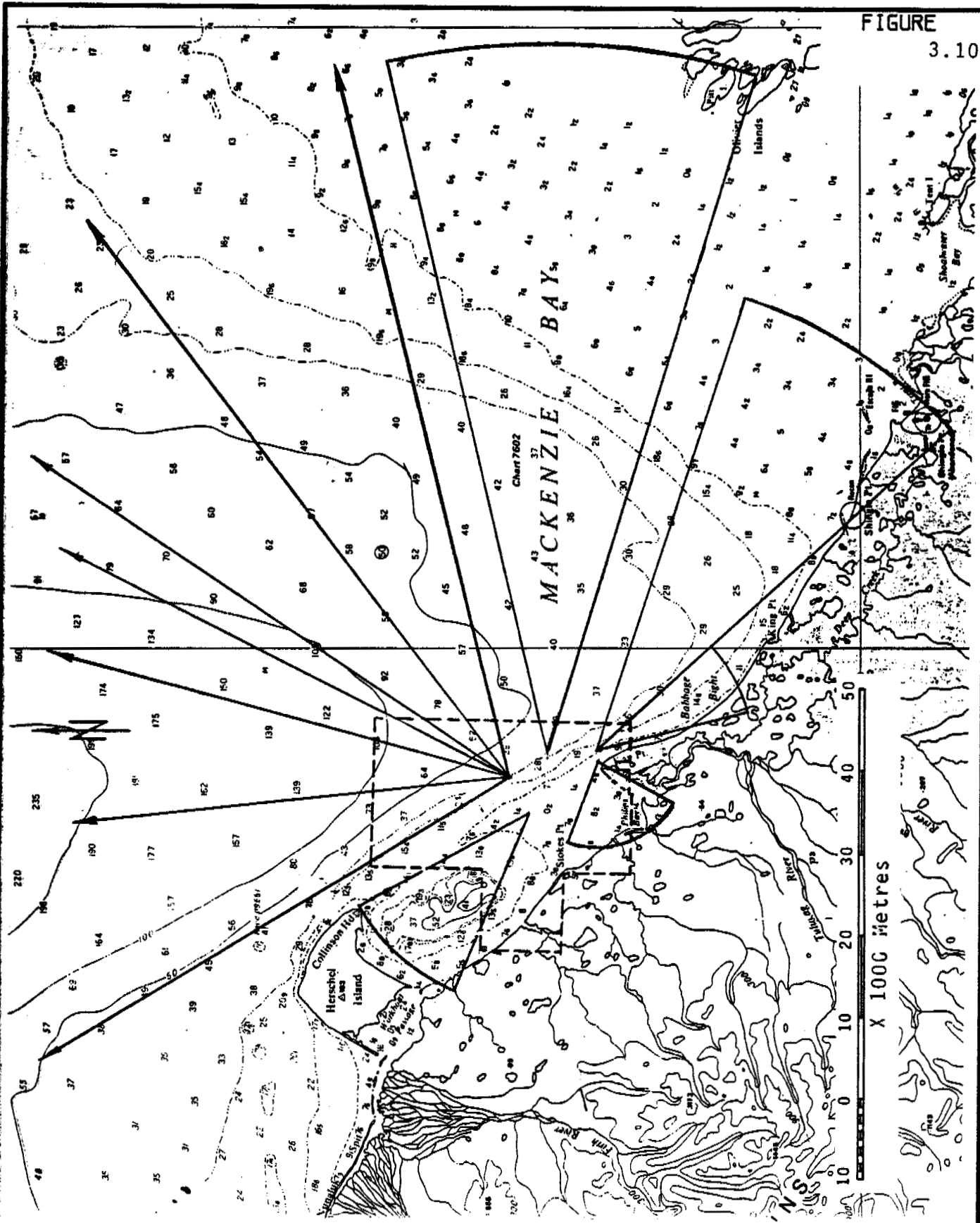


BEAUFORT SEA COASTAL SEDIMENT STUDY

Stokes Point: Local Hindcast Fetch Sectors

Date: 21 Mar 85

Checked by:
Keith Philpott
Consulting Limited



BEAUFORT SEA COASTAL SEDIMENT STUDY

Date: 21 Mar 85

Key Point: Local Hindcast Fetch Sectors

Checked by:

Keith Philpott

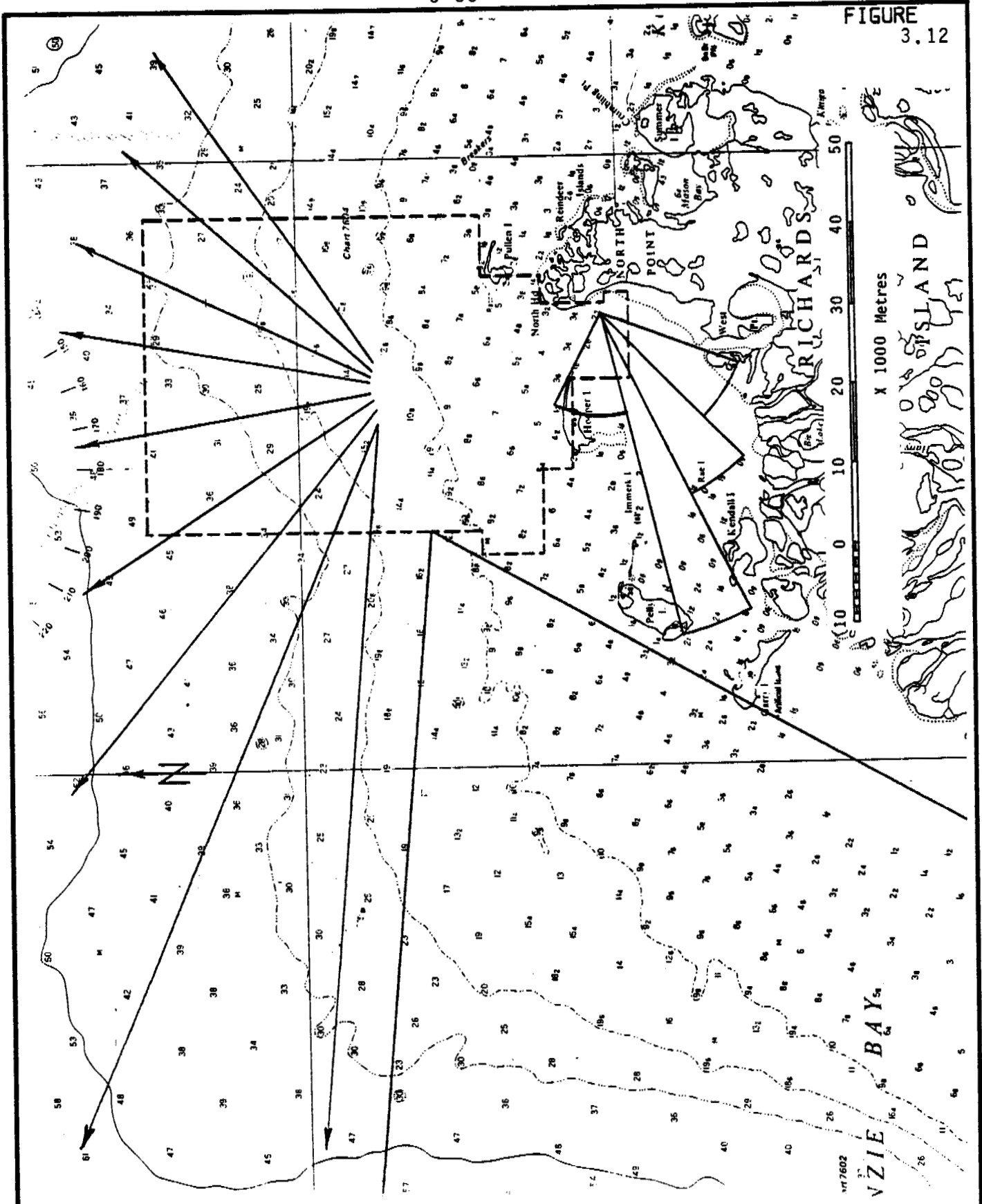
Consulting Limited

mean direction of 200 degrees (back azimuth) to refract to the inshore nodes. Since the wave refraction analysis results apply to wave conditions at the refraction grid boundaries, this meant that the North Head deep water hindcast fetches had to include, for the southwest sectors, Mackenzie Bay. This sector is shown in Figure 3.12. However, southwest winds would also generate waves over the shallow bay to the southwest of North Head and south of Hooper Island. This meant that two separate wave trains could be generated by the same winds and reach the same inshore points from two separate paths.

This overlap was handled by performing two fourteen-year hindcasts for North Head. The first hindcast, referred to as the "deep water hindcast", used the eight northern fetches and one western fetch shown in Figure 3.12. These results were then transferred inshore using the refraction analysis results. The second hindcast, referred to as the "local shallow water hindcast" was performed using the five fetch sectors in the immediate vicinity of North Head. The two wave data sets were combined at the inshore nodes, i.e, after refraction effects were considered (section 4.2).

3.6.3 Hindcasting at Tuktoyaktuk

An outline of the Tuktoyaktuk refraction grids is shown along with the Tuktoyaktuk deep water hindcast fetches in Figure 3.13.

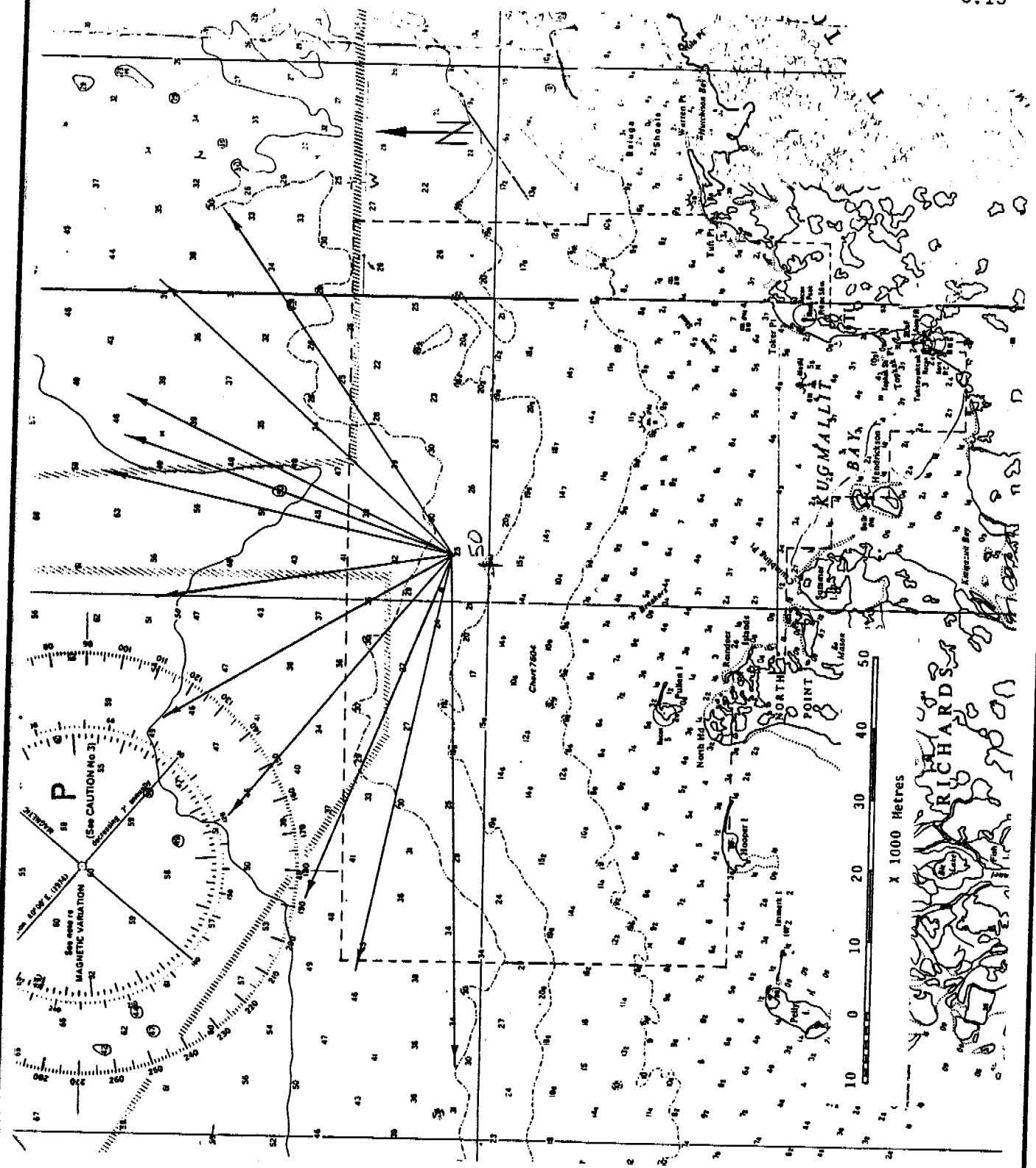


BEAUFORT SEA COASTAL SEDIMENT STUDY

North Head: Local Hindcast Fetch Sectors

Date: 21 Mar 85
Checked by:
Keith Philpott Consulting Limited

FIGURE
3.13



BEAUFORT SEA COASTAL SEDIMENT STUDY

Tuktoyaktuk: Local Hindcast Fetch Sectors

Date: 21 Mar 85

Scales as shown

Checked by:

Keith Philpott

Consulting Limited

When the deep water hindcast wave data was transferred inshore, using the results of the wave refraction analysis, the resulting inshore wave heights were considered to be unrealistically low. This was attributed to the problems caused by running a conservative spectral transfer model (no energy input or losses) over such a large shallow area. In essence the model results suggested that very few waves would make it from the outer grid boundaries to the inshore nodes when the model was run under the specified conditions. This matter is elucidated in section 4.3.

The ideal solution to this problem would be to refract each wave condition independantly, adding energy due to wind generation and removing energy due to bottom effects as the wave propogates inshore. This sort of solution, however, was not feasible within the scope of this project. The solution chosen was to bring the refraction boundaries closer to Tuktoyaktuk and to allow for bottom effects on wave height by using wave heights from the S.M.B. shallow water parametric model. The S.M.B. deepwater model was used to hindcast the wave periods because bottom effects do not significantly alter wave periods. This combination of parametric models was referred to as the "frictional hindcast" model. When the edge of the ice was close to Tuktoyaktuk all hindcasting was done with the S.M.B. shallow water parametric model.

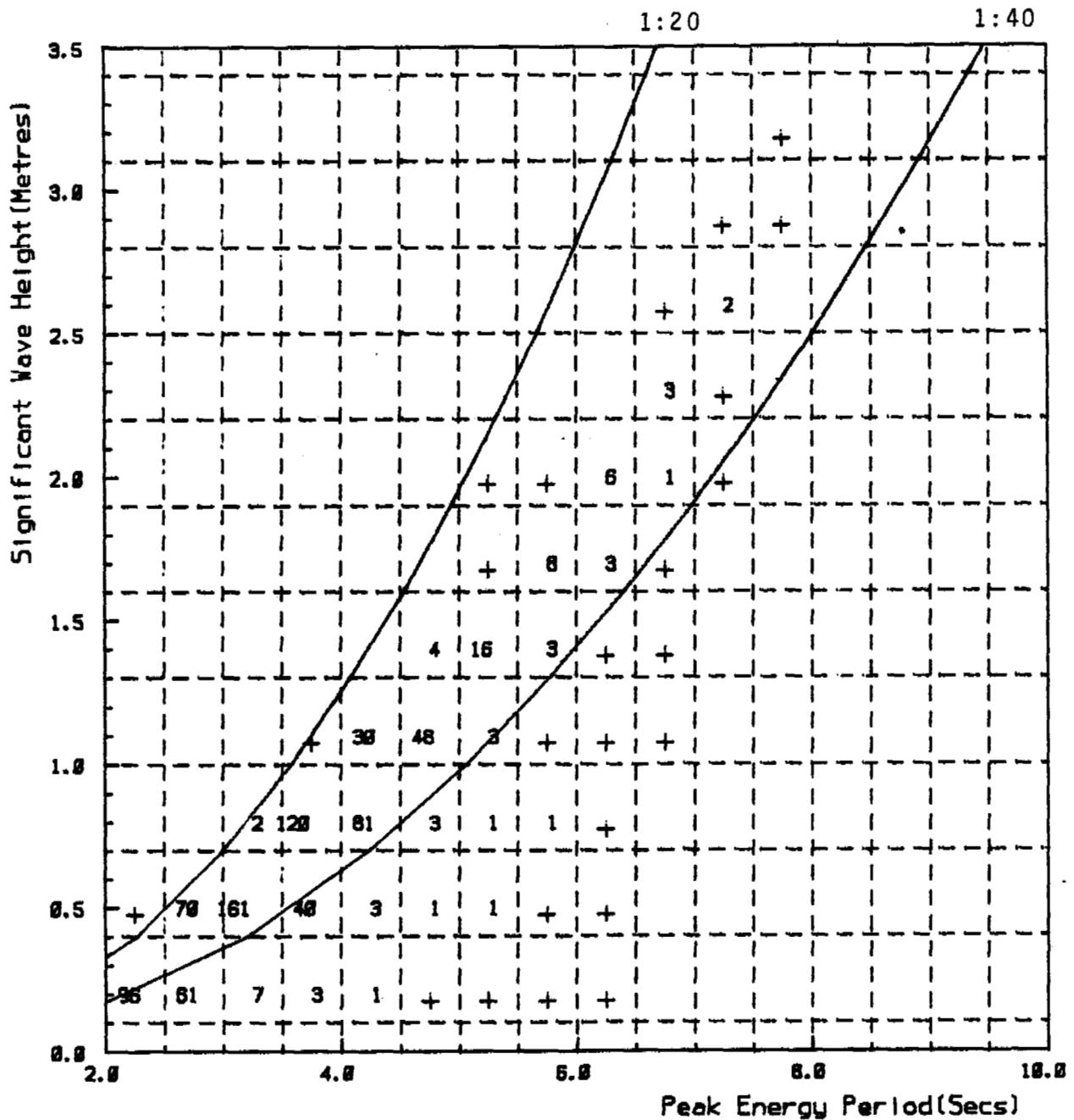
3.6.4 Wave Statistics Plots and Tables

The results of the fourteen-year hindcasts have been converted into statistical plots and tables. Results for each of the seven study sites are presented in Part II. An example and explanation of each plot is presented as follows:

1. Scatter Diagram of Significant Wave Height vs. Peak Period (Figure 3.14)

These diagrams represent the fourteen years of hindcast data in parts per thousand. Two wave steepness lines are shown, 1:20 and 1:40. The 1:20 line is in the proximity of a limiting steepness for deep water waves, the 1:40 line is shown for reference purposes.

FIGURE
3.14



Direction Limits: 0.0 TO 360.0

Values in parts per : 1000

Calms: 19.4 %

+ - Values less than 1 ppt

Dates: 2/7/78 to 7/9/83

Season: Summer, Fall

Total No. of Records: 34065

Waves Hindcast Using Wind Data from Tuktoyuktuk N.W.T.

BEAUFORT SEA COASTAL SEDIMENT STUDY

Date: 17 Feb 85

Scales as shown

King Point: Scatter Diagram for Deep Water Wave Data

Checked by:

1978 - 1983

Keith Philpott

Consulting Limited

2. Weibull Long-Term Distribution of Wave Heights

This is a standard Weibull analysis where $\text{Log}(\text{Log}(1/P))$ is plotted against $\text{Log}(\text{wave height})$, and P is the probability of exceedance of a given wave height. The wave data is collated into cumulative wave height groups as shown in Table 3.5. The cumulative probability of occurrence is computed by dividing the number of occurrences in each group by the total number of occurrences. A least squares curve fit is then performed on the logarithmic data points as shown in Table 3.6 and Figure 3.15.

A coefficient of correlation of 0.99 can be achieved by excluding the lower one and sometimes two wave height groups. This is standard with a Weibull analysis. Results such as in the form of Tables 3.5 - 3.8 and Figure 3.15 are given in Part II for each of the seven study sites.

TABLE 3.5 WEIBULL PROBABILITY ANALYSIS - KING POINT

WHT LIMIT	CUM TOTAL	CUM PROB(P)	LOGLOG(1./P(H))	LOG(WHT)
< .4	32736	.999969	-4.877672	-.397940
< .7	21067	.643523	-.717976	-.154902
< 1.0	11126	.339860	-.329105	.000000
< 1.3	4151	.126798	-.047263	.113943
< 1.6	1453	.044304	.131225	.204120
< 1.9	711	.021719	.220936	.278754
< 2.2	379	.011577	.286995	.342423
< 2.5	148	.004521	.370102	.397940
< 2.8	69	.002100	.427517	.447158
< 3.1	29	.000886	.484676	.491362
< 3.4	6	.000183	.572510	.531479

TABLE 3.6 LEAST SQUARES CURVE FIT ON LOGLOG(1/(1-P)) - KING POINT

LOG(WHT)	LOGLOG(1./P(H))	CURVE FIT	RESIDUAL
-.39794	-4.87767	-.51204	-23.10418
-.15490	-.71798	.14179	98.01048
.00000	-.32911	.20291	59.55455
.11394	-.04726	.24721	35.91456
.20412	.13123	.27526	17.79970
.27875	.22094	.28937	2.47347
.34242	.28699	.29975	-9.35083
.39794	.37010	.31281	-17.00017
.44716	.42752	.32104	-25.06626
.49136	.48468	.33082	-30.90318
.53148	.57251	.34463	-34.96507

SLOPE= 15718 INTERCEPT=.25464 CORR COEFF=.84019

TABLE 3.7 LEAST SQUARES CURVE FIT ON REDUCED DATA - KING POINT

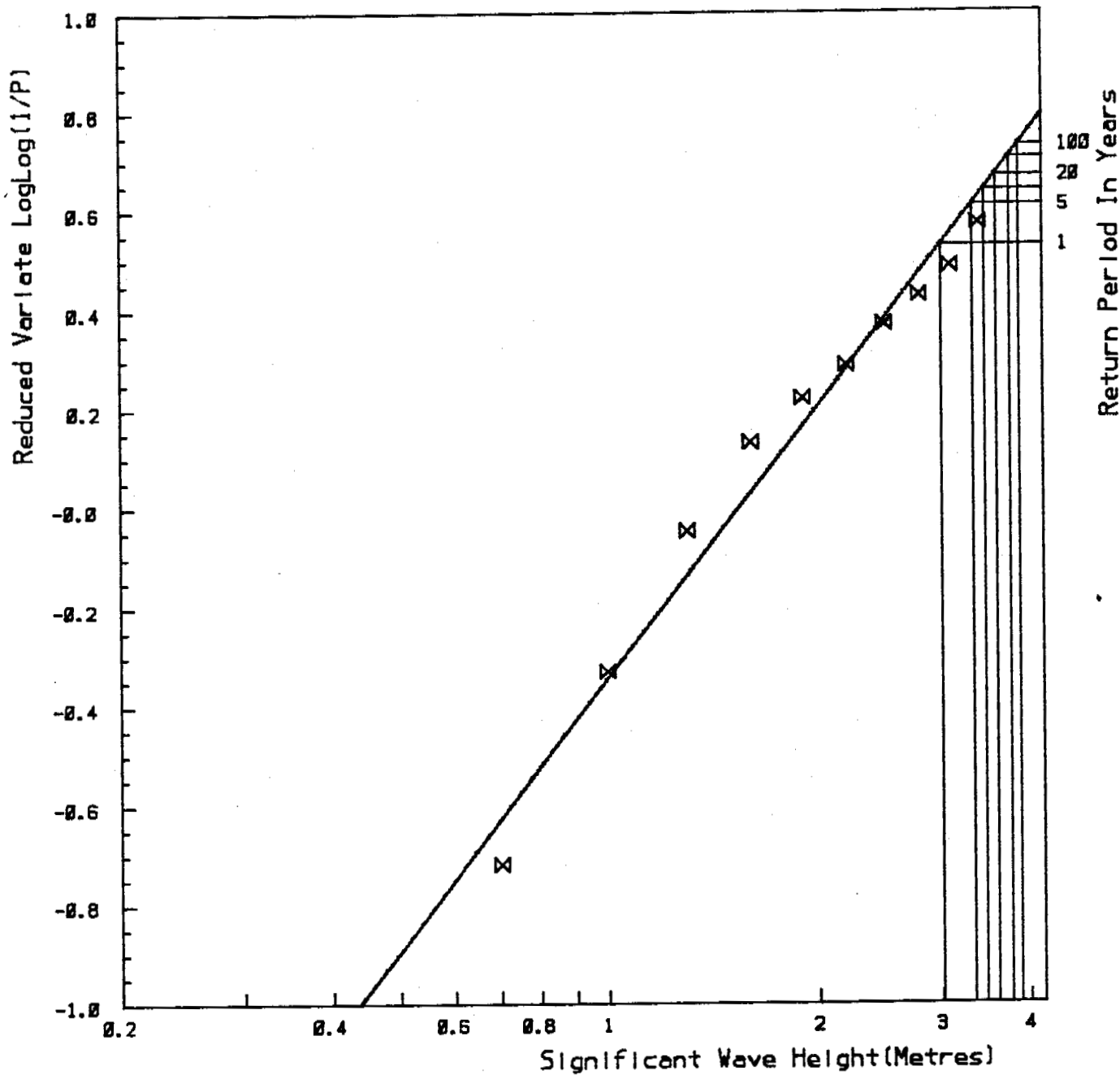
2 GROUPS OMITTED FROM FIT:		LOG(WHT)	LOGLOG(1./P(H))	CURVE FIT	RESIDUAL
< .4	32736	.00000	-.32911	-.04056	-8.91699
< .7	21067	.11394	-.04726	.13545	5.07721
		.20412	.13123	.24692	10.35701
		.27075	.22094	.30295	5.72856
		.34242	.28699	.34420	.41010
		.39794	.37010	.39610	-.42242
		.44716	.42752	.43196	-3.43935
		.49136	.48468	.46765	-5.31243
		.53140	.57251	.52251	-2.04435

SLOPE= 62451 INTERCEPT=.16497 CORR COEFF=.98940

TABLE 3.8 PREDICTED WAVE HEIGHTS FOR GIVEN RETURN PERIODS - KING POINT

RETURN PERIOD(YEARS)	WAVE HEIGHT(HS)
1.0	3.1
5.0	3.5
10.0	3.7
20.0	3.8
50.0	4.0
100.0	4.2

FIGURE
3.16



Direction Limits: 0.0 TO 360.0

Calms: 16.2 %

Dates: 2/7/70 to 7/9/83

Season: Summer, Fall

Total No. of Records: 32736

Waves Hindcast Using Data from Tuktoyaktuk N.W.T.

BEAUFORT SEA COASTAL SEDIMENT STUDY

King Point: Weibull Long Term Distribution of
Wave Heights

Date: 18 Mar 85

Scales as shown

Checked by:

Keith Philpott
Consulting Limited

3. Deep Water Wave Energy Distribution

Wave energy distributions are presented as shown in Table 3.9 and Figure 3.16. The fourteen-year hindcast is collated into wave height, period, and direction groups with user defined group sizes. The total energy for each direction sector is computed using the mean wave height, mean period and number of waves for each wave height and period group in that sector.

The energy (kinetic and potential) per metre width of wave crest per wave is found by:

$$E = \frac{1}{8} \rho g H_{rms}^2 L \quad (3.2)$$

where ρ = density

g = acceleration of gravity

H_{rms} = root mean square wave height

L = peak period wave length

The percentage energy in table 3.9 is found by dividing the total energy from all waves in each sector by the total energy of all waves at the site. The percentage frequency is the total time of waves per sector divided by the total time of all waves. The mean wave power is the weighted

average of the power per wave group and the time of occurrence of each wave group. The wave power is calculated as:

$$P = \frac{C_g E}{L} \quad (3.3)$$

where C_g is the wave group velocity and E and L are as defined for Equation 3.2.

TABLE 3.9 PERCENTAGE WAVE POWER DISTRIBUTION - KING POINT

DIRECTION SECTOR	PERCENTAGE FREQUENCY	MEAN POWER (KW)	PERCENTAGE ENERGY
270. - 280.	4.44	.88	2.84
280. - 290.	3.90	.88	2.48
290. - 300.	4.16	.75	2.27
300. - 310.	2.96	.70	1.52
310. - 320.	5.33	1.51	5.86
320. - 330.	4.30	2.34	7.33
330. - 340.	3.13	2.37	5.40
340. - 350.	1.95	3.10	4.40
350. - 360.	3.33	2.40	5.81
360. - 10.	2.85	1.82	1.53
10. - 20.	2.47	1.86	1.90
20. - 30.	3.68	1.18	3.17
30. - 40.	3.93	1.81	5.18
40. - 50.	3.52	2.22	5.69
50. - 60.	6.10	3.43	15.25
60. - 70.	4.73	1.13	3.90
70. - 80.	8.93	1.66	10.81
80. - 90.	4.73	.76	2.60
90. - 100.	6.28	.90	4.89
100. - 110.	4.79	.77	2.69
110. - 120.	5.74	.71	2.96
120. - 130.	1.62	.48	.56
130. - 140.	2.24	.38	.62
140. - 150.	3.17	.37	.86
150. - 160.	.34	.13	.03
160. - 170.	.49	.13	.05
170. - 180.	.87	.15	.09
180. - 190.	.82	.16	.09

4. Wave Height Exceedance and Wave Period Exceedance

The wave height exceedance and wave period exceedance plots (Figures 3.17 and 3.18) show the percentage of time that the significant wave height and peak periods exceed any values.

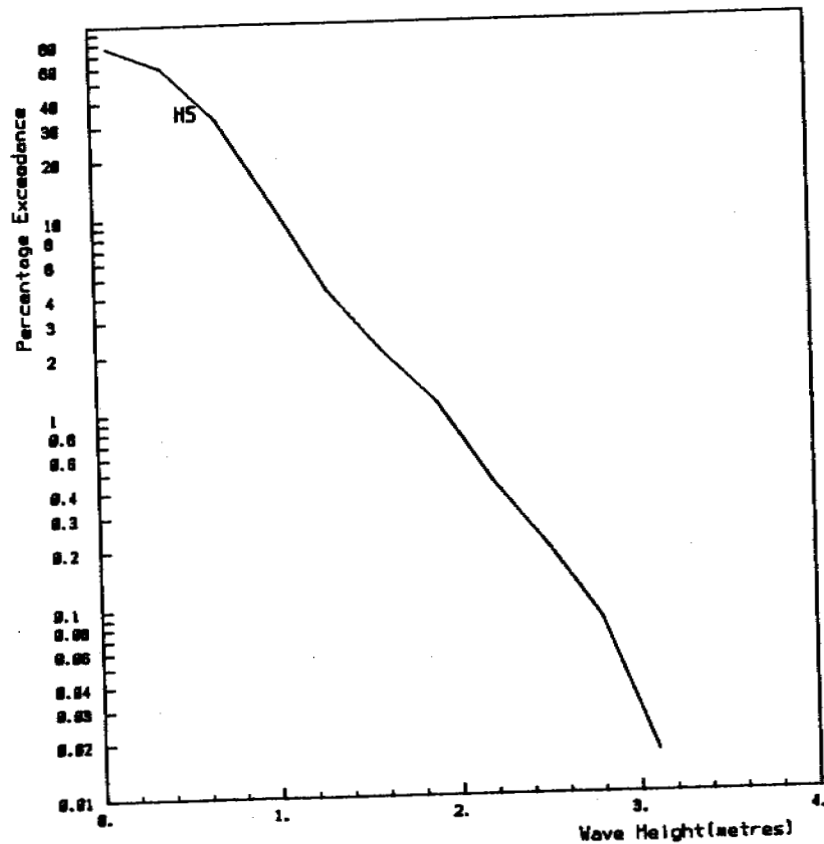
5. Wave Period Occurance

Figure 3.19 shows the percentage occurrence for the peak wave periods in each of the user defined wave period groups.

6. Wave Height Persistence

Figure 3.20 shows an example of both favourable and unfavourable wave height persistence diagrams. These show the number of times that wave heights are either above (unfavourable) or below (favourable) certain wave heights (1.0, 2.0, 2.5, and 3.0 m here) for continuous durations. For example, the waves were below 1.0 m for 100 continuous hours approximately ninety times in the fourteen open-water season. The waves were above 2.0 m for 24 continuous hours four times.

FIGURE
3.18



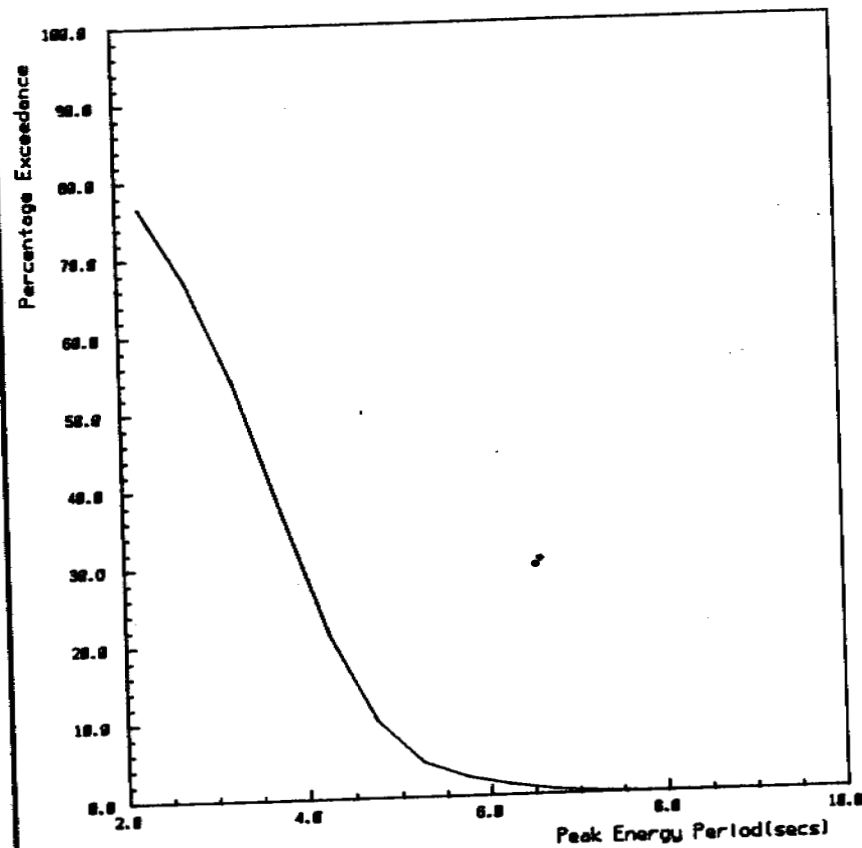
Direction Limits: 270.0 TO 190.0
 Calms: 19.4 %
 Dates: 2/7/78 to 7/9/83
 Season: Summer, Fall
 Total No. of Records: 34885
 Waves Hindcast Using Wind Data from Tuktoyaktuk N.W.T.

BEAUFORT SEA COASTAL SEDIMENT STUDY

King Point: Deep Water Wave Height Exceedance
 1978 - 1983

Date: 17 Feb 85
 Scales as shown
 Checked by:
 Keith Philpott
 Consulting Limited

FIGURE
3.19

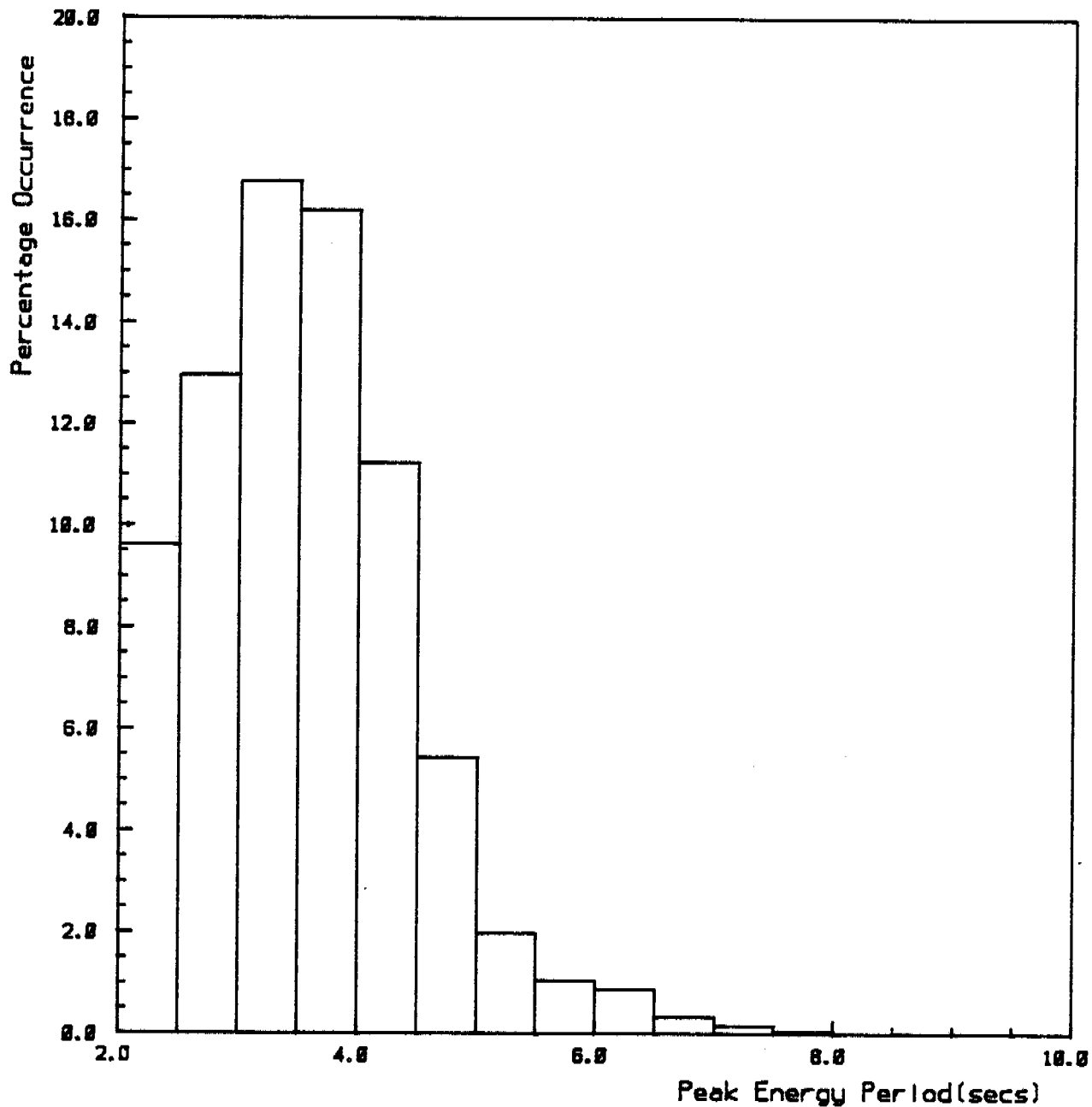


Direction Limits: 270.0 TO 190.0
 Calms: 19.4 %
 Dates: 2/7/78 to 7/9/83
 Season: Summer, Fall
 Total No. of Records: 34885
 Waves Hindcast Using Wind Data from Tuktoyaktuk N.W.T.

BEAUFORT SEA COASTAL SEDIMENT STUDY

King Point: Deep Water Wave Period Exceedance
 1978 - 1983

Date: 17 Feb 85
 Scales as shown
 Checked by:
 Keith Philpott
 Consulting Limited

FIGURE
3.20

Direction Limits: 270.0 TO 190.0

Calms: 19.4 %

Dates: 2/7/78 to 7/9/83

Season: Summer, Fall

Total No. of Records: 34065

Waves Hindcast Using Wind Data from Tuktoyaktuk N.W.T.

BEAUFORT SEA COASTAL SEDIMENT STUDY

King Point: Deep Water Wave Period Occurrence
1970 - 1983

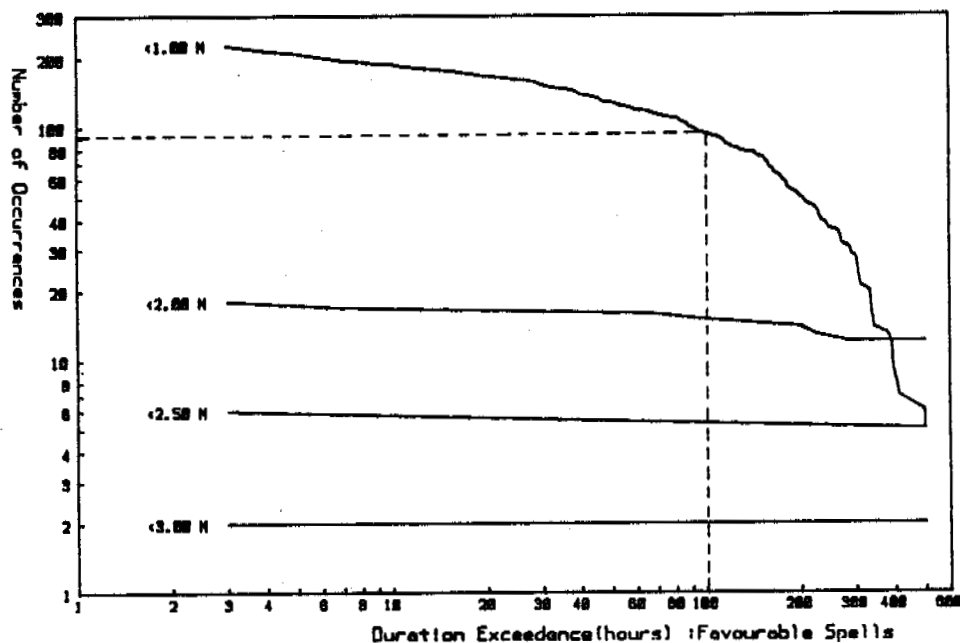
Date: 17 Feb 85

Scales as shown

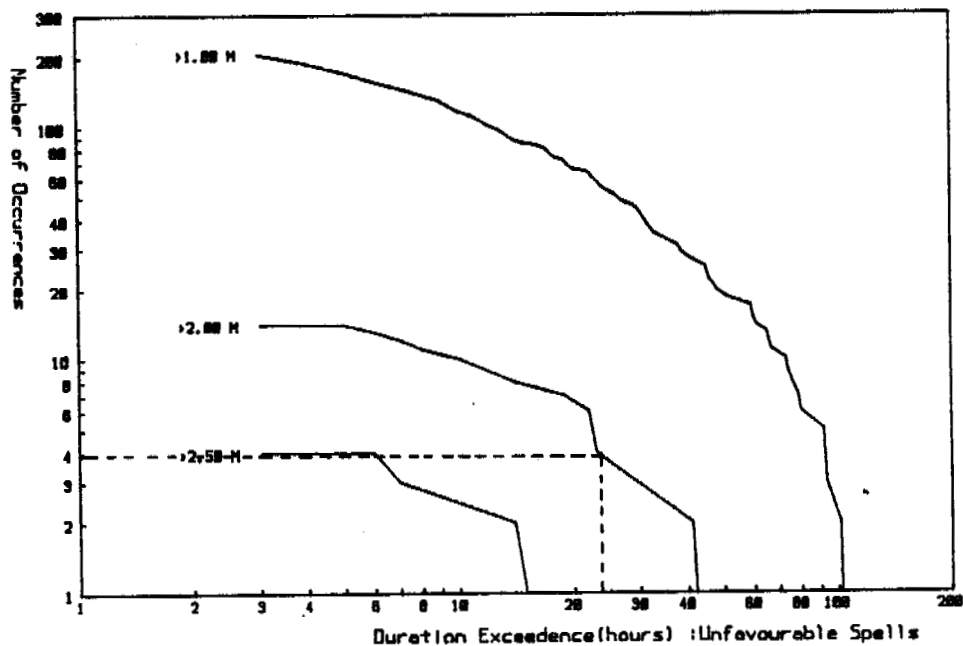
Checked by:

Keith Philpott
Consulting Limited

FIGURE
3.21



Date: 2/7/78 to 7/9/83
 Season: Summer, Fall
 Waves Hindcast Using Wind Data from Tuktoyaktuk N.V.T.



Date: 2/7/78 to 7/9/83
 Season: Summer, Fall
 Waves Hindcast Using Wind Data from Tuktoyaktuk N.V.T.

BEAUFORT SEA COASTAL SEDIMENT STUDY

King Point: Deep Water Wave Height Persistence
 Favourable and Unfavourable Spells

Date: 17 May 85

Scales as shown

Checked by:

Keith Philpott
 Consulting Limited

7. Wave Tables

Wave height and period tables are presented for each of the user defined direction sectors as well as one table for all directions. Table 3.10 is an example of an all-direction table.

TABLE 3.10 ALL DIRECTIONS WAVE TABLE - KING POINT

ALL DIRECTIONS

WAVE HT(N)	Wave Period(secs)										Total
	2	3	4	5	6	7	8	9	10	-	
.10	5300	303	37	8	3	0	0	0	0	0	5659
.40	2385	6824	111	34	2	0	0	0	0	0	9356
.70	0	4182	2809	41	1	0	0	0	0	0	6953
1.00	0	2	2593	94	6	0	0	0	0	0	2695
1.30	0	0	132	601	9	0	0	0	0	0	742
1.60	0	0	0	250	82	0	0	0	0	0	332
1.90	0	0	0	3	227	1	0	0	0	0	231
2.20	0	0	0	0	77	2	0	0	0	0	79
2.50	0	0	0	0	3	37	0	0	0	0	40
2.80	0	0	0	0	0	23	0	0	0	0	23
3.10	0	0	0	0	0	6	0	0	0	0	6
3.40	0	0	0	0	0	0	0	0	0	0	0
3.70	0	0	0	0	0	0	0	0	0	0	0
4.00	0	0	0	0	0	0	0	0	0	0	0
TOTAL	7693	11231	5682	1031	410	69	0	0	0	0	26116

SUMMARY :

NO. IN TOTAL SECTOR = 32736
 NO. OUTSIDE TOTAL SECTOR = 1329
 NO. OF CALMS = 6620
 TOTAL NO. OF ALL RECORDS = 32736
 PERCENTAGE CALMS = 19.4%

SECTION 4 NEARSHORE WAVE TRANSFORMATION

4.1 Wave Refraction Analysis and Spectral Transfer

4.1.1 Outline of Procedure

The following paragraphs outline the overall process by which the deepwater wave climate is transformed into a corresponding shallow water wave climate at or near the breaker line. The shallow water wave data is in a form that may be directly applied to the alongshore sediment transport models described in Section 6 of this report. The two principal components of the computational software are the linear wave refraction model LINREF and the spectral transfer post-processor, SPECTRANS. The latter calculates the wave transfer functions which in turn provide wave height coefficients and direction changes from deep to shallow water. A more comprehensive explanation of these models including relevant equations can be found in Pinchin et al., (1985).

The wave refraction program computes wave ray paths using either forward or backward tracking techniques. The seabed is defined by a series of digitized depth grids. Waves of specified period and initial direction are refracted over the numerical bed for any specified tide level. For each ray traced, the program outputs a file containing initial and final ray conditions.

When backward tracking with high ray density, wave spectra may be transferred from one location to another by using the directional ray concentration information produced by the refraction program. By transferring a number of offshore spectra encompassing the full range of possible mean wave directions and peak spectral periods, it is possible to compute wave height factors and direction shifts for all offshore wave conditions. These factors are a function of offshore mean direction and peak period only.

Wave ray backtracking is not essential to a wave spectrum transformation calculation. It merely ensures that all direction and frequency components are represented at a point of interest. In mathematical terms, the identical wave ray path will be calculated irrespective of whether the start point is in deep or shallow water, given that the boundary conditions are identical. However, backtracking provides much the simplest way of obtaining comprehensive data at a specified inshore location.

4.1.2 Wave Ray Tracking

Wave refraction is the bending of wave crests in response to seabed topography. It is a function of wave speed

which is itself a function of water depth and wave period. When constructing wave refraction diagrams it is convenient to work with wave orthogonals, often called wave rays, which are perpendicular to the wave crests.

The techniques used in LINREF are based on the "circular arc" method originally developed at the Hydraulic Research Station, Wallingford (Abernethy and Gilbert, 1975). Briefly, the method assumes that within a small triangular element the variation of wave speed can be closely approximated by linear interpolation. The wave ray path is then described by a circular arc within each element and is tangential to the corresponding arcs in adjacent elements. With appropriate boundary conditions wave rays can be refracted over the numerical bed to some unknown destination.

4.1.3 Preparation of Grids

For refraction analysis, the bathymetry was reduced to a number of rectangular grids with dimensions and grid size varied according to proximity to the area of interest, the absolute value of depth, and the bottom gradient. The general principles for selecting grid sizes are as follows:

- The grid spacing in the shallow water area of interest should be of the same order of magnitude as the wave lengths to be considered.
- The solution technique makes the basic assumption that wave speed varies linearly within each of the elements of the grid. It follows therefore that the wave speed corresponding to depths at adjacent grid points should closely follow the curve described by the shallow water wave speed relationship, that is, the departure from the curve at the mid-point between two nodes should be no more than a few percent.
- Taking the above into account, experience has shown that a grid size of 50 m is adequate for the inshore grid area in the immediate area of interest.
- These conditions may be relaxed in the shoreline regions outside the area of interest. Here one is only concerned with identifying those highly oblique wave rays which are invalid as they return to shallow water.
- As the water depth increases, so may the spacing since the change in wave speed becomes progressively less dependent on the change in water depth.
- In the interest of computational economy grid spacing is increased as quickly as possible. At the same time, significant bottom features cannot be overlooked.
- The seaward limits of the grids should be in "deepwater" or at a point where offshore wave data is available. The former is theoretically half a wave length but in practice wave refraction at such depth is so slight that a depth of about 30 m is usually sufficient.

The sources of the bathymetric data are given in Section 2.2.2.

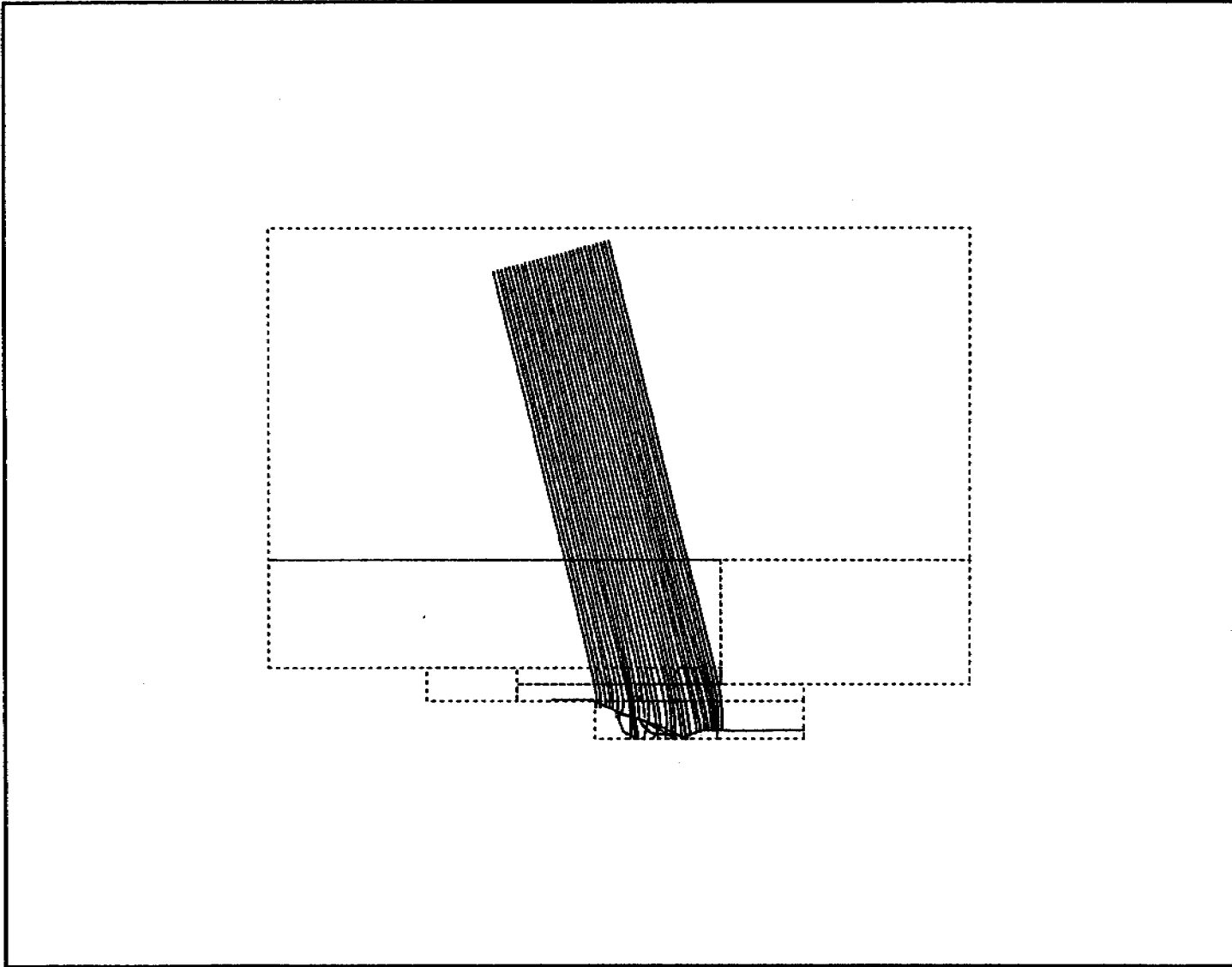
A number of difficulties had to be overcome in preparing the depth grids. These include:

- field sheets using different U.T.M. zones
- field sheets in geographic coordinates only
- field sheets in different units
- field sheets with different scales
- field sheets with different datum
- sparse data at some sites
- overlapping field sheets with different depths.

Diagrams showing the location, nodal dimensions, and mesh sizes of the refraction grids are presented for each site in the appropriate sections of Part II of this report.

4.1.4 Forward and Back-tracked Refraction Diagrams

Forward-tracked ray diagrams may be constructed by tracking a number of rays from the offshore boundary to cover the inshore area of interest. Such a diagram for King Point is shown in Figure 4.1. Whilst this method provides a good picture of general wave refraction patterns in an area, associated methods of calculation of wave refraction coefficients are unsatisfactory for a number of reasons which are fully discussed in Abernethy and Gilbert (1975), but may be summarized as follows:



WAVE RAY DETAILS

Tide Level= 0.50 m.

Wave Period= 6.5 secs

Direction= 194.8 Degrees True

Bathymetry information used for
grids obtained from the following
sources:

- C.H.S. Field Sheets numbered:
V.A. 10070 (1978)
V.A. 10071 (1978)
- Soundings taken by Peter Kiewit
Construction Co. Ltd. (1984).
- Original notes by B. McDonald
& a scaled version by D. Frobel



BEAUFORT COASTAL SEDIMENT STUDY

King Point Forward-Track
Ray Diagram

Date: 31 Jan 85

Scale 1:100000

Checked by:

**KEITH PHILPOTT
CONSULTING LTD.**

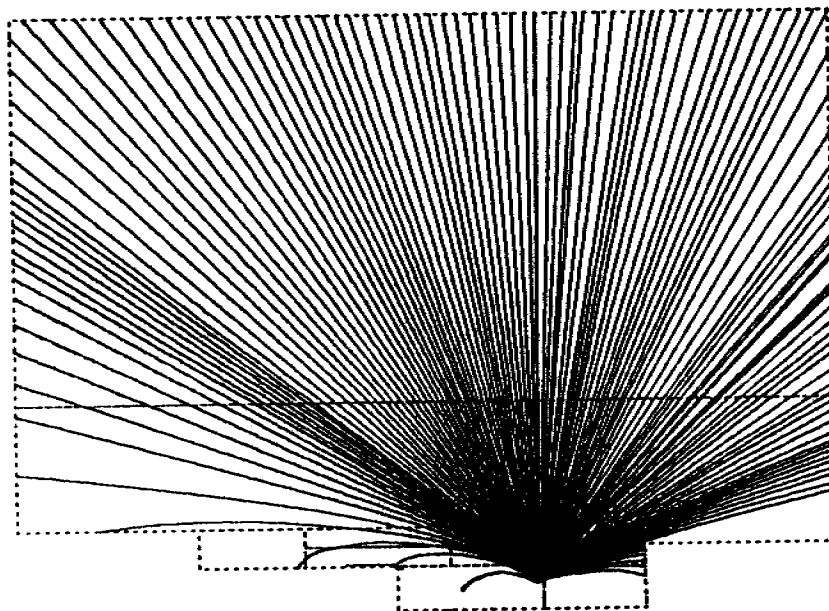
FIGURE 4.1

- (i) Wave refraction coefficients calculated from the wave intensity equation are highly sensitive to wave ray position and wave frequency for non-uniform topography.
- (ii) Forward-tracking tests using different wave ray spacings give significantly different results.
- (iii) Results are sensitive to initial wave ray direction.
- (iv) Bottom topography smoothing can reduce the variability, but the results then tend to become a function of the smoothing strategy adopted (Poole, 1975).
- (v) As a result of the above, it was concluded that refraction results from forward-tracking rays used to evaluate a wave intensity relationship exhibit an inherent bias towards high wave heights, an excessive sensitivity to frequency, offshore direction and position which is greatest in regions where refraction coefficients are large.

These difficulties may be overcome by constructing a large number of wave rays at very small angular increments for a number of wave periods from each single point of interest. This process is known as backtracking. It allows an inshore two-dimensional frequency-direction wave spectrum to be subdivided into elements by frequency and direction each of which is individually tracked during the spectrum transfer process. Abernethy and Gilbert (1975) showed that this technique gives more stable and realistic results even in regions of caustics.

Caustics are regions where forward-tracked wave rays converge and cross producing singularities with theoretically infinite concentrations of wave energy (Pierson, 1951). With backtracked wave rays the phenomenon does not explicitly arise. By using spectral transfers wave energy concentrations are diffused in a manner which more accurately reproduces what is actually observed.

In contrast with forward-tracking, backward-tracked ray diagrams are not visually enlightening. Hence, only one back-tracking diagram for each site is presented in Part II. An example of a back-track diagram for King Point is shown in Figure 4.2.



WAVE RAY DETAILS

Tide Level= 0.50 m.

Wave Period= 5.8 secs

Position No:4

Bathymetry information used for grids obtained from the following sources:

- C.N.S. Field Sheets numbered:
V.R. 10070 (1970)
V.R. 10071 (1970)
- Soundings taken by Peter Kiewit Construction Co. Ltd. (1984).
Original notes by B. McDonald & a scaled version by D. Frobel



BEAUFORT COASTAL SEDIMENT STUDY

KING POINT BACKWARD-TRACK
RAY DIAGRAM

Date: 8 Mar 85

Scale 1:100000

Checked by:

Keith Philpott
Consulting Limited

4.1.5 Wave Spectrum Transfer

The process of refracting a wave spectrum is based on the assumption that the wave energy flux in a frequency band of width df centered about frequency f will remain in that band as the wave spectrum is transferred inshore. With this assumption it is possible to take a discrete element from an offshore spectral density distribution and to independently transfer it inshore applying only shoaling and refraction coefficients. This conservative method applies over distances where the shoaling and refraction effects dominate over dissipative effects, i.e. outside the breaker zone. This method also neglects local generation.

The selection of the initial inshore directions and periods will partition the inshore spectra into a corresponding number of discrete elements of size $df.d\theta$. Each element of the inshore spectrum will thus be represented by a single wave ray.

The principal output from the wave refraction analysis is the deep water direction of all wave rays. This gives the original deep water direction θ_0 of the energy flux in each element $df.d\theta$ of the inshore spectra. The deep water energy flux that is present at any deep water direction at a given frequency is dependent on the deep water directional spectrum model used.

4.1.6 The Deep Water Spectrum Model

The offshore spectrum model used was the JONSWAP as described by Hasselman et al., (1973). Having specified a series of wave periods for wave ray backtracking the corresponding peak frequencies were used to construct JONSWAP deep water spectral density distributions $S(f)$.

A value of $\gamma = 2.2$ was used for the JONSWAP "peakedness parameter" which relates a JONSWAP spectrum to a fully developed Pierson-Moskiwitz spectrum. This value was determined by comparing theoretical with measured spectra from the Beaufort Sea (Leblond et al., 1982).

Each JONSWAP spectrum is assumed to be directly distributed according to the power cosine function

$$F(\theta_0) = \cos^n |\bar{\theta}_0 - \theta_0| \quad (4.1)$$

where $\bar{\theta}_0$ is the mean deep water direction of wave propagation and n is the direction spreading index. An index value of 2 corresponds to a broad-banded energy distribution characteristic of locally generated waves, whereas an index value of 10 corresponds to a narrower spectrum which would be more characteristic of a wave condition generated outside the area.

The direction and frequency components of the spectral energy term are assumed to be independent such that

$$S_0(f, \theta_0) = S_0(f) \cdot F(\theta_0) \quad (4.2)$$

It is important when applying the power cosine function $F(\theta)$ that the values are normalized so that the area under the two-dimensional spectral density surface is equal to the area under the one-dimensional JONSWAP curve. The deepwater significant wave height is computed from the zeroth moment of the one-dimensional JONSWAP spectrum

$$H_{S_0} = 4\sqrt{\int S_0(f) df} \quad (4.3)$$

4.1.7 The Conservative Inshore Directional Wave Spectra

To summarize the above steps, it is possible to compute the spectral density for each frequency-direction element of an inshore spectrum $S(f, \theta)$. Each such element is then uniquely represented by one wave ray and hence one deep water wave direction. The deep water spectral density element which is transferred along a ray path is computed using a directionally distributed JONSWAP spectrum. It is therefore necessary to define the mean direction $\bar{\theta}_0$ and peak frequency f_p of the deep water spectrum. The elements of the deep water spectrum are then refracted inshore by applying refraction and shoaling coefficients.

A conservative one-dimensional inshore spectral density $S(f)$ can then be defined by the following Equation:

$$S(f) = \int S(f, \theta) d\theta \quad (4.4)$$

The zeroth moment and first moment of direction of the inshore spectra are computed as:

$$M_{0i} = \iint S(f, \theta) df d\theta \quad (4.5)$$

$$M_{1D_i} = \iint S(f, \theta) (\bar{\theta}_0 - \theta) df d\theta \quad (4.6)$$

where $\bar{\theta}_0$ is the mean offshore wave direction. The inshore significant wave height and mean inshore direction are then found by:

$$H_{S_i} = 4 \sqrt{M_{0i}} \quad (4.7)$$

$$\bar{\theta}_i = \bar{\theta}_0 + \frac{M_{1D_i}}{M_{0i}} \quad (4.8)$$

4.1.8 The Inshore Wave Height Factor

An inshore wave height factor for each offshore complete JONSWAP spectrum is computed by dividing the inshore significant wave height (Equation 4.7) by the offshore significant wave height (Equation 4.3). Because the offshore directional JONSWAP spectrum is dependant on only the spectral peak frequency and mean direction of wave propagation, the wave height factor is also a function of only peak frequency and mean offshore direction.

For any offshore wave condition the significant wave height can be multiplied by the appropriate inshore wave height factor (as determined by the offshore mean direction and peak period) to predict the corresponding inshore wave height.

This procedure for predicting inshore wave heights was recently applied to measured offshore wave data during the Canadian Coastal Sediment Study (Pinchin et al, 1985). The results, when compared with measured inshore wave data, showed a substantial overestimation of the predicted inshore wave heights. This discrepancy was corrected by allowing for energy dissipation due to wave-wave interaction using the shallow water equilibrium spectrum theory of Kitaigorodskii et al., (1975). The inshore wave heights computed using spectral transfers that allowed for wave-wave interactions compared very well with the

measured wave data. The Kitaigorodskii theory was therefore incorporated in the spectral transfers performed for each of the seven study sites of this project.

4.1.9 Shallow Water Saturated Spectrum

Kitaigorodskii et al., (1975), proposed that the maximum spectral density that can be sustained in a given depth of water is

$$S_m(f) = \frac{\alpha g^2 f^{-5} \phi(\omega_h)}{16\pi^4} \quad (4.9)$$

where $\omega_h = 2\pi f \sqrt{h/g}$ (4.10)

α is the Phillips constant 0.0081, h is the water depth, and $\phi(\omega_h)$ is the dimensionless function shown in Figure 4.3.

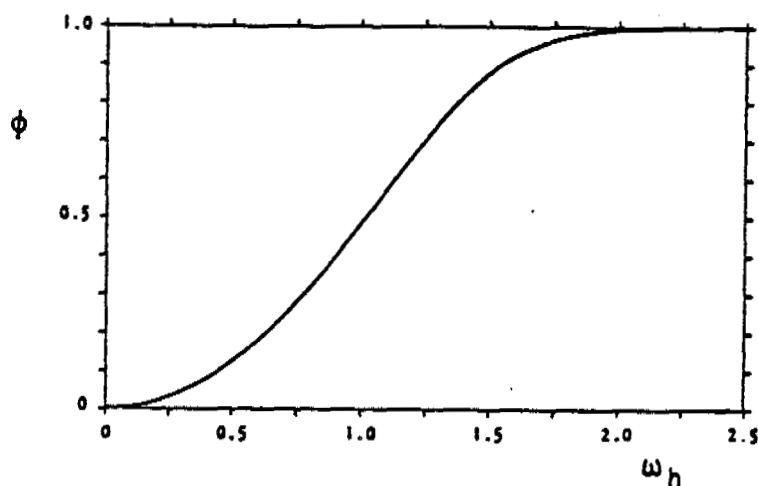
Dimensionless Function $\phi(\omega_h)$

FIGURE 4.3

This theory is incorporated into the spectral transfer process by comparing the value of the computed inshore conservative spectral density $S(f)$, from Equation 4.4, with the value of the saturated inshore spectral density from Equation 4.5. When the computed density $S(f)$ is greater than the saturated density, all values of $S(f, \theta)$ (Equation 4.4) are factored linearly by the ratio $S_m(f)/S(f)$.

The inshore significant wave height and mean inshore wave direction are again computed by Equations 4.7 and 4.8, and the inshore wave height factor is computed as in Section 4.1.8.

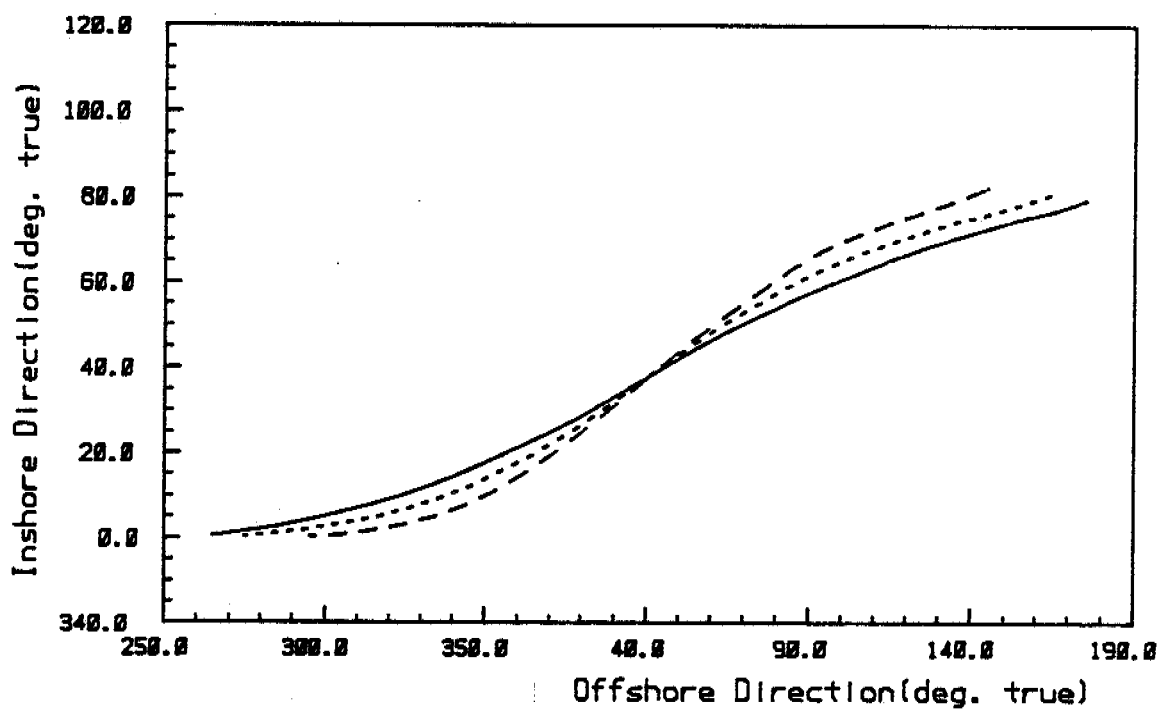
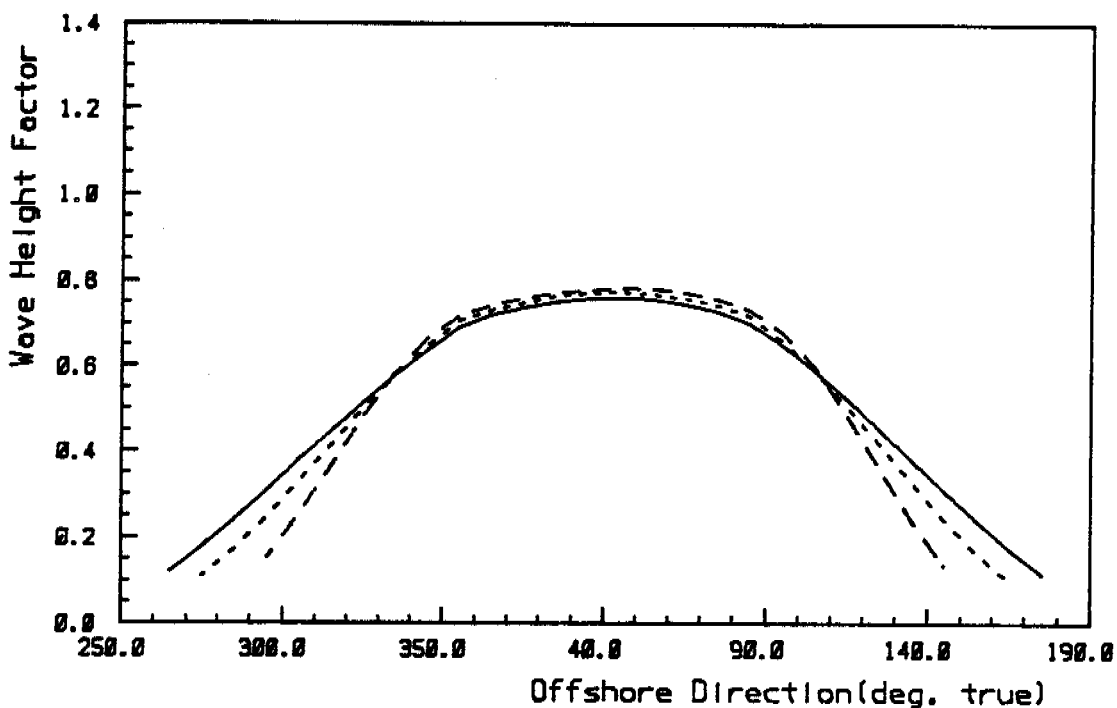
4.1.10 Computed Nearshore Wave Conditions

Two inshore points of interest, or nodes, were chosen for each of the seven field sites. The node locations are shown in Figures 2.1 to 2.7. An additional three nodes were chosen at King Point in connection with the beach plan shape modelling (Section 8).

For each inshore node, wave height factors and mean inshore wave directions were computed for spectra with frequencies corresponding to wave periods of 3.2, 4.0, 5.0, 6.3, 7.9, 10.0 and 12.6 seconds and ten degree increments of deepwater wave direction covering the complete range of possible deepwater conditions. Thus, for any offshore wave condition the corresponding inshore wave condition can be computed by applying the appropriate wave height factor and direction shift. The peak periods are assumed to remain unchanged from offshore to inshore.

Plots of the inshore wave height factor and inshore wave direction as a function of deepwater wave direction have been prepared for periods 3.2, 5.0, 7.9, and 10.0 seconds. An example of the 5.0 second plots for King Point are shown in Figure 4.3. The complete sets of plots for each site are presented in Section II. The wave height factors refer to the significant wave height associated with the deepwater sea state and not to any individual spectral constituent.

FIGURE
4.4



Node No: 1	Spreading Index: 2	_____
Tide Level: 0.50 m.	
Peak Period: 5.0 secs		-----

BEAUFORT SEA COASTAL SEDIMENT STUDY

Date: 15 Apr 85

Scales as shown

Checked by:

Keith Philpott
Consulting Limited

King Point: Wave Spectrum Transformation Results for
Node Number 01

Three values of the power cosine direction index n (Equation 4.1) were considered: 2, 4, and 10. In the absence of field data a moderately focused value of 4 was used to compute the fourteen years of inshore wave conditions for use in the rest of the project.

4.2 Inshore Wave Statistics

Wave height factors and direction shifts were applied to the fourteen years of offshore hindcast wave data to compute fourteen years of inshore wave data at each of the seven study sites. Detailed inshore wave statistics were computed and plotted for one node at King Point, using the procedures described in Section 3.6.4 and presented in Part II.

4.3 Wave Transformations at North Head

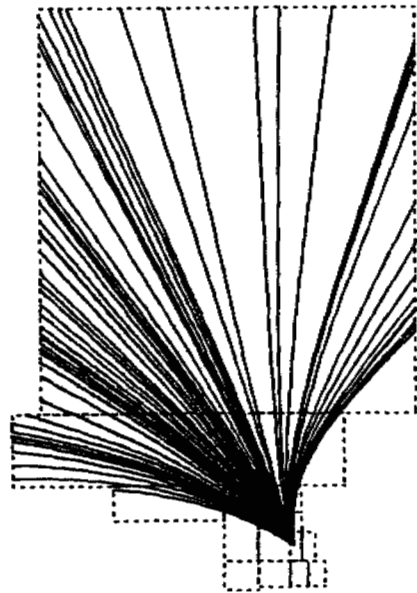
Since the offshore directions of the wave rays define the amount of wave energy that is transferred along a ray path, it is essential that only one offshore wave condition exists for any one direction at any one time. At North Head, however, the

back-track diagrams showed the wave rays could exit the western edge of the refraction grids both to the north and south of Hooper Island. These two areas are defined by two very different hindcast fetches as shown in Figure 3.12. As explained in Section 3.6.2, this meant that two separate wind-wave hindcasts had to be performed.

It was obvious that these two hindcast data sets could not use the results of the same refraction analysis. In order to compute the offshore to onshore wave transformation functions for the deepwater data set, it was essential that the wave rays be restricted from exiting the refraction grids south of Hooper Island. A back-track diagram for this case is shown in Figure 4.4.

Spectral transfers were performed using backtracks with this restriction and the deepwater wave climate was transferred to the inshore nodes. The spectral transfer results for the 7.9 second case are shown in Figure 4.5. It can be seen here that deepwater spectra with a mean back-azimuth of 200 degrees will have constituent waves that can refract to the inshore nodes.

Because the local shallow water hindcast was performed in essentially the same depth of water as the wave refraction nodes were located, it was concluded that the shallow water wave data did not need to be refracted before it was combined



WAVE RAY DETAILS

Tide Level= 0.50 m.

Wave Period= 5.0 secs

Position No:2

Bathymetry information used for grids obtained from the Canadian Hydrographic Service. Field Sheets numbered:

M.A. 10101 (1970)



BEAUFORT SEA COASTAL STUDY

NORTH HEAD BACKWARD-TRACK
RAY DIAGRAM

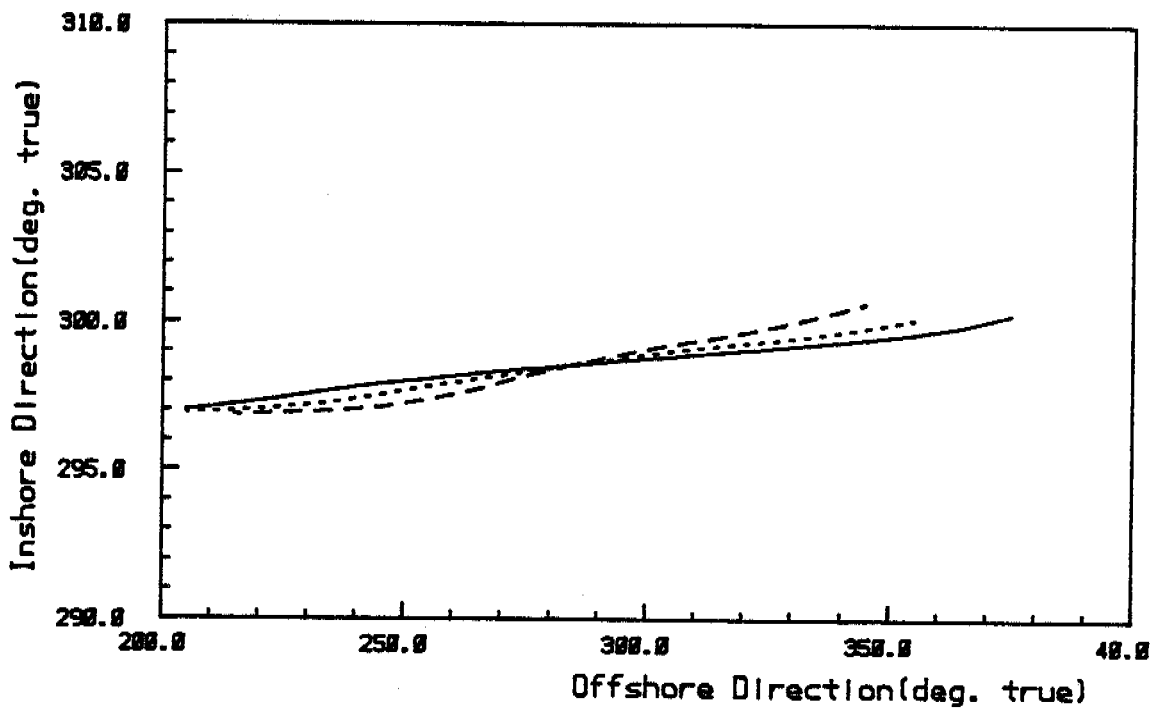
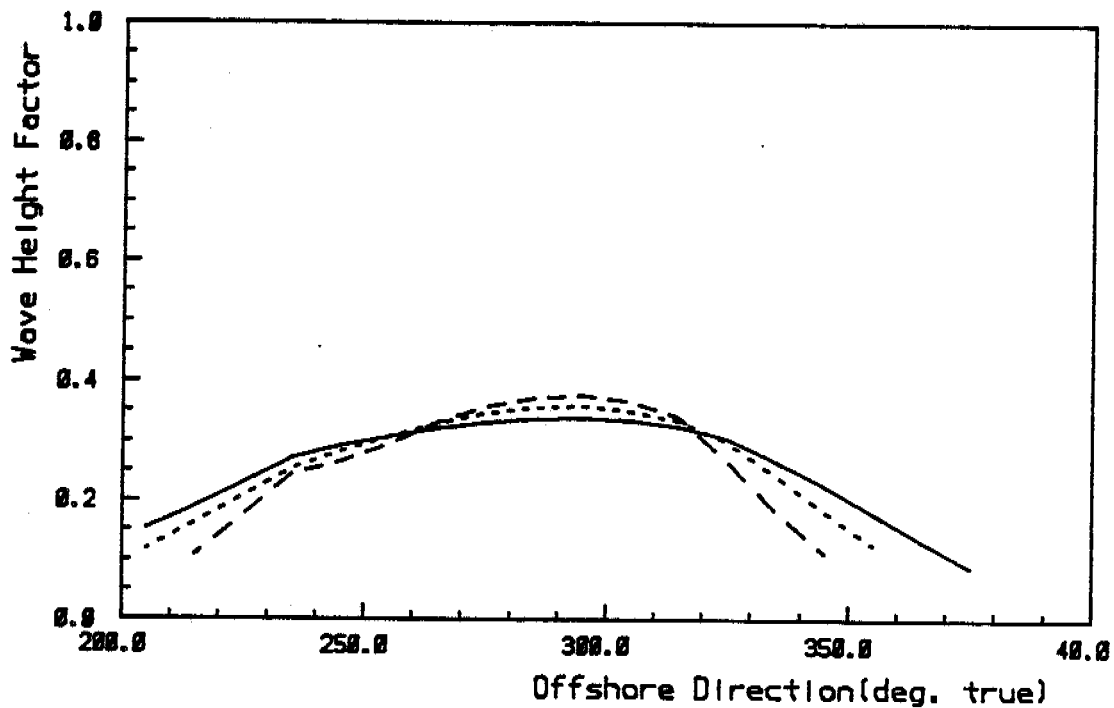
Date: 16 Apr 85

Scale 1:500000

Checked by:

Keith Philpott
Consulting Limited

FIGURE
4.6



Node No: 1	Spreading Index: 2	_____
Tide Level: 0.50 m.	4
Peak Period: 7.9 secs	10	-----

BEAUFORT SEA COASTAL SEDIMENT STUDY

North Head: Wave Spectrum Transformation Results for
Node Number 01

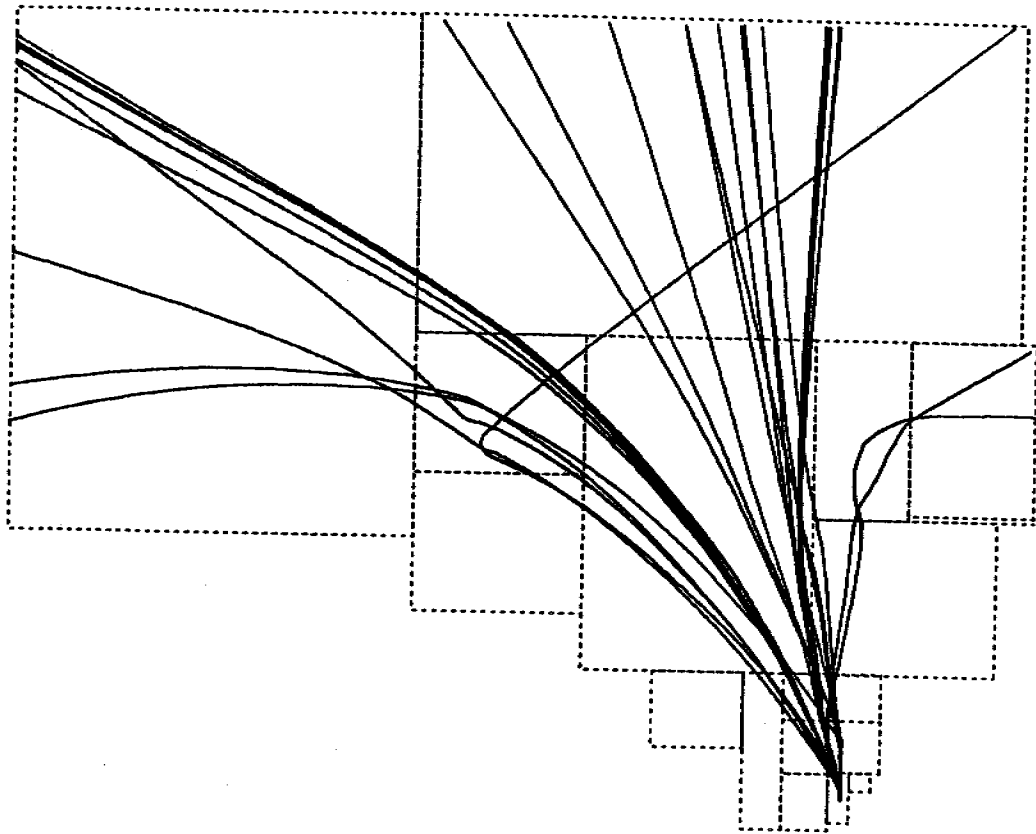
Date: 27 Mar 85
Scales as shown
Checked by:
Keith Philipott Consulting Limited

with the refracted deepwater wave data. It is therefore important to note that the spectral transfer results which are presented in Part II of the report do not apply to the local hindcast wave data.

4.4 Wave Transformations at Tuktoyaktuk

A deepwater wave refraction analysis similar to that at North Head was performed at Tuktoyaktuk. In this case, wave rays were not permitted to exit the western edges of the refraction grids within Kugmallit Bay (See Figure 3.13). Figure 4.6 shows a wave ray back-track diagram computed with this restriction.

When the deepwater hindcast data was transferred inshore, the resulting inshore wave data seemed unrealistically low. It was concluded that this was caused by considering such a large refraction area and not considering wind energy input within the grids. The refraction grid sizes are shown in Figure 4.7. The ideal solution to this problem would be to refract each wave condition independently, adding energy due to wind generation and subtracting energy due to bottom effects. As this sort of solution was not feasible within the scope of this project, the chosen solution was to reduce the area of refraction grids.



WAVE RAY DETAILS

Tide Level= 0.50 m.

Wave Period= 5.0 secs

Position No:2

Bathymetry information used for
grids obtained from the Canadian
Hydrographic Service. Field Sheets
numbered:

M.A. 10128 (1970)
F.S. 2758 (1957)



BEAUFORT SEA COASTAL STUDY

TUKTOYAKTUK BACKWARD-TRACK
RAY DIAGRAM

Date: 0 Mar 85

Scale 1:500000

Checked by:

Keith Philpott
Consulting Limited

FIGURE 4.7

KEY

Grid Number
Nodal Dimensions (XxY)
Mesh Size (metres)

1
39X47
50X50

7
28X8
600X600

2
53X23
100X100

16
2X27
500X500

3
37X37
150X150

4
40X33
150X150

5
38X33
150X150

6
9X18
600X600

8
14X17
600
X
600

10
37X45
400X400

11
37X45
400X400

9
24X17
1500X1500

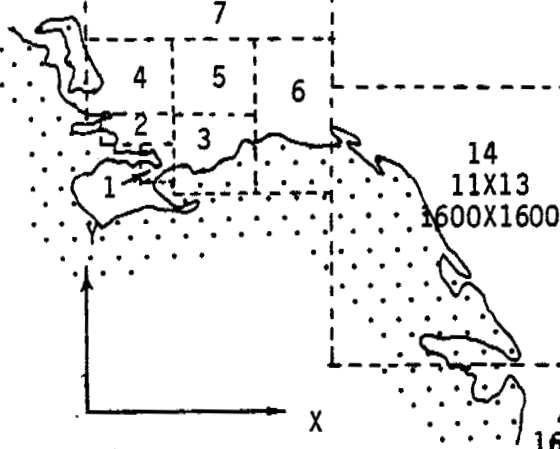
12
12X22
3000X3000

14
11X13
1600X1600

13
38X21
500X500

15
19X14
1000X1000

17
19X15
3000X3000



X 1000 Metres

BEAUFORT SEA COASTAL SEDIMENT STUDY

Tuktoyaktuk: Nodal Dimensions and Mesh Size of
Refraction Model Grids

Date: 14 May 85

Scales as shown

Checked by:

Keith Philpott
Consulting Limited

As part of the initial wave refraction analysis at Tuktoyaktuk, a separate series of wave back-tracks had been performed using grids 1 to 5. This was originally going to be used to refract the results of a local hindcast from southwest of Tuktoyaktuk. However, this analysis was not completed once the problem with the deepwater wave transformation was identified.

The problem with the deepwater wave transformation was solved by re-hindcasting the wave climate using the "frictional" model described in Section 3.6.3. These results were then refracted through the small grid system. The spectral transfer results are presented in Part II.

SECTION 5 SURGE SENSITIVITY ANALYSIS

5.1 Objective

The objective of the work described here is to determine the sensitivity of alongshore and onshore-offshore sediment transport to positive storm surges. It shows that surges have an important influence on nearshore profile adjustments but only a secondary influence on alongshore transport which may be increased or decreased by a positive surge. These results are used to evaluate the influence of surges on yearly estimates of alongshore and onshore-offshore sediment transport presented in Sections 6 and 7 respectively.

5.2 Effects of a Surge on the Numerical Models

Before examining results from surge analyses it is important to have a general understanding of how surges influence the various models used in this study.

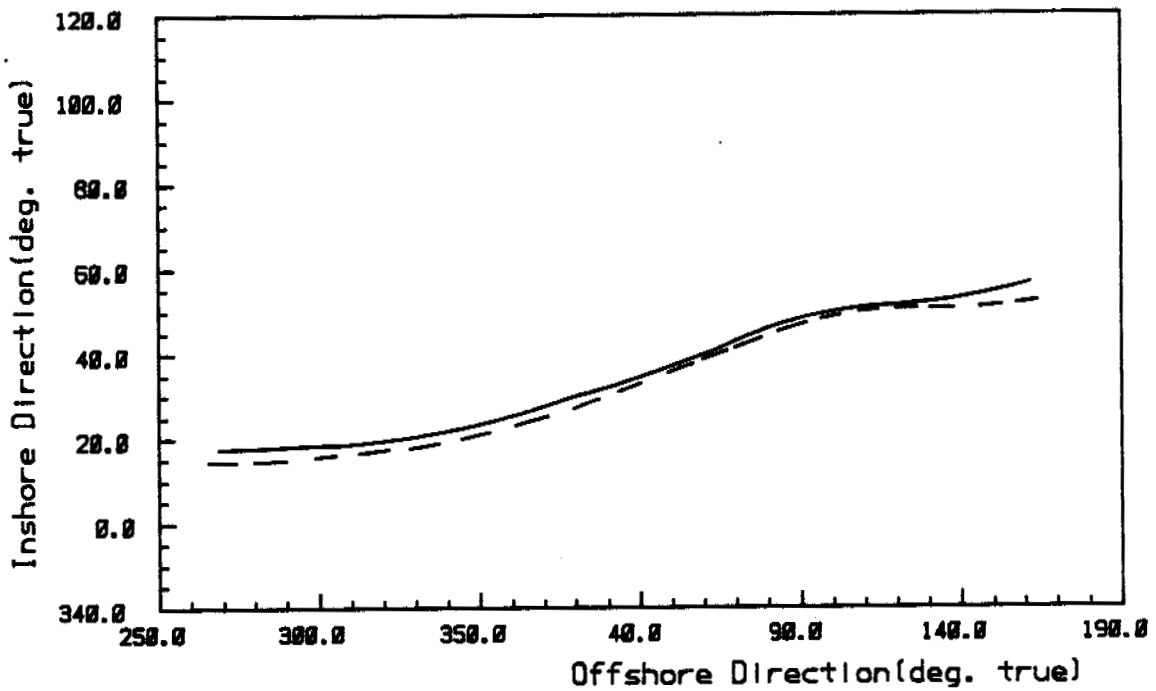
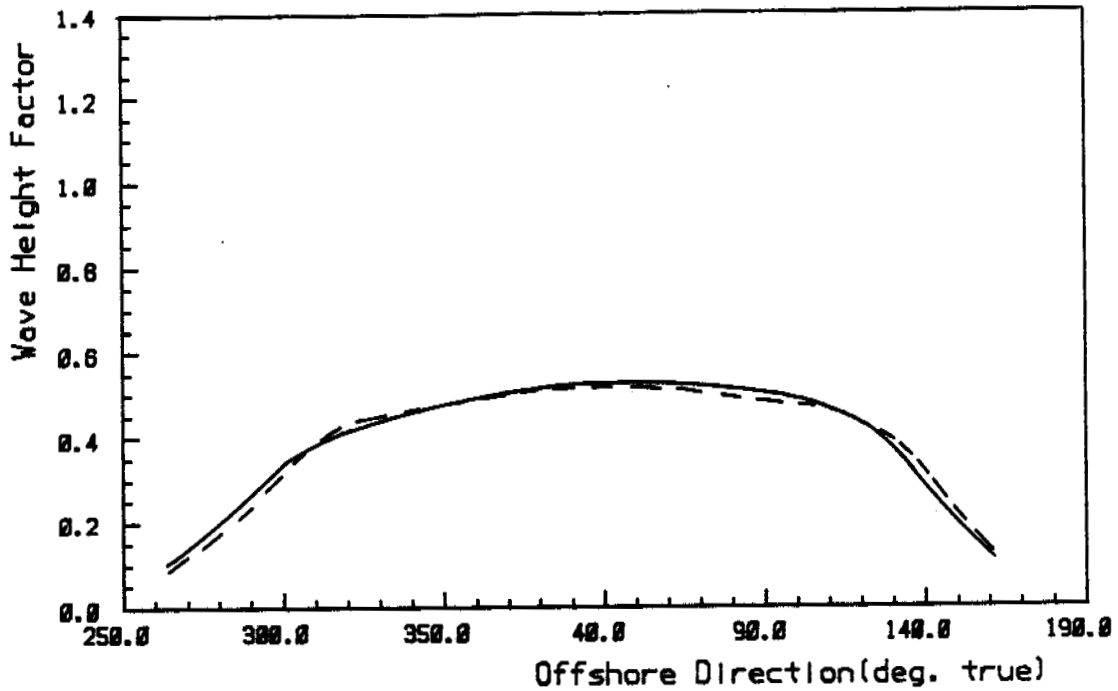
5.2.1 The Hindcast and Wave Transformation Models

The deepwater wave hindcast remains unaffected by surges. However, at sites where shallow water hindcasts were performed (North Head and Tuktoyaktuk), there will be a significant effect due to the reduced friction losses over fetches with increased water depth.

In comparing wave transformations at different water levels it is first noted that the node locations are automatically adjusted to maintain a specified water depth when the water level is changed. Consequently, if the bathymetric contours were regular and parallel to the shoreline, the wave transformation would not be influenced by a change in water level. However, due to the irregular nature of the bathymetry in the Beaufort Sea some differences are inevitable. Figures 5.1 to 5.4 show spectral transfer results for King Point at two different water levels (0.50 m and 2.25 m above CHS datum) for wave periods of 3.2 s, 5.0 s, 7.9 s and 10.0 s. The comparison shows only very small differences in the wave height factors and direction changes. This indicates that surges do not significantly affect nearshore wave transformation results at King Point.

One water level related effect which is not within the scope of the wave transformation technique used in this study concerns wave breaking over offshore shoals. A close examination of the study sites reveals that with the exception of Stokes Point and Kay Point, shoals are either very localized and some distance offshore or non-existent. At Stokes Point the shoal affects waves originating from the east, which is not the prevailing direction of wave attack. The same shoal affects the Kay Point inshore climate, where it will have had some effect. However, due to the blurring effect of directional wave spectra, the shoal has less influence than one might expect from consideration of idealized uni-directional wave fields.

FIGURE 5.1

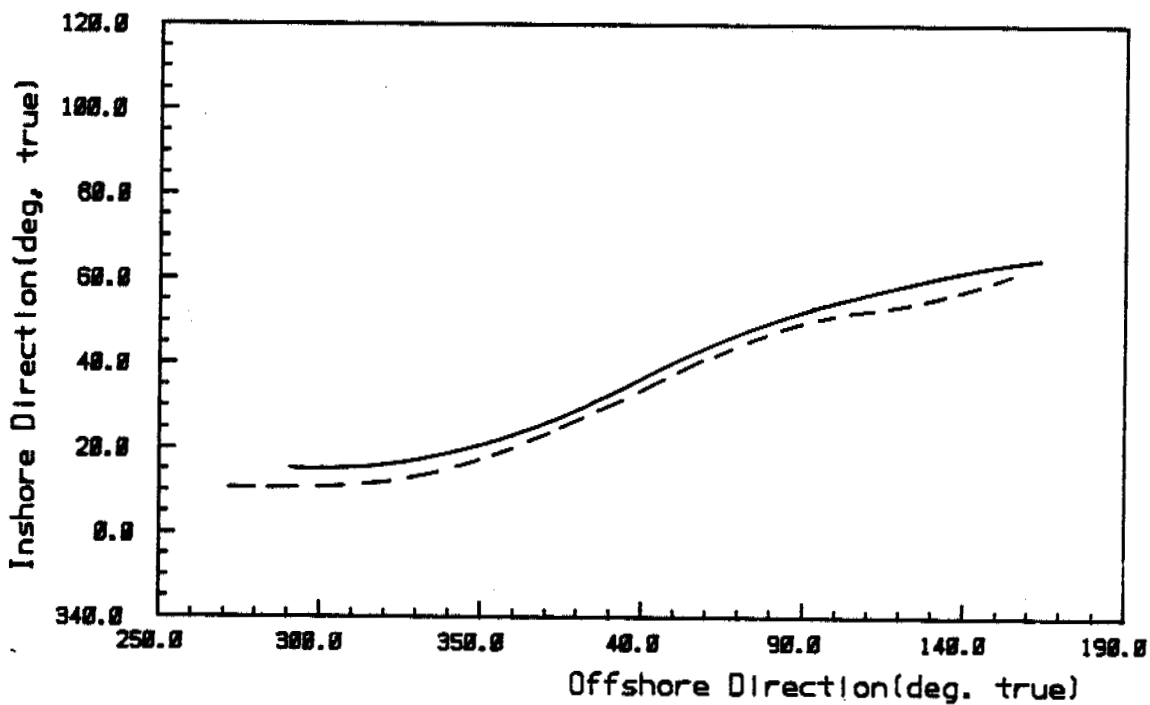
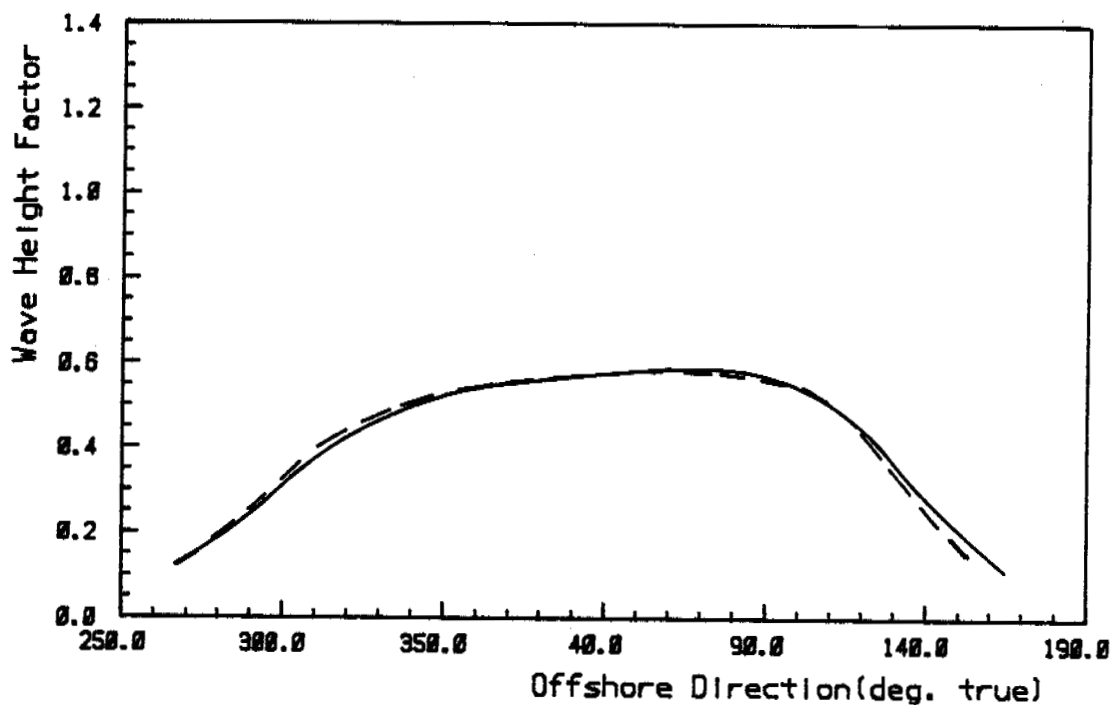


Node No: 1
Peak Period: 10.0 sec.

Spreading Index: 4
Tide Level: 0.50m ----
 2.25m ———

BEAUFORT SEA COASTAL SEDIMENT STUDY	Date: 7 May 85
	Scales as shown
King Point: Comparison of Spectral Transfer Results at Different Water Levels	Checked by:
	Keith Philpott
	Consulting Limited

FIGURE 5.2



Node No: 1

Spreading Index: 4

Peak Period: 7.9 sec.

Tide Level: 0.50m ----
2.25m ———

BEAUFORT SEA COASTAL SEDIMENT STUDY

Date: 7 May 85

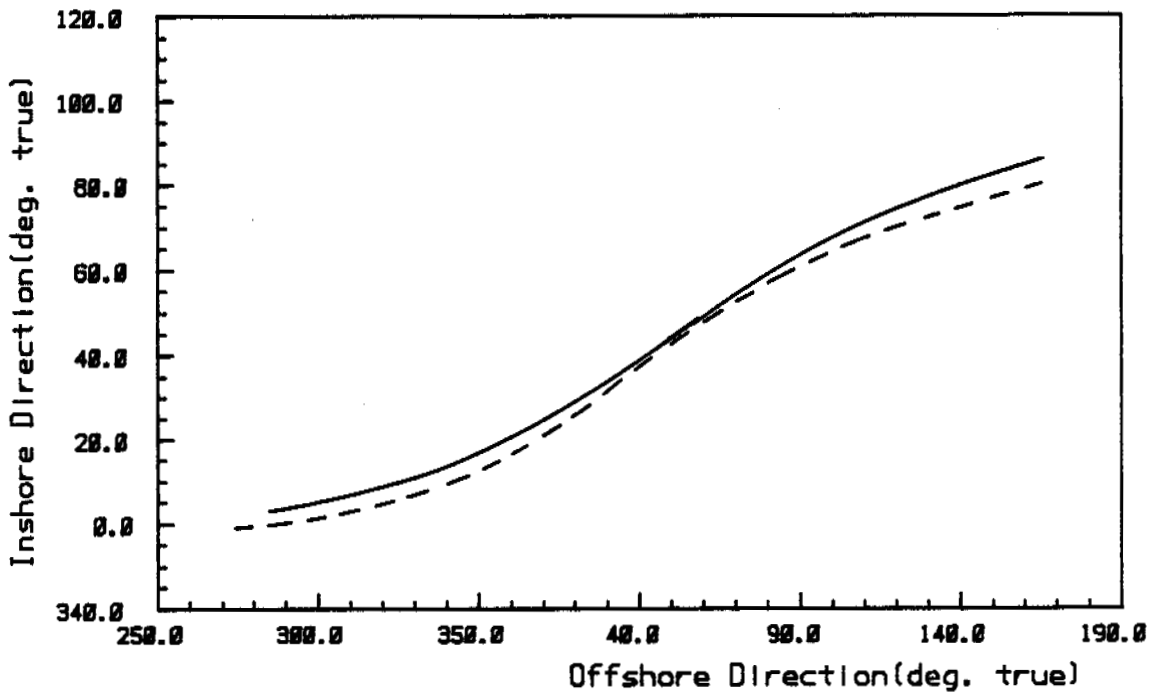
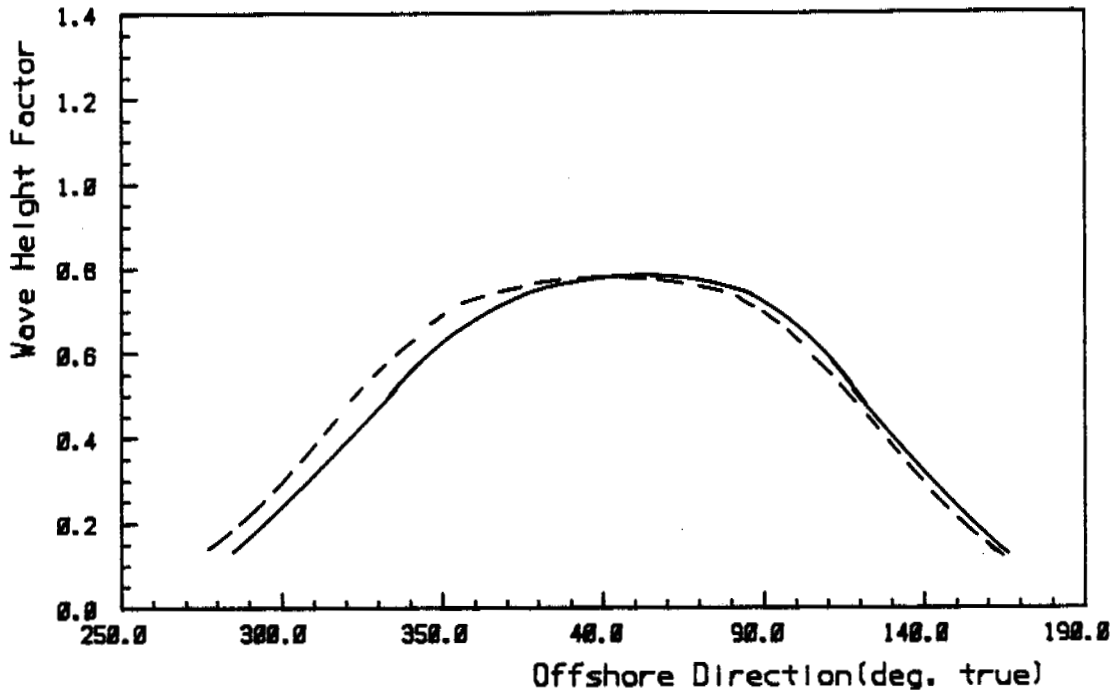
Scales as shown

Checked by:

Keith Philpott
Consulting Limited

King Point: Comparison of Spectral Transfer Results at
Different Water Levels

FIGURE 5.3



Node No: 1

Peak Period: 5.0 sec.

Spreading Index: 4

Tide Level: 0.50m ----
2.25m ———

BEAUFORT SEA COASTAL SEDIMENT STUDY

King Point: Comparison of Spectral Transfer Results at
Different Water Levels

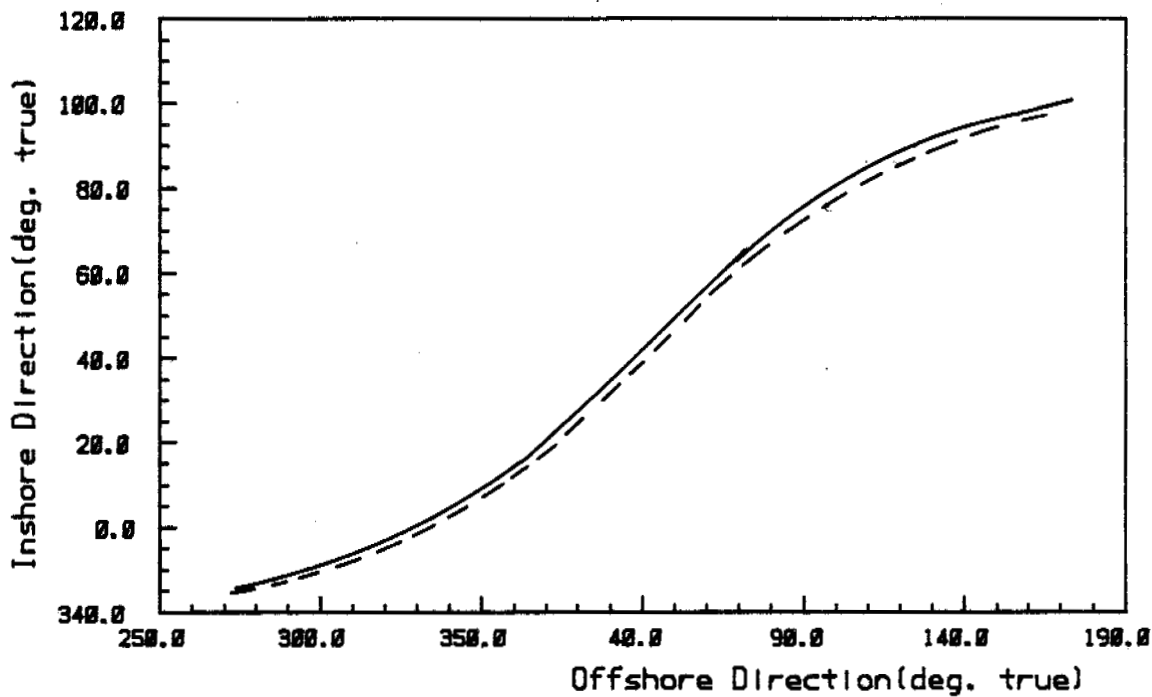
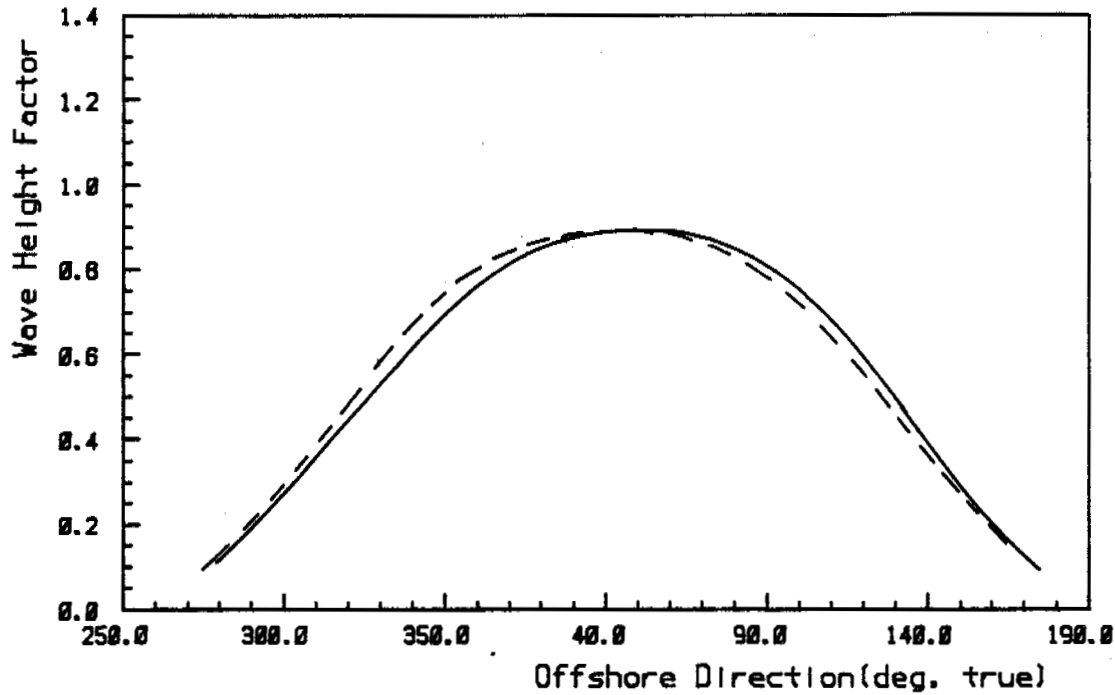
Date: 7 May 85

Scales as shown

Checked by:

Keith Philpott
Consulting Limited

FIGURE 5.4



Node No: 1

Spreading Index: 4

Peak Period: 3.2 sec.

Tide Level: 0.50m - - - -
2.25m ————

BEAUFORT SEA COASTAL SEDIMENT STUDY

Date: 7 May 85

Scales as shown

Checked by:

Keith Philpott

Consulting Limited

King Point: Comparison of Spectral Transfer Results at
Different Water Levels

5.2.2 The Alongshore Sediment Transport Package

The breaker zone moves inshore with a rise in water level and offshore with a fall. Its width may increase or decrease depending on the profile shape. Thus an increase or decrease in water level could result in a change in the effective beach slope within the zone of active sediment transport and near the beach. It may also alter the sediment particle size distribution across the surf zone due to the change in position. Evidently there would be no change in sediment transport for the case of a plane beach slope with a uniform sediment particle size distribution.

The preconception that alongshore sediment transport is always increased by raised water levels is also not supported by a detailed study of the behaviours of the various models. Changes in the slope and grain size distributions may have somewhat different effects on each of the sediment transport models employed. Thus, in profiles having varying slopes (concave, convex or undulating) with varying sediment texture, a surge may cause either an increase or decrease in transport rates. This issue is investigated further in Section 5.5.1.

5.2.3 The Nearshore Profile Adjustment

The profile adjustment model is based on the concept that a developing part of the nearshore profile evolves toward an equilibrium

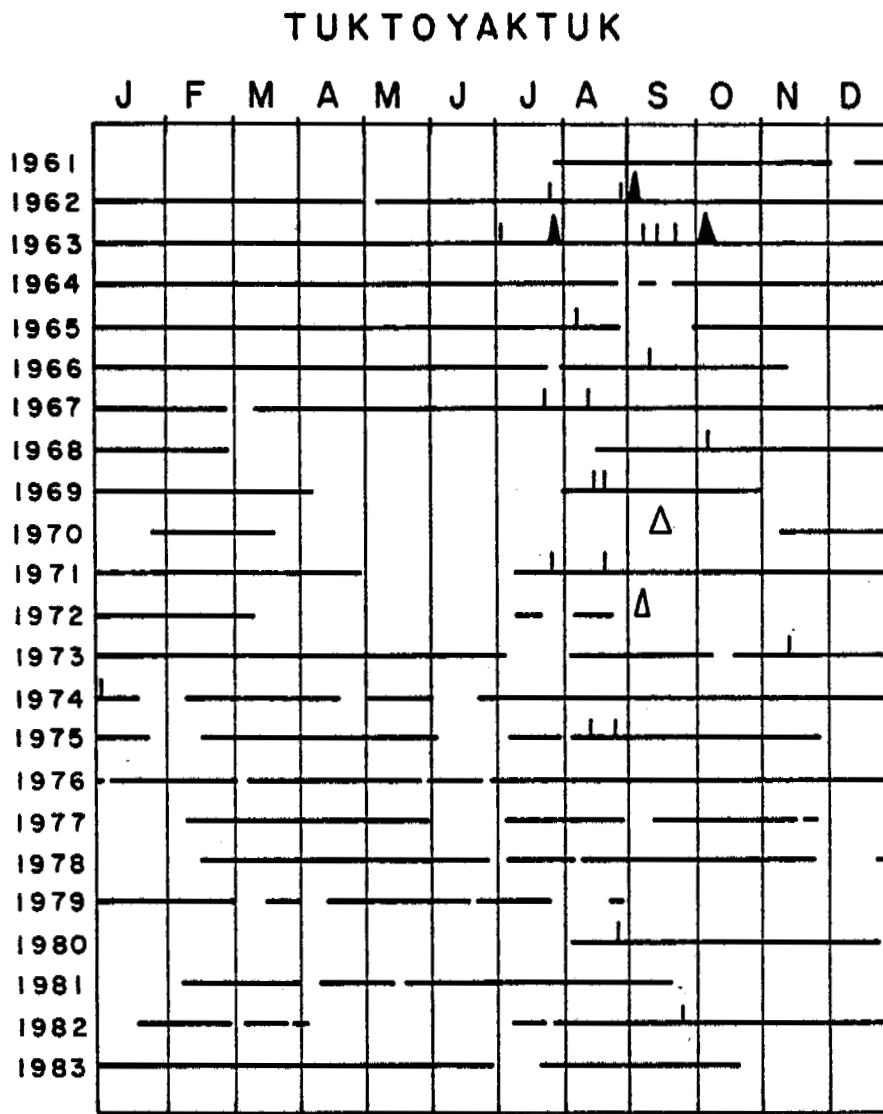
form corresponding to a specific wave condition. As the water level changes the position of the developing profile changes and consequently surges have a significant effect on profile adjustment. Section 7 of this report deals specifically with the effect of surges on the profile adjustment.

5.3 Surges in the Beaufort Sea

Both positive and negative surges are common in the Beaufort Sea. The occurrence of both types has been examined by Henry and Heaps (1976). The coastline of the Beaufort Sea is subject to positive surges when strong northwesterly to westerly winds occur during ice-free periods. The surges are amplified by the bathymetric features of Kugmallit Bay and also by the outflow of the Mackenzie River into Mackenzie Bay and to a lesser extent into Kugmallit Bay.

Negative surges occur during periods of offshore and easterly winds in the Beaufort Sea; while these surges are quite frequent, they seldom drop the water level more than a metre. (Henry and Heaps, 1976).

Tide gauges have been in operation at Tuktoyaktuk intermittently since 1961 and temporary gauges have been used elsewhere (see Figures 5.5 and 5.6). The periods of tide gauge operation and the recorded and unrecorded surges are shown in Figure 5.5 (after Henry, 1984). During the past ten years surges have been relatively insignificant. The largest known surges occurred in 1944

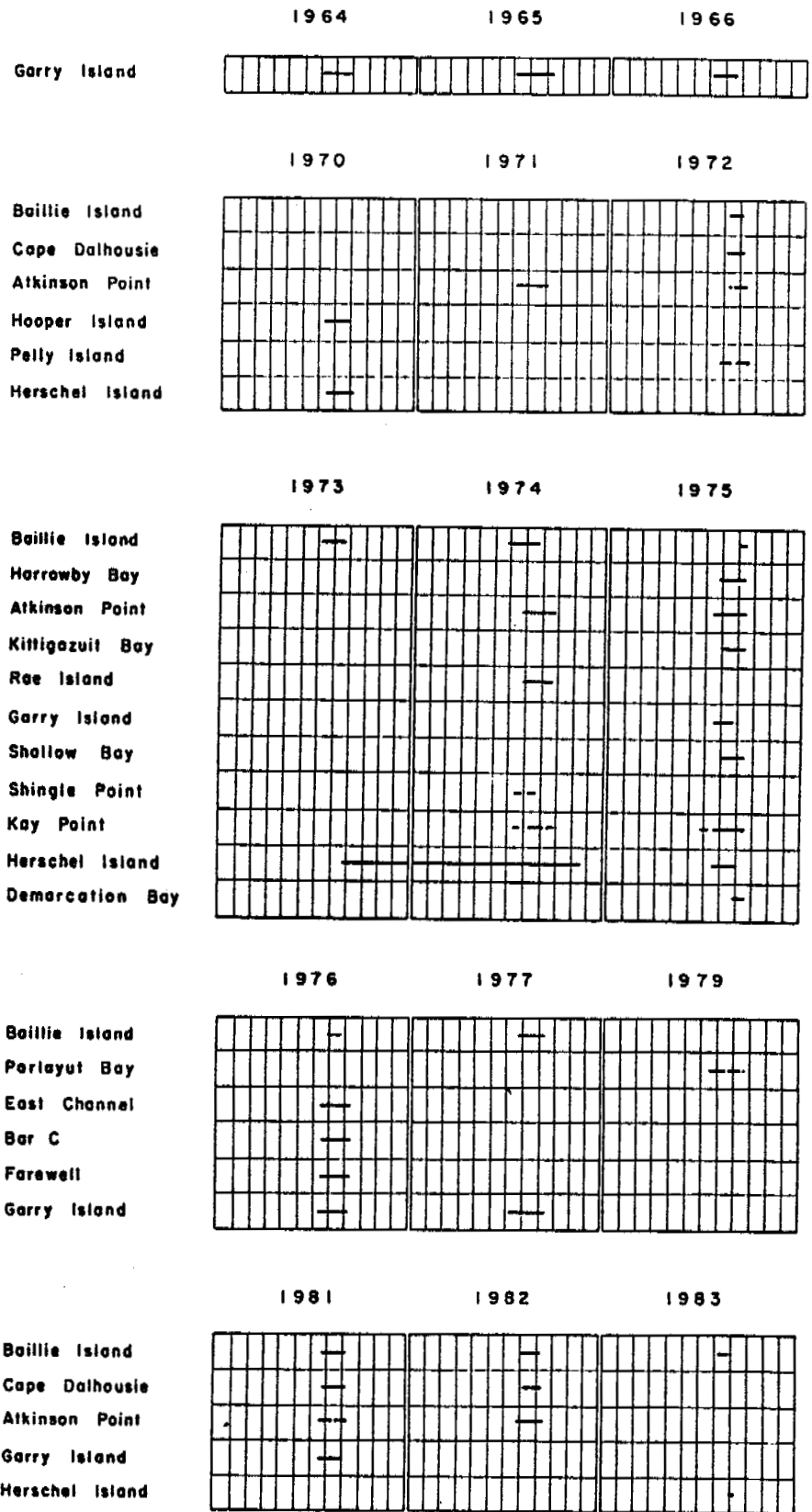


- ▲ Recorded surge > 1.5m.
- △ Unrecorded surge > 1.5m
- ⊥ Recorded surge < 1.5m

(after Henry, 1984)

BEAUFORT SEA COASTAL SEDIMENT STUDY	Date: 8 May 85
	Scales as shown
Periods of Tide Gauge Operation and Surge Occurrences	Checked by:
	Keith Philpott
	Consulting Limited

FIGURE 5.6



(after Henry, 1984)

BEAUFORT SEA COASTAL SEDIMENT STUDY

Periods of Temporary Tide Gauge Operation

Date: 15 May 85

Scales as shown

Checked by:

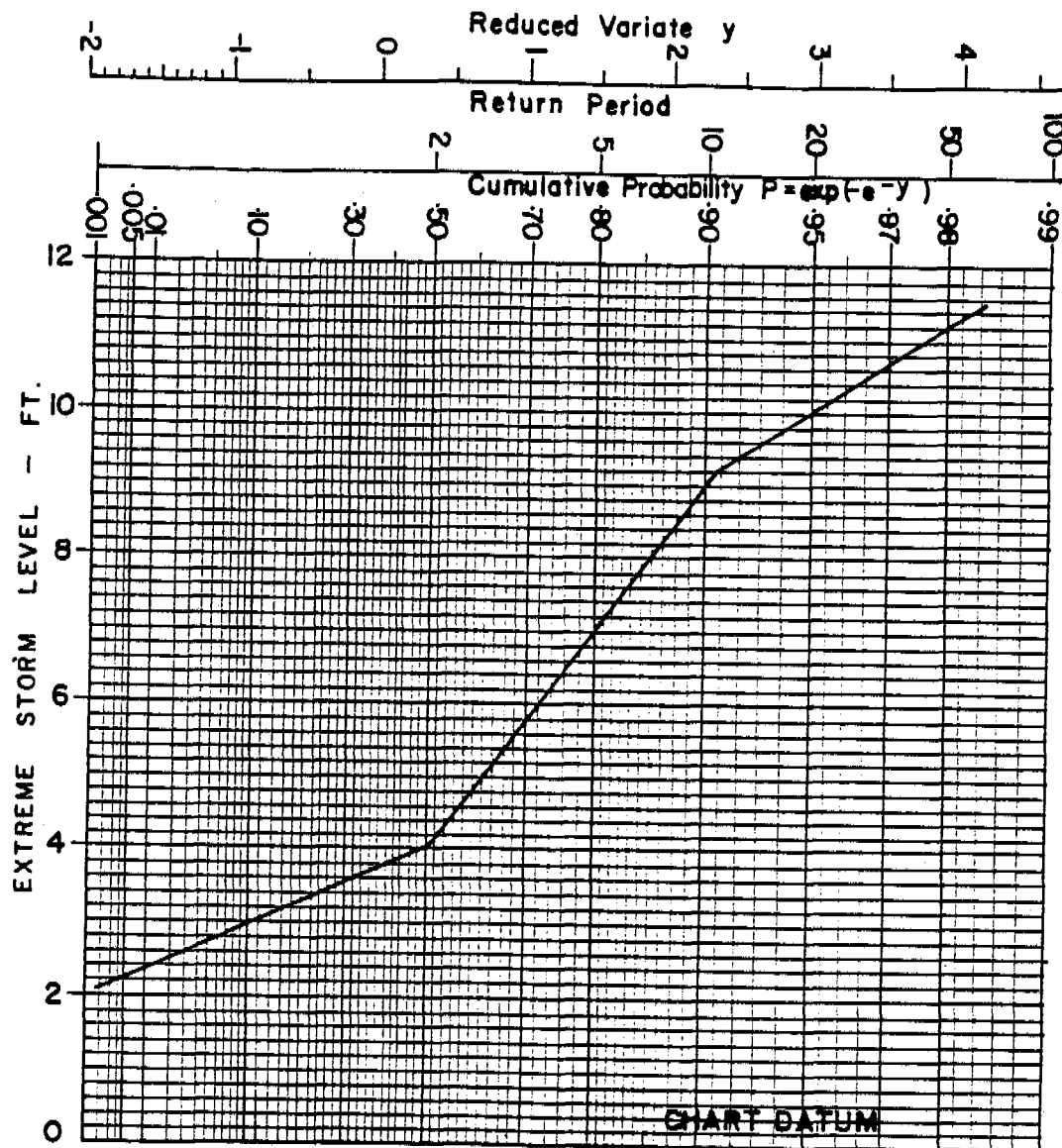
Keith Philpott
Consulting Limited

and 1970, although both were unrecorded they have been estimated to be in the neighbourhood of 3 m at Tuktoyaktuk. Henry (1984) suggested 3 m (above MWL) could be taken as a rough lower limit of the 100-year surge height at Tuktoyaktuk, including tide but excluding wind wave effects.

Henry (1984) used an explicit finite difference model to predict the 100-year storm surge. The numerical details are described in Henry (1975) and Henry and Heaps (1976). Wind stresses corresponding to a 70-year design storm were used to drive the storm surge model to determine the 100-year surge level (this was based on assumptions by Burns, 1973, and Markham, 1975, that ice cover is sufficient to prevent large storm surges in 3 summers out of 10). A 100-year surge level of 3.5 m above CHS datum was predicted at Tuktoyaktuk by the model. However, Henry (1984) qualified the result as tentative since a proper calibration was not possible due to insufficient water level data.

An earlier study at Tuktoyaktuk by Kolberg and Shah (1976) provides estimates of approximate return periods for various water levels (See Figure 5.7). These were determined using data on storm water level occurrences obtained from available references and available tidal and wind records. The estimate of the 100-year return period water level is about 3.5 m above CHS datum which agrees with the more recent study by Henry (1984).

The sensitivity analysis at King Point was performed with a large surge and also with an average surge. The large surge was



(after Kolberg and Shah, 1976)

BEAUFORT SEA COASTAL SEDIMENT STUDY

Approximate Return Periods of Extreme Storm Water
Levels at Tuktoyaktuk

Date: 8 May 85

Scales as shown

Checked by:

Keith Philipott
Consulting Limited

based on a peak height of 2.75 m above CHS datum at Tuktoyaktuk which would have an approximate return period of 1 in 20 years (according to Kolberg and Shah). The average surge was taken as one metre, typically a yearly occurrence.

5.4 Description of the Storm Even Used in the Sensitivity Analysis

The initial surge sensitivity analysis was performed at King Point using a two-day storm surge. The hybrid storm event that was simulated consisted of waves from the largest hindcast storm series (around 2 September 1972 at most sites) superimposed on a typical large storm surge water level profile represented numerically in step form. The surge was based on an assumed peak height of 2.75 m above mean water level at Tuktoyaktuk. The 2.75 m surge at Tuktoyaktuk can be translated to surge heights at the other study sites using results of the numerical model of Henry and Heaps. At King Point the factor is 0.6 and the peak surge would be 1.65 m above MWL or 2.15 m above CHS datum. Surge factors at all of the seven sites, normalized relative to Tuktoyaktuk, are presented in Table 5.1. Figure 5.8 shows the wave climate and water level time series used at King Point for the surge analysis.

5.5 Results and Comments

Table 5.1

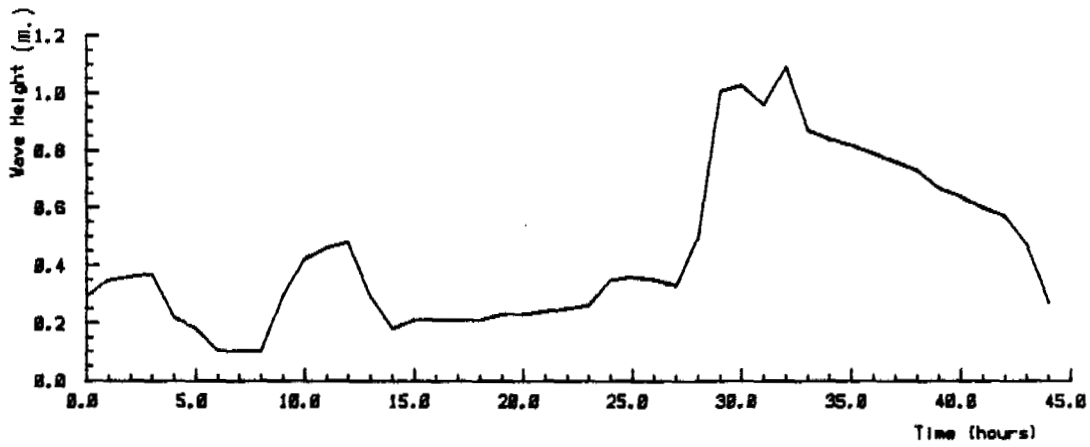
Surge Factors (after Henry, 1976)

Site	Factor
Atkinson	1.0
Kay Point	0.4
King Point	0.6
North Head	1.0
Pauline Cove	0.15
Stokes Point	0.2
Tuktoyaktuk	1.0

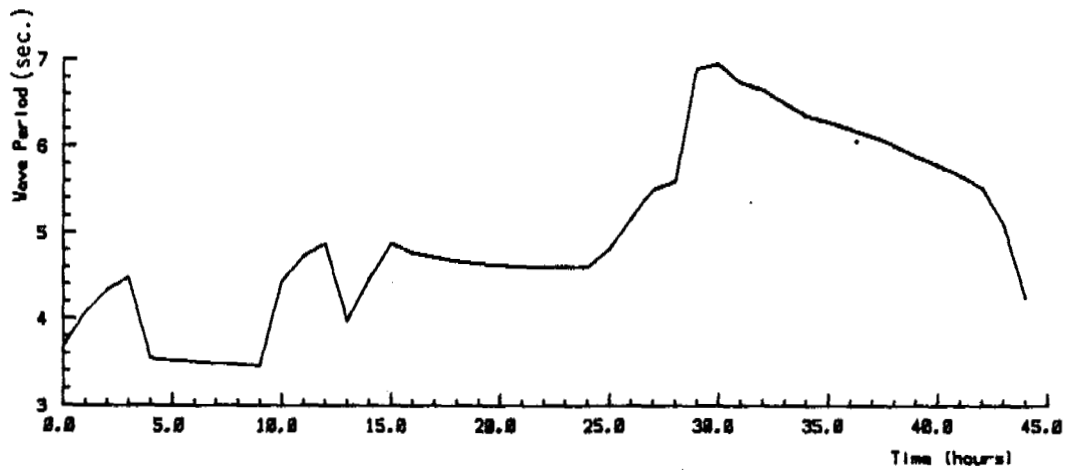
Table 5.2

Comparison of Net Sediment Transports in cubic metres at Mean Water Level and with a large Two Day Surge at King Point (node 1)

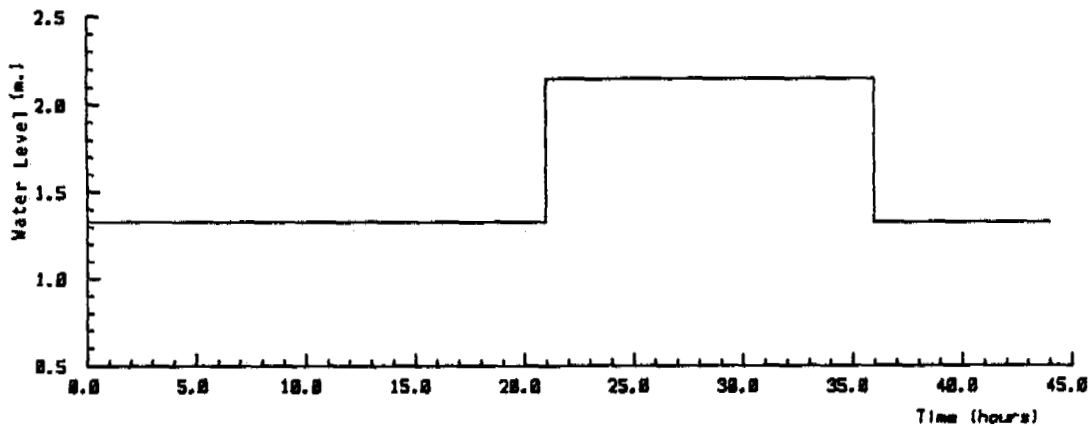
Model	At MWL	Storm Surge
CERC	5703	2722
Queen's modified CERC	3315	2536
Swart modified CERC	4886	2338
Bijker	42	0
Engelund and Hansen	2197	1602
Swart model	171	38
Willis model	3568	2318
Van Der Graaf and Overeem model	3289	2042
Nielsen model (breaking waves)	4168	3051
Nielsen model (non-breaking wave)	1794	1311
Fleming model	679	670
Swart and Lenhoff model	1970	1114



Wave Height vs Time



Wave Period vs Time



Water Level Above CHS Datum vs Time
(Mean Water Level = 0.5m)

BEAUFORT SEA COASTAL SEDIMENT STUDY

Two Day Storm Surge used for the Sensitivity Analysis
at King Point

Date: 2 May 85

Scales as shown

Checked by:

Keith Philpott
Consulting Limited

5.5.1 Alongshore Sediment Transport

The initial sensitivity analysis was performed at King Point. The results of sediment transport runs using the SEDX package, a) at mean water level and, b) with the synthesized storm surge are presented in Table 5.2.

According to all of the models used in SEDX, there is less alongshore sediment transport at the higher water level of 2.15 m above CHS Datum at node 1 at King Point. A similar result was found at node 2 with a very different upper beach profile.

A closer examination of the implications of large surges at King Point explains these results. At node 2 a 2.15 m surge would partially submerge a very steep bluff which causes a significant reduction in the width of the active sediment transport zone, and reduces the alongshore sediment transport rate.

At node 1, a 2.15 m surge would submerge the barrier beach, creating in effect, a profile with a very large bar which the model was not designed to accommodate. Consequently, a modified profile was introduced in which a long gentle upward slope was connected to the crest of the barrier at the same slope as the top of the barrier in place of the back slope. Therefore, the decreased sediment transport at node 2 during the surge can be attributed to a much less steep slope in the zone of active transport at the raised water level. This is believed to be a good simulation of what occurs in reality except that overwashing of the barrier was not included.

The analysis was repeated for a smaller surge with a peak height of 0.9m above MWL. A slight decrease in sediment transport was observed at both nodes.

The greatest effect was found at Atkinson Point where similar surge sensitivity calculations were made. There, large surges (with a peak height of 2.75m above MWL) were found to increase the alongshore transport to a significant extent (by approximately 50%). Smaller surges with a peak height of 1.5m above MWL do not significantly increase the transport (less than 10% during a storm event). In that case the profile was moderately convex and the grain size was taken to be constant. Taking account of surge frequencies it is inferred that the effect of surges on the annual rate at Atkinson Point would be to increase it by 5-10%, which is not significant compared to the standard deviation of sediment transport estimates (see Section 6.4.2).

A sensitivity analysis was also completed at Tuktoyaktuk. The shallow water wave hindcast and the wave transformations were repeated at storm surge depths. While the inshore wave heights were greater, the sediment transport during the storm surge decreased significantly because the sediment distribution changes in the shoreward direction from sand to gravel, which is less mobile. A similar trend was evident for small surges.

Surges at Kay Point, Stokes Point, and Pauline Cove are not significant (see Table 5.1). A surge sensitivity analysis could not

be completed at North Head due to a lack of profile data above mean water level.

The sensitivity analyses at Atkinson Point, King Point and Tuktoyaktuk demonstrate that the response of alongshore sediment transport to water level changes is site dependent. The response is very sensitive to input parameters which characterize the raised water level zone of active transport. It would appear that in cases where the slope of the surge-inundated area is either much steeper (in the case of bluffs) or much more shallow (in the case of low-lying areas), sediment transport will tend to be reduced.

The foregoing results, in general, show that the effects of elevated water levels on alongshore sediment transport cannot on their own account for large shoreline recessions known to have occurred. However because they usually occur in conjunction with severe wave conditions, storm surges are, in fact, normally associated with major sediment transport events that accompany the more striking examples of coastal change.

5.6 Implications of the Surge Sensitivity Analysis

The onshore-offshore sediment transport model (SEGAR) shows much greater sensitivity to water level changes associated with storm surges, this is reported in Section 7. It can be postulated that alongshore sediment transport plays an important interactive role in profile adjustment. However, this is not reproduced directly with the techniques employed in this study.

Considering that the sensitivity of the profile adjustment model to water level changes overshadows the sensitivity of the alongshore sediment transport models, the fourteen year sediment transport runs have been performed at mean water level (0.5 m above CHS datum) for each site. The assessment of the recession rates and the change in morphology at each of the study sites will have to incorporate both the sediment transport results and the onshore-offshore profile change results.

SECTION 6 LITTORAL TRANSPORT ESTIMATION

The sediment transport numerical modelling package, SEDX, was implemented at two inshore nodes for each of the following sites: Stokes Point, Kay Point, King Point, North Head, Tuktoyaktuk, and Atkinson Point. A detailed description of SEDX is given in Fleming, Philpott, and Pinchin (1984); only a summary is provided herein.

6.1 Outline of Method

The sediment transport rates were computed using data from the hindcast, statistical analysis, spectral transfer and refraction analysis stages. The procedure used was as follows:-

- .Hindcast hourly deep water significant wave conditions for the fourteen year period 1970-1983.
- .Collate these wave conditions into statistical groups of 10 degree directional increments, 0.3 m wave height increments and 0.5 s wave period increments.
- .Transfer the offshore statistics to corresponding inshore statistics. This was done by combining the offshore statistics with the spectral transfer output.
- .Apply the alongshore sediment transport suite SEDX to the inshore wave conditions to compute alongshore transport rates using twelve different models.

6.2 Alongshore Sediment Transport Package

The sediment transport package, SEDX, incorporates three variants of the bulk energy model and nine different detailed predictor models (see Table 6.1). The detailed predictor models are coupled with a longshore current model.

6.2.1 Bulk Energy Models

The three total energy bulk alongshore sediment transport models assume that the available energy of waves approaching the shoreline can be related to the alongshore sand transport rate. All three methods are variants of the U.S. Army Coastal Engineering Research Centre, Shore Protection Manual original model. The metric version of the original formula is:

$$q_{ls} = 0.01974 T_p (H_{OS} K_R)^2 \sin(2\alpha_b) \quad (6.1)$$

where q_{ls} is the alongshore sediment transport rate in m^3/s , T_p is the peak wave period, H_s is the deepwater significant wave height, K_R is the refraction coefficient and α is the wave breaker angle to the shoreline. Swart (1976b) introduced a parameter to account for the grain size of the bed material. This parameter can be represented as a factor,

$$K = 1.466 \log_{10} \left(\frac{0.00146}{D_{50}} \right) \quad (6.2)$$

to be applied to Equation 6.1 (D_{50} is the median grain diameter).

Table 6.1

The Sediment Transport Models - References
and General Classification

Model/Name	References	General Classification
1. CERC Formula	U.S. Army Coastal Engineering Research Centre - CERC (1977)	Bulk energy model
2. Queen's modified CERC Formula	Kamphuis and Sayao (1982) Davies (1984)	Bulk energy model
3. Swart modified CERC Formula	Swart (1976b)	Bulk energy model
4. Bijker Formula	Bijker (1971)	Based on bed and/or suspended load concentration
5. Engelund and Hansen (by Swart)	Swart (1976b)	Based on bed and/or suspended load concentration
7. Swart model	Swart (1976a)	Adaptation of Ackers and White
8. Willis model	Willis (1978)	Adaptation of Ackers and White
9. Van der Graaf and Van Overeem	Van der Graaf and Van Overeem (1979)	Adaptation of Ackers and White
10. Nielsen model (breaking waves)	Nielsen et al., (1978) Nielsen (1979)	Based on bed and/or suspended load concentration
11. Nielsen model (non-breaking waves)	Nielsen et al., (1978) Nielsen (1979)	Based on bed and/or suspended load concentration
12. Fleming model	Fleming (1977)	Based on bed and/or suspended load concentration
13. Swart and Lenhoff model	Swart and Lenhoff (1980)	Adaptation of Ackers and White

Sayao and Kamphuis (1982) introduced the surf similarity parameter to account for the effect of beach slope and the rate of wave energy dissipation. To be applied to Equation 6.1 this parameter can be described as a multiplying factor,

$$\kappa = \frac{\kappa 2m \sqrt{\gamma_b}}{0.77} \quad (6.3)$$

where γ_b is the breaker index and m is beach slope.

Recently, Davies (1984) has developed an expression for κ from a study of field experiments. He found κ was related to suspended sediment concentration which was a function of energy density per wave at breakpoint, E_{bw} , defined as

$$E_{bw} = \frac{\rho g^{3/2} H_b^2 d_b^{1/2} T}{8} \quad (6.4)$$

where ρ is the density of water and d_b is the breaker depth.

The expression for κ was found to be:

$$\kappa = \left[\frac{E_{bw}}{E_{bw_c}} \right]^{0.54} \quad (6.5)$$

with $E_{bw_c} = 0.95$ KJ/wave/m crest.

6.2.2 Detailed Predictors

The remaining models may be classed as detailed sediment transport predictors. These provide either, a) suspended load plus bed load, or b), total estimates of sediment concentration

which is then transported by the action of background currents. All such models have been developed for use with linear wave theory and require a current to be applied for any net movement to take place. A brief description of these models is provided here. The models fall into two very general categories, those which are similar to the Bijker (1971) derivation (e.g. includes a suspended load distribution and usually a bed load expression) and those which are modifications of the Ackers and White (1973) formula.

6.2.2.1 Bijker Related Models

Bijker's original formula developed in 1967 is one of the earliest attempts to describe in detail both bed load and suspended load due to waves and currents. The bed load formula was adapted from the Frijlink (1952) formula for sediment transport in unidirectional flow by modifying the shear stress terms to account for the stirring action of waves. The suspended load is found by defining the Rouse-Einstein distribution of suspended material from the bed to the free surface and integrating the product of this distribution and instantaneous velocity through the depth. (See Einstein, 1950). Although the formula contains no inception of motion criterion, the transport rates predicted for shear stresses below the threshold shear are very low.

Swart (1976a) adapted the original formula by Engelund and Hansen (1967) for the prediction of total sediment transport rates in any depth under steady flow conditions in an analogous manner to the Bijker formula. The expression does not contain an initiation of movement criterion either.

Fleming (1977) developed a transport formula from which the bed load and suspended load for wave action can be predicted. He defined a reference concentration close to the bed and used a force balance of bed particles to derive a theoretical expression for its value. It contains an incipient motion criterion. It also assumes that the concentration at the bed cannot exceed 0.52 and that the eddy diffusivity is constant above the bed load region. Integration of the product of concentration and a one-seventh power law velocity distribution through the depth provides the transport rate.

Nielsen (1979) and Nielsen et al. (1978) determined the distribution of suspended sediment with distance from the bed for breaking (spilling breakers) and non-breaking wave conditions in the laboratory. The data were used to develop quantitative predictors for the eddy diffusivity, which were found to be constant with distance from the bed for non-breaking waves and increasing strongly with distance from the bed for breaking waves. Nielsen also defined a reference concentration at the top of the bedforms. It contains an incipient motion

criterion. The total load transport rate is determined by integrating the product of the respective concentration distribution (either for non-breaking or breaking waves) with the one-seventh power law velocity distribution. The Nielsen derivation assumes all transport is by suspension.

6.2.2.2 Adapted Ackers and White Models

Ackers and White (1973) developed a technique for estimating sediment load in unidirectional flow by considering that the work done in moving sediment is the product of the power available to move the sediment and the efficiency of the system. Their derivation makes a distinction between bed load and suspended load on the basis of dimensionless grain size and not on the basis of position in the water column. Distinct ranges of dimensionless grain size are considered to be moved predominantly as bed load, as suspended load or by a mixture of both. A threshold of sediment movement criterion is included.

In his version of the Ackers and White formula, Syart (1976b) adapted the fine grained component of shear stress to include the effect of wave action. A subsequent version adjusted initiation of movement relationships.

Willis (1978) concluded that the critical (incipient motion) value of mobility number given by Ackers and White is different for combined wave and current action from the value for currents alone. To compensate for this difference he multiplied the wave induced shear stresses by an empirical coefficient which is a function of grain size. Willis also adapted both the fine grained and coarse grained components of shear stress to include the effect of wave action.

Van der Graff and Van Overeem (1979) added the effect of waves on shear stresses to both the fine-grained and coarse-grained components of shear. At the same time, they used the same critical mobility number as for steady state conditions as well as a steady state formulation for wave power.

Another version of the Ackers and White formula has been developed by Swart and Lenhoff (1980). This version integrates all instantaneous time dependent variables through a wave period. Values for instantaneous resultant velocity at the bed and instantaneous shear stress at the bed are found by vector addition of the contributions by the waves and the currents. An empirical formulation of critical mobility number is developed from 800 data sets for a wide range of flow conditions including:

- observed incipient motion on a flat bed for waves only
- observed incipient motion on a rippled bed for waves only
- observed incipient motion on a flat bed with waves and currents
- sediment load data over rippled beds for waves only
- sediment load data over rippled bed with waves and currents.

6.2.3 Alongshore Current Model

The rationale behind the SEDX package approach is explained by Swart and Fleming (1980). In order to objectively compare results from the different sediment transport formulae the input variables must be determined consistently. Accordingly, the same longshore current model should be used in each detailed predictor. A new framework for the prediction of alongshore currents was proposed by Fleming and Swart (1982). A brief summary of the principles and assumptions they applied follows.

The magnitude and distribution of the wave-driven alongshore current in the breaker zone depends on the momentum balance, which in turn depends on the underwater profile, the incident wave characteristics and the wave breaking mechanism.

In 1970 Longuet-Higgins solved this momentum balance equation in the alongshore direction in the shore area by making specific assumptions regarding three individual terms; namely, the driving force or radiation stress term, the bed shear and the lateral mixing, the latter two being dissipative terms.

The momentum balance in the alongshore direction x as given by Longuet-Higgins is:

$$\frac{\partial R_{yx}}{\partial y} + B_x + \frac{\partial D_y}{\partial y} = 0 \quad (6.6)$$

where $\frac{\partial R_{yx}}{\partial y}$ = variation in flux of x -momentum with distance y offshore;

B_x = bed shear in the direction of the longshore current; and

$\frac{\partial D_y}{\partial y}$ = exchange of momentum due to lateral mixing.

The type of solution obtained, or more specifically the variation of the current with distance offshore, depends on the assumptions made regarding these three terms.

Predicted alongshore sediment transport rates are very sensitive to the distribution and magnitude of the alongshore current. An error in prediction of the alongshore current of 10 percent could cause an error in the prediction of the alongshore

sediment transport of as high as 70 percent. (Fleming and Swart, 1982).

In a laboratory study into current patterns in the vicinity of a proposed coastal structure, it was observed that alongshore current velocities generated by regular waves on a very flat beach (a slope of 1 in 100) were between 2 and 5 times higher than predictions with the Longuet-Higgins model would tend to indicate (CSIR, 1978). This anomaly is seemingly coupled to the bed roughness.

Fleming and Swart in a reanalysis of the data originally used by Longuet-Higgins, developed a functional expression for the roughness parameter C_{LH} used by Longuet-Higgins to determine bed shear. Many investigators have assumed C_{LH} to be a constant equal to 0.01; Fleming and Swart have shown it is in fact related to bed slope and bed roughness as follows:

$$C_{LH} = 25 \left[\frac{f_w g}{2C_h} \right]^{0.5} (\tan m)^{0.85} \quad (6.7)$$

where

C_h = Chezy roughness coefficient

f_w = wave friction factor.

m = beach slope

A theoretical framework for the prediction of alongshore currents generated by random waves was developed by Battjes (1974) which yielded reliable results. It is comparable to the Longuet-Higgins approach for regular waves except that wave set-up was not neglected and for the obvious differences between regular and random waves. The method has to be applied numerically since no analytical solution was found. Battjes draws the very important conclusion that lateral mixing is not important in the determination of the velocity profile for random waves and may therefore be omitted.

For SEDX a derivation for random waves was carried out at the same level of assumption as used by Longuet-Higgins for regular waves:-

- (i) Linear wave theory is used;
- (ii) Waves are random with a Rayleigh height distribution;
- (iii) Waves break as spilling breakers with a constant breaker index $\gamma_b = H_b/d_b$ throughout the breaker zone;
- (iv) The wave spectrum within the breaker zone is treated in the same way as by Battjes (1974), that is, waves in excess of γ_b times the

water depth are reduced to γ_b times the water depth;

- (v) Wave set-up is initially neglected and the implication is discussed in Fleming and Swart (1982);
- (vi) The bed slope m in the breaker zone is considered constant;
- (vii) The bed roughness coefficient C_{LH} is constant over the breaker zone; and
- (viii) Lateral mixing is neglected (Battjes, 1974).

The final expression for longshore currents is given as

$$V = V_{oir} f(y) \quad (6.8)$$

where

$$V_{oir} = \frac{5\pi}{16} \frac{\gamma_b (gd_{bs})^{0.5}}{C_{LH}} \tan m \sin \alpha_{bs} \cos \alpha_{bs} \quad (6.9)$$

and

$$f(y) = \left(\frac{d}{d_{bs}}\right) \left(\frac{d}{H}\right) \gamma_b \exp\left(-\frac{\alpha_b^2 d^2}{H_{frms}^2}\right) \quad (6.10)$$

where H_{frms} = fictitious rms wave height at water depth d , which would have existed under the influence of shoaling, refraction, and bed friction if no wave breaking had occurred.

\bar{H} = mean wave height at depth d , after including the effect of wave breaking and subscript bs refers to the significant breaker line.

6.3 Application of the Alongshore Sediment Transport Model

6.3.1 Optional Modes of Operation

A complete summary of the different operational modes in the sediment transport package is presented in Fleming, Philpott, and Pinchin (1984). Only an update of additional features which have been incorporated into the model in the interim is presented.

In order to apply SEDX to shorelines with coarse-grained sediment a change had to be made to allow the option of calculating the roughness length on the basis of $2 \cdot D_{90}$ instead of ripple height. This alteration reflects the assumption that ripples do not form on gravel beds.

For the detailed predictor transport models, the profile is divided into sediment transport zones. The availability of sediment distributions at different depths along the profile prompted another change in SEDX to incorporate this more detailed information.

6.3.2 Input Data

Several input parameters were common to the six sites where SEDX was implemented. At each site an average water temperature of one degree Celsius was used for the computation of kinematic viscosity. Also, for each site, for the sediment, a relative mass density of 1.52 and a porosity of 0.6 were used. The porosity is required for mass transport to volume conversions.

Site specific information is summarized for each node at each site in tables preceding the detailed sediment transport results given in Part II of this report. As an example, the data at King Point is examined herein (See Table 6.2). Information is presented for both nodes on this table. The first item is the profile data and the corresponding profiles for King Point are shown in Figure 6.1. (Beach profiles are presented for each site in Part II of this report). The profile data is followed by the input grain size distributions. At node 1, the first distribution shown (a gravel) applies to zone 1 on the profile, profile zones 2 to 8 are characterized by the second grain size distribution which is a medium to fine sand. The chosen option for calculating bottom roughness is also shown alongside the grain size distributions. The next data item is the depth at the node which was set in the refraction analysis. The U.T.M. coordinates of each node used in the study are

Table 6.2 - King Point, Input for SEDX (Nodes 1 and 2)

BEAUFORT SEA COASTAL SEDIMENT STUDY

Current date is 02/27/85
Current time is 17:45:45.45

14 YEAR AVERAGE SEDIMENT TRANSPORT HINDCAST

WAVE DATA IS HINDCAST FROM TUKTOYAKTUK N.W.T. WINDS

This run used the following sediment transport models

- 1 CERC formula
- 2 Queen's modified CERC (March 1985)
- 3 Swart modified CERC
- 4 Bijker formula
- 5 Engelund and Hansen (by Swart)
- 7 Swart model
- 8 Millis model
- 9 Van Der Graaf and Overveen model
- 10 Nielsen model (breaking waves)
- 11 Nielsen model (non breaking waves)
- 12 Fleming model
- 13 Swart and Lenhoff model

KING POINT NODE 1 MEAN WATER LEVEL

Profile Data

	Zone	1	2	3	4	5	6	7	8
Shoreline O/S to mid-zone		3.2	12.7	25.2	44.0	131.5	356.5	586.5	886.5
Sed. Transport Zone Width		6.5	12.5	12.5	25.0	150.0	300.0	160.0	280.0
Depth at Centre of Zone		.25	.75	1.25	2.00	3.00	4.50	6.75	9.25
Sediment Transport Switch		On	On	On	On	On	On	On	On

Input Grain Size Distribution (mm)

Zone	D16	D25	D35	D50	D65	D75	D84	D90	
1	.710	1.900	4.900	8.300	12.700	16.200	21.200	25.000	Roughness Based on 2090
2 to 8	.168	.210	.265	.380	.520	.730	1.045	1.390	Roughness Based on Ripple Height

refraction analysis was to a depth of 4.0 meters
beach normal azimuth = 43.5 degrees
weighted breaker depth = .67 meters

KING POINT NODE 2 MEAN WATER LEVEL

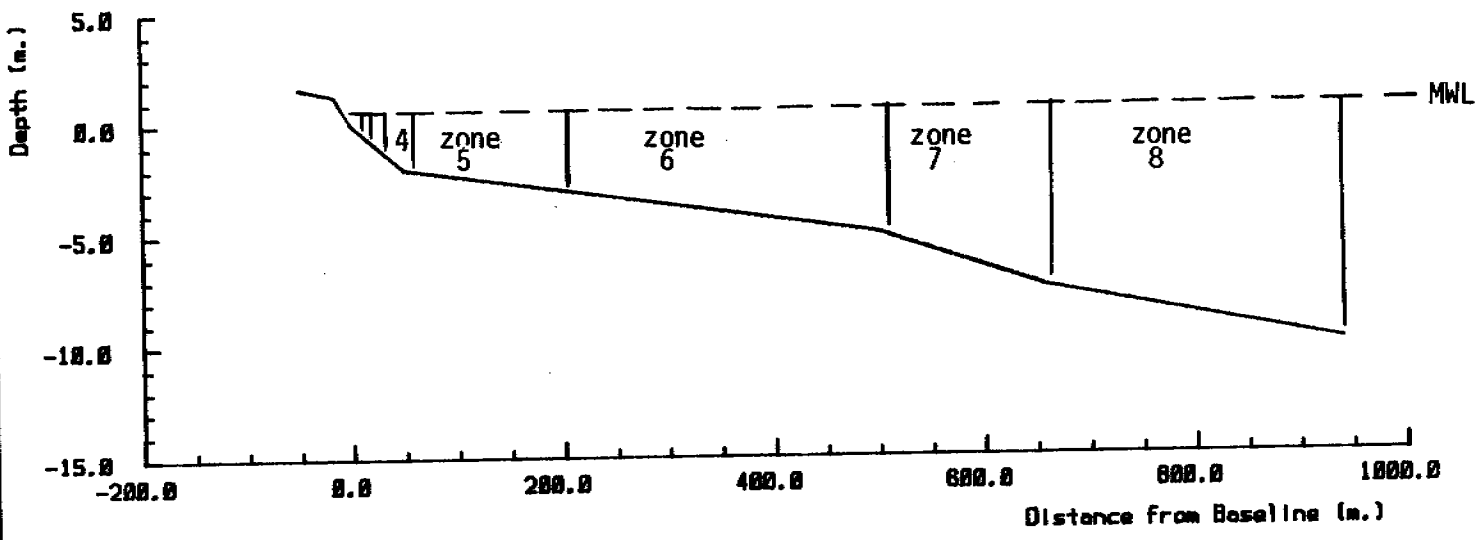
Profile Data

	Zone	1	2	3	4	5
Shoreline O/S to mid-zone		3.6	12.3	32.3	107.3	282.3
Sed. Transport Zone Width		7.3	10.0	30.0	120.0	230.0
Depth at Centre of Zone		.25	.75	1.75	4.00	8.00
Sediment Transport Switch		On	On	On	On	On

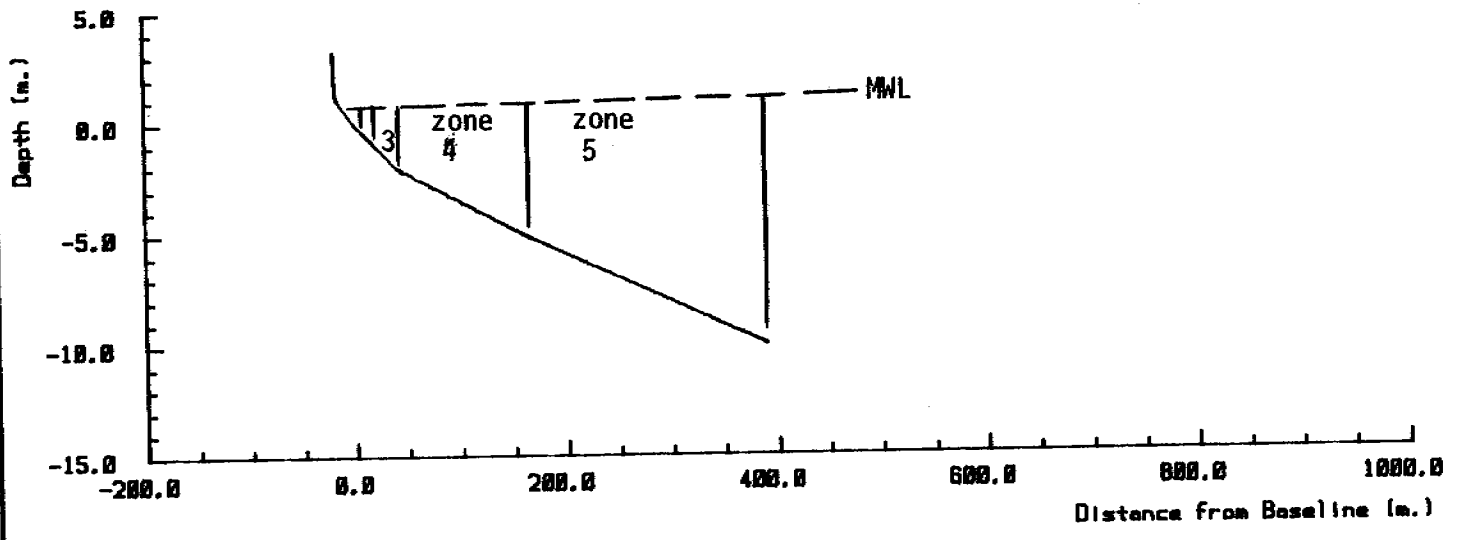
Input Grain Size Distribution (mm)

Zone	D16	D25	D35	D50	D65	D75	D84	D90	
1	.710	1.900	4.900	8.300	12.700	16.200	21.200	25.000	Roughness Based on 2090
2 to 5	.168	.210	.265	.380	.520	.730	1.045	1.390	Roughness Based on Ripple Height

refraction analysis was to a depth of 4.0 meters
beach normal azimuth = 38.0 degrees
weighted breaker depth = .68 meters



(a) Profile at Node 1



(b) Profile at Node 2

BEUFORT SEA COASTAL SEDIMENT STUDY

King Point: Beach Profiles used in Sediment Transport Predictions

Date: 15 Mar 85
 Scales as shown
 Checked by:
 Keith Philippott
 Consulting Limited

provided on the location plans in Part II of this report. The beach normal azimuth of the profile used in the sediment transport calculations is also given. Finally, the weighted (or average) breaker depth provides an indication of the intensity of the inshore wave climate.

6.4 Sediment Transport Results

6.4.1 Form of Results

The results for King Point (node 1) are presented in the following pages. Complete sets of results (excluding Pauline Cove) are presented in Part II of this report. The six basic forms of output are described as follows:

Tables 6.3 and 6.4. Gross, net, positive and negative sediment transport rates for each profile zone and in total across the profile. Positive values are defined as clockwise with respect to the beach normal and negative is counter-clockwise with respect to the beach normal. Cumulative distribution of net sediment transport and percentage distribution of net sediment transport across the profile. The detailed output for King Point is also presented in graphical form in Part II of this report.

Table 6.3 - King Point SEDX results (I) - Node 1

RESULTS OF ALL WAVE CONDITIONS

KING POINT NODE 1, MEAN WATER LEVEL

GROSS SEDIMENT TRANSPORT RATES (cu.m./m./yr.)

Model	B(1)	B(2)	B(3)	B(4)	B(5)	B(6)	B(7)	B(8)	Total Transport (cu.m./yr.)
1									.4480E+05
2									.1652E+05
3									.4032E+05
4	.0000E+00	.1665E+02	.2880E+02	.7312E+00	.1191E-32	.0000E+00	.0000E+00	.0000E+00	.4864E+03
5	.2612E+02	.1645E+04	.7743E+03	.1353E+03	.7252E+01	.7803E-02	.0000E+00	.0000E+00	.3488E+05
7	.0000E+00	.7431E+02	.8427E+02	.1888E+02	.2021E-01	.0000E+00	.0000E+00	.0000E+00	.2257E+04
8	.6346E+02	.2284E+04	.1268E+04	.2943E+03	.3195E+02	.1877E+00	.0000E+00	.0000E+00	.5592E+05
9	.5236E+01	.2284E+04	.1159E+04	.1968E+03	.8007E+01	.7574E-02	.0000E+00	.0000E+00	.4928E+05
10	.2337E-01	.2388E+04	.1863E+04	.1916E+03	.1031E+02	.1386E-01	.0000E+00	.0000E+00	.4949E+05
11	.4850E+00	.9129E+03	.4555E+03	.1210E+03	.1038E+02	.1385E-01	.0000E+00	.0000E+00	.2168E+05
12	.1564E+02	.5127E+03	.2846E+03	.3531E+02	.2073E+01	.6996E-02	.0000E+00	.0000E+00	.1026E+05
13	.0000E+00	.1328E+04	.6859E+03	.1853E+03	.3234E+01	.8864E-02	.0000E+00	.0000E+00	.2829E+05
MEAN	.1233E+02	.1263E+04	.6343E+03	.1212E+03	.8128E+01	.2740E-01	.0000E+00	.0000E+00	.2951E+05
S.D.	.2125E+02	.9351E+03	.4703E+03	.9692E+02	.9813E+01	.0000E+00	.0000E+00	.0000E+00	.1919E+05

KING POINT NODE 1, MEAN WATER LEVEL

NET SEDIMENT TRANSPORT RATES (cu.m./m./yr.)

Model	B(1)	B(2)	B(3)	B(4)	B(5)	B(6)	B(7)	B(8)	Total Transport (cu.m./yr.)
1									.5809E+04
2									.5813E+04
3									.2855E+04
4	.0000E+00	.1188E+02	.2847E+02	.7312E+00	.1191E-32	.0000E+00	.0000E+00	.0000E+00	.4226E+03
5	-.5809E+01	.9136E+01	.4876E+03	.1209E+03	.7224E+01	.7803E-02	.0000E+00	.0000E+00	.9285E+04
7	.0000E+00	.2947E+02	.7583E+02	.1886E+02	.2021E-01	.0000E+00	.0000E+00	.0000E+00	.1591E+04
8	-.1655E+02	.2947E+02	.5898E+03	.2362E+03	.3177E+02	.1877E+00	.0000E+00	.0000E+00	.1836E+05
9	-.1422E+01	.1428E+03	.7478E+03	.1837E+03	.7985E+01	.7574E-02	.0000E+00	.0000E+00	.1691E+05
10	.4820E-02	.1925E+03	.6712E+03	.1812E+03	.1029E+02	.1386E-01	.0000E+00	.0000E+00	.1688E+05
11	-.9852E-01	.9124E+02	.2359E+03	.1186E+03	.1029E+02	.1385E-01	.0000E+00	.0000E+00	.8488E+04
12	-.3938E+01	-.6818E+01	.9634E+02	.2996E+02	.2863E+01	.6996E-02	.0000E+00	.0000E+00	.2154E+04
13	.0000E+00	.1349E+03	.4866E+03	.9951E+02	.3224E+01	.8864E-02	.0000E+00	.0000E+00	.1874E+05
MEAN	-.3889E+01	.7842E+02	.3782E+03	.1882E+03	.8097E+01	.2740E-01	.0000E+00	.0000E+00	.8281E+04
S.D.	.5429E+01	.7178E+02	.2735E+03	.8276E+02	.9759E+01	.0000E+00	.0000E+00	.0000E+00	.6376E+04

KING POINT NODE 1, MEAN WATER LEVEL

POSITIVE SEDIMENT TRANSPORT RATES (clockwise wrt. beach normal)

Model	B(1)	B(2)	B(3)	B(4)	B(5)	B(6)	B(7)	B(8)	Total Transport (cu.m./yr.)
1									.2491E+05
2									.1117E+05
3									.1384E+05
4	.0000E+00	.1426E+02	.2864E+02	.7312E+00	.1191E-32	.0000E+00	.0000E+00	.0000E+00	.4545E+03
5	.1852E+02	.8268E+03	.5989E+03	.1281E+03	.7238E+01	.7803E-02	.0000E+00	.0000E+00	.2288E+05
7	.0000E+00	.5189E+02	.8885E+02	.1887E+02	.2021E-01	.0000E+00	.0000E+00	.0000E+00	.1924E+04
8	.2345E+02	.1117E+04	.9249E+03	.2653E+03	.3186E+02	.1877E+00	.0000E+00	.0000E+00	.3714E+05
9	.1987E+01	.1213E+04	.9537E+03	.1982E+03	.7996E+01	.7574E-02	.0000E+00	.0000E+00	.3385E+05
10	.1418E-01	.1298E+04	.8673E+03	.1864E+03	.1038E+02	.1386E-01	.0000E+00	.0000E+00	.3318E+05
11	.1972E+00	.5821E+03	.3457E+03	.1158E+03	.1038E+02	.1385E-01	.0000E+00	.0000E+00	.1584E+05
12	.5854E+01	.2529E+03	.1585E+03	.3264E+02	.2868E+01	.6996E-02	.0000E+00	.0000E+00	.6289E+04
13	.0000E+00	.7315E+03	.5863E+03	.1824E+03	.3229E+01	.8864E-02	.0000E+00	.0000E+00	.1952E+05
MEAN	.4668E+01	.6666E+03	.5822E+03	.1147E+03	.8112E+01	.2740E-01	.0000E+00	.0000E+00	.1814E+05
S.D.	.7938E+01	.4981E+03	.3698E+03	.8969E+02	.9786E+01	.0000E+00	.0000E+00	.0000E+00	.1234E+05

Table 6.4 - King Point SEDX results (II) - Node 1

KING POINT NODE 1, MEAN WATER LEVEL								
NEGATIVE SEDIMENT TRANSPORT RATES (counter clockwise wrt. beach normal)								
Model	B(1)	B(2)	B(3)	B(4)	B(5)	B(6)	B(7)	B(8) Total Transport (cu.m./yr.)
1								.1998E+05
2								.5354E+04
3								.1019E+05
4	.0000E+00	.2387E+01	.1646E+00	.1533E-19	.0000E+00	.0000E+00	.0000E+00	.3190E+02
5	.1560E+02	.8177E+03	.1833E+03	.7167E+01	.1403E-01	.0000E+00	.0000E+00	.1280E+05
7	.0000E+00	.2242E+02	.4223E+01	.5709E-02	.0000E+00	.0000E+00	.0000E+00	.3332E+03
8	.4000E+02	.1007E+04	.3352E+03	.2905E+02	.8962E-01	.0000E+00	.0000E+00	.1878E+05
9	.3329E+01	.1071E+04	.2058E+03	.6543E+01	.1079E-01	.0000E+00	.0000E+00	.1615E+05
10	.9276E-02	.1090E+04	.1961E+03	.5211E+01	.8700E-02	.0000E+00	.0000E+00	.1631E+05
11	.2878E+00	.4100E+03	.1098E+03	.5209E+01	.8774E-02	.0000E+00	.0000E+00	.6641E+04
12	.9705E+01	.2590E+03	.5412E+02	.2675E+01	.5058E-02	.0000E+00	.0000E+00	.4054E+04
13	.0000E+00	.5966E+03	.9961E+02	.2874E+01	.5153E-02	.0000E+00	.0000E+00	.8775E+04

MEAN	.7669E+01	.5962E+03	.1320E+03	.6526E+01	.1580E-01	.0000E+00	.0000E+00	.9942E+04
S.D.	.1333E+02	.4467E+03	.1089E+03	.8834E+01	.0000E+00	.0000E+00	.0000E+00	.6895E+04

KING POINT NODE 1, MEAN WATER LEVEL								
CUMULATIVE DISTRIBUTION OF NET SEDIMENT TRANSPORT (cu.m./yr.)								
Model	B(1)	B(2)	B(3)	B(4)	B(5)	B(6)	B(7)	B(8)
4	.0000E+00	.1404E+03	.4043E+03	.4226E+03	.4226E+03	.4226E+03	.4226E+03	.4226E+03
5	-.3288E+02	.8132E+02	.5176E+04	.8200E+04	.9283E+04	.9283E+04	.9283E+04	.9283E+04
7	.0000E+00	.3604E+03	.1316E+04	.1588E+04	.1591E+04	.1591E+04	.1591E+04	.1591E+04
8	-.1069E+03	.2614E+03	.7633E+04	.1354E+05	.1830E+05	.1836E+05	.1836E+05	.1836E+05
9	-.9189E+01	.1766E+04	.1111E+05	.1571E+05	.1690E+05	.1691E+05	.1691E+05	.1691E+05
10	.3115E-01	.2407E+04	.1000E+05	.1533E+05	.1607E+05	.1600E+05	.1600E+05	.1600E+05
11	-.5849E+00	.1140E+04	.4089E+04	.6853E+04	.8396E+04	.8400E+04	.8400E+04	.8400E+04
12	-.2540E+02	-.1105E+03	.1094E+04	.1843E+04	.2152E+04	.2154E+04	.2154E+04	.2154E+04
13	.0000E+00	.1686E+04	.7769E+04	.1026E+05	.1074E+05	.1074E+05	.1074E+05	.1074E+05

MEAN	-.1944E+02	.8600E+03	.5488E+04	.8193E+04	.9407E+04	.9415E+04	.9415E+04	.9415E+04
S.D.	.3500E+02	.9102E+03	.4096E+04	.5982E+04	.6967E+04	.6977E+04	.6977E+04	.6977E+04

KING POINT NODE 1, MEAN WATER LEVEL								
PERCENTAGE DISTRIBUTION OF NET SEDIMENT TRANSPORT								
Model	B(1)	B(2)	B(3)	B(4)	B(5)	B(6)	B(7)	B(8)
4	.00	35.90	61.89	2.21	.00	.00	.00	.00
5	-.94	1.69	75.51	22.40	1.34	.00	.00	.00
7	.00	25.37	65.27	9.35	.02	.00	.00	.00
8	-1.90	3.30	67.72	27.12	3.65	.02	.00	.00
9	-.13	13.15	69.24	17.01	.74	.00	.00	.00
10	.00	18.24	63.61	17.17	.98	.00	.00	.00
11	-.02	20.37	52.67	24.68	2.30	.00	.00	.00
12	-3.34	-5.79	81.90	25.47	1.75	.01	.00	.00
13	.00	18.62	67.19	13.74	.45	.00	.00	.00

MEAN	-.70	14.55	67.22	17.68	1.25	.00	.00	.00
S.D.	1.18	12.96	8.26	8.26	1.18	.00	.00	.00

6.4.2 Summary of Results

The totals of positive and negative sediment transport estimates from each model are presented for each node at each site in Table 6.5. It is apparent that at each site estimates of sediment transport vary among the models by at least two orders of magnitude. Best estimates of sediment transport (as shown on Table 6.5 and on Figures 6.2 to 6.7) were produced by screening out invalid results. Those models which were considered to produce valid results are identified on Table 6.5. The choice of valid models varies from site to site since it depends on environmental conditions such as beach slope and sediment size distribution. A full description of the beach profiles and sediment distributions is given for each site in Part II of this report. The selection of valid models is described in the following sub-section.

It should be recognized that the variation in results could have been reduced by individually tuning the models. However, the package deal approach was adopted specifically to facilitate objective intercomparison of models. (6.2.3)

6.4.3 Selection of Valid Models

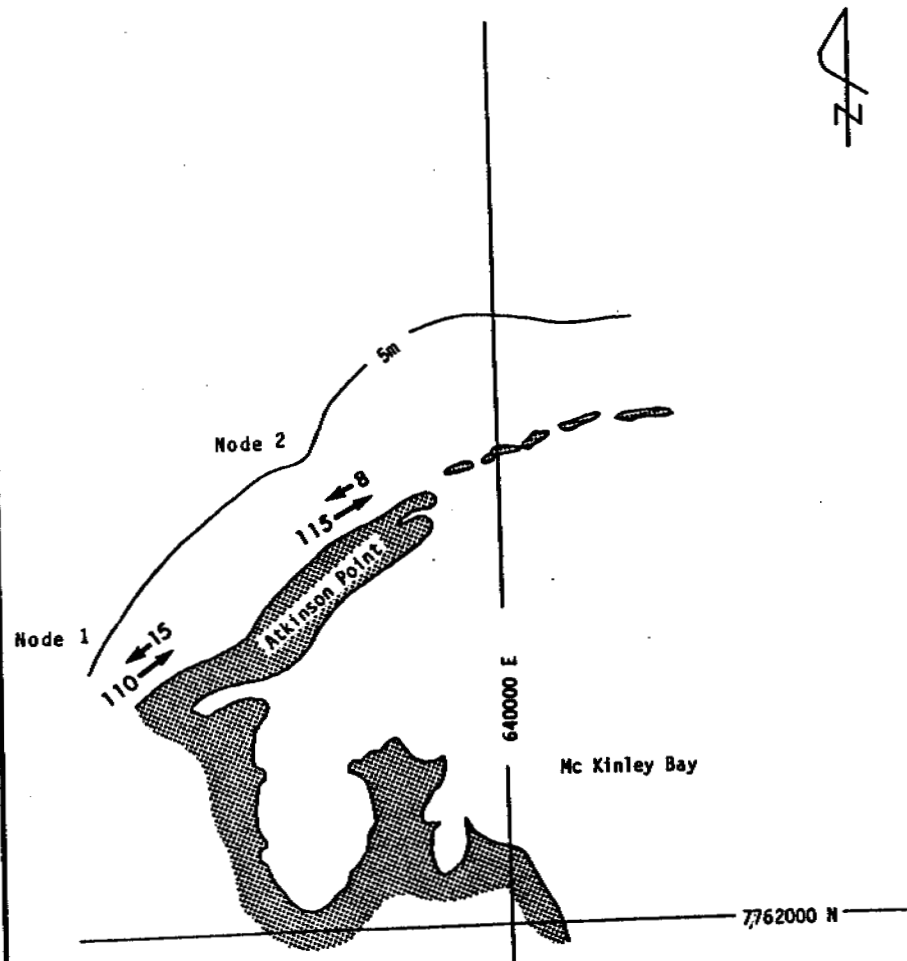
The principal conclusion from the SEDX runs is that some of the detailed predictors yield unreasonably high

TABLE 6.3 Summary of Sediment Transport Results and Best Estimates - All Sites (m³ per annum)

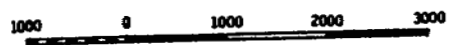
Stokes Point Node 1			Stokes Point Node 2			North Head Node 1			North Head Node 2		
Model	S/E	N/W	Model	S/E	N/W	Model	N/W	S/E	Model	N/W	S/E
1	48818	7871	1	44798	8	1	1261	37498	1	1382	118788
2	13888	1849	2	11358	8	2 *	11	861	2 *	29	14238
3	52988	18228	3	58328	8	3	1519	45168	3	1665	143888
4	18888	5919	4	5844	8	4 *	8	918	4 *	8	12988
5	186588	42878	5	188588	8	5	1766	88558	5	1288	173588
7 *	1.8E+86	162188	7	16978	8	7	8	17978	7	1	115288
8 *	1.4E+86	385788	8 *	164188	8	8 *	3293	228888	8 *	1922	475388
9 *	1.9E+86	526888	9 *	198388	8	9 *	1967	283888	9 *	1468	546488
10	19258	8593	10	26378	8	10	1284	62788	10	916	68188
11	14358	6884	11	14248	8	11	382	29458	11	266	36898
12	93488	37888	12	47848	8	12	1232	53888	12	787	185788
13 *	1.8E+86	265788	13	88898	8	13	572	76618	13	413	244688
Best Estimate	44986	14951	Best Estimate	48471		Best Estimate	1882	51376	Best Estimate	888	188613
Kay Point Node 1			Kay Point Node 2			Tuktoyaktuk Node 1			Tuktoyaktuk Node 2		
Model	N/E	S/W	Model	N/E	S/W	Model	N/E	S/W	Model	N/E	S/W
1	8	59788	1	8	69878	1	568	22498	1	569	26858
2	8	12578	2	8	28848	2	24	1522	2	58	2548
3	8	65188	3	8	58438	3	265	18538	3	322	14758
4 *	8	9329	4 *	8	7287	4 *	8	8	4 *	8	8
5	8	96188	5	8	68828	5	636	18888	5	551	11338
7	8	82188	7	8	73688	7 *	8	8	7 *	8	8
8 *	8	287988	8 *	8	214688	8	818	14588	8	999	22448
9 *	8	356888	9 *	8	263888	9	232	4369	9	294	7271
10	8	15388	10	8	8797	10	243	7338	10	248	18268
11	8	12898	11	8	7552	11	143	4221	11	146	6178
12	8	55328	12	8	37898	12	183	3865	12	286	4118
13 *	8	177888	13 *	8	135688	13	186	2184	13	158	38868
Best Estimate		49885	Best Estimate		43825	Best Estimate	321	8833	Best Estimate	353	18882
King Point Node 1			King Point Node 2			Atkinson Point Node 1			Atkinson Point Node 2		
Model	S/E	N/W	Model	S/E	N/W	Model	N/E	S/W	Model	N/E	S/W
1	24915	19988	1	24668	25888	1	74188	15218	1	153288	11368
2	11178	5354	2	12588	9488	2 *	17818	1525	2	44548	1538
3	13848	18198	3	12948	16268	3	98748	28278	3	284288	15148
4 *	454	32	4 *	218	163	4	137188	16198	4	186488	588
5	22888	12888	5	18588	15288	5 *	722288	98718	5 *	545988	3588
7 *	1924	333	7 *	958	862	7 *	6.7E+86	466388	7 *	5.3E+86	76168
8	37148	18788	8	16728	23398	8 *	7.2E+86	714788	8 *	5.5E+86	197488
9	33858	16158	9	15728	21398	9 *	9.7E+86	973588	9 *	7.4E+86	266988
10	31188	16318	10	15618	21578	10	138488	21688	10	184588	7748
11	15848	6441	11	6526	9155	11	181788	14818	11	79658	5224
12	6289	4854	12	3813	4545	12 *	688888	92658	12 *	513188	32738
13	19528	8775	13	9316	12278	13 *	4.7E+86	443588	13 *	3.6E+86	116588
Best Estimate	21334	11895	Best Estimate	12759	15922	Best Estimate	118888	14948	Best Estimate	115415	7688

* models NOT used in Best Estimate

FIGURE 6.2



Universal Transverse Mercator Projection
Zone 8



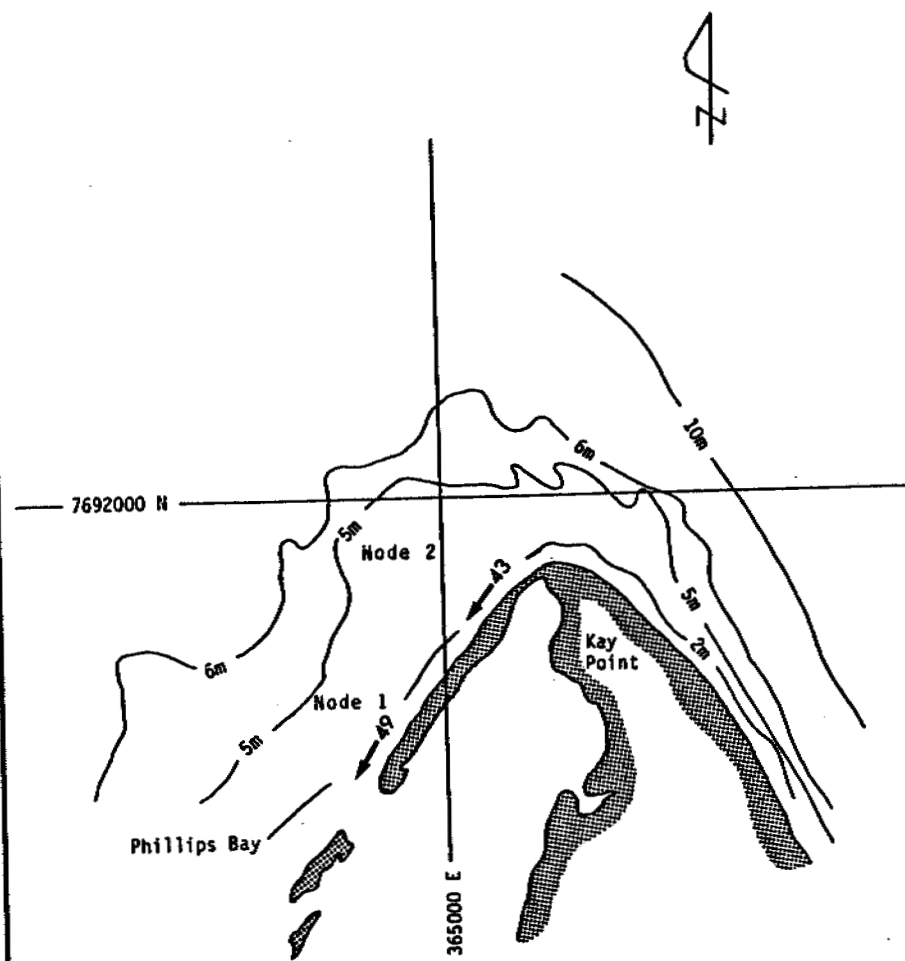
Scale
in
Metres

BEAUFORT SEA COASTAL SEDIMENT STUDY

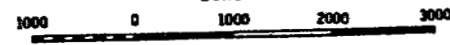
Atkinson Point: Best Estimate of Net Potential Sediment
Transport Rates $1000's m^3$

Date: 2 May 85
Scales as shown
Checked by:
Keith Philpott
Consulting Limited

FIGURE 6.3



Universal Transverse Mercator Projection
Zone 8



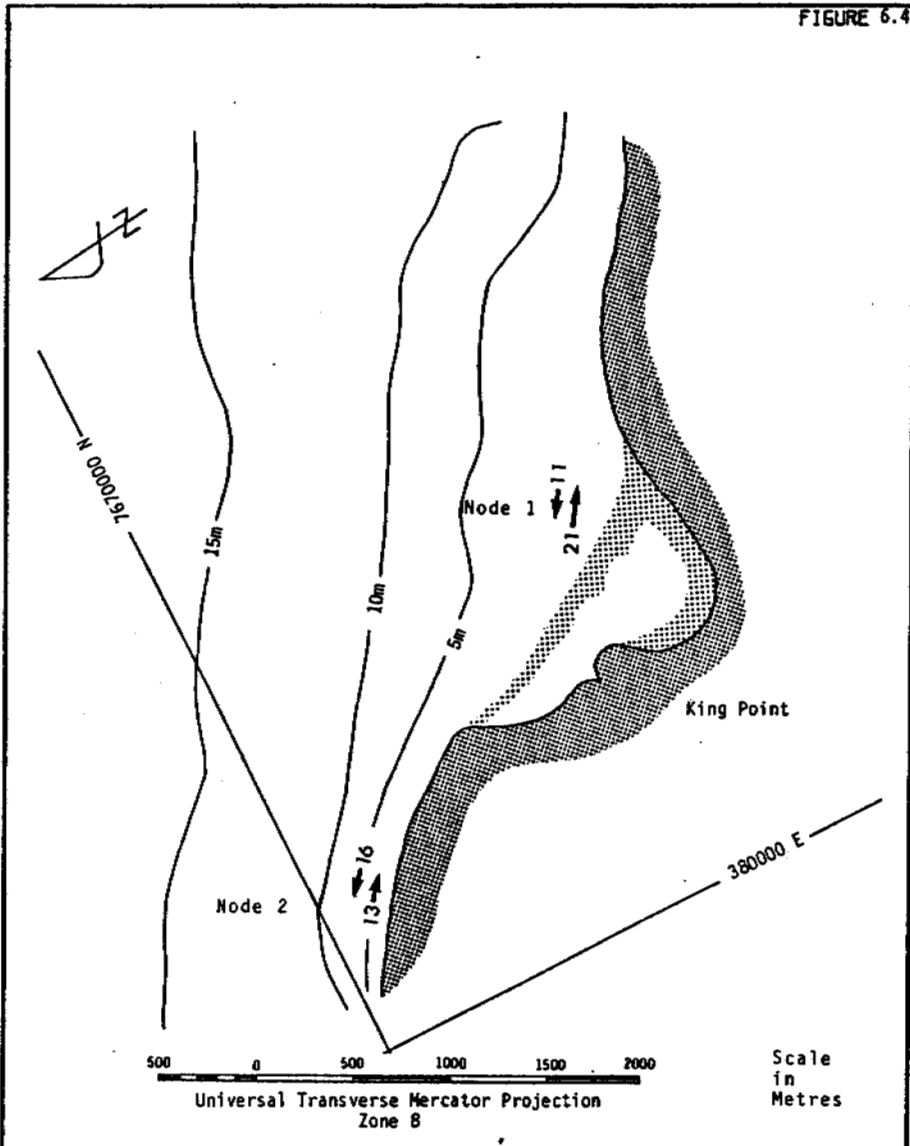
Scale
in
Metres

BEAUFORT SEA COASTAL SEDIMENT STUDY

Kay Point: Best Estimate of Net Potential Sediment
Transport Rates $1000's m^3$

Date: 2 May 85
Scales as shown
Checked by:
Keith Philpott
Consulting Limited

FIGURE 6.4

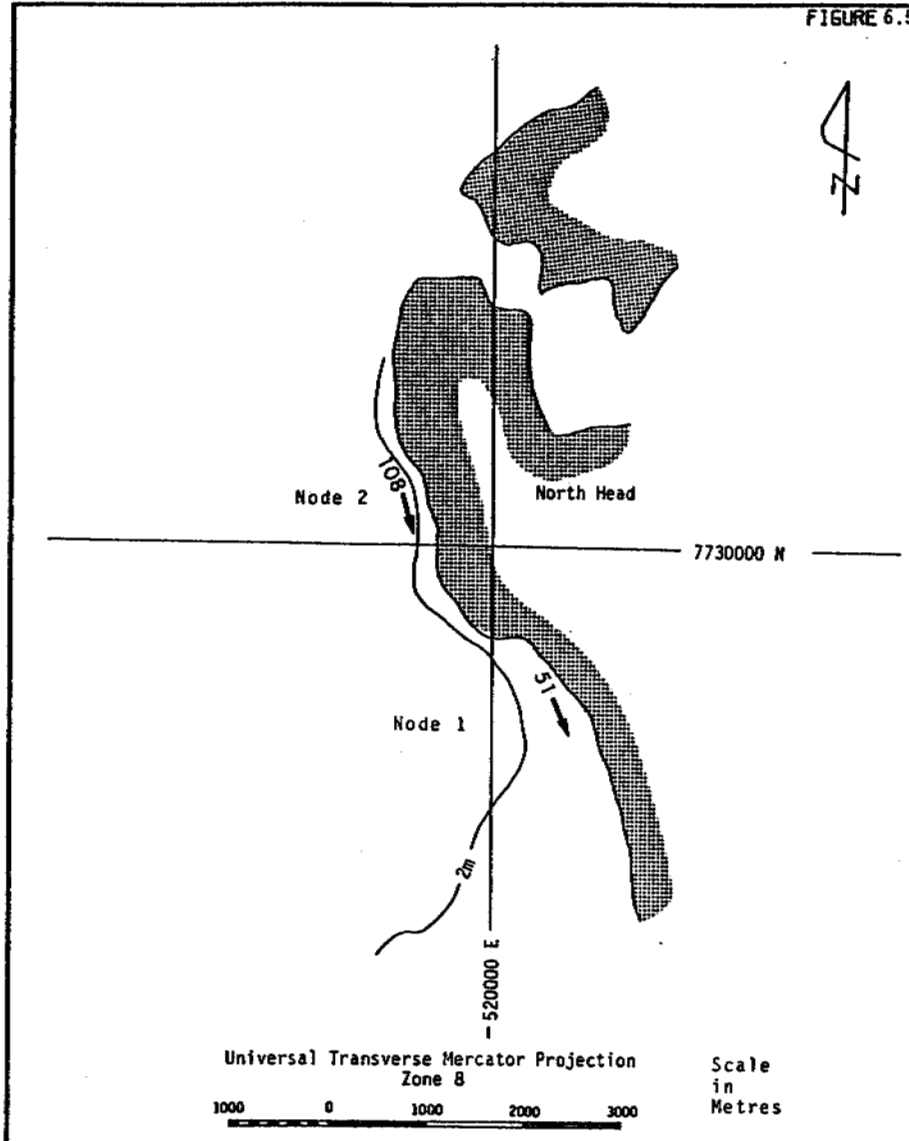


BEAUFORT SEA COASTAL SEDIMENT STUDY

King Point: Best Estimate of Potential Sediment
Transport Rates 1000's m³

Date: 2 May 85
Scales as shown
Checked by:
Keith Philpott
Consulting Limited

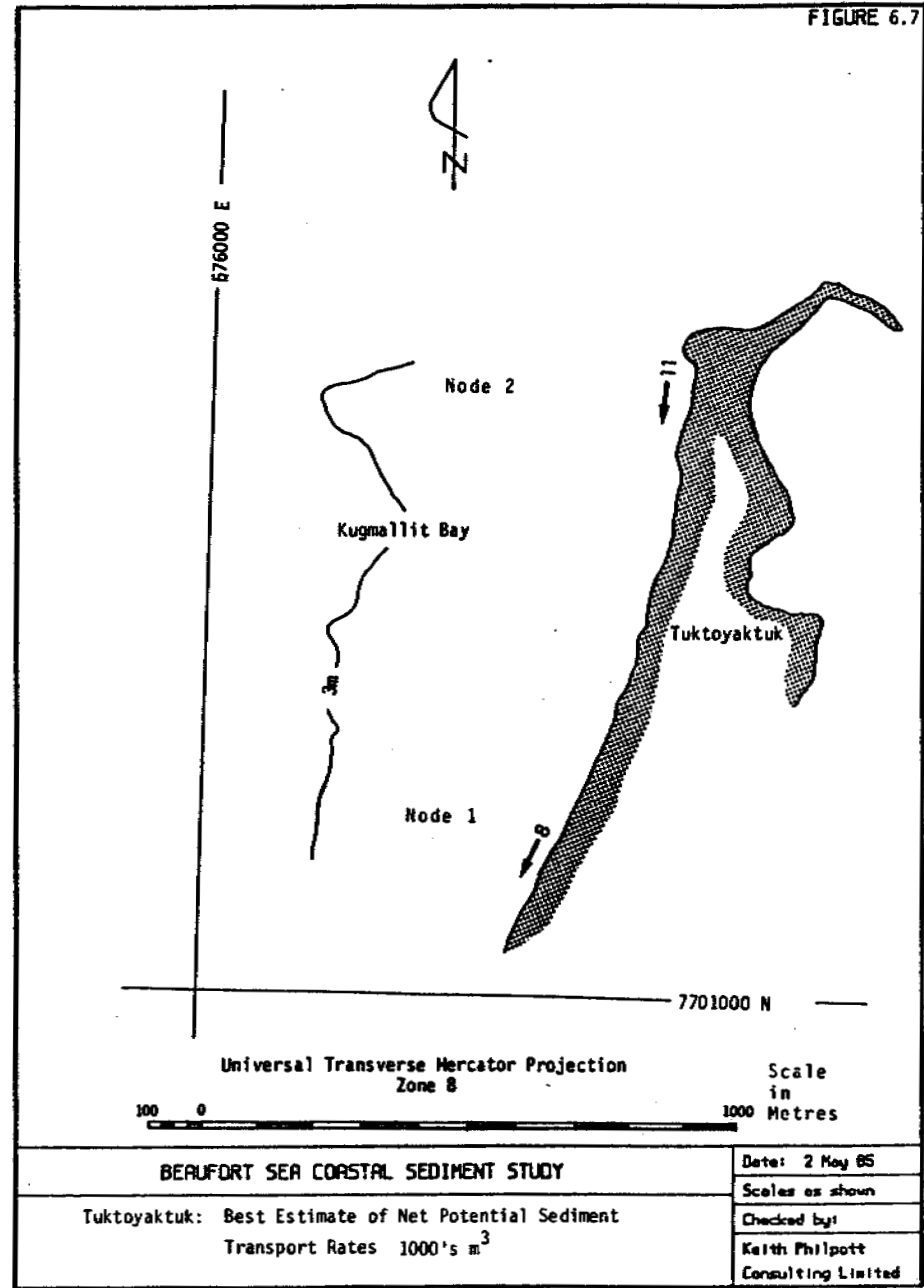
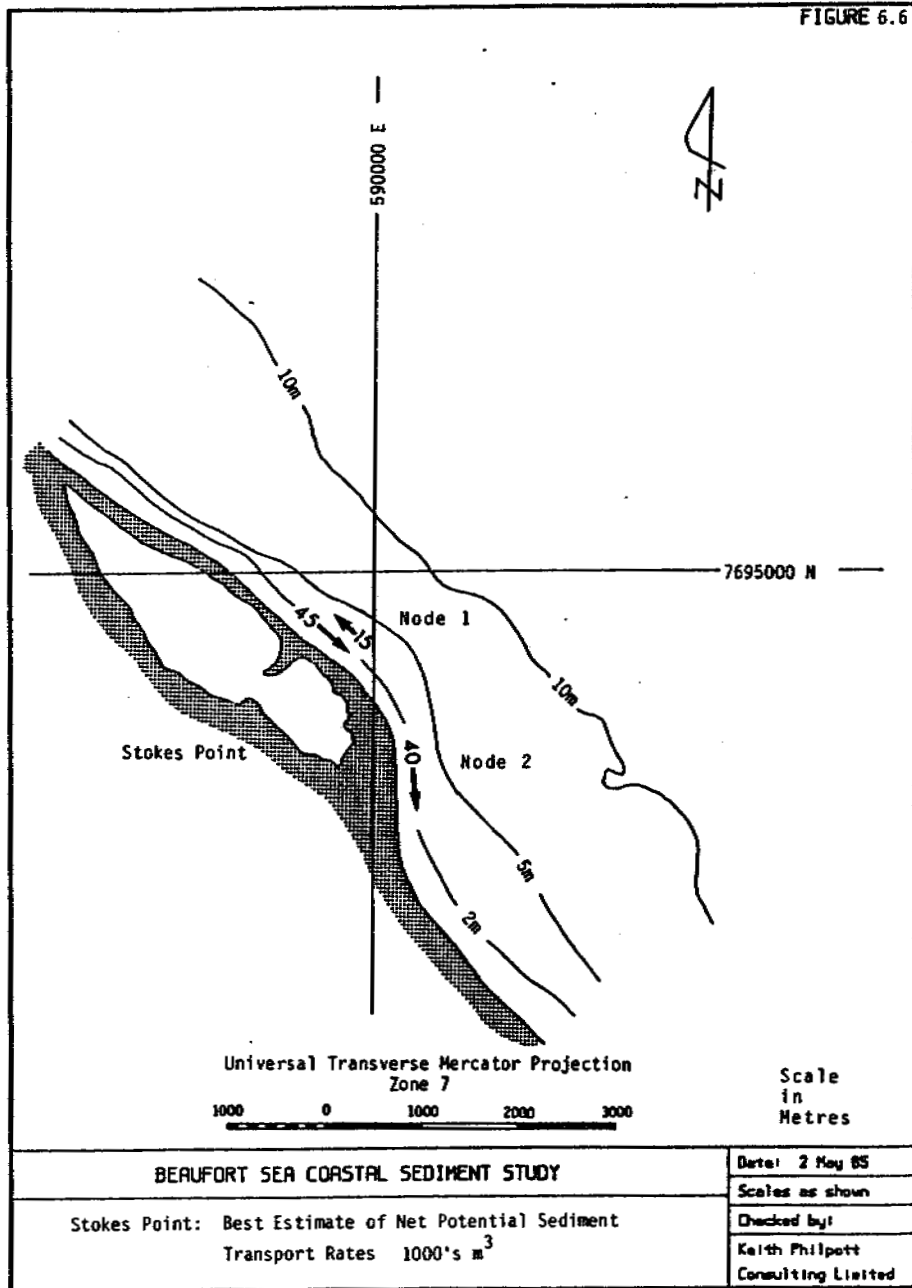
FIGURE 6.5



BEAUFORT SEA COASTAL SEDIMENT STUDY

North Head: Best Estimate of Net Potential Sediment
Transport Rates 1000's m³

Date: 2 May 85
Scales as shown
Checked by:
Keith Philpott
Consulting Limited



sediment transport rates for fine grain size distributions. Since all the models are to some degree empirical, they will have been formulated for a specific range of grain sizes and slopes, and extrapolation outside of these ranges can cause instability in places which have a median grain size less than about 0.25 mm. This is especially true at Atkinson Point where results from models 5 to 9, 12, and 13 were not included in the best estimate. It is also apparent to varying degrees at Stokes Point and Kay Point. Part of the reason for instability of these models at fine grain sizes may be related to the threshold for incipient sediment motion. A recent paper by Wang and Shen (1985) suggests that the threshold of motion at fine grain sizes and with turbulent flow may be much higher than under the laminar sub-layer condition assumed in this modelling system. If this is true, the Ackers and White models would be expected to overpredict sediment transport at fine grain sizes.

At Atkinson Point and at node 1 at Stokes Point the Engelund and Hansen model and the Fleming model were not included in the best estimate of sediment transport. Again, the instability is probably related to applying the model outside of the range of environmental conditions used to derive the empirical coefficients. The Fleming model was specifically developed for one particular site which had a relatively flat profile with fine sand.

Results from the Bijker model were also omitted from best estimates at many sites because the sediment transport rates were very low. This is a specific instance where individual calibration would have provided more reasonable results. Typically, exaggerated roughness lengths are used in conjunction with this model.

The North Head results bring the influence of another important factor to light: beach slope. Almost all of the models at this site produce apparently reasonable results even though the median grain size diameter was taken as 0.20 mm. The difference at North Head is an extremely flat beach slope ranging from 1:200 to 1:425 in the zone of active transport. The mild slope would act to spread the surf zone producing a less concentrated zone of wave energy dissipation. Consequently, the shear stresses would be significantly reduced thus offsetting the influence of fine grain diameters.

The results at King Point, where the median grain size was 0.27 mm, proved to be quite reasonable. Only the results from the Bijker and Swart (Ackers and White, adaptation) models were not included in the best estimate since the estimates from these two models were quite low.

6.4.4 Evaluation of Sediment Transport Models and Possible Sources of Error

Some limitations of the twelve sediment transport models have been revealed through an analysis of the results. Other probable limitations which exert an influence on the results, but yet have not been explicitly identified, will also be discussed in the following paragraphs.

Bulk Models:

Because they have a strong empirical basis the results from the bulk models have been generally accepted as valid. However, a weakness is that these models do not possess a threshold criterion for incipient motion and all alongshore wave energy even that due to minimal wave heights is assumed to be equally capable of causing sediment transport. Obviously this is erroneous. Although the strong empirical basis of the formulae tends to counteract this deficiency, it does mean that the models can only be accurate within the range of environmental conditions for which they were derived. These include wave climate, beach profile, and sediment characteristics.

Along the Beaufort coast both very fine and very coarse grain sediments are common, and the results from the bulk

models should therefore be cautiously interpreted. For example, the original CERC model was derived from field data with median grain sizes of 0.2 mm, 0.4 mm, and 0.6 mm. Also, mathematical instability precludes the use of the Swart CERC model for a sediment distribution which has a median diameter greater than 1.5 mm.

Detailed Predictors:

Before proceeding to specific comments on the causes for the wide range of results obtained with the detailed predictors, some general comments may be in order. First and foremost it should be appreciated that the development of detailed alongshore sediment transport models is still in its infancy. Also, most models have not been thoroughly tested against data other than that used in their original derivations. Possibly more important are the facts a) that most of the models derive from modifications of unidirectional flow sediment transport techniques; and b) that they depend on a complex chain of interrelated computations several parts of which were originally derived under rather different boundary cases, often only at laboratory scale. The bulk models avoid the resulting instability problems by making the transport rate a simple proportion of the alongshore wave power. However, they do not provide details of the process that are required in many applications. A final general comment addresses the package deal approach. Many of the models would produce more realistic

results if they were calibrated individually, however, the package deal approach was chosen for this study for the purpose of objective comparison between sediment transport models.

The calculation of bed roughness and shear stress is one of the most important steps in the sediment transport model. These parameters influence both the amount of sediment mobilized as well as the velocity of the longshore current which moves the mobilized sediment. The effect of bed roughness on the magnitude of longshore currents has been quantified with the aid of over 350 individual data sets by Fleming and Swart (1982) and included in the longshore current model. The effect of bed roughness on shear stress and the amount of sediment being mobilized is treated differently in almost every model. However, the modified Ackers and White formulae exhibit a greater dependence on shear stress in this respect than do the Bijker related formulae (with suspended and bed load expressions) and presumably errors in shear stress will be magnified in these models. This may partially explain the instability in these models at fine grain sizes, especially considering the possible error in threshold shear stress at fine grain sizes discussed in Section 6.4.3.

The influence of breaking waves will affect the validity of all model results in several ways. Both sediment mobility (or suspended concentration) calculations and longshore current determination are affected. The effect of breaking

waves has been shown by Nielsen et al., (1978) to significantly influence the level of turbulence in a region of the water column extending down from the free surface to five times the ripple height above the bed. Those models which are based either partly or wholly on the suspended load distribution through the water column should include the influence of the increased turbulence caused by breaking waves. Of the five models of this type only one of the Nielsen models does this. A comparison of the Nielsen non-breaking and breaking wave versions reveals that including the influence of turbulence causes sediment transport rates to increase by up to a factor of two. Nielsen et al., (1978) determined empirical coefficients for eddy diffusivity from laboratory measurements of suspended sediment under spilling breaking and non-breaking waves. The data set included a wide range of grain sizes from 0.08 mm to 0.55 mm which may be the reason the Nielsen models are the only detailed predictors which give consistently reasonable results at fine grain sizes. It should be stressed that none of the detailed predictors consider plunging breakers which can occur at some of the Beaufort Sea sites.

There are several other inaccuracies related to the influence of breaking waves. The wave characteristics inside the surf zone are definitely not sinusoidal, as assumed. Also, the bed roughness and wave-induced bedforms, derived for non-breaking waves are probably not valid inside the breaker zone.

There are also several sources of error related to the longshore current model which could affect the estimated sediment transport rates. The effect of bed roughness on longshore currents has already been mentioned. One assumption in the development of the longshore current package (described in section 6.2.3) is that all waves break as spilling breakers and this in turn leads to the assumption that lateral mixing can be ignored for random waves (Battjes, 1974). However, the steep nearshore slopes at King Point will cause most waves to form plunging breakers, and many breakers will be of plunging form at Stokes Point and Kay Point. Fleming and Swart (1982) suggest that in the case of longshore currents generated by random waves breaking as plunging breakers lateral mixing should be included.

Steep beach slopes also cause reflections which effectively increase the breaker index according to recent field studies by Thornton and Wu (1984), and hence the constant value of 0.78 is probably a non-conservative assumption.

SECTION 7 NEARSHORE PROFILE ADJUSTMENT

7.1 Introduction

The nearshore profile adjustment model, SEGAR, computes changes in beach profile geometry due to changes in wave and water level conditions such as those due to storm surges. It was implemented at one inshore node for each of the five following sites: Atkinson Point, Kay Point, King Point, Stokes Point and Tuktoyaktuk. There was not sufficient data to use this model at North Head or Pauline Cove.

SEGAR was developed by D.H. Swart based on his onshore-offshore sediment transport theory, Swart (1974). The model computes changes in the nearshore profile as a function of gradients in onshore-offshore sediment transport based on the difference between the current profile and an equilibrium corresponding to current wave and water level conditions.

This model has been verified at several oceanic sites. Also, Swain and Houston (1983, 1984) using the same theory and computational approach have independently developed and verified their own model using different field and laboratory data.

7.2 Theoretical Background

The principles underlying the model may be summarized:

- i) A beach profile is characterized by three distinct zones, each with its own transport mechanism. These are:
 - the backshore which is the area above the wave run-up limit;
 - a developing profile (D-profile) where a combination of bedload and suspended load transport takes place;
 - a transition area, seaward of the D-profile and landward of the point where sediment transport by wave action is initiated and where only bed load transport normally takes place.
- (ii) The most basic assumption is that the developing D-profile will eventually reach a stable configuration under steady wave attack conditions. This profile is then considered to be stable in both form and position.

- (iii) The sediment transport rates into (or out of) the D-profile from (or to) the backshore or transition area provide the boundary conditions for the change in the D-profile.

- (iv) The rate of onshore/offshore sediment transport at a given time is a function of the deviation of the profile at that time from the equilibrium condition. Consequently, the time dependent profile development may be examined in relation to a time series of wave conditions.

A more detailed explanation of these principles and the computational methods used in the model are presented in a paper by Swart (1976) which has been appended to this report.

7.3 Outline of Methods

7.3.1 Calibration

The initial step in the analysis is to calibrate the model against a measured profile. The purpose of calibration is to tune the model to reproduce a representative measured profile under the action of the given wave climate. It therefore has to be assumed that the measured profile is a good representation of the mean annual profile, a typical wave formed profile undistorted by antecedent storm or ice action.

For calibration purposes the fourteen year hindcast wave data set was collated into statistical groups by wave height, period and direction. The frequency of occurrence of each group was then divided by fourteen to produce an average year of wave data. This data set was treated as a time-series and then randomized to remove any biases introduced in the statistical collation process.

The process of calibration begins by running the model with the one year of randomized wave data using the measured profile as the initial condition. Surges were not considered in the calibration process because they could not be related to the randomized wave data. The objective of calibration is to produce a computed profile at the end of the run that closely matches the measured profile used at the start of the run.

This can generally be achieved by varying a scaling factor WSKAAL. This factor is used to adjust the active length of the developing D-profile. A better calibration fit can sometimes be achieved by also adjusting the mean water level used during the calibration run.

Once an adequate calibration fit is achieved the measured profile is recalibrated using a "one-third rollback" of the initial wave data set. This consists of taking the first one third of the randomized time-series of waves and splicing it to the end of the data set. The rollback calibration is a check on the validity of the initial "random" data set.

The assumption that the input profile should return to its initial form and position following one year of average wave data will be valid providing that the wave climate follows an annual cycle and no sediment is lost from the profile or added to it.

Four factors which weaken the validity of the calibration process in the region under study are listed:

1. The annual cyclic variation of the wave climate in the Beaufort Sea is accentuated by the fact that the open water season is very short, leaving the possibility of very large year to year variations in the wave climate.

2. The fact that the shoreline is retreating at many of the sites indicates that sediment is being lost either offshore or alongshore, contrary to one of the assumptions.
3. While surges have a pronounced effect on the coastal morphology they are not considered in the calibration process used in this study.
4. Only instantaneous profile measurements were available at the study sites, and these were not necessarily representative of the average profiles at those sites.

Quite often the profile that resulted from a trial calibration run was different from the input profile. In some cases the subsequent surge analysis was then performed with the output profile resulting from the calibration run rather than the measured profile. In these instances the measured profile was assumed to be non-typical due to profile composition or antecedent conditions such as ice effects which are not accounted for by the model.

7.3.2 Storm Surge Analysis

The nearshore profile adjustment analysis is in effect a surge sensitivity study of nearshore profiles including estimates for shoreline retreat during large storms. At some sites rates of annual retreat could also be estimated based on the recession during individual storm surges. (See section 9).

The storm events used in this analysis are identical to those used in the surge sensitivity analysis of alongshore sediment transport (Section 5). Typically, a two to three day storm event was synthesized using the largest wave event in the fourteen year hindcast series (around 2 September 1972 at most sites) superimposed on varying storm surge water level profiles represented numerically in step form. Each site was usually run first with no surge and then with at least two different levels of peak surge.

7.4 Application of the Nearshore Profile Adjustment Model

7.4.1 Operational Modes

The SEGAR package has two basic operational modes - perpendicular or oblique wave attack. In the latter case shear stresses are increased to account for the presence of nearshore

currents generated by oblique waves. For this study only the perpendicular wave attack mode was employed since most of the previous verification for SEGAR has been associated with this mode.

7.4.2 Input Data

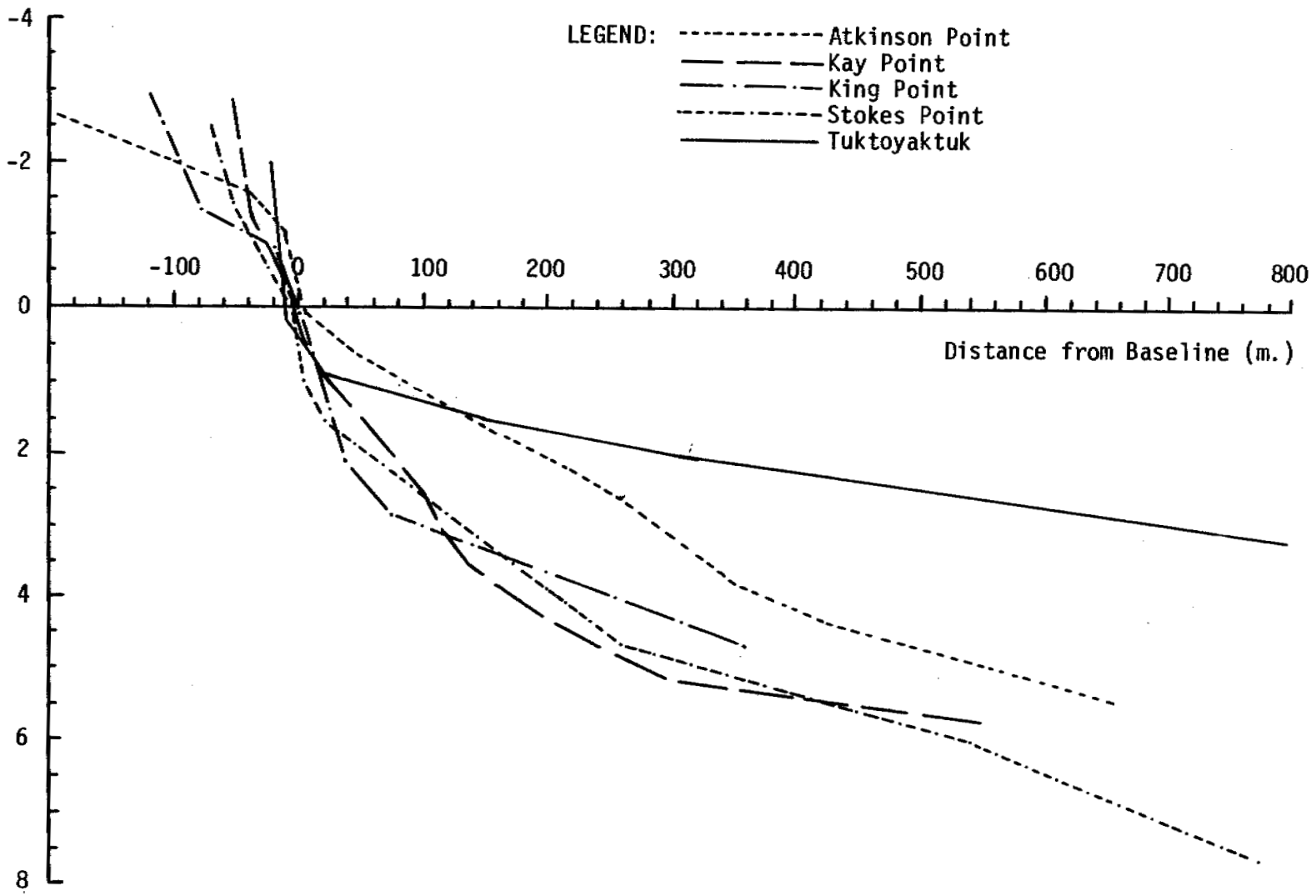
Several input parameters were common to the five sites investigated. At each site an average water temperature of one degree Celsius was used for the computation of kinematic viscosity. A relative mass density of 1.52 was used for the sediment at each site.

A single sediment size distribution is required for each profile. The distribution was taken as the shoremost sediment distribution used for the alongshore sediment transport modeling.

The profiles used at each site were derived from the measured profiles used in the alongshore sediment transport runs. However, in some cases these profiles had to be slightly altered to be compatible with the software. The profiles are shown superimposed in Figure 7.1.

Initial Profiles for the
Nearshore Profile Adjustment Analysis

Date: 24 Apr 85
Scales as shown
Checked by: Keith Philippott
Consulting Limited



A table showing the maximum wave height and period during the storms at each site is provided (Table 7.1). The listing of the wave data files for the storm events are given in Part II.

Table 7.1

Maximum Wave Condition During Simulated
Storm Surges for SEGAR Runs

Site	Inshore Maximum		Total Storm	Surge Levels
	Hs (m)	Tp (s)	Duraton (hrs) (No. of wave conditions)	Tested (peak surge) (m.)
Atkinson	2.31	9.06	45	0.0,1.0,1.5,2.75
Kay	2.26	8.48	46	0.0,0.5,1.1
King	1.19	6.65	42	0.0,1.0,1.65
Stokes	1.61	8.48	42	0.5,1.0
Tuktoyaktuk	1.00	6.29	54	0.5,1.5,2.75

7.5 Form of the Results

In this study the results are presented as figures showing both initial and final profiles. The model also provides the amount of retreat or advance at any point along the profile. The recession at Mean Water Level is given on the figures under the heading Supplementary Data.

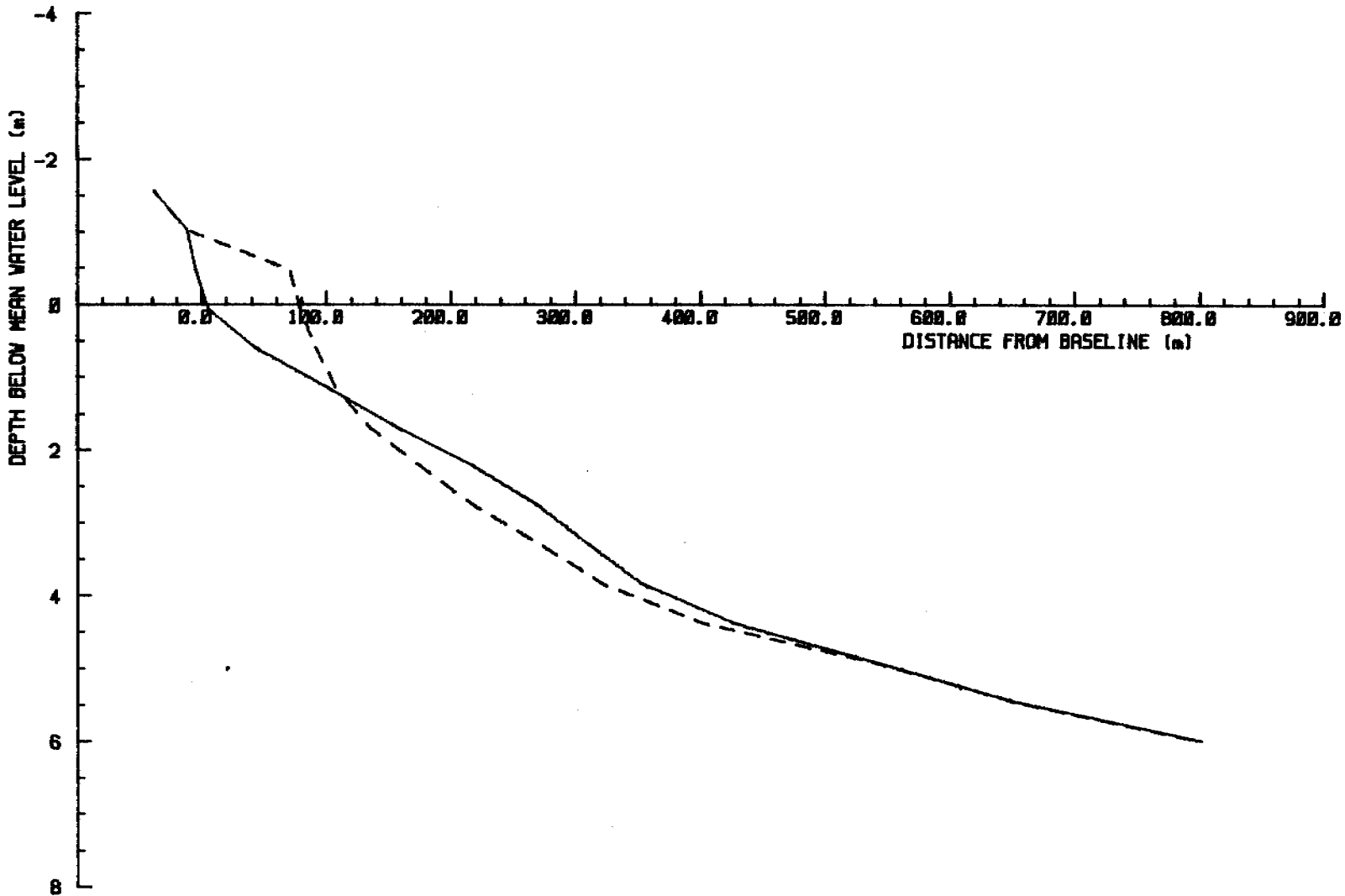
7.6 Discussion of Results

7.6.1 Atkinson Point

Calibration runs were attempted at Atkinson Point on the measured profile using WSKAAL values of 0.7, 1.0 and 1.25 (See Figures 7.2-7.4). The best fit was achieved with a WSKAAL of 1.25, however it was still not a good representation of the shape of the measured profile. A further calibration run was performed with a one metre rise in water level (referred to as "tide" in Figure 7.5) This produced a very good fit below MWL, but a relatively poor fit above MWL. Possible reasons for obtaining a better fit at a raised water level could be:

1. The majority of waves occur at increased water levels.
2. The datum associated with the profile measurement could be inaccurate.

FIGURE 7.2



CALIBRATION RUN / WSKARL = 0.7 / MEASURED PROFILE

ATKINSON POINT PROFILE ADJUSTMENT

LEGEND

————— Initial profile

----- End of run profile

CALIBRATION RUN 2

SUPPLEMENTARY DATA

Calibration run for 98 wave conditions
Total time all waves was 1312.1 hours

Shoreline advance = 74.55 metres

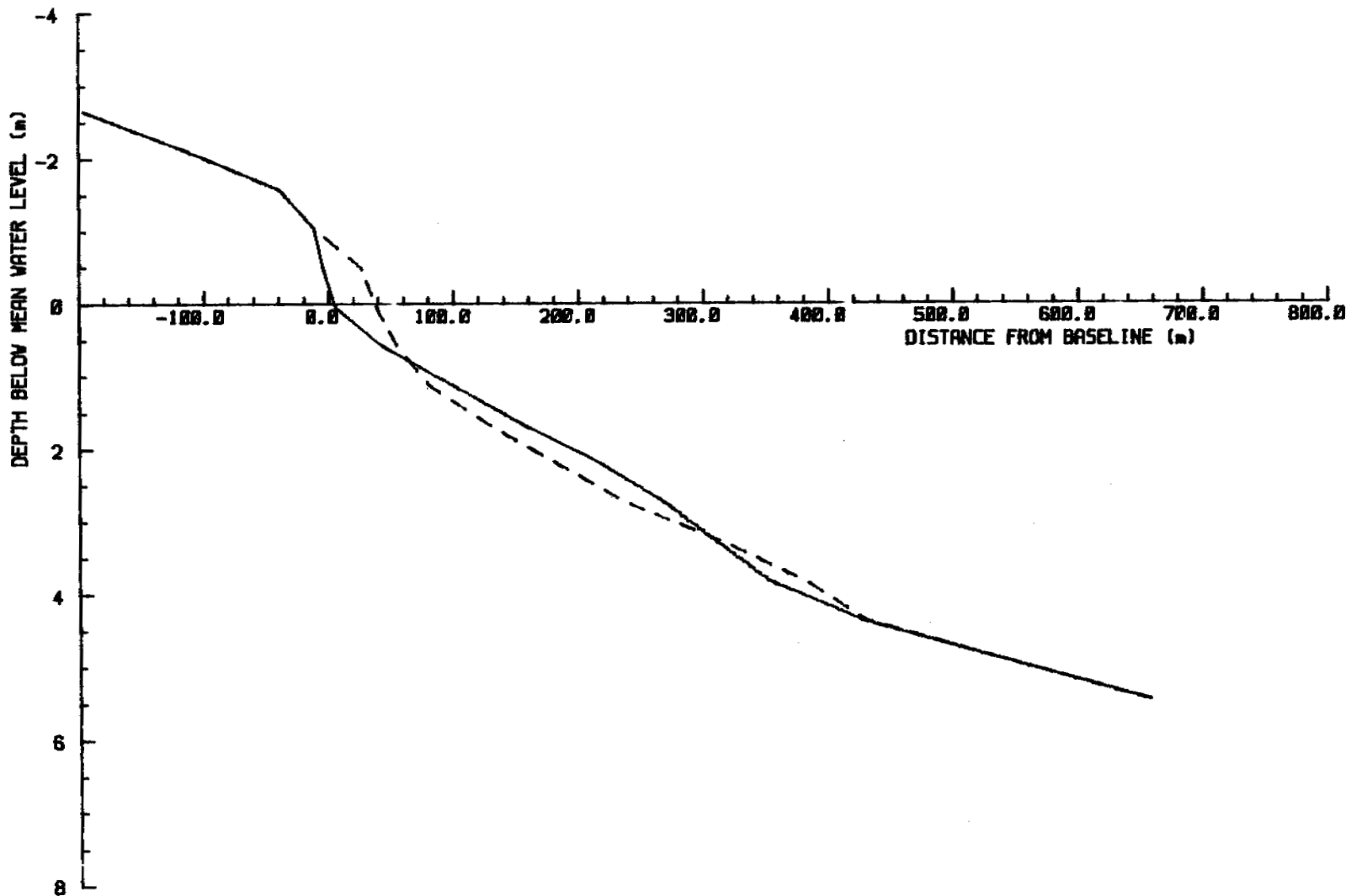
Date: 24 Apr 85

Scale: as shown

Checked by:

Kaith Philipp

Consulting Limited



ATKINSON POINT PROFILE ADJUSTMENT

CALIBRATION RUN / WSKRAL = 1.0 / MEASURED PROFILE

Date: 24 Apr 85

Scales as shown

Checked by:

Keith Philippot

Consulting Limited

LEGEND

———— Initial profile

----- End of run profile

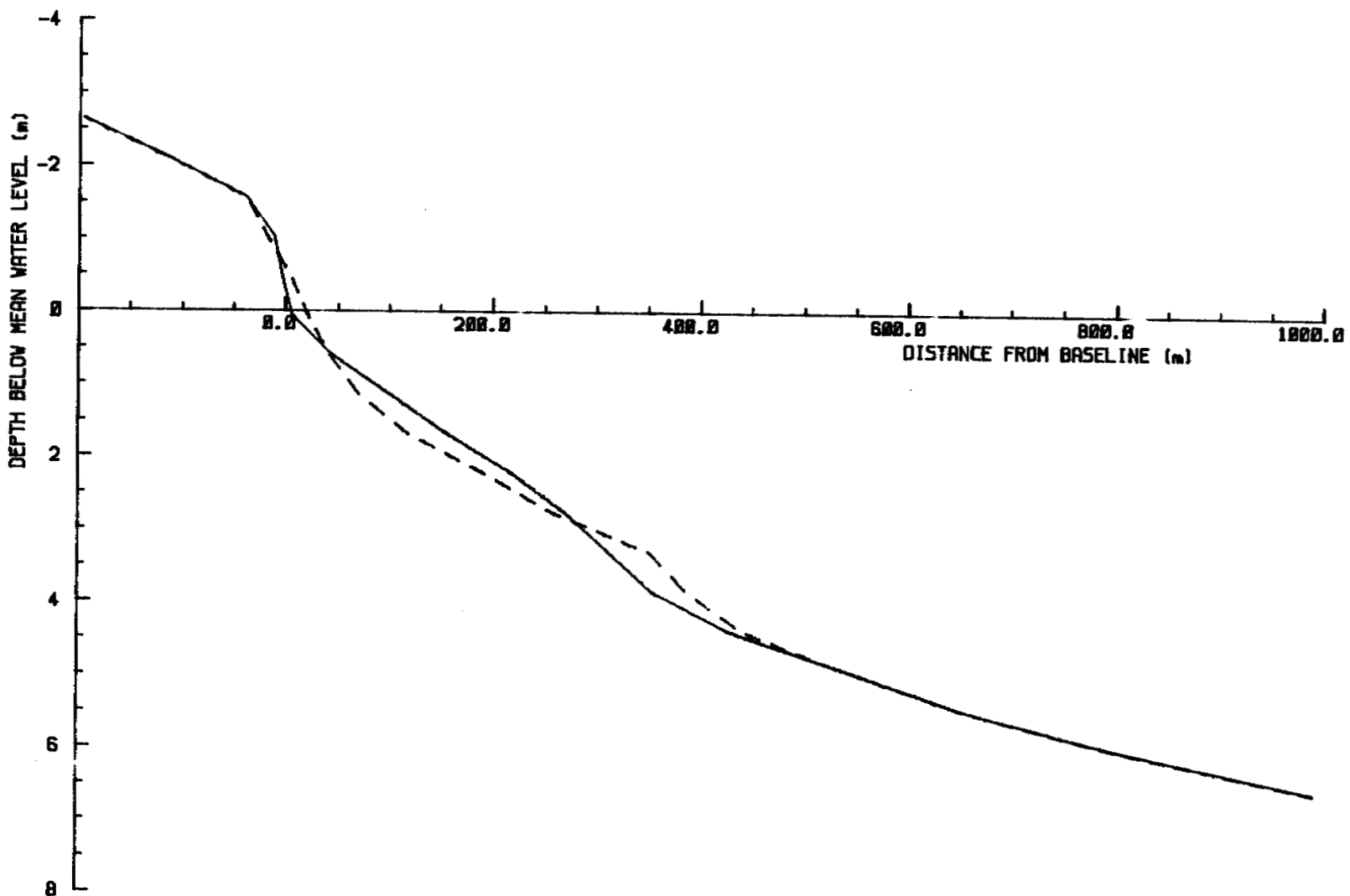
CALIBRATION RUN 1

SUPPLEMENTARY DATA

Calibration run for 90 wave conditions
Total time all waves was 1312.1 hours

Shoreline advance = 32.98 metres

FIGURE 7.3



ATKINSON POINT PROFILE ADJUSTMENT

CALIBRATION RUN / WSKRRL = 1.25 / MEASURED PROFILE

LEGEND

————— Initial profile

- - - - - End of run profile

CALIBRATION RUN 3

SUPPLEMENTARY DATA

Calibration run for 90 wave conditions
Total time all waves was 1312.1 hours

Shoreline advance = 14.58 metres

FIGURE 7.4

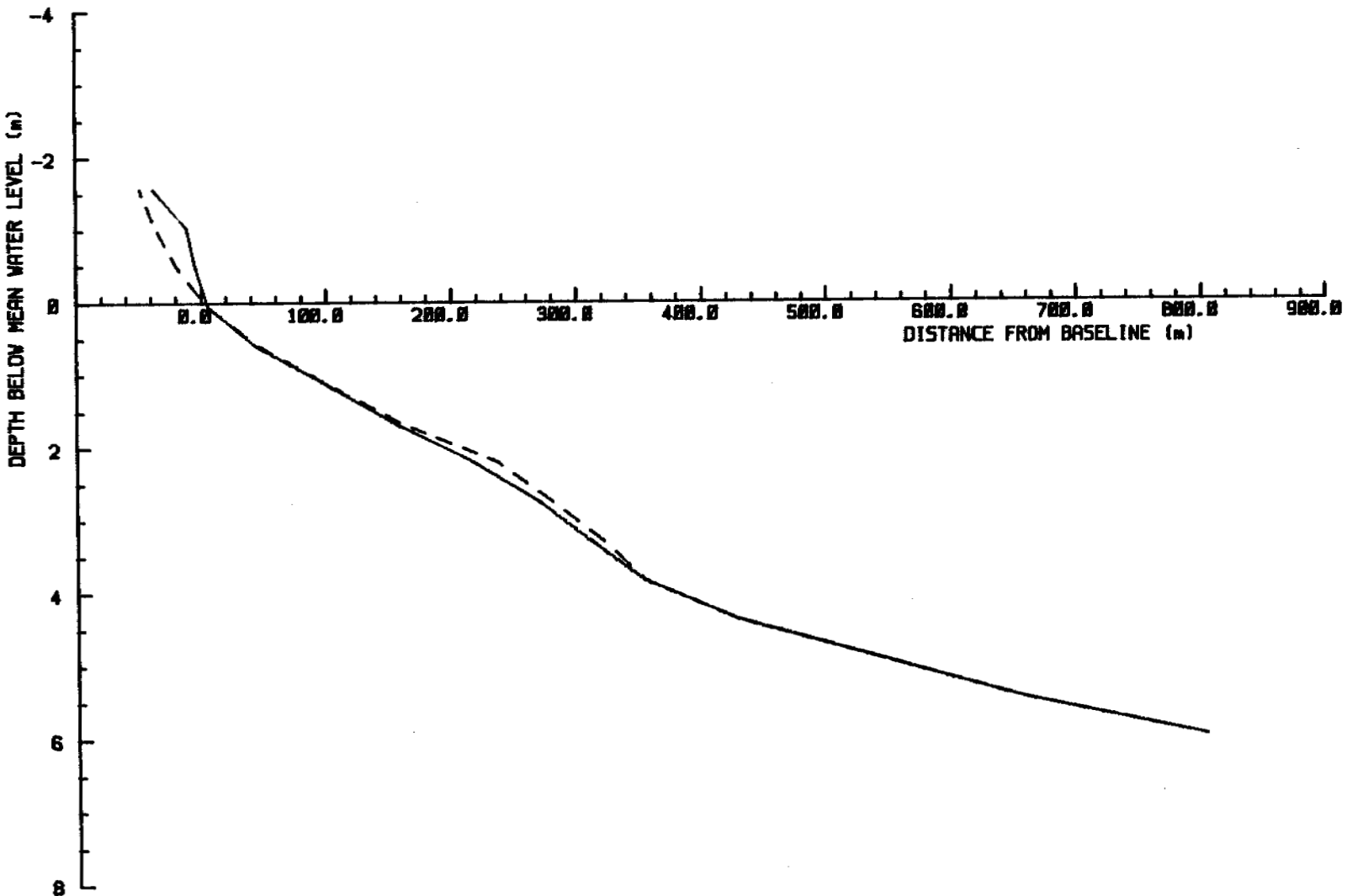
Date: 24 Apr 85

Scales as shown

Checked by:

Kelth Philippot

Consulting Limited



ATKINSON POINT PROFILE ADJUSTMENT

CALIBRATION RUN / VSKAPL = 1.0 / MEASURED PROFILE

TIDE = 1.0 m

Date: 24 Apr 85

Scales as shown

Checked by:

Kaith Philippot

Consulting Limited

LEGEND

————— Initial profile

----- End of run profile

CALIBRATION RUN 8

SUPPLEMENTARY DATA

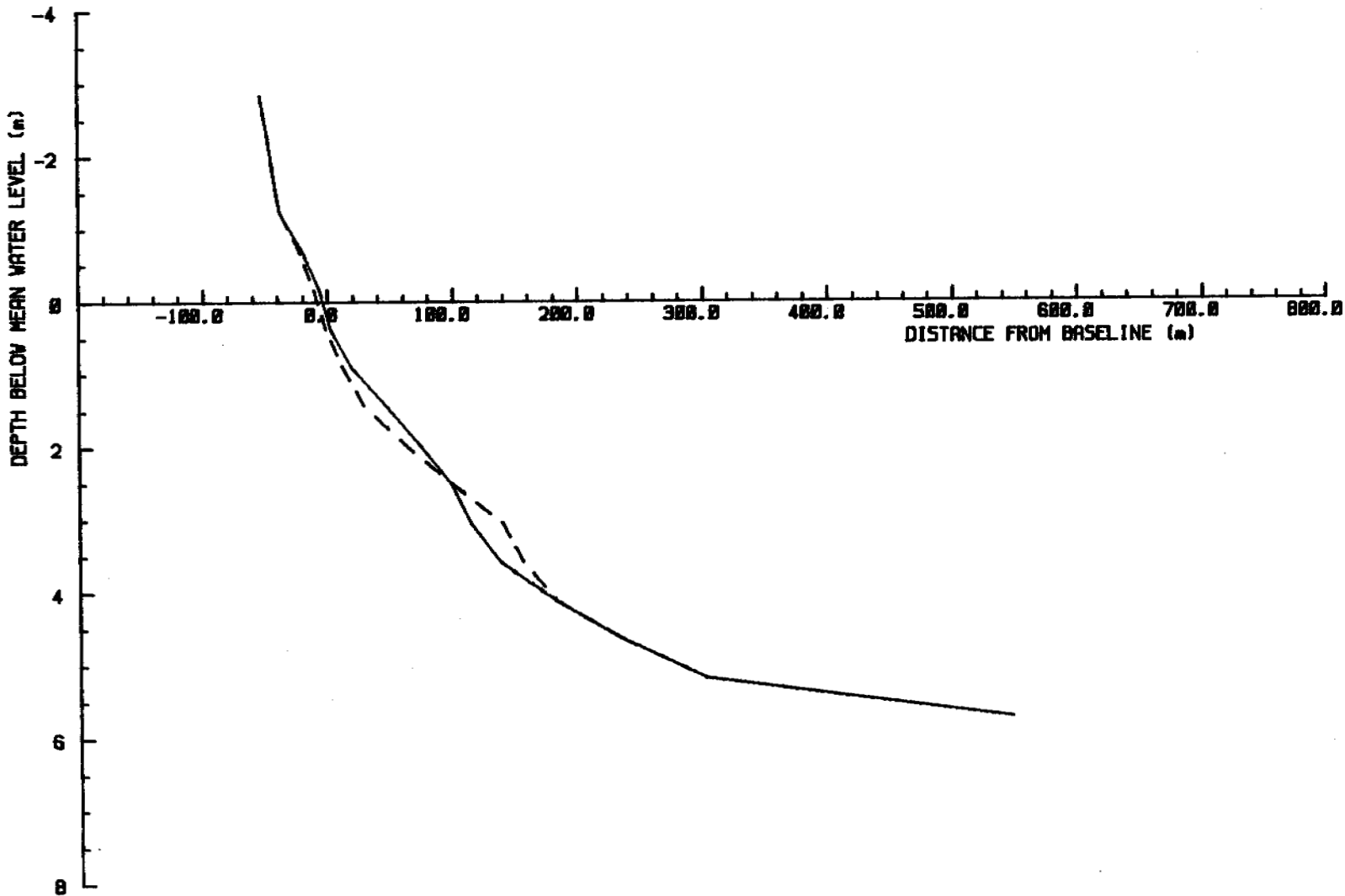
Calibration run for 90 wave conditions
Total time all waves was 1312.1 hours

Shoreline retreat = 2.53 metres

It is also probable that the poor fit above MWL is related to the fact that the beach at Atkinson Point is actually on a spit which experiences overtopping. SEGAR was not designed for spits or barrier beaches. The calibration at Atkinson Point was deemed unsuccessful because the match above mean water level was inadequate. Hence the analysis was terminated. It appeared that the measured profile was inconsistent with the theory underlying SEGAR.

7.6.2 Kay Point

A series of calibration runs produced the best fit at Kay Point with WSKAAL = 0.7. There is some deviation between the final profile from the calibration run and the measured profile (see Figure 7.6). However, both profiles were thought to be plausible and consequently storm surge runs were performed with both. The results are presented for both profiles for three storm runs, one with no surge, one with a constant surge of 0.5 m and one with a step form surge series with a peak height of 1.1 m. The latter corresponds to a 2.75 m surge at Tuktoyaktuk. The results indicate that shoreline retreat increases at Kay Point as the surge level increases. During a two day storm with a peak surge of 1.1 m, wave height of 2.26 m, and wave period of 8.48 s, SEGAR predicted the shoreline would retreat 9-10 m depending on which initial profile (measured or calibrated) is adopted. A constant 0.5 m surge produced a shoreline retreat of about 6.5 m on average. (Results are presented in Figures 7.7-7.9).



CALIBRATION RUN / WSKRAL = 0.7 / MEASURED PROFILE

KRY POINT PROFILE ADJUSTMENT

Date: 24 Apr 85

Scales as shown

Checked by:

Kaith Philpott

Consulting Limited

LEGEND

———— Initial profile

----- End of run profile

CALIBRATION RUN 2

SUPPLEMENTARY DATA

Calibration run for 66 wave conditions
Total time all waves was 1364.0 hours

Shoreline retreat = 4.40 metres

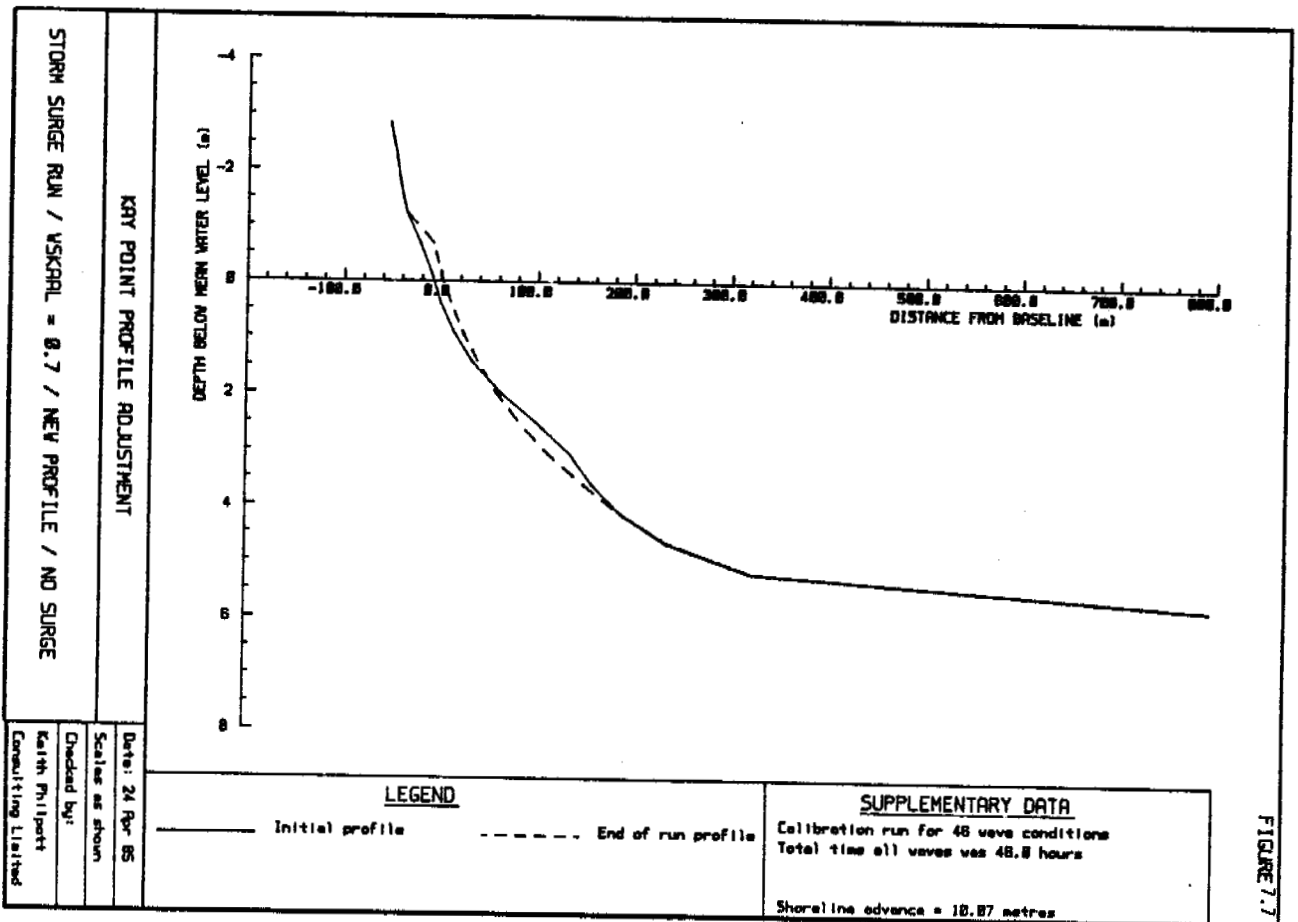
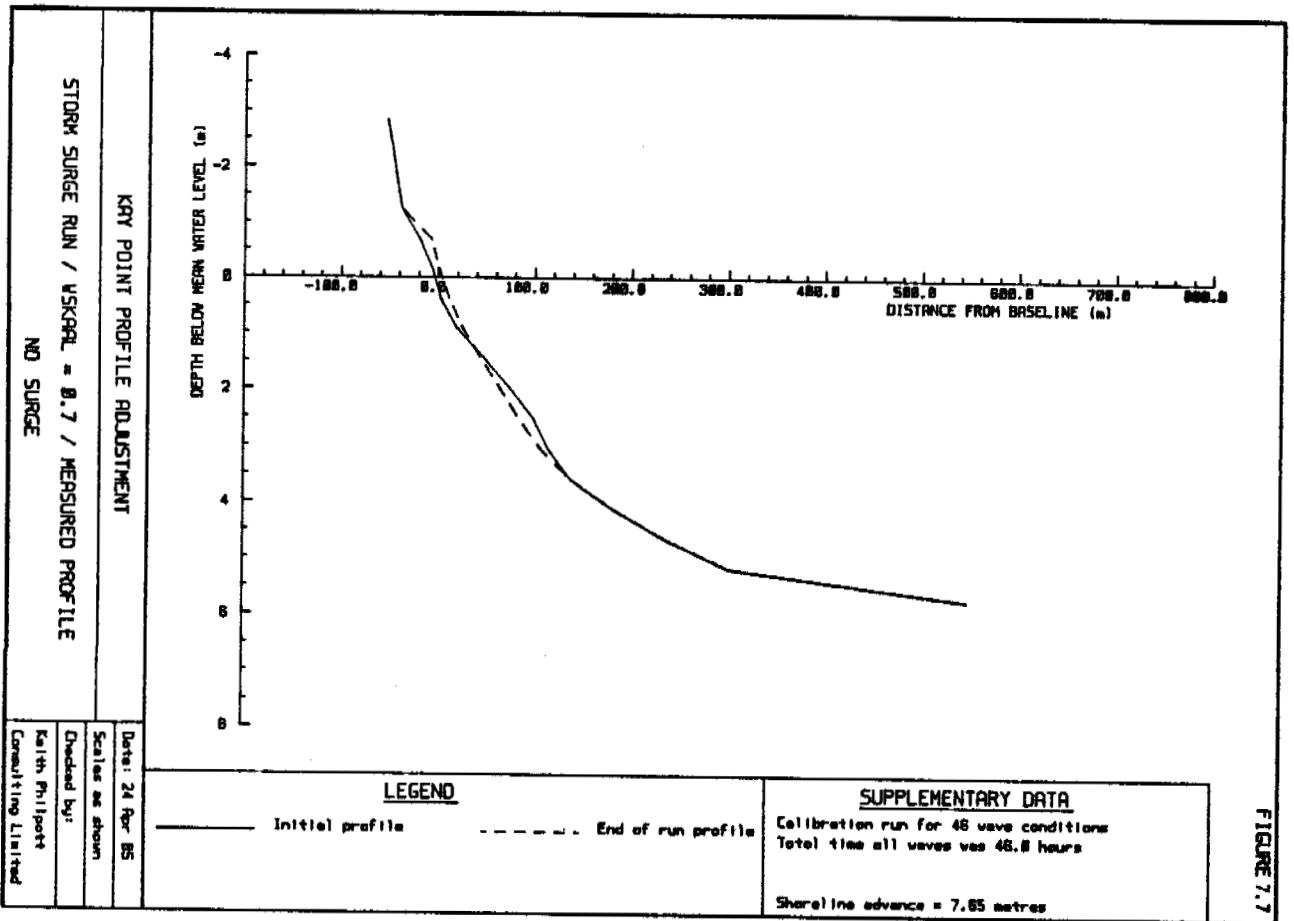


FIGURE 7.7

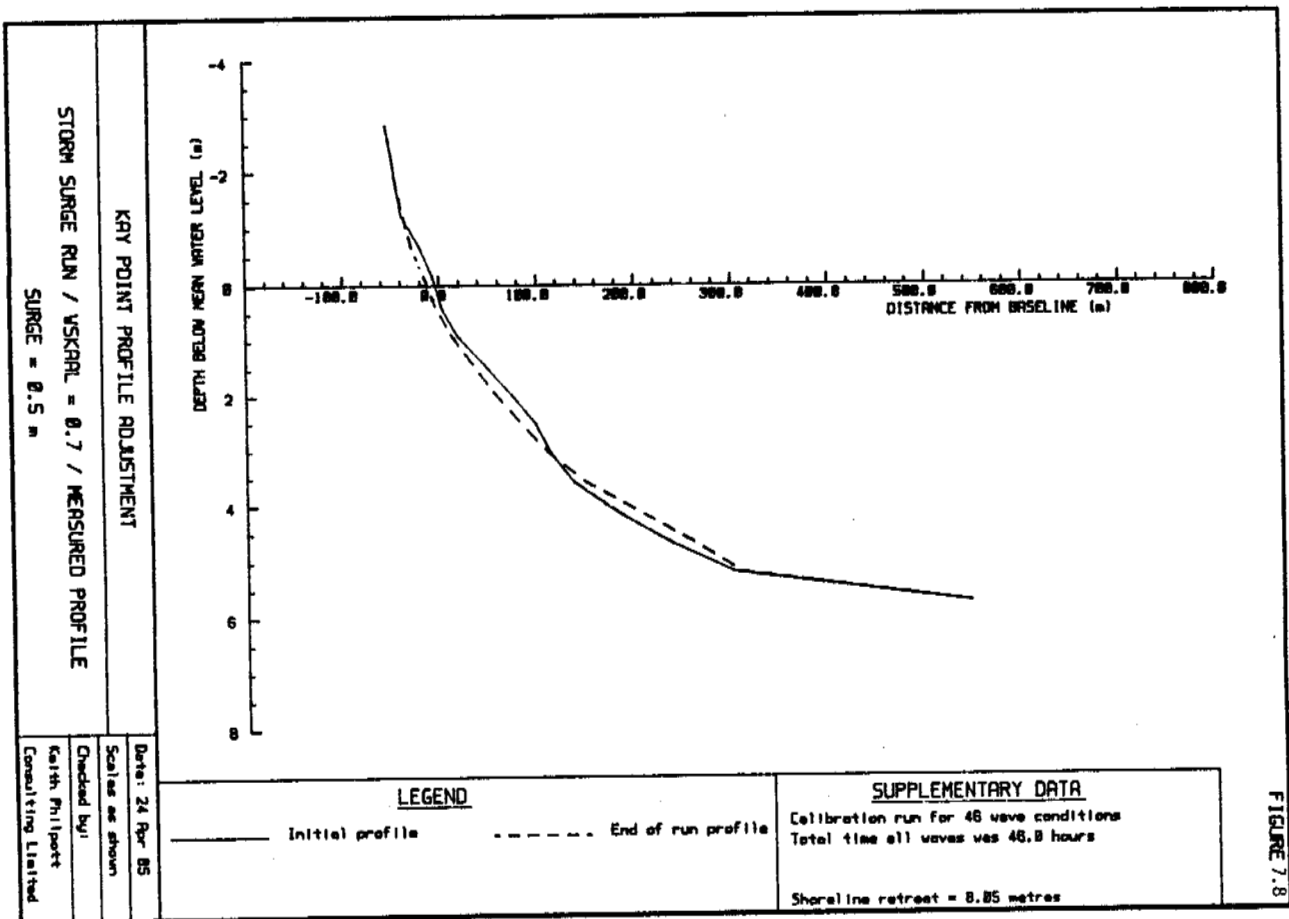
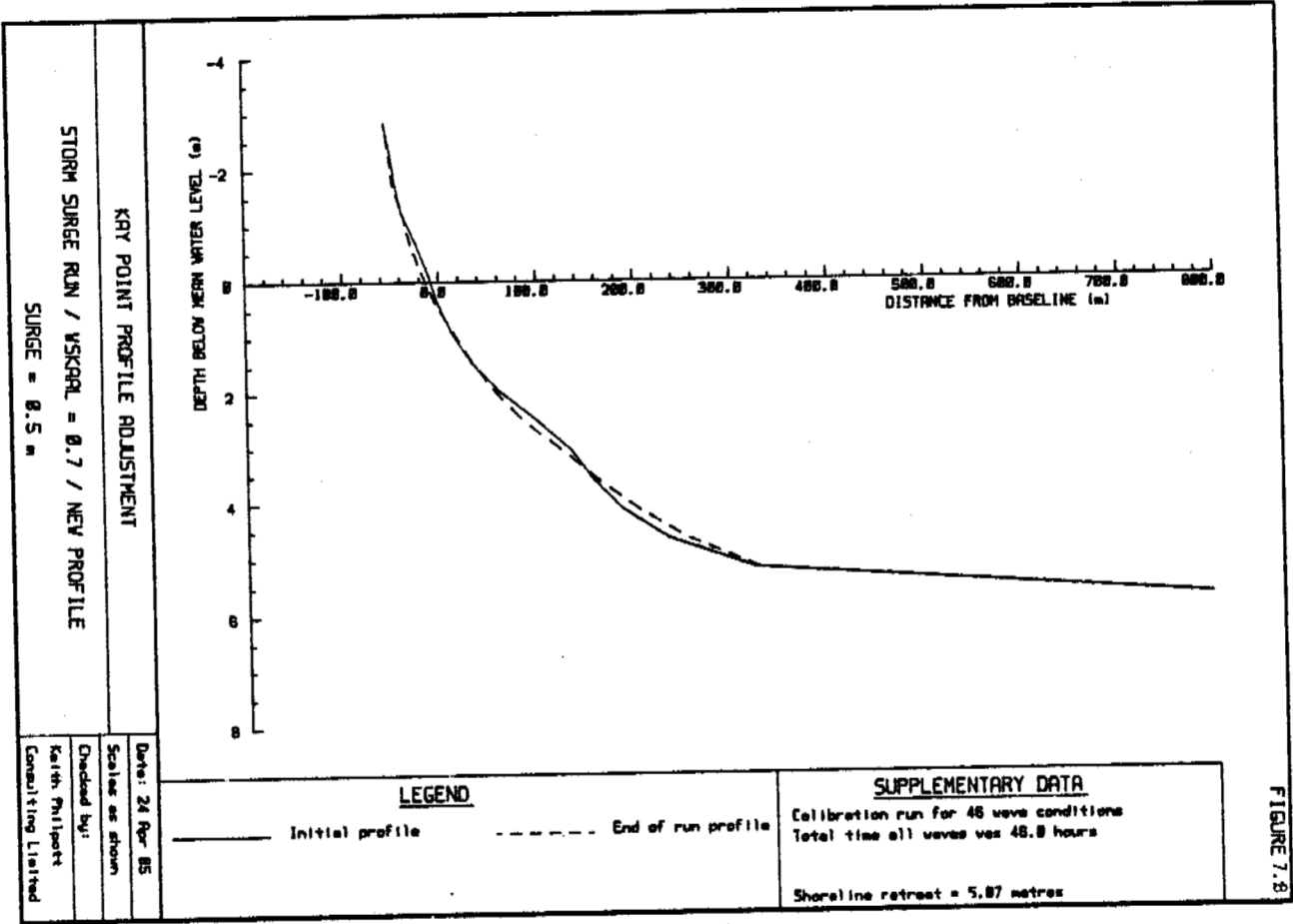


FIGURE 7.8

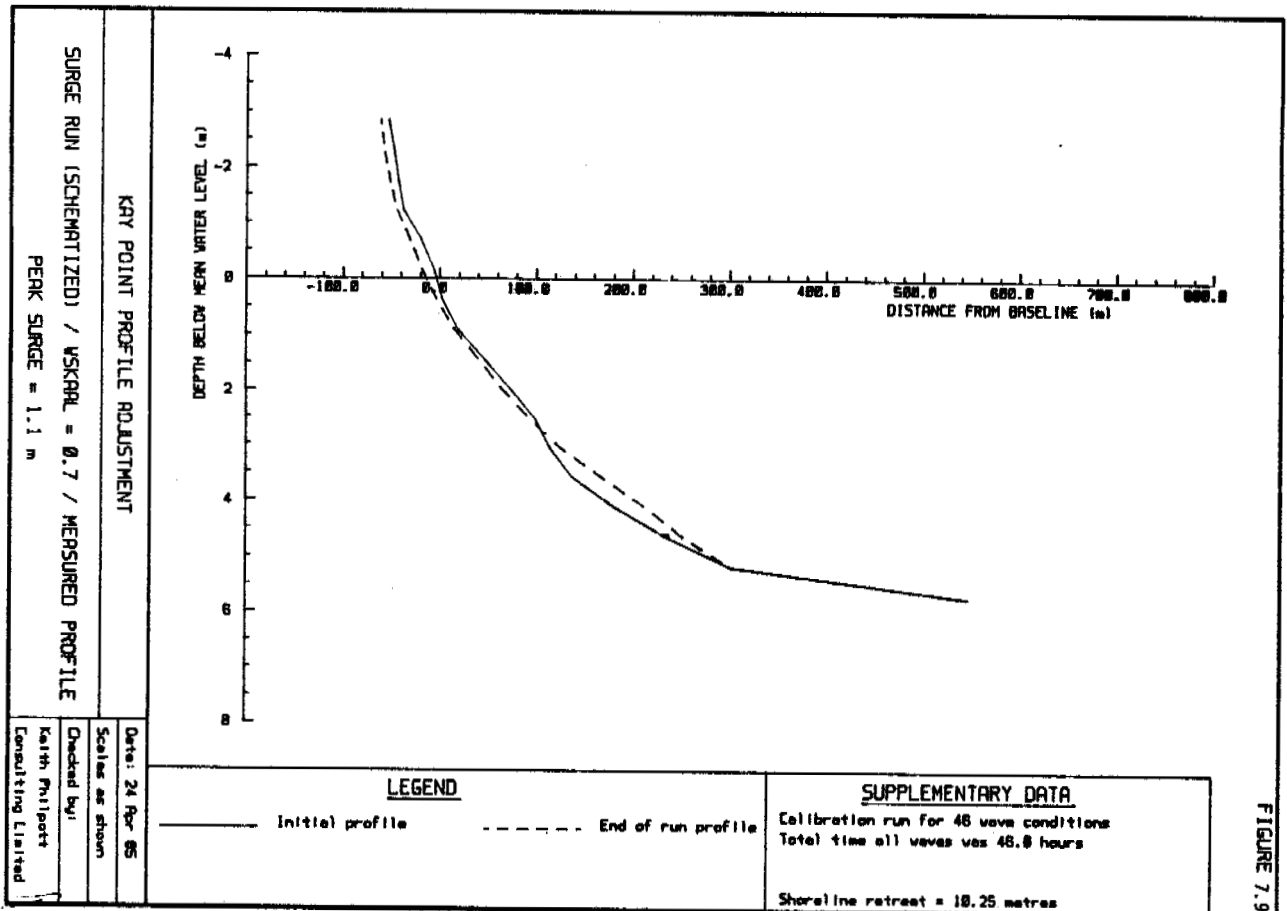


FIGURE 7.9

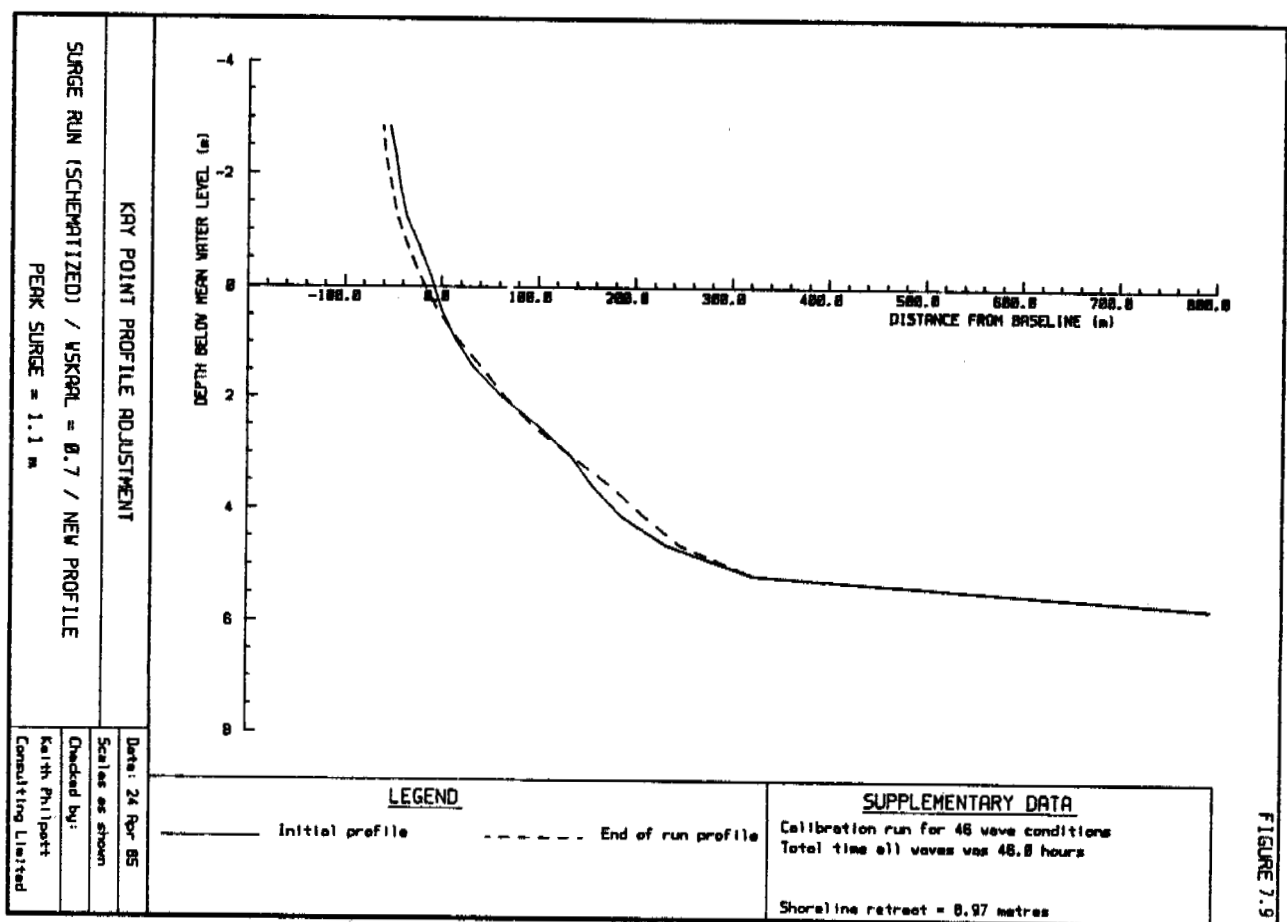


FIGURE 7.9

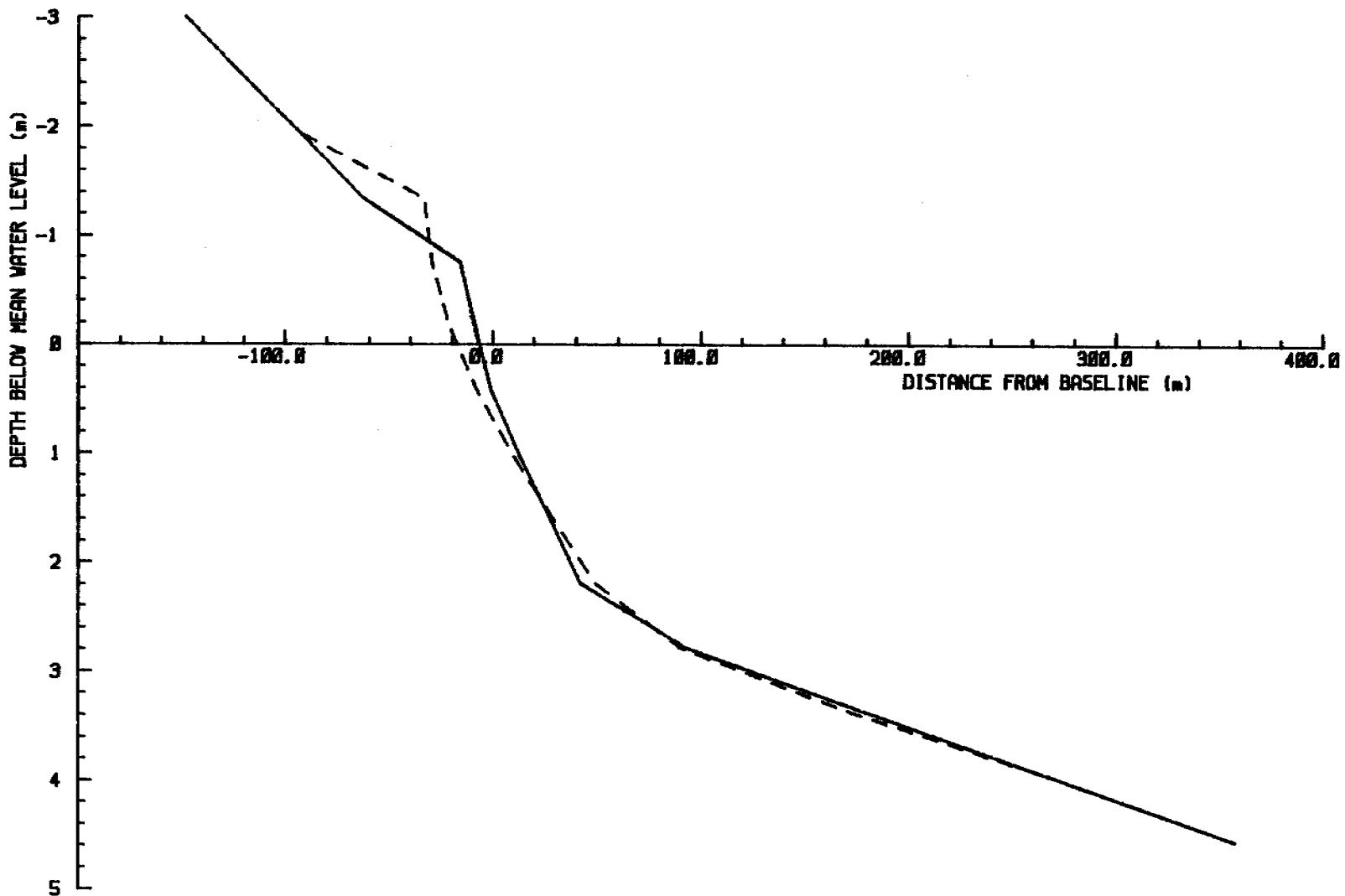
FIGURE 7.9

7.6.3 King Point

Calibration runs on the measured profile at King Point did not prove to be entirely successful. The best match occurred with a WSKAAL of 0.7, however the resulting profile was higher and less steep than the actual measured profile (see Figure 7.10). As with Atkinson Point it is believed that part of the reason for the poor match relates to the fact that King Point is a barrier beach subject to overwashing. Consequently, the resultant profile from the calibration run, rather than the measured profile, was chosen as the representative profile at this site. Calibration runs with the initial wave data set and with a one third roll-back on the data set gave consistent results for the adopted profile. (See Part II of this report for a full set of figures showing all the model runs).

Figures 7.11-7.13 show the results of three storm runs at varying surge levels. Again, shoreline retreat at mean water level increases with a rise in water level to a maximum of 4.75 m for a peak surge of 1.65 m above MWL.

Figure 7.13 also shows major flattening of the beach face in which the crest of the beach berm retreated about 50 metres and rose more than a metre in elevation. Although such changes are probably not fully realizable on the barrier beach at King Point they may be interpreted as an indication of overwashing on the real beach.



KING POINT PROFILE ADJUSTMENT

CALIBRATION RUN / WSKARL = 0.7 / SLT = 0.3 / UNSHOALED

Date: 24 Apr 85

Scales as shown

Checked by:

Keith Philippott

Consulting Limited

LEGEND

————— Initial profile - - - - - End of run profile
 Wave 1 Equilibrium

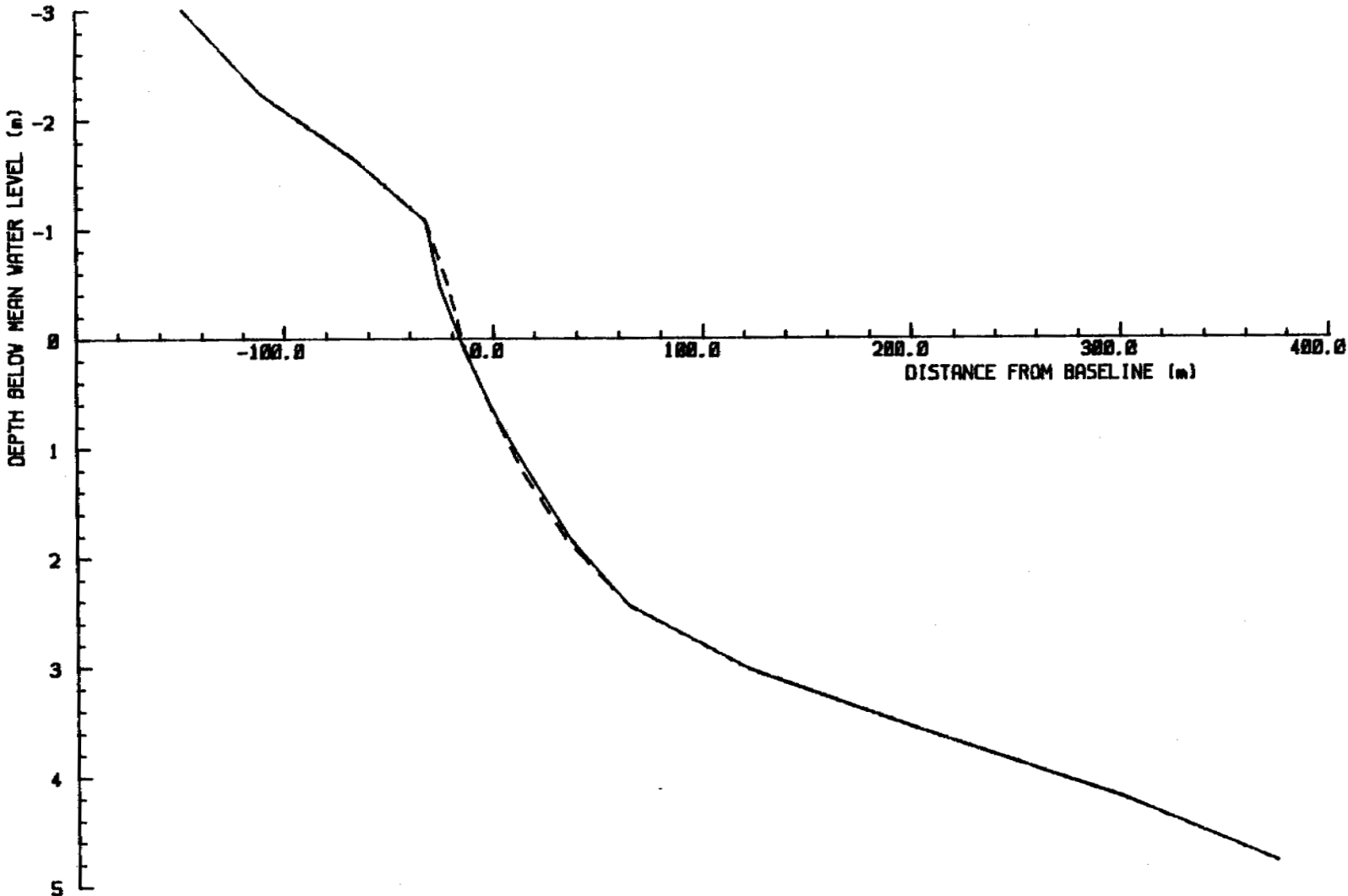
CALIBRATION RUN 5

SUPPLEMENTARY DATA

Calibration run for 57 wave conditions
 Total time all waves was 600.8 hours

Shoreline retreat = 10.76 metres

FIGURE
7.10



KING POINT PROFILE ADJUSTMENT

STORM SURGE RUN / NO SURGE / VSKAAL = 0.7

LEGEND

————— Initial profile - - - - - End of run profile

SUPPLEMENTARY DATA

Calibration run for 42 wave conditions
Total time all waves was 42.0 hours

Shoreline advance = 1.17 metres

FIGURE 7.11

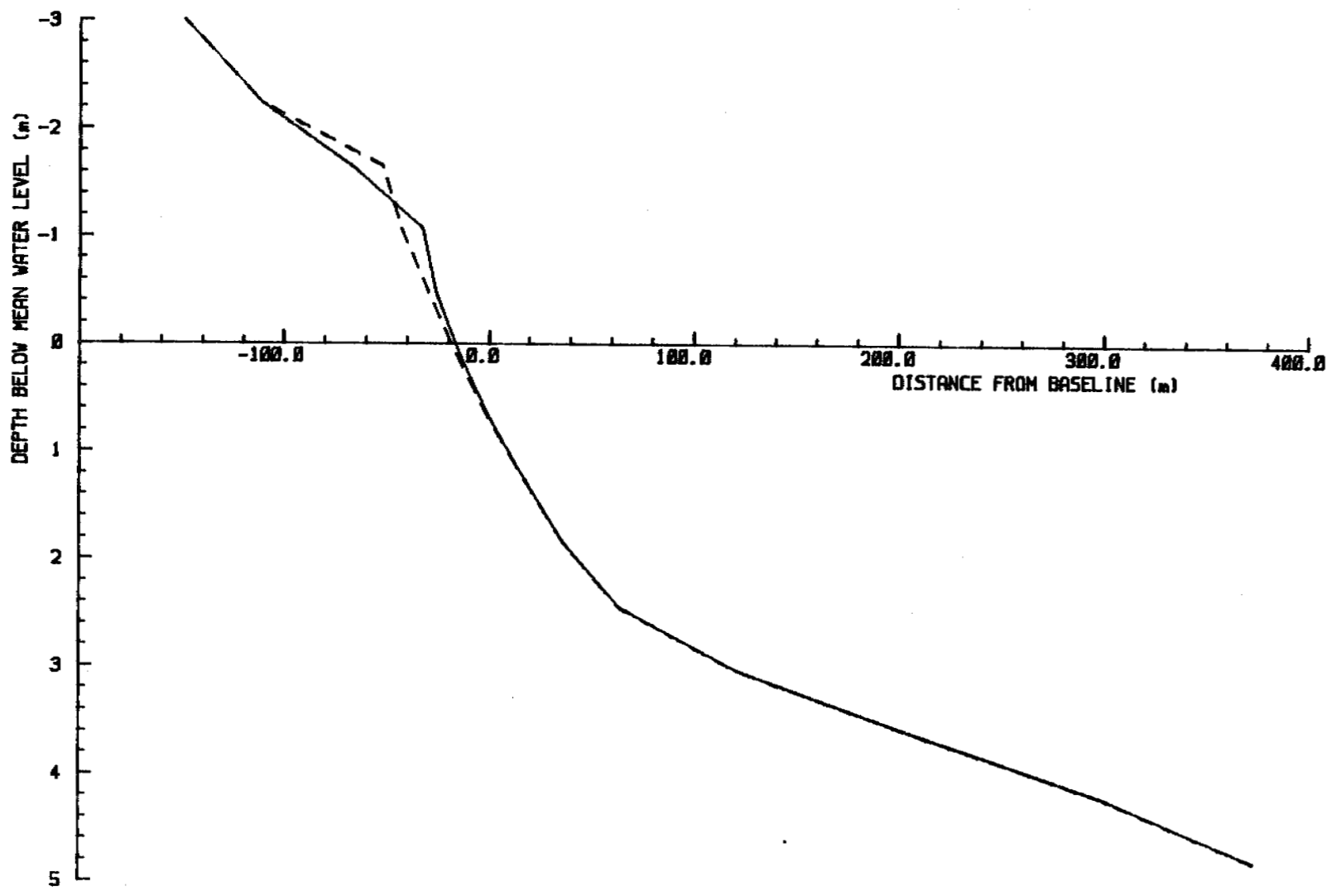
Date: 24 Apr 85

Scales as shown

Checked by:

Keith Phillipott
Consulting Limited

FIGURE 7.12



KING POINT PROFILE ADJUSTMENT

STORM SURGE RUN / SURGE = 1.0 m

LEGEND

Initial profile
 End of run profile

SUPPLEMENTARY DATA

Calibration run for 42 wave conditions
 Total time all waves was 42.0 hours

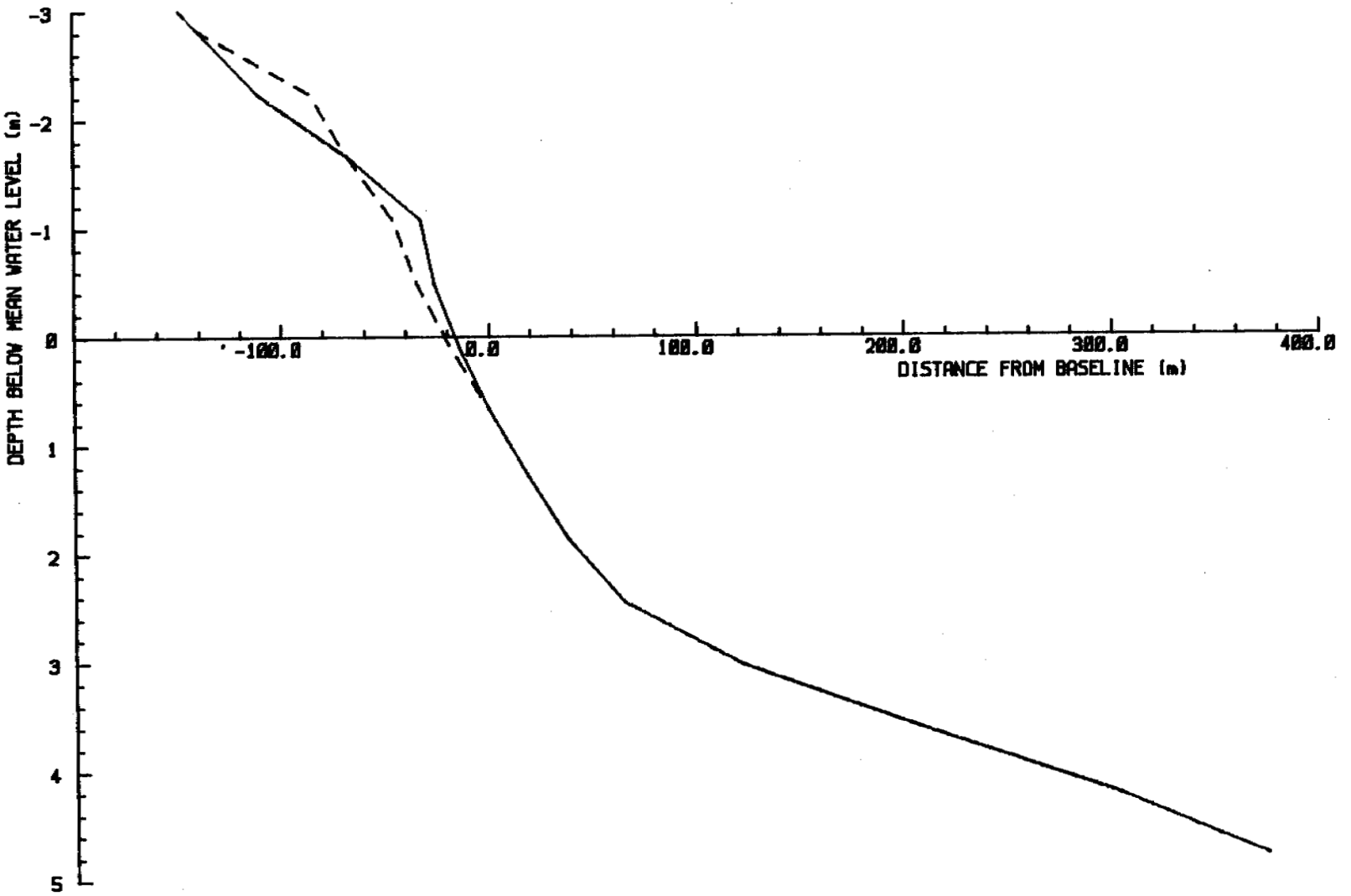
Shoreline retreat = 1.60 metres

Date: 24 Apr 85

Scales as shown

Checked by:

Kaith Philpott
Consulting Limited



KING POINT PROFILE ADJUSTMENT

STORM SURGE RUN / SCHEMATIZED SURGE / WSKARL = 0.7
 PEAK SURGE = 1.65 m above MWL

LEGEND

————— Initial profile - - - - - End of run profile

SUPPLEMENTARY DATA

Calibration run for 42 wave conditions
 Total time all waves was 42.0 hours

Shoreline retreat = 4.74 metres

Date: 24 Apr 85

Scales as shown

Checked by:

Kalith Philippott
 Consulting Limited

FIGURE 7.13

7.6.4 Stokes Point

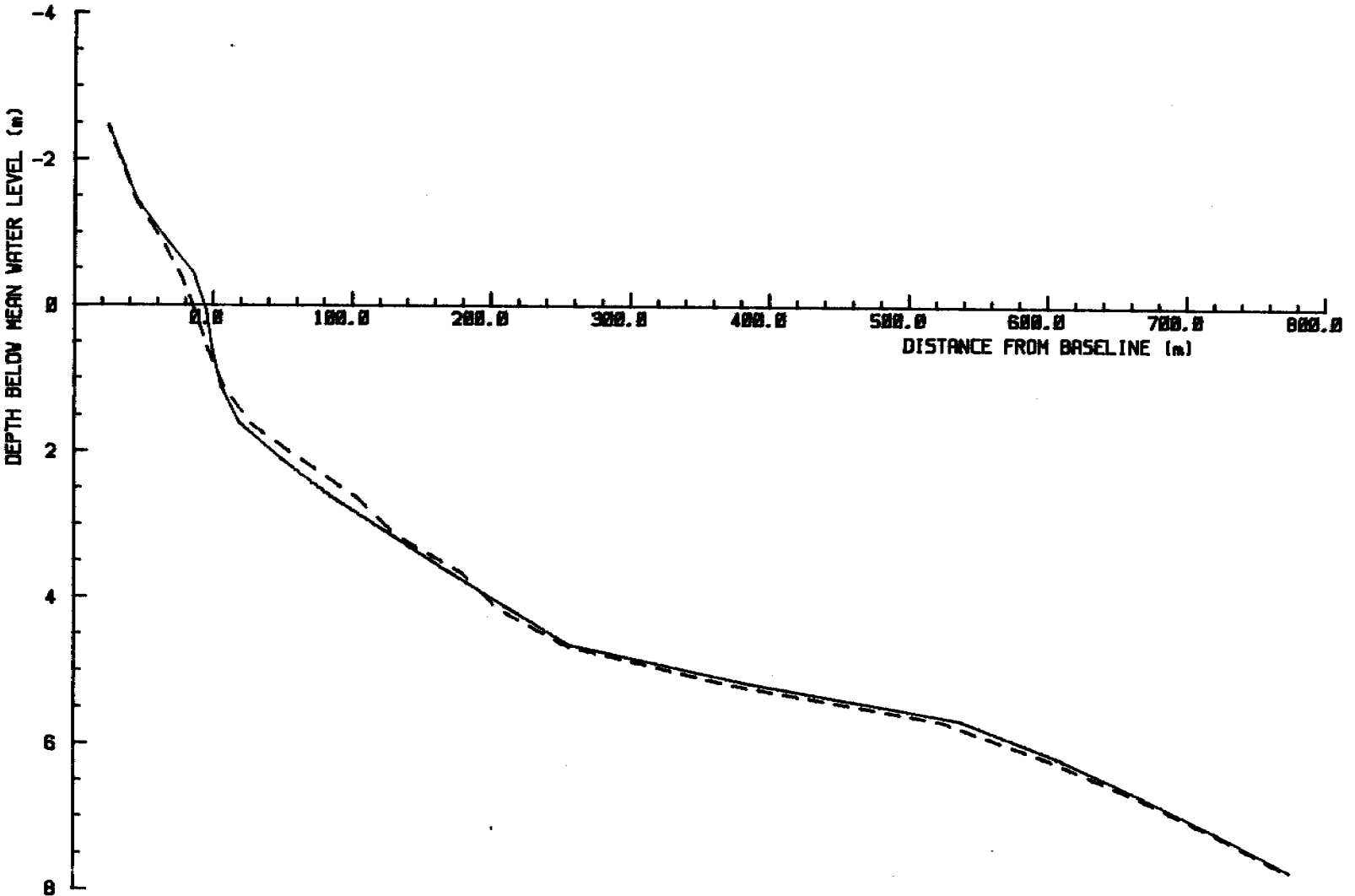
The most successful calibration run on the measured profile of Stokes Point was obtained with a WSKAAL value of 0.7 and a water level adjustment (or tide) of -0.5 m (see Figure 7.14). The need for a negative water level adjustment may indicate that the reported profile datum is in error.

Storm surge runs were performed on the measured profile with surges of 0.5 m and 1.0 m which in light of the calibration results levels may represent 0.0 m and 0.5 m surges.

The surge runs once again indicated that shoreline retreat increases as water level increases. At the larger surge the two day storm produced about 2 m of shoreline retreat at MWL. (Figure 7.15)

7.6.5 Tuktoyaktuk

In order to obtain a successful calibration run on the measured profile at Tuktoyaktuk the water level had to be adjusted by the addition of a 0.5 positive tide (see Figure 7.16). Again, this either indicates an error in establishing the datum of the measured profile, or it suggests that a majority of the waves which influence the profile occur when the water level is 0.5 m higher than the MWL.



STOKES POINT PROFILE ADJUSTMENT

CALIBRATION RUN / VSKRQL = 0.7 / MEASURED PROFILE TIDE
= -0.5 m

Date: 24 Apr 85

Scales as shown

Checked by:

Kaith Philippott
Consulting Limited

LEGEND

————— Initial profile - - - - - End of run profile

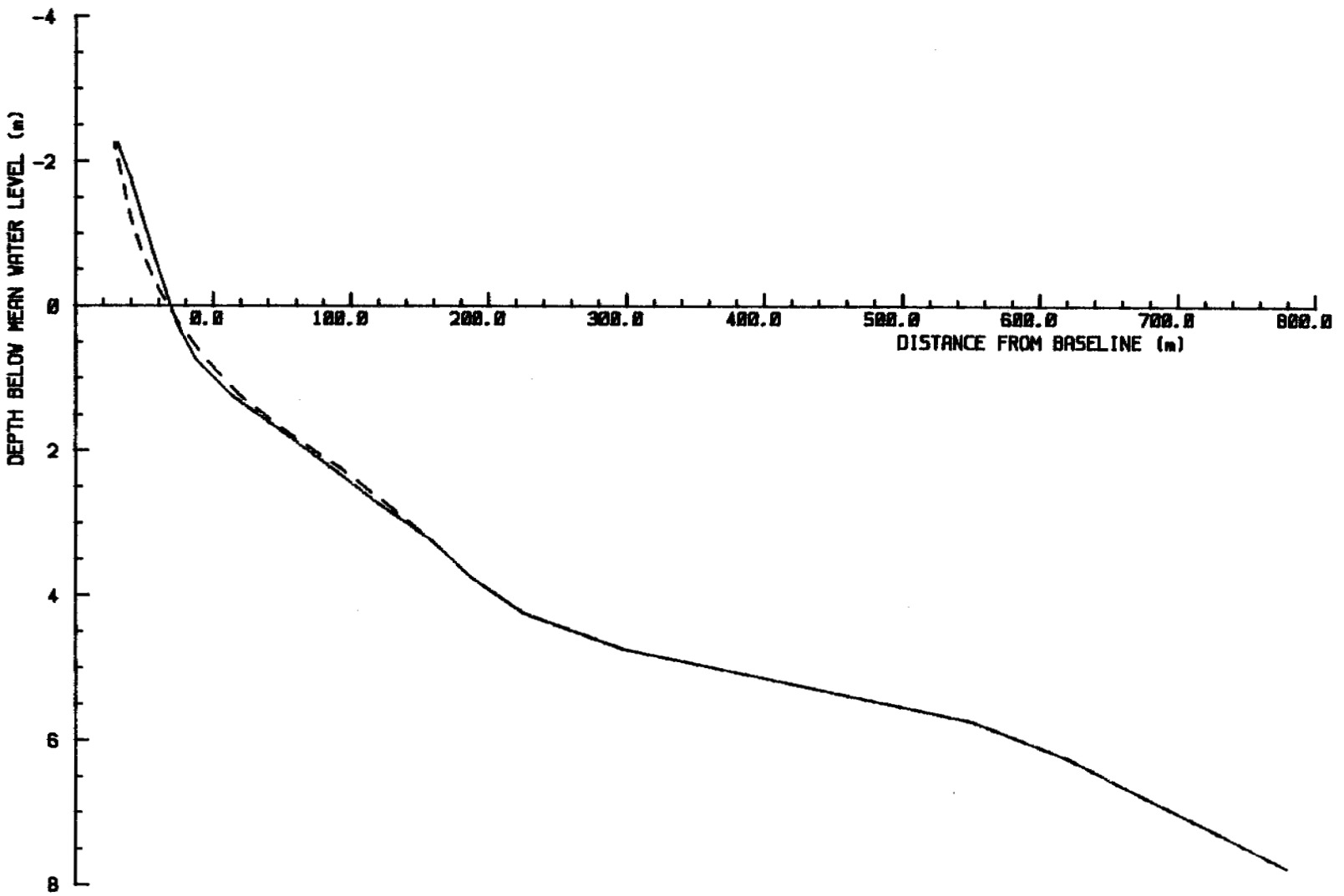
CALIBRATION RUN B

SUPPLEMENTARY DATA

Calibration run for 82 wave conditions
Total time all waves was 643.4 hours

Shoreline retreat = 7.91 metres

FIGURE 7.14



STORM SURGE RUN / SURGE = 1.0 m

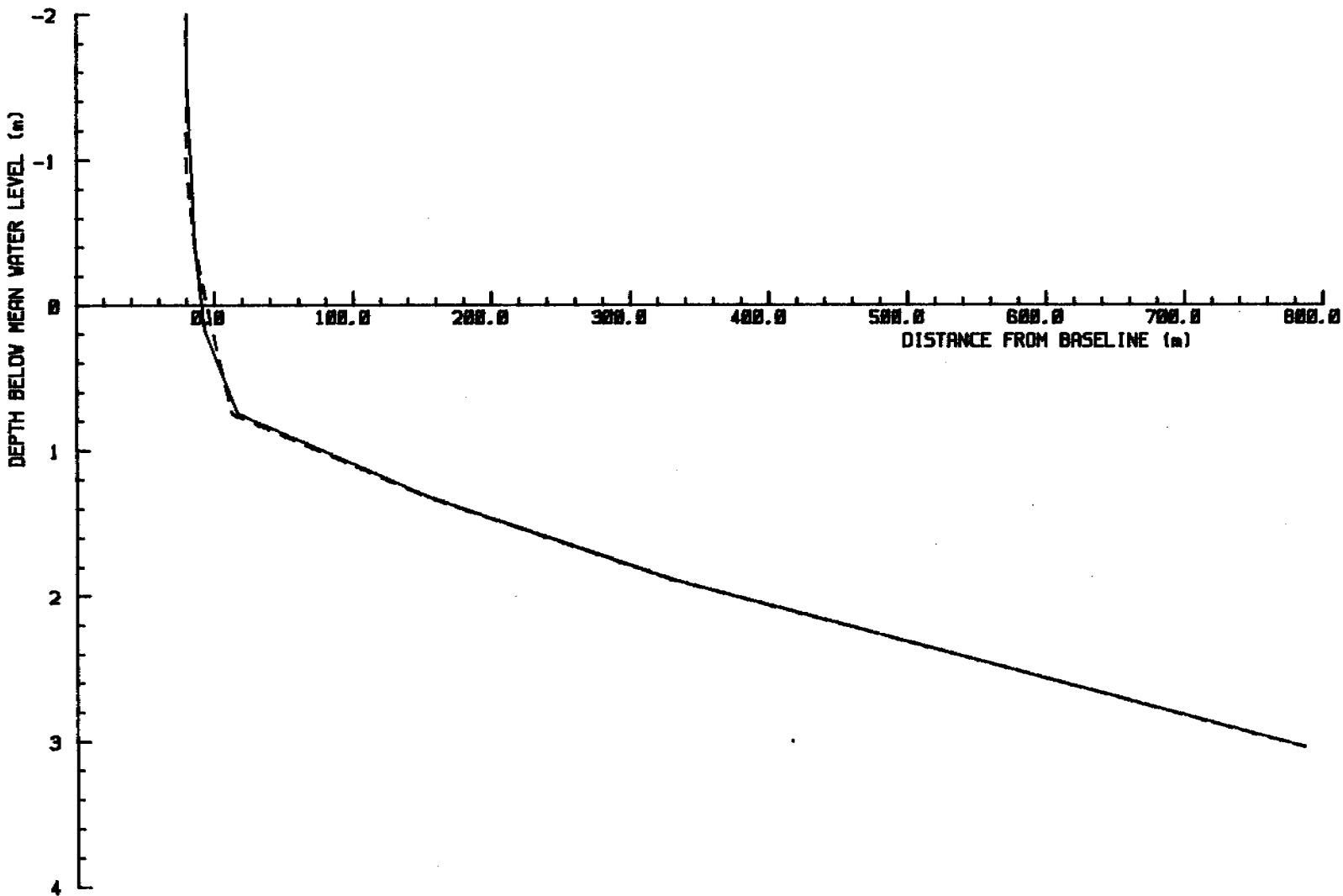
STOKES POINT PROFILE ADJUSTMENT

Date: 24 Apr 85
 Scales as shown
 Checked by:
 Keith Philippott
 Consulting Limited

LEGEND
 ——— Initial profile - - - - - End of run profile

SUPPLEMENTARY DATA
 Calibration run for 42 wave conditions
 Total time all waves was 42.0 hours
 Shoreline retreat = 1.83 metres

FIGURE 7.15



TUKTOYAKTUK PROFILE ADJUSTMENT

CALIBRATION RUN / VSKRAL = 0.7 / MEASURED PROFILE

TIDE = 0.5 m

LEGEND

————— Initial profile

----- End of run profile

CALIBRATION RUN 4

SUPPLEMENTARY DATA

Calibration run for 56 wave conditions
Total time all waves was 912.0 hours

Shoreline advance = 3.85 metres

Date: 24 Apr 85

Scales as shown

Checked by:

Kaith Philpott

Consulting Limited

FIGURE
7.16

The surge runs gave unusual results at Tuktoyaktuk, in which a shoreline advance rather than a retreat was recorded at mean water level for all surge levels. Several explanations can be offered for this. The primary points are that above MWL the profile is composed (at least on the surface) of very coarse material and consequently the upper backshore profile is very much steeper than the relatively gentle sloping nearshore which is covered with fine sediment. This made it impossible to choose a single representative sediment distribution for the entire profile.

SECTION 8 EFFECTS OF A STRUCTURE AT KING POINT

8.1 Introduction

The objective was to determine the effect of a hypothetical structure located at the west end of the barrier beach at King Point. The structure, in the form of a jetty or causeway, was assumed to be a total littoral barrier allowing no bypassing of littoral sediment.

The beach plan shape evolution model (BPLAN) was used to investigate this problem. The model computes changes in the planform of a shoreline due to spatial and temporal variations in alongshore sediment transport rates. It uses wave data in strict chronological order and updates shoreline geometry at the end of each wave condition so as to simulate the actual evolution. Coastal planform adjustments from 1970 to 1983 were determined with and without the coastal structure.

There is also a discussion of the feasibility of having an opening in the structure near the shore to facilitate fish migrations.

8.2 Description of the Model

8.2.1 Theoretical Background

The model (BPLAN) is a one-line shoreline change model based on the Pelnard-Considerere (1956) principle which assumes that the shoreline erodes or accretes in parallel slices. A simple equation of continuity illustrates the basic principle, as follows:

$$\frac{\partial Q_x}{\partial x} + h \frac{\partial y}{\partial t} = 0 \quad (8.1)$$

where Q_x is the littoral transport rate at point x ,

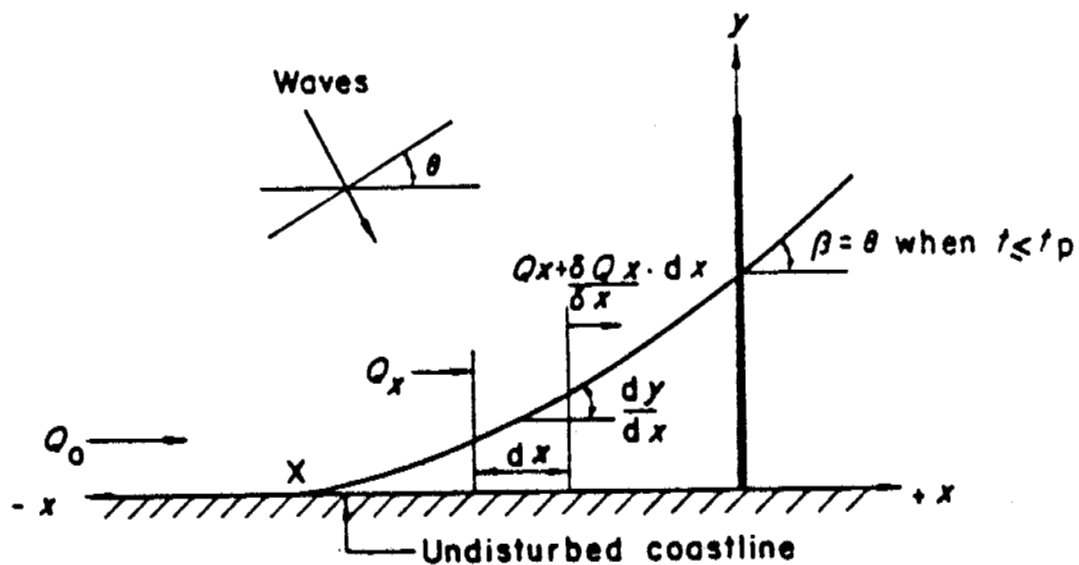
h is the active beach height below and above water,

$\partial y / \partial t$ represents the rate of shoreline change.

(See Figure 8.1).

With the present limits of knowledge, only potential alongshore transport rates, which assume unlimited availability of sand, can be computed directly. Similarly, there is an underlying assumption that all of the material eroded from the active beach face is transported as littoral material; possible offshore losses of fine material or overwash losses of coarser material are neglected. However, where field data is available for calibration it is possible to approximate the effects of restricted sand supply and offshore or inshore losses in BPLAN.

Assume the actual alongshore transport rate Q_x is equal to αQ_p , where Q_p is the potential transport rate and α is a factor less than 1. Also, if part of the erosion product of an eroding



(after Muir Wood and Fleming, 1981)

BEAUFORT SEA COASTAL SEDIMENT STUDY

Date: 2 May 85

Scales as shown

Checked by:

Figure 8.1 Reference Diagram for Beach Evolution Models

Keith Philpott
Consulting Limited

face of height h is lost offshore then the second term in equation 8.1 becomes $\beta h \partial y / \partial t$ where β is the fraction of erosion product that is not lost offshore. The case of an accreting beach face where a proportion of the material is either "lost" over a barrier beach, or offshore, can be similarly represented, although in that case β is greater than unity. With these two adjustments, equation 8.1 becomes

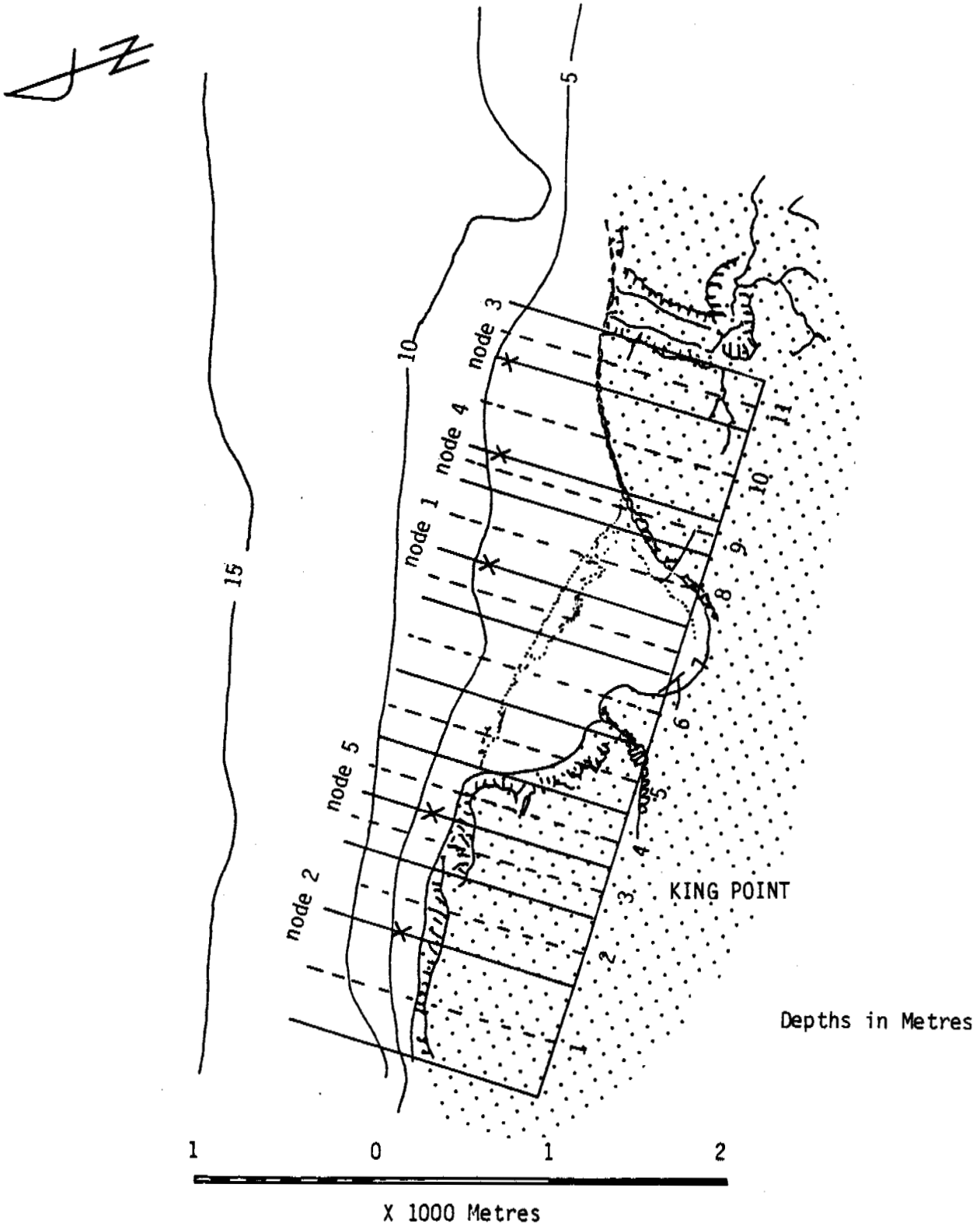
$$\alpha \frac{\partial Q_p}{\partial x} + \beta h \frac{\partial y}{\partial t} = 0 \quad (8.2)$$

For simplicity the two factors may be combined:

$$\frac{\partial Q_p}{\partial x} + \frac{\beta}{\alpha} h \frac{\partial y}{\partial t} = 0 \quad (8.3)$$

It will be clear from Equation 8.3 that the application of a single factor to the beach height, in effect the use of a fictitious height, suffices to calibrate the model to account for either or both of actual alongshore transport rates and losses from the beach face. The factor can be varied from one segment of beach to another as required. Generally, different factors apply to zones of erosion and accretion.

The BPLAN model also includes facilities to allow for the effects of beach nourishment, and for partial littoral barriers as well as total littoral barriers as used in this study.



<p>BEAUFORT SEA COASTAL SEDIMENT STUDY</p>	<p>Date: 8 Mar 85</p>
	<p>Scales as shown</p>
<p>Baseline Location for Beach Plan Evolution Model</p>	<p>Checked by:</p>
	<p>Keith Philpott Consulting Limited</p>

8.2.2 Input Data and Operation

The definition of the shoreline at King Point is shown in Figure 8.2. The coast was divided into 11 sections and the shape was determined by the offset from a baseline (dashed lines in Figure 8.2). The 1970 shoreline was used to define the initial condition. A fictitious erodable beach height was assigned to each section of beach. The input data for runs without and with a structure are shown in Tables 8.1 and 8.2 respectively.

The inshore wave climate was defined at five nodes shown on Figure 8.2. Nodes 1 and 2 were used for the alongshore sediment transport estimations described in Section 6. The inshore wave climate for each of the three additional nodes was determined specifically for application of the beach plan shape model. The three additional node locations were selected located with the aid of forward tracking wave refraction diagrams (see example in Figure 8.3)

The wave characteristics were interpolated at seven more locations to provide twelve littoral drift calculation points (these points fall on the solid lines in Figure 8.2). The model was applied using fourteen years of sequential hindcast data (1970-1983). Waves are refracted from the inshore node (at a depth of 4 m) to the breakpoint using plane beach refraction, assuming the contours are locally parallel to the shoreline. The potential littoral drift rate is then calculated for the twelve points using the Swart (1976b)

Table 8.1

Application of the Beach Plan Model at King Point

Conditions Without a Structure

Operating Conditions for Final Run 1970-1983

Beach Plan Shape Model Results - Without a Structure - Run KPBP7

No. of beach sections = 11

Initial beach offsets

at each section(1 to 11): 810.0, 900.0, 900.0, 900.0, 870.0, 780.0, 720.0, 640.0, 530.0, 720.0, 870.0

Length of each section(1 to 11): 650.0, 400.0, 300.0, 300.0, 400.0, 400.0, 300.0, 400.0, 200.0, 500.0, 300.0

Angle of baseline normal to true north = 47.0

Refraction data specified at

drift calculation points: 2, 4, 8, 10, 11

Refraction data given at 4.0 m. contour

Calibration height

(for sections 1 to 11): 50.0, 50.0, 50.0, 50.0, 5.0, 5.0, 25.0, 25.0, 25.0, 25.0, 25.0

Drift calculation point 1 is an open boundary

Drift calculation point 12 is an open boundary

- Notes: 1. Distances and heights are in metres; angles are in degrees.
 2. Calibration beach height equals (actual height) X (height factor).

Table B.2

Application of the Beach Plan Model at King Point

Conditions With a Structure

Operating Conditions for Final Run 1970-1983

Beach Plan Shape Model Results - With a Structure - Run KPBPB

No. of beach sections = 11

Initial beach offsets

at each section(1 to 11): 810.0, 900.0, 900.0, 900.0, 870.0, 780.0, 720.0, 640.0, 530.0, 720.0, 870.0

Length of each section(1 to 11): 650.0, 400.0, 300.0, 300.0, 400.0, 400.0, 300.0, 400.0, 200.0, 500.0, 300.0,

Angle of baseline normal to true north = 47.0

Refraction data specified at

drift calculation points: 2, 4, 8, 10, 11

Refraction data given at 4.0 m. contour

Calibration height

(for sections 1 to 11): 5.0, 5.0, 5.0, 5.0, 5.0, 5.0, 25.0, 25.0, 25.0, 25.0, 25.0

Drift calculation point 1 is an open boundary

Drift calculation point 5 is a long groyne

Drift calculation point 12 is an open boundary

- Notes: 1. Distances and heights are in metres; angles in degrees.
 2. Calibration beach height equals (actual height) X (height factor).

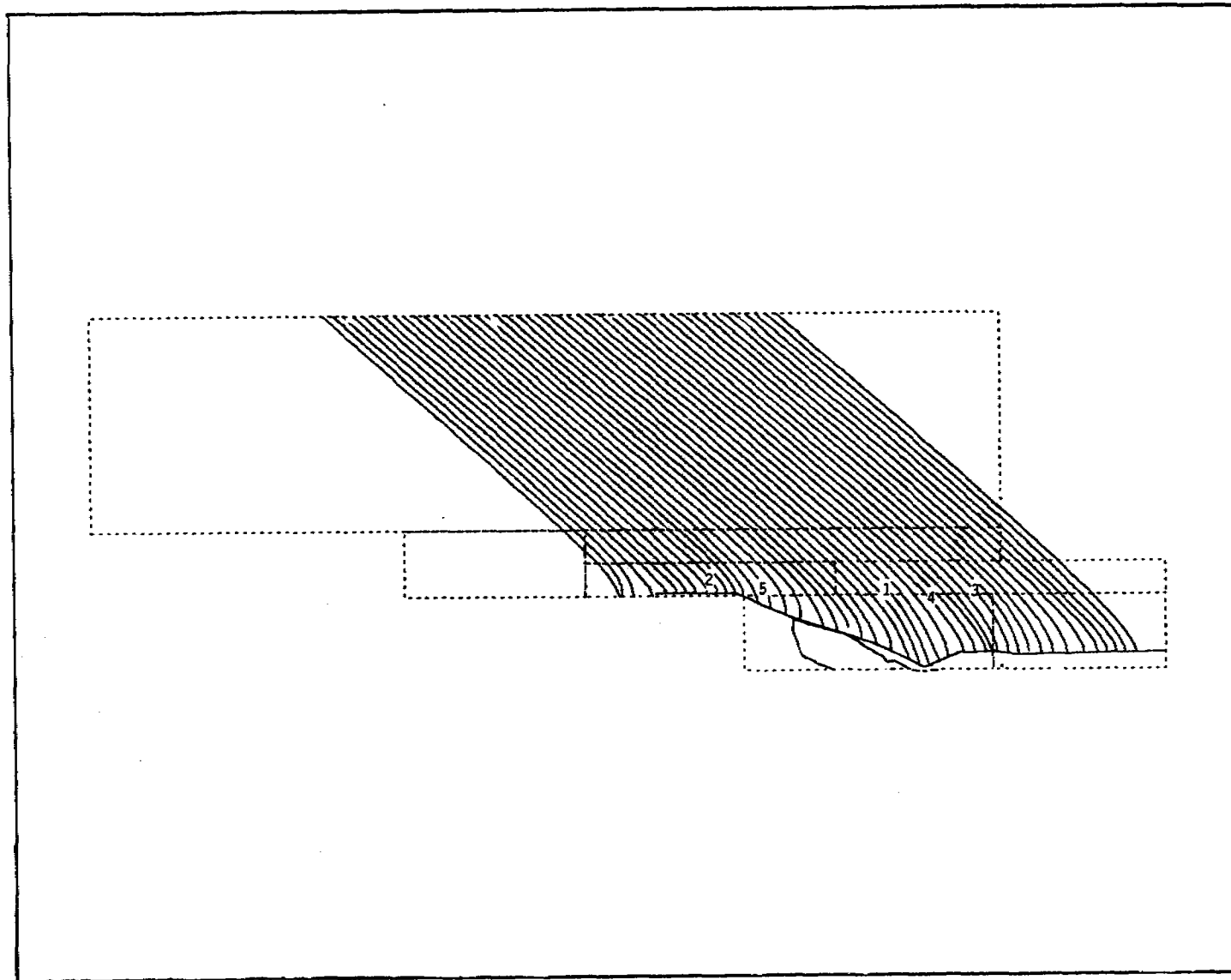


Figure 8.3

WAVE RAY DETAILS

Tide Level= 0.50 m.
 Wave Period= 5.0 secs
 Direction= 229.0 Degrees True

Bathymetry information used for grids obtained from the following sources:
 - C.H.S. Field Sheets numbered:
 V.R. 10070 (1970)
 V.R. 10071 (1970)
 - Soundings taken by Peter Kiewit Construction Co. Ltd. (1984).
 Original notes by B. McDonald & a scaled version by D. Frobel



BEAUFORT COASTAL SEDIMENT STUDY

Wave Refraction Analysis for
 King Point - Beaufort Sea
 showing Node Locations

Date: 31 Jan 85	
Scale 1:50000	Checked by:
Keith Philpott Consulting Limited	

modified CERC bulk energy model. The amount of erosion or accretion is determined by the difference in the littoral drift entering and leaving a beach section. The shoreline position offsets change with each wave condition and therefore the beach plan shape is redefined after each wave. This ensures that shoreline change is properly evolutionary (i.e. in correct chronological sequence).

8.3 Potential vs. Actual Littoral Drift

All sediment transport models determine the potential maximum alongshore transport rate which is only realized when there is an unlimited supply of sand. Ideally, beach plan shape models should only be applied where there is a fully developed beach with an unlimited sand supply. At King Point, the potential transport is often not realized since there are no fully developed beaches east or west of the barrier beach.

At King Point the actual sediment transport was estimated by using recession rates of the bluffs east and west of the barrier beach (McDonald and Lewis, 1973; Harper et al., 1985). Confidence in this approximation was strengthened by a separate calculation of infilling of the barrier beach over a period of fourteen years, 1956-1970.

Through a personal communication from R. Gillie, Dobrocky Seatech, the composition of the bluff was estimated from information included

in McDonald and Lewis (1973). The information included sediment particle size distribution and the percentage ice content. The volume of sand and gravel which might be expected to be moved as littoral drift was then taken as a percentage of the total volume per metre alongshore (bluff height multiplied by the recession rate). This calculation indicated that actual drift was about 15,000-25,000 m³/year from the west and 2500 m³/year from the east. The separate analysis for the infilling of the barrier beach produced an estimate for gross littoral transport of 21,000 m³/year which agrees well with the result determined from the recession rates.

The potential littoral drift along the coast at King Point reaches a maximum gross potential transport rate of 183,000 m³/year, according to the beach plan model. This is obviously much greater than the actual transport rate. Input to the beach plan shape model had to be adjusted to accommodate the discrepancy between actual and potential rates of transport.

Initial calibration runs were performed with estimated actual beach height parameters. The results from these runs showed an unreasonably large amount of deposition at the east end of the barrier beach and larger recession rates along the bluff west of the beach than actually occurred. It was possible to compensate for the artificially high accretion and erosion by applying a factor to the beach height to restrict shoreline change (using the principle described by Equation 8.3). A reasonable estimate of the required beach height factor could be made in both cases. The excessive

erosion was thereby brought into correspondance with the known recession rates. To calibrate for accretion at the east end of the beach, the beach height was multiplied by the ratio of deposition predicted from potential transport rates to the deposition calculated from the actual sediment transport rates.

Some of the calibrated beach heights were adjusted when the structure was added. West of the structure, the calibration beach height factors were reduced to reflect the altered coastal processes in this area. East of the structure calibration factors remained the same.

8.4 Form of Results

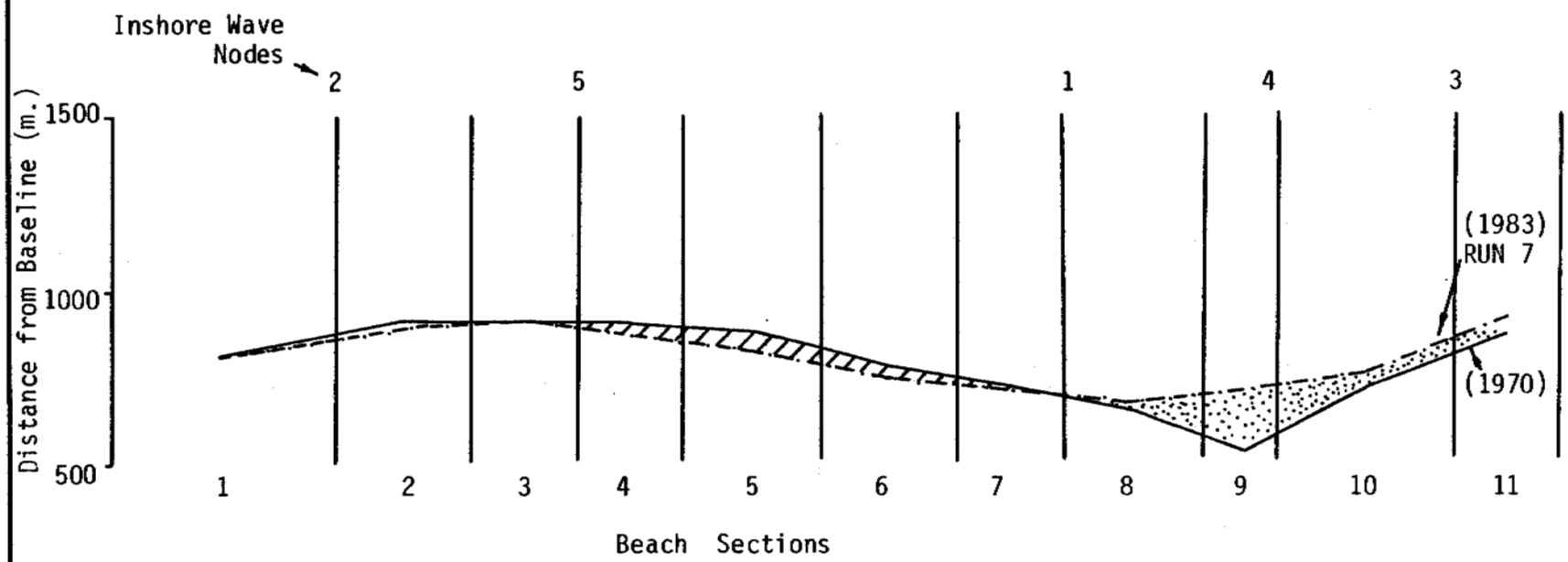
The results are presented in Part II of this report in the form of summary tables for the end of each open water season (1970-1983). The tabular results consist of yearly and cumulative values of beach line position (offset) changes and beach volume changes at each littoral drift calculation point. The tables also include the littoral drift estimates (left, right and net) at each calculation point. The BPLAN model has the facility to produce summaries for any chosen period of time.

8.5 Discussion of the Results

The beach plan shape change between 1970 and 1983 for the run without a structure is shown in Figure 8.4. The noticeable changes include some erosion at the west end of the barrier beach and a very large area of deposition at the east end of the barrier beach. The results from this model could be checked against aerial photographs, but unfortunately no photographs have been taken by EMR since 1970. The depositional feature does seem to be overestimated; 150 m of accretion was predicted at beach in section 9. The calibration would have been improved if an estimate of the amount of sediment lost over the barrier beach into the lagoon was available. This could also be accounted for by an increase in apparent beach height to limit the extent of accretion.

The second run was performed with an impermeable structure at the west end of the beach. This hypothetical coastal structure has been included in some conceptual designs proposed for a King Point harbour development (for instance, the Beaufort Sea Environmental Impact Statement, 1982.)

The run with a structure in place again probably overestimates deposition east of the barrier beach for the reasons presented above. (See Figure 8.5). Furthermore, the area of erosion immediately east of the structure for a distance comparable to its length will have been overestimated because the sheltering of the structure on local wave action is not taken into account.



Legend: — 1970 shoreline
- - - 1983 shoreline (Run 6)
/// erosion
••• accretion

BEAUFORT SEA COASTAL SEDIMENT STUDY

Beach Plan Shape Evolution without Structure at King Point 1970 - 1983

Date: 8 Mar 85
Scale: 1:20,000

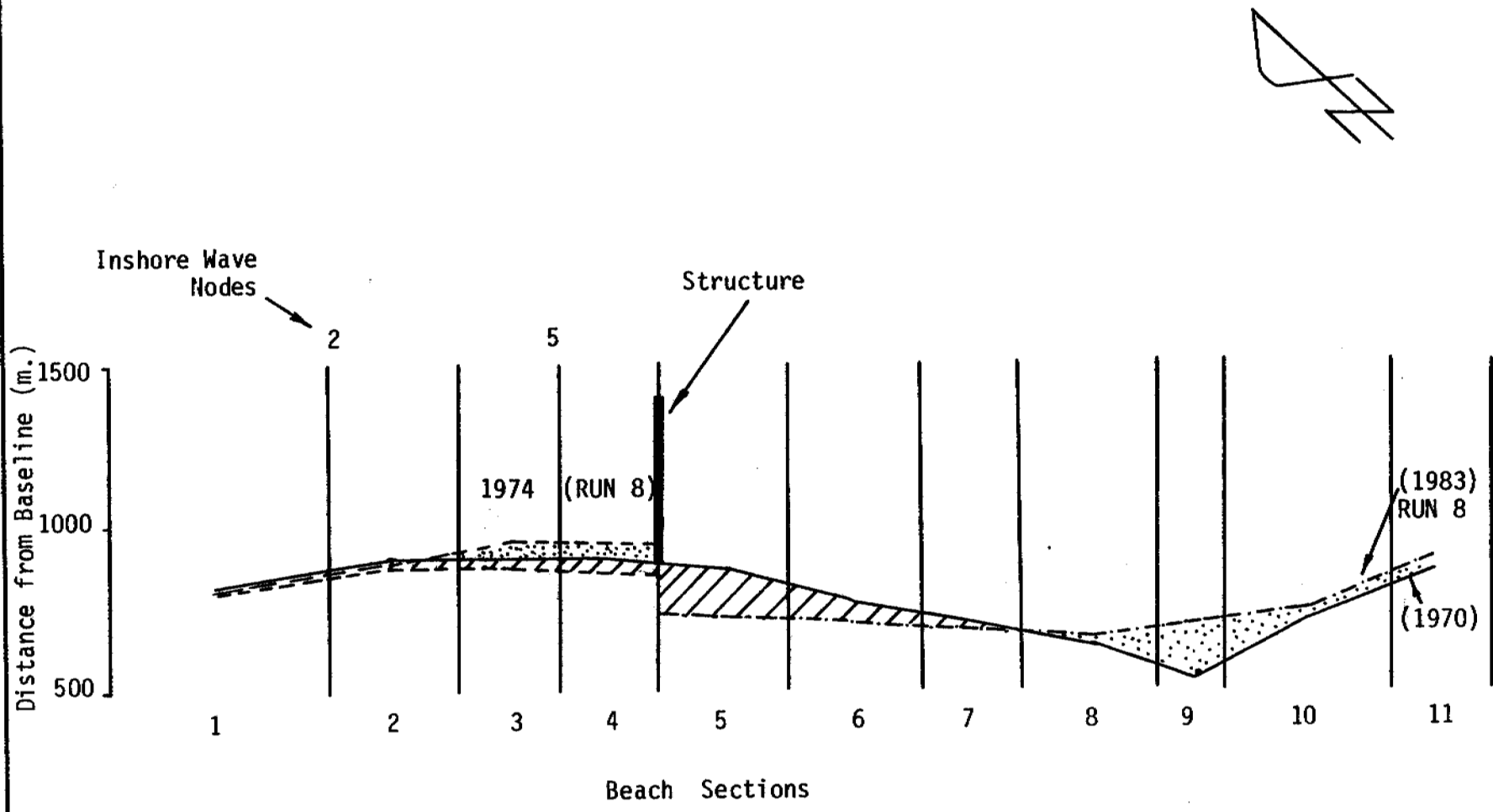
Checked by:
Keith Philippott
Consulting Limited

FIGURE 8.4

BEAUFORT SEA COASTAL SEDIMENT STUDY

Beach Plan Shape Evolution with Structure at King Point
1970 - 1983

Date: 8 Mar 85
 Scale: 1:20,000
 Checked by:
 Keith Philippott
 Consulting Limited



Legend:

- 1970 shoreline
- 1983 shoreline (Run 8)
- - - 1974 shoreline (Run 8)
- /// erosion
- accretion

FIGURE 8.5

Considering that this volume of erosion is overestimated and that no bypassing occurs at the structure, deposition east of the beach would be considerably less than computed. One interesting conclusion from the model is that net deposition west of the structure is not likely to occur in the long term, although in some years deposition may occur, (resulting from net transport to the east), as evidenced by the predicted shoreline position after 1974. In Figure 8.5 the structure appears to have been outflanked, however, the erosion in the immediate vicinity of the structure will be reduced or even reversed by the effects of sheltering, thus reducing the risk of outflanking.

8.6 Feasibility of Fish Migration Passages

Environmental concern has arisen over the impact of an impermeable structure on coastal fish migration. The possibility of leaving gaps in the structure would not be advisable in the nearshore zone. During years when westerly storms are significant, accumulation of sediment occurs west of the structure (see predicted shoreline position in 1974-Figure 8.5).

The effects of gaps near the shoreward ends of littoral

barriers on littoral currents and littoral transport have been examined on a number occasions: For example during preliminary studies for Fifty Point Marina on Lake Ontario (personal communication, Public Works Canada), and in Oman (Philpott, 1980). It was also tried unsuccessfully at Rungsted Harbour in Denmark (since rebuilt).

The concept of leaving a gap to permit passage of cuments, sediment and fish does not work well unless the complete structure is "transparent" to waves. This is because alongshore sediment transport is reduced in any partially sheltered "wave shadow" area leading to deposition and eventual filling of the gap.

To build a sufficiently "open" structure in the Arctic is evidently not feasible and would furthermore defeat the objective if it is to serve as a breakwater. Under these circumstances the only feasible alternative the fish migratioin passage is essential would be to pierce the structure with large culverts and to reopen them when they become blocked. Depending on the water depth requirement it could be more economical to install several culverts and simply abandon those close to shore as they become filled with sand.

This topic requires further consideration.

SECTION 9 DISCUSSION OF METHODOLOGY AND RESULTS

9.1 Overview of Methodology

This is a discussion of both the techniques used in this study and of the results obtained by their use. The techniques are reviewed through examining the numerical models implemented. The results are presented on a site by site basis.

In this it is also necessary to make a clear distinction among the three types of numerical models used and their relative merits. These are: 1) wave hindcasting; 2) nearshore wave transformation; and 3) coastal sediment transport. These three types of models are designed to be interfaced although they are separate and distinct modelling systems which are commonly used independently or with other models. They are discussed under separate headings following this overview.

The conventional sequence in wave analysis is to commence with hindcasting and then proceed to grid preparation, backtracking, etc. However, in the present study where complex sheltering conditions were encountered at several sites it was found to be essential to consider the grid boundaries before deciding on wave hindcasting stations. From this came a clearer recognition that any given wave sheltering problem may be resolved in a number of ways;

that selection of a particular set of grid boundaries is most important and will influence the proper selection of the hindcasting stations and the range of fetch directions that must be taken into account. The derived inshore wave climates from the wave modelling systems are then used as input to the coastal process models. The wave data is used in either sequential or statistical format depending on the particular model application.

9.2 Wave Hindcasting

The wave hindcasting procedure PHEW was successfully adapted to incorporate time varying fetches to allow for the changing position of the ice limit. Two other modifications were required to cope with unusual shallow water conditions at North Head and Tuktoyaktuk. The PHEW procedure, a "one-dimensional" parametric wave hindcasting system, was designed to imitate some features of more complex two-dimensional systems and to incorporate several features to facilitate calibration. Calibration tests with the limited amount of available directional wave measurements (none in the Beaufort Sea) have shown that this procedure is significantly more accurate than the common practice of defining offshore wave angles to the nearest 45 degrees. However, a wider range of good quality measured wave data is still needed to continue calibrating and verifying its output. In the present study the shallow water modifications were introduced because they were obviously better than

previously available facilities though they could not be properly calibrated for lack of measured data.

Some other possible refinements also await suitable measured data and the opportunity for undertaking calibration and verification tests. The complete lack of directional wave data and shallow water nearshore measurements in the Beaufort Sea is an important constraint that should be remedied.

9.3 Nearshore Wave Transformations

The refraction of directional spectra using LINREF and SPECTRANS has proved to be of special value because of the complex patterns of coastal sheltering and/or the shallows that were found in varying degrees at virtually all of the seven sites other than Atkinson Point.

The late addition of a facility to limit the spectrum according to the form of the shallow water equilibrium spectrum provides an important refinement to the technique. According to measurements at Pointe Sapin, New Brunswick, this phenomenon can reduce inshore wave heights by as much as 50%. It is especially worth noting here that the use of the shallow water saturated spectrum to limit the inshore wave height appears to make it usually redundant to perform complex wave friction calculations. There is still a strong need, however, for inshore directional wave

measurements at places like Kay Point, Stokes Point, North Head and Tuktoyaktuk to further confirm these methods and assumptions.

By comparison with the spectral transfer technique, the conventional use of forward-tracked refraction and unidirectional mono-chromatic waves is too primitive to cope with any coastal boundary conditions other than simple open coasts. Even in these cases, errors remain due to the failure to take spectral saturation into account.

The complexities of some of the sites required the development of a special procedure in addition to the software modifications discussed elsewhere. For example, the North Head site is exposed to two independently generated wave fields. One is the "deepwater" wave field from Mackenzie Bay which is quite strongly refracted before reaching the site. The other is the locally generated shallow water wave field which is subject to much less refraction. Two separate wave hindcasts were required here.

9.4 Alongshore Sediment Transport Models

The alongshore sediment transport package SEDX, was originally developed for research purposes and not as an operational tool. It was intended to be a "test-bench" for making objective comparisons among different models by applying exactly the same input data set to all models. For this reason no facility for individual "

tuning" of inputs to each model was provided, as normally done when only one model is in use. On the other hand, in an operational application, such as this, the SEDX format can produce a startling range of answers that serves to dispel any misconception about the accuracy of coastal sediment transport estimates that might be engendered by having only one model.

This study confirms that there are major shortcomings with the available models for the prediction of alongshore transport. The difficulties are exemplified by the wide range of results the different models can yield from the same set of input data. To some extent the problems arise from the specific morphology of Beaufort Sea coasts which evidently differ substantially from the conditions used in the derivation of the models. However, this is not the whole story, and another part of the problem lies in the fact that most of the models have been synthesized from somewhat heterogeneous combinations of theoretical, laboratory, and field data sources.

9.4.1 Bulk Energy Predictor Models

The bulk energy models, the first of which appeared nearly 30 years ago, relate alongshore transport directly to a simple fraction of the alongshore component of wave power. They produce stable results, and are believed to be accurate to within half an order of magnitude under appropriate circumstances. However, they provide no detail and little insight into the sediment transport process, just a number for the alongshore transport rate, based on the accumulated total work done by the dissipation of the alongshore component of wave power.

The most familiar, and still most widely used, the CERC bulk energy model, is least appropriate for the Beaufort Sea coastline since it does not include a threshold criterion for sediment motion, and does not relate alongshore transport to wave breaker characteristics, beach slope, and grain diameter. The sediment sizes ranged from fine sand to gravel and the CERC model does not differentiate between them. The Swart (1979) adaption can be regarded as a modest improvement to the CERC model but it only works over a restricted range of sediment size and wave characteristics and cannot produce results outside that range. The most promising version of a bulk energy model was developed by Kamphuis and Sayao (1982) and improved by Davies (1984). It includes the effect of beach slope, wave steepness and sediment suspension. It implicitly

includes a threshold criterion. The most recent refinement of this expression also incorporates grain diameter in the manner described by Sayao, Nairn and Kamphuis (1985).

9.4.2 Detailed Predictors

The detailed predictors exhibit notable instabilities and sometimes the range of answers from the various models for a single set of input data is as high as three orders of magnitude. Since nature is not so unstable, this variation must be attributed to the model formulations and to interactions between the models and computed inputs which rely in turn on other theories or research results.

The detailed predictors all use a common set of results to compute bottom roughness and the alongshore current distribution but then differ more or less in the sediment transport models they use and their way of dealing with suspended sediment. While the package deal approach can lead to instances of instability which may have been avoided through individual tuning, it does not provide an objective evaluation of the variation in results that can be expected from these models.

The longshore current model that Fleming and Swart (1982) developed from theory by Longuet-Higgins (1970) assumes that waves

break as spilling breakers. This assumption is not entirely valid at some of the study sites and the confidence in prediction would be improved if the model could accommodate plunging breakers by introducing lateral mixing to the alongshore current velocity distribution where necessary. Furthermore, the original Longuet-Higgins development was not intended for steeply sloping beaches or barred profiles. While barred profiles did not exist at the study sites, in some cases steep beach slopes did. Unfortunately, an acceptable formulation for longshore currents on steep slopes is not presently available.

Of the two families of detailed predictors the most advanced from each category are the Swart and Lenhoff (1980) model and the Nielsen et al., (1978) model. The Ackers and White adaptation by Swart and Lenhoff is unstable at fine grain sizes and deserves improvement in this aspect - possibly by calibrating bed roughness to produce reasonable results or by improving on the incipient motion threshold criterion based on recent discoveries. The more reasonable sediment transport estimates provided by the Nielsen models (even at very fine grain sizes) most likely result from the inclusion of very fine grain sizes (eg. 0.08 mm) in the laboratory tests Nielsen used to define his empirical coefficients. One possible improvement to this model might be to extend it to include an expression for

sediment concentration in a surf zone characterized by plunging breakers. However, this would present considerable problems concerning spatial or temporal variation of sediment concentration due to the nature of plunging breakers.

Finally, none of the models tested are distinctly applicable to gravel beaches. Although an option has been incorporated in the system to accommodate coarser grain sized sediments there has been no opportunity to calibrate it. More research is required on this topic also.

9.5 Coastal Profile Adjustment with SEGAR

The nearshore profile adjustment model, SEGAR was implemented with modest success at five of the seven study sites. Several limitations became apparent in this work, including the special characteristics of arctic region coastal conditions which differ from the theoretical assumptions underlying the model and the paucity of coastal profile data.

In the Beaufort Sea the variability of the length of the open water season and the relatively short length of season (approximately 3-4 months) contribute to cause an extremely variable

annual wave climate. The calibration exercise of the nearshore profile adjustment process (described in Section 7.3.1) is based on the assumption that a relatively consistent year to year or cyclic variation in wave climate exists. The large annual variation that occurs in the Beaufort Sea may interfere with the calibration process because the mean annual profile can vary widely from year to year with variation in the wave climate.

The method in which a representative measured profile was obtained also presents problems for the calibration process. The measured profile measurement may not be representative of a mean annual profile, especially if it is measured following ice action or a severe storm. It is preferable to synthesize a mean profile from a series of profile measurements made throughout one or more open water seasons.

Another difficulty that was encountered concerns the reported datum level for the measured profiles. Atkinson Point, Stokes Point and Tuktoyaktuk required adjustment in the datum level during the tuning process. There is the possibility that the reported datum was in error in these cases. However, since the adjustment was to raise the water level at Atkinson and Tuktoyaktuk it may indicate that surges are particularly important at those sites. Unfortunately, surges could not be considered during the calibration process adopted for this study.

It would be advantageous to augment the calibration process by calibrating against an actual storm sequence with measured environmental conditions, including initial and final profiles. This type of approach would address several of the shortcomings that have arisen in the calibration process used for this study.

A major limitation of the nearshore profile adjustment model and its application at the study sites arises when barrier beaches or spits are considered. Overtopping of spits at Atkinson Point and Kay Point probably occurs in most years and at the barrier beach at King Point during extreme events (see Table 9.1). Overtopping and subsequent overwashing of sediment on barrier beaches must have some effect on the profiles. However, the equilibrium profile developed by Swart did not explicitly consider barrier beaches or spits which undergo overtopping. This may account for the poor matching of the upper parts of the profiles above mean water level at some of the sites. It is also cause for exercising caution when interpreting the results from sites which can be characterized as beaches which experience overwashing.

Table 9.1
 Beach Profile Heights & Estimated Surge Heights
 Beach Profile Calibration Sites

Location	Surge Height (m)	Beach Profile Height Data
King Point Node 1	1.65	barrier beach 1.5 m above MWL
Stokes Point Node 1	1.0	highest land 1.4 m above MWL storm limit 0.5 m above MWL
Kay Point Node 2	1.1	spit 1.05 m above MWL
Tuktoyaktuk Node 2	2.75	measured to 5 m above MWL
Atkinson Point Node 1	2.75	spit 0.96 m above MWL

Swart's development of onshore-offshore sediment transport theory conserves sand mass thereby implying that no long term shoreline retreat or advance occurs. However, a strong influence of surges at sites where overwashing of spits or barrier beaches occurs will invalidate this assumption since transgression of the feature will occur. Furthermore long term changes in coastal morphology also occur through gradients in alongshore sediment transport (as computed with BPLAN), and the changes inferred from the coastal profile adjustment model will only be valid where net alongshore transport gradients are negligible.

9.6 Beach Plan Evolution Modelling

In this study a one-line beach plan evolution model, BPLAN, was successfully applied at King Point to a shoreline that differs considerably from the idealized beach coast for which it was designed. The model takes advantage of the inshore wave climate from the advanced spectral transfer technique and combines it with a simple bulk model - stable but not necessarily very accurate. The advantage of this type of model is that it can provide results for a sequence of points along a shore and can test the reasonableness and consistency of those results by calibration against shoreline position data.

Apart from its use of spectral transfer output, BPLAN as it stands is a rather simplistic model. Still it gives a clearer insight into macro-scale coastal processes for the effort expended than the application of SEDX at two or more nodes. The point of this discussion is to raise the question whether it would be worthwhile to invest some effort in the further development of BPLAN as a routine operational method of evaluating alongshore sediment transport? Such an approach would eventually incorporate detailed predictors and other advanced features when there are suitable stable models.

9.7 Evaluation of Results

This discussion concludes with an evaluation of the results on a site by site basis.

9.7.1 Atkinson Point

Atkinson Point lies between two bays. It consists of a headland with low cliffs to which are anchored opposed spits one extending north eastwards part way across the mouth of McKinley Bay and the other south westwards part way across the adjacent Bay. It appears to be a closed system, a littoral cell. The only obvious source of littoral sediment is erosion of the headland. The only other possible source, an unlikely one, is from the sea by onshore transport. From a study of the coastal planform, divergent net transport away from the cliffs towards the ends of the two spits would be expected. The actual rates of alongshore transport might be deduced from a simple sediment budget taking into account cliff composition, cliff and beach recession rates less beach overwash. The alongshore transports would only be equal to the cliff erosion rate if the spits transgressed without change in profile. Unfortunately, the data required for such a computation was not available and hence it is not possible to compare estimates of actual alongshore transport with the computed values shown in Figure 6.2.

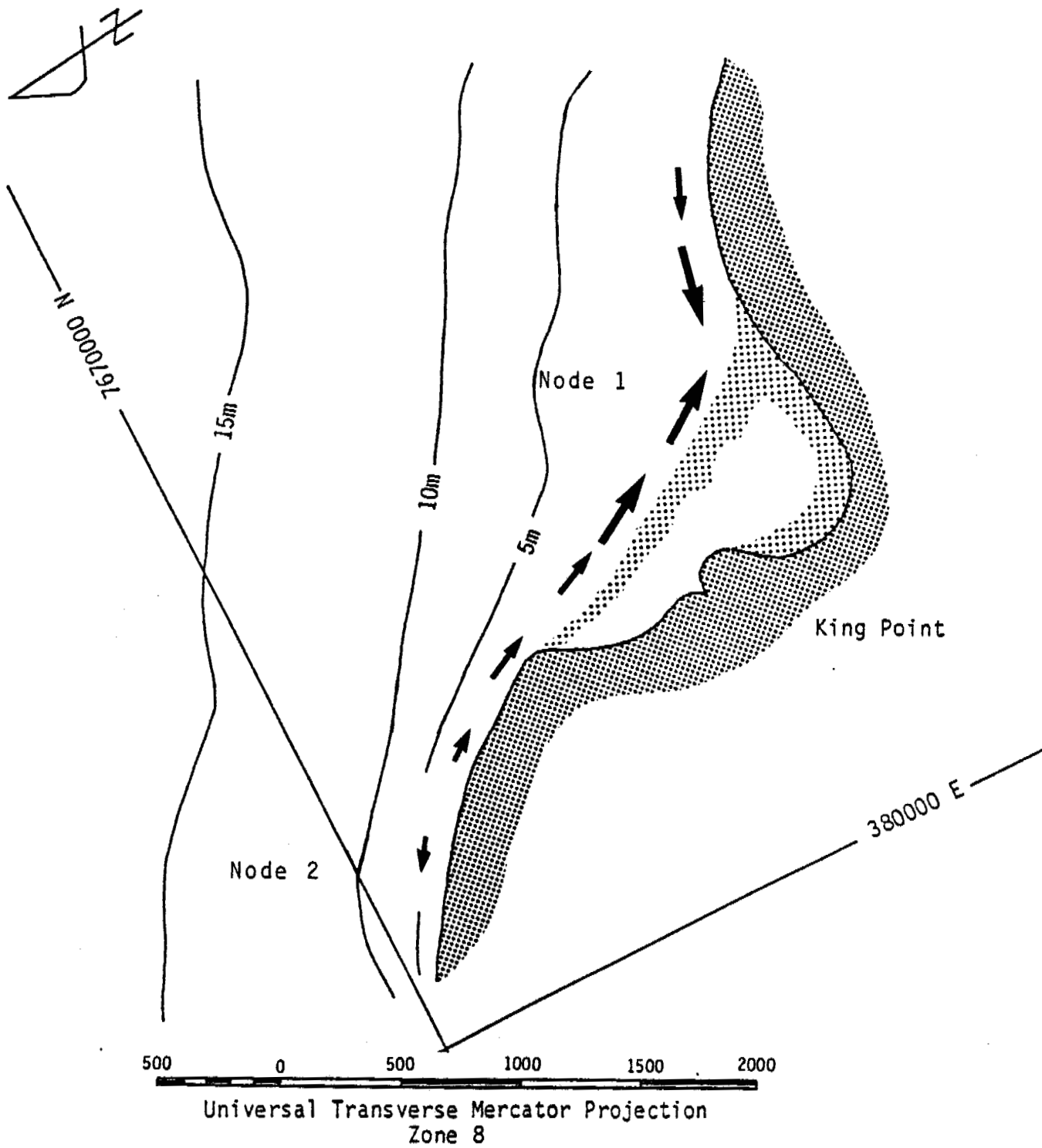
The estimates of sediment transport rates are very similar at nodes 1 and 2 with net eastward transports of 107,000 m^3/a and 95,000 m^3/a respectively. Either the spit is

prograding or the mouth of McKinley Bay is filling as a result of overwashing - or both. The potential sediment transport rates are probably indicative of the actual transport rate because of apparent abundance of sand depositional features. Therefore, the predicted sediment transport rate is probably a reasonable estimate of the infilling rate in McKinley Bay. This site displays the greatest sediment transport rates of the six sites considered. The high rates of coastal recession from earlier periods would substantiate these results but recent observations by Forbes and Frobel (1985) do not. However, if the actual alongshore transport is significantly less than the potential rates the difference would presumably be due to ice bonding or overwashing since there does not appear to be any lack of sand.

The investigation of profile adjustment at Atkinson Point was not completed due to a poor fit in calibration of the measured profile. This probably results from overwashing of beach which gives rise to a different equilibrium profile shape than that determined by Swart.

To deal with barrier beaches or spits there is an obvious need for a method of estimating the overwashing of sediment - the process by which such features transgress. When overwashing occurs, how are the alongshore transport and nearshore profile affected?

Note: Arrows represent relative magnitude and direction of net sediment transport.



BEAUFORT SEA COASTAL SEDIMENT STUDY

Coastal Processes at King Point

Date: 15 May 85

Scales as shown

Checked by:

Keith Philpott
Consulting Limited

9.7.2 Kay Point

Kay Point is a transgressive spit four kilometres long anchored to an eroding cliff headland (Forbes, 1981). Here a sediment balance would be required to obtain an independent estimate of the net alongshore transport which was computed at 43,000 m³/a to 49,000 m³/a. See Figure 6.3. Most, if not all, of the sediment entering the spit at its north end is derived from cliff erosion. However, the coastal geometry is such that only a short length of the cliff, probably less than 500 m is suitably oriented to supply the spit. Could it supply over 40,000 m³/a? Again, more data would be required to perform a sediment budget, but forty- or fifty-thousand cubic metres is considered to be a high estimate.

In this case, where there is direct evidence of rapid transgression, there is also a need for a means of systematically estimating overwash and its influence on alongshore transport.

If overwashing is neglected the results from the SEGAR runs can be accepted at face value. From the results presented in Section 7.6.2 and from the frequency of surges a recession rate at MWL of about 3 m/yr can be inferred.

9.7.3 King Point

The King Point site consists of a 2 km long barrier beach which interrupts an eroding bluff shoreline. The barrier beach was formed by extension of a spit. It closed off the lagoon prior to 1970.

The alongshore sediment transport results as computed by SEDX show a gross potential transport rate near the east end of the beach of about $32,000 \text{ m}^3/\text{a}$ which is similar to sediment budget estimates of actual littoral transport from bluff recession rates and beach infilling rates. The net transport along the cliffs to the west of the barrier beach is only $3,000 \text{ m}^3/\text{a}$ directed to the west.

A more detailed examination of the littoral cell in the vicinity of King Point is possible through the results of the beach plan shape model BPLAN. It was run from 1970 to 1983, without a structure. The relative magnitudes and directions of sediment transport are shown in Figure 9.1.

It is evident that there is a divergent sediment transport node just west of the west end of the barrier beach and a convergent node at the east end of the beach. The shoreline is probably transgressing throughout the littoral cell except at the convergent node which will be a zone of deposition.

It is difficult to estimate the rate of progression of the shoreline at the convergent node since overwashing of the barrier beach will play an important role. In other words the barrier beach is also growing back further into the lagoon. However, it is evident that the beach at King Point is a rapidly developing feature.

The sediment transport runs for the storm surge sensitivity analysis give an indication of the episodic nature of sediment transport in the region. A large part of the sediment transported during a year may occur during one large storm. While this has been recognized as a common phenomenon on many beach coasts (Seymour and Castel, 1985) it is particularly important in the Beaufort Sea since open water seasons are short and since storms are usually separated by periods of calms.

The possibility of leaving gaps in a coastal structure at King Point to protect fish migration patterns would be a costly feature. The rapid development of depositional features at this site would suggest constant dredging would be required to retain open passages through the structure.

The profile adjustment analysis revealed a shoreline retreat of almost 5 m during a large storm (equivalent of a 2.75 m

9-10

surge at Tuktoyaktuk combined with the largest storm during the 14 year hindcast period). However, the accretion due to changes in the beach plan arising for the spatial variation of alongshore transport far overshadows profile adjustment during surges.

9.7.4 North Head

The North Head site is tucked in on the west side of North Head. It is understood to have a flat fine grained beach with an approximate north-south orientation. The water depth immediately offshore of the beach is shallow and decreasing southwards to less than two metres. The site is also partly sheltered from dominant westerly storms by Hooper Island.

As expected, under these circumstances, the northerly node is much more exposed and potential sediment transport rates are higher there than to the south; $108,000 \text{ m}^3/\text{a}$ versus $51,000 \text{ m}^3/\text{a}$. This suggests that an area of deposition exists south of the site. The extent of deposition would depend on the actual rates of transport. The main source of sediment is presumably shoreline erosion. Hence the actual alongshore transport may be much less than the computed values. Very little detailed site information was available for this site and no sediment budget could be attempted.

A recent decision by Gulf Canada Resources to treat sediment transport in the area as a "mud flow" suggests that the application of sandy beach coast models was inappropriate at North Head. Implementation of the profile adjustment model was not possible due to a lack of profile data above MWL.

9.7.5 Pauline Cove

At Pauline Cove the numerical modelling process terminated with the computation of the inshore wave climate when it became apparent that there was insufficient data for coastal sediment modelling. However, the location of the beach site at the foot of a long cliff near the distal end of a sharply pointed cliffed headland suggests that this would also have been a difficult site for the application of the coastal sediment transport models.

9.7.6 Stokes Point

Stokes Point, a large depositional feature, is apparently relatively stable. Moderate alongshore transport rates were computed to be around $30,000 \text{ m}^3/\text{a}$. Much higher rates and inferred rapid erosion, Readshaw (1983) are judged improbable at his site.

Large accretions like Stokes Point tend to form on reaches of coast where there is a downdrift reduction or reversal in the alongshore transporting capacity of the waves, and/or an increase in sediment supply. In the present instance it is not self-evident what the main cause is although it may well be related to the sheltering effect of the offlying shoals.

An examination of nearshore profile adjustment revealed recession rates of 2 m in large surges (equivalent to a 2.75 m at Tuktoyaktuk) and 1 m in average surges (with a return period of about 1 year). From the results it is estimated that shoreline recession would be approximately 1 m/yr. Since there doesn't appear to be a gradient in alongshore sediment transports at Node 1 the estimate of 1 m/yr recession should be valid and unaffected by alongshore transport.

This would be an excellent site for the application of the BPLAN model using perhaps three additional backtracking nodes.

9.7.7 Tuktoyaktuk

This site is on a sand-gravel barrier about 1.5 km long oriented north-south and exposed to the shallow waters of Kugmallit Bay. The direction of net drift is southwards

and there is virtually no drift in the opposite direction. The section of shoreline involved appears to be a complete littoral cell. Therefore, unless there is an onshore transport of sand it would appear that the only source of littoral material is recession of the coast itself.

The computed potential alongshore transport rates were found to be 11,000 and 8,000 m³/a. That the rate is less at the southern node suggests accretion rather than erosion is occurring there. This is probably correct because the node is close to the accreting spit which forms the main sink for the littoral cell. The low alongshore transport values computed reflect the mildness of the wave climate due to the shallowness of Kugmallit Bay and the rather coarse grained material found in the zone of active transport. By comparison Kolberg and Shah (1976) obtained a result about four times as great (30,000 m³/a) using conventional procedures which would exaggerate the wave climate and disregard actual grain size.

While 30,000 m³/a is certainly too high, 8,000 m³/a may well be too low because it is likely that the sediment transported along the shore is finer than that found on the profile. It is a potential weakness of current methodology

that the particle sizes of sediment found on the profile are taken to be representative of the particle sizes of sediment that moves through an area. That is not necessarily so. A sediment budget approach based on textural analysis of eroding material and erosion rates might be useful.

The nearshore profile adjustment analysis at Tuktoyaktuk did not produce reasonable results. The very coarse grained and steep backshore probably gave rise to the unrepresentative results of this site.

SECTION 10 CONCLUSIONS

The conclusions presented herewith summarize the findings of each stage of this study.

10.1 Data

This study has highlighted a shortage of data for coastal process studies in the Beaufort Sea. Some of these deficiencies are known to be receiving attention in ongoing EMR (AGC) and DIAND programmes; others lie in the domain of other agencies.

10.1.1 Wind Records

There is a need to maintain homogeneous sets of complete wind recordings at more places in the area besides Tuktoyaktuk.

Such records should comprise 24-hourly observations per day with 36 directions to meet the needs of high quality hindcasting. A possible alternative would be eight observations per day at consistent three-hourly intervals, again with 36 directions.

Pending implementation of the above there is a need for a comprehensive once-for-all comparative study of all measured wind records plus the AES computed geostrophic wind data set to provide the best possible over-water wind data set. The output should be available as conversion factors to be applied to measured wind records and as modified synthetic data sets that can be directly applied to air-sea modelling.

10.1.2 Water Level Records

Water level gauge records in the area are inadequate for detailed comparisons of storm surges. Hence, reliance has had to be placed on the discontinuous records at Tuktoyaktuk together with the results of numerical storm surge models. Apart from the need to maintain the Tuktoyaktuk gauge at all times, there would seem to be a case for installing at least one more permanent gauge, somewhere on the Yukon coast, say at the location of the anticipated new shore-base.

10.1.3 Wave Measurements

Although there is a rapidly growing data base of wave records from artificial island sites in the Beaufort Sea, there are significant deficiencies with respect to needs for

calibration of hindcasting procedures for coastal process studies.

1. None of the measurements made to date are directional and hence cannot be used to calibrate direction outputs of hindcast models such as the one used in this study.
2. Station records are all of very short duration only one to two months, and stations are not occupied in consecutive seasons. Hence, records are too short for fully effective calibration of hindcasting procedures.
3. Data acquisition problems at many of the stations have resulted in sparse data sets that are ineffective for calibrating hindcasts.
4. No wave records suitable for calibration purposes are available in sheltered and shallow inshore areas that characterize sites such as Kay Point, North Head, Pauline Cove, Stokes Point and Tuktoyaktuk.

10.1.4 Geomorphology and Sediment

1. Nearshore profile data was generally minimal for this type of study. Ideally, there should be repeated measurements at several transects per site. Repetition is needed to delineate the range of variation and to define the time-averaged mean profile. This is required to calibrate profile adjustment models such as SEGAR.
2. Where overwashing of spits or barrier beaches is anticipated, the profiling should be carried over the beach crest and down the back face into the adjacent lagoon or embayment.
3. Sediment texture data was also sparse. There should be at least half a dozen sample analyses per profile to provide adequate input to the alongshore transport rate system SEDX.
4. There are indications of unusual combinations of profile slope and particle size on the Beaufort Sea coasts. Occurrences of cohesive material and/or ice bonding are likely causes. More detailed investigations, coring and continuous monitoring of the ice bonding interface within the profile are desirable to better define site conditions.

5. Wherever possible, sufficient data on shoreline changes, cliff composition, and cliff recession should be obtained to permit the preparation of a simple sediment budget. This was only performed at the King Point site in the present study where it made an important contribution to understanding coastal processes.

10.2 Nearshore Wave Climates

Wave Hindcasting and Wave Transformation

1. It has been found necessary in this study to redefine the ice limits on a weekly basis and to interpolate daily fetch values in order to obtain more accurate wave hindcasts.
2. It has also been necessary to devise a method of changing from deepwater to shallow water hindcast models as the ice edge moves in. This is in addition to having fetch depth vary with fetch direction.
3. With long fetches at Tuktoyaktuk, it was found necessary to use the deepwater model to define

wave periods but to use the shallow water model for heights to allow for the fact that wave heights there are controlled by bottom friction due to the width and shallowness of Kugmallit Bay. There is a need to verify this procedure against wave measurements.

4. To deal effectively with complex combinations of deepwater and shallow water fetches with sheltering effects, it was found to be necessary to select the refraction grid boundaries before choosing the hindcasting locations. Different boundaries were often used for different fetches at the same site.
5. It was found necessary to use additional hindcast stations, one for the outer deepwater fetches; and one or more others for shallow water fetches. These were located in the vicinity of the edge of the applicable refraction grids.
6. Again, with complex combinations of deep and shallow water fetches and with sheltering, it was found necessary to split the backtracking for individual nodes into phases using different grid boundaries for each phase.

7. The introduction of the shallow water spectral saturation limit into the nearshore wave transformation routine has eliminated a major source of error which has evidently led to serious overestimation of inshore waves and coastal sediment transport rates in previous studies. The method is based on Canadian Coastal Sediment Study field and numerical work which has shown that nearshore wave heights were previously being overestimated by 50% or more in some cases (Pinchin et al, 1985).
8. The wave analysis software brought to this study, with the addition of spectral saturation, had already been well proven in "normal" environments. To fully develop its potential there is an urgent need for directional wave measurements in shallow, sheltered waters.
9. On the basis of comparison of methods and results of this and previous studies, it must be concluded that the conventional refraction analysis technique with forward tracking of unidirectional monochromatic waves can produce misleadingly inaccurate results concerning inshore wave climates. Its use in this context should be discontinued forthwith.

10.3 Effects of Surges on Coastal Processes

1. Surges have little effect on mean alongshore sediment transport rates at the study sites considered. For a plane beach with uniform sediment distribution, raising or lowering the water level, as in a surge, makes no significant difference to the alongshore sediment transport rate. In practical cases a positive surge may either increase or decrease the transport rate depending on the shape of the profile and the variation in sediment size over its surface. The largest effect found was at Atkinson Point where the impact on the annual mean rate was less than 10%.
2. In contrast to the above, surges do have a major impact on nearshore profiles. This is readily apparent from results of SEGAR. Profiles can be stable at MWL and yet show recession at a raised water level under the same set of wave conditions. It is not surprising because the profile is a function of water level as well as wave conditions. The whole profile is displaced by a change in water level.
3. Reported instances of sudden massive recessions due to the combination of surges and melting of ground ice are no doubt correct but cannot be directly confirmed with the present models.

10.4 Numerical Estimates of Alongshore Sediment Transport

1. The twelve alongshore sediment transport predictors used in the SEDX system have produced a wide, even bewildering range of results when applied to the six sites on the Beaufort Sea. In all cases the estimates represent values of the potential or maximum possible transport rates. The wide scatter is in contrast to applications to more typical oceanic beach coasts where most predictors have given consistent results.
2. The cause of the scatter in results is believed to be due to non-typical combinations of wave climate, profile geometry, and sediment texture that are found in the arctic region.
3. The detailed predictors produced the widest scatter, and at most sites several had to be excluded because their results were judged to be invalid. The Nielsen et al., (1978) breaking wave model was judged best overall among detailed predictors.
4. The bulk models gave more stable results but these are not necessarily more accurate. Also they provide little insight into the process.

Nevertheless, in their most developed forms they are, at present, perhaps more useful in some applications than detailed predictors, pending further detailed calibration of the detailed predictors.

5. The application of SEDX to two or more independent nodes generates a large volume of local-scale data related specifically to the nodes but gives only a limited insight into the macro-scale coastal processes acting in the area. On its own, it gives no indication of places where actual transport is less than the potential rates.
6. To overcome the above mentioned shortcoming requires:
 - a) data at more nodes, say at least five;
 - b) data on the implications of continuity among the nodes;
 - c) field data on shoreline change and sediment budget for calibration purposes.
7. It would appear that, at most of the sites examined in this study, actual sediment transport rates must differ from the potential rates computed by the models. In most cases the actual rates will be less than the computed potential rates; but the reverse may also be true in some instances.

8. Actual sediment transport rates may exceed potential rates from detailed predictors in places where the sediment found on the active profile is coarser than the sediment actually transported over the profile. This may be true at the Tuktoyaktuk site.
9. There is another potential problem in the standard assumption that the texture of sediment on a segment of a profile is the same as the sediment transported over that segment. This assumption leads to continuity problems where sediment texture varies from node to node and from one part of a profile to another.
10. There is a need for better procedures to deal with situations where fully developed beaches do not exist and alongshore transport rates are less than potential rates. This occurs on shores where the thin layers of beach material are underlain with cohesive, ice-bonded or rocky materials, including places where eroding cliffs and bluffs are present.
11. Another situation encountered in this study, where actual transport rates, are evidently less than computed potential rates occurred with spits and barrier beaches subject to transgression caused by

overwashing. A special method is also needed to model this situation.

12. Generally speaking the SEDX modelling system appears to be in need of considerably more development to give consistent results under non-typical coastal conditions such as those of the Beaufort Sea. As it stands, it has apparently been calibrated to give good results under typical oceanic beach coast conditions. The fact that most component models can display instability under other conditions suggests that none of the present detailed predictors, with the possible exception of the Nielsen breaking wave model, can be regarded as a general purpose model. Since these models display a degree of instability not found in nature the problem must lie in the formulation and/or numerical manipulation applied.

10.5 Nearshore Coastal Profile Adjustments

1. Difficulty was encountered in calibrating the coastal profile adjustment model SEGAR at several of the sites for various reasons summarized in points 2-6.

2. Variability of the year to year wave climate causes difficulty in obtaining a representative mean annual profile.
3. The profile measurements acquired for this study are single measurements and it is likely they may not be representative of a mean profile.
4. In some cases the reported datum for the measured profile may be in error.
5. Surges appear to have a significant effect on the mean equilibrium profile and this cannot be taken into account in the present calibration process due to the lack of a continuous water level record at all sites, and the lack of documented profile change during a storm sequence.
6. Overwashing of the beach occurs at three of the five sites investigated with SEGAR. This would probably alter the equilibrium shape derived by Swart (1974) which would affect any results predicted by SEGAR.
7. The successful SEGAR runs do show that shoreline retreat increases with increased water levels.

8. If the alongshore transport is constant over a reach of shoreline (i.e. no gradient exists), the results of SEGAR may be taken at face value. However, if there is a large alongshore transport gradient shoreline recession may be much more or much less than predicted by SEGAR.

9. Coastal profile adjustments which are related to onshore-offshore sediment transport account for some of the larger more rapid coastal changes. However, the most striking changes are probably associated with characteristic arctic phenomena such as ground-ice melt, surge-accelerated slumps, and the rarely occurring ice override.

10.6 Use of the Beach Plan Model at King Point

1. The BPLAN model was successfully calibrated and used to predict shoreline changes at King Point under much less than ideal conditions.

2. The modification of the beach plan evolution model to non-typical conditions at King Point indicates the potential value of this simple type of model.

3. Because it computes littoral transport rates at a number of points along the shore for successive years, and because it also accounts for continuity from node to node it provides a means of calibration and verification that is not possible using SEDX at individual non-connected nodes.
4. At sites where morphological features are rapidly developing such as the deposition at the convergent sediment transport node at King Point, profile adjustment is not significant and a two-dimensional beach plan model provides sufficient accuracy in prediction of shoreline change.
5. For future arctic coastal process studies a beach plan evolution model might well be developed as the primary model for use at all sites to investigate macro scale changes in morphology - for example by incorporating the best available bulk model.
6. In the long run of course, there will be a ready demand for an economical three-dimensional coastal evolution model incorporating an improved detailed alongshore predictor, and a profile adjustment feature, together with plotting of resulting shoreline changes.

References

- Abernethy, C.L., Gilbert, G. 1975. Refraction of wave spectra, Hydraulics Research Station (U.K.) Report No. INT 117.
- Acres-Philpott. 1983. Interim report for numerical model of caisson island berm erosion for Esso Resources Canada Ltd. Unpublished.
- Ackers, P., White, W.R. 1973. Sediment transport, new approach and analysis. Journal of the Hydraulics Division. A.S.C.E. Vol. 99. No. HY11, pp. 2041-2060.
- Atlantic Geoscience Centre North Head borehole report. Moran/AGC. Don Forbes. Unpublished data.
- Atlantic Geoscience Centre. Atkinson Point beach profile, nearshore profiles and beach sample. Peter Lewis. Unpublished data.
- Atlantic Geoscience Centre. Kay Point nearshore samples and profile, beach sample and beach profiles. Unpublished data.
- Atlantic Geoscience Centre. Stokes Point nearshore profile and sample, beach profile, and beach sample. Unpublished data.
- Atlantic Geoscience Centre. Tuktoyaktuk beach profile, nearshore profiles, and one nearshore sample. Unpublished data.
- Aubrey, D.G., Spencer, W.D. 1984. Inner shelf sand transport wave measurements, Pointe Sapin, New Brunswick, Canada. Report prepared for National Research Council of Canada by Woods Hole Oceanographic Institution.
- Baird, W.F., Hall, K.R. 1980. Wave hindcast study, Beaufort Sea. Hydrotechnology Ltd. for Gulf Canada Resources Inc. Report and Appendices A, B, and H with results for Tarsuit and North Issungnak and wave data report.
- Battjes, J.A. 1974. Computation of set-up, longshore currents, run-up and overtopping due to wind-generated waves. Ph.D. thesis, Technisches Hogeschool, Delft.
- Beaufort Sea Environmental Impact Statement 1982. Volume 2. Development Systems. Dome, Esso, Gulf.
- Bettes, P., Fleming, C.A., Hanrich, T.C., Zienkiewicz, O.C., Austin, D.J. 1978. Longshore currents due to a surf zone barrier. 16th Coastal Engineering Conference, Hamburg, A.S.C.E.

- Bijker, E.W. 1971. Longshore transport computations. Journal of Waterways, Harbours and Coastal Engineering Division. Proc. A.S.C.E. Vol. 97, WW4, pp. 687-701.
- Bretschneider, C.L. 1973. Prediction of waves and currents. Look Laboratory Report. Vol. III, No. 1, pp. 1-17.
- Burns, B.M. 1973. The climate of the Mackenzie Valley - Beaufort Sea. 2 Vols., Climatological Studies No. 24, Atmospheric Environment Service, Toronto.
- Carter, T.G. 1980. Private communication concerning the parameterization of Darbyshire and Draper (1963) hindcasting curves.
- CERC 1977. Shore protection manual. Coastal Engineering Research Centre, U.S. Army Corps of Engineers.
- Croasdale, K.R. 1978. Factors governing ice ride up on sloping beaches. Symposium on Ice. Lulea, Sweden. I.A.H.R.
- Croasdale, K.R. 1983. The present state and future development of Arctic offshore structures. P.O.A.C. Helsinki, Finland.
- Croasdale, K.R. 1983. Ice action on artificial islands and wide structures.
- CSIR 1978. Koeberg Nuclear Power Station, Report No. 8, Sediment transport study, Current tests. CSIR Report. Stellenbosch, South Africa.
- Danard, M. 1983. Meteorological conditions for maximum storm surges in the Beaufort Sea. For Institute of Ocean Sciences, Fisheries and Oceans Canada. Sidney, B.C. Atmospheric Dynamics Corp'n. Unpublished.
- Danard, M., Gray, M. (1984). Extreme wind stresses over the Beaufort Sea as determined from Tuktoyaktuk winds. For Institute of Ocean Sciences. Fisheries and Oceans Canada. Sidney, B.C. Atmospheric Dynamics Corp'n. Unpublished.
- Darbyshire, M., Draper, L. 1963. Forecasting wind generated sea waves. Dock and Harbour Engineering.
- Davies, M.H. 1984. Littoral Transport Rate Prediction. M.Sc. Thesis, Queen's University, Kingston, pp. 123.
- Dome Petroleum et al. 1982. Hydrocarbon development in the Beaufort Sea - Mackenzie Delta Region.

D.P.W. 1970. Herschel Island, feasibility of a marine terminal. Department of Public Works. Ottawa, Canada.

Einstein, H.A. 1956. The bed-load function for sediment transportation in open channel flows. Tech. Bull. soil Conserv. Serv. U.S. Dep. Agric., 1026.

Engelund, F., Hansen, E. 1967. A monograph on sediment transport in alluvial streams. Teknisk Vorlag, Copenhagen.

Fissel, D.B., Birch, J.R. 1984. Sediment transport in the Canadian Beaufort Sea. For Atlantic Geoscience Centre, E.M.R. Bedford Inst. Oceanography. Dartmouth, N.S. Arctic Sciences. Sidney, B.C. Unpublished.

Fleming, C.A. 1977. The development and application of a mathematical sediment transport model. Ph.D. Thesis, University of Reading.

Fleming, C.A., Swart, D.H. 1982. New framework for prediction of longshore currents. Proc. 18th Coastal Conference, Cape Town, South Africa, A.S.C.E.

Fleming, C.A., Philpott, K.L., Pinchin, B.M. 1984. Evaluation of coastal sediment estimation techniques. Phase I: Implementaiton of alongshore sediment transport models and calibration of wave hindcasting procedure. Canadian Coastal Sediment Study. Associate Committee for Research on Shoreline Erosion and Sedimentation. National Research Council of Canada. Report No. C2S2-10.

Forbes, D.L., Frobel D. 1985. Coastal erosion and sedimentation in the Canadian Beaufort Sea. Part B. Geological Survey of Canada Paper 85-18. (Preprint).

Frijlink, H.C. 1952. Discussion des Formules de Debit Solide de Kalinske, Einstein et Meyer-Peter et Muller, compte tenu des Mesures Recentes de Transport dans les Rivieres Neerlandaises. 2eme journal Hydraulique, Societe Hydraulique de France, Grenoble, pp. 98-103.

Hardy. 1983. Yukon offshore geotechnical program data report - Phase I. For Gulf Canada Resources Inc. Calgary, Canada. Hardy Associates. Unpublished.

Harper, J.R. 1978. The physical processes affecting the stability of tundra cliff coasts. Doctoral dissertation. Louisiana State U. Unpublished.

Harper, J.R. 1978. Coastal erosion rates along the Chukchi Sea coast near Barrow, Alaska. Arctic. 31:4. Dec. 1978., pp. 428-433.

- Harper, J.R. 1983. Shore-zone ice scour statistics: implications to coastal development. Proc. Ice Scour Conf. Montebello, Quebec. National Research Council of Canada.
- Harper, J.R., Owens, E.H., Wiseman, W.J. 1978. Arctic beach processes and the thaw of ice-bonded sediments in the littoral zone. Proc. Third Intl. Permafrost Conference., pp. 195-199.
- Harper, J.R., Owens, E.H. 1981. Analysis of ice-overide potential along the Beaufort Sea coast of Alaska. Proc. P.O.A.C., pp. 974-984.
- Harper, J.R., Penland, S. 1982. Beaufort Sea sediment dynamics. For the Geological Survey of Canada, EMR. Woodward-Clyde. Unpublished.
- Hasselmann, K., Barnett, T.P., Bouws, E., Carlson, H., Cartwright, D.E., Enke, K., Ewing, J.A., Gienapp, H., Hasselmann, D.E., Kruseman, P., Meerburg, P., Muller, P., Olbers, D.J., Richter, K., Sell, W., Walden, H. 1973. Measurements of wind-wave growth and swell decay during the joint North Sea wave project (JONSWAP). Deutschen Hydrographischen Zeitschrift, Reihe A, Nr. 12.
- Henry, R.F. 1984. Flood hazard delineation at Tuktoyaktuk. For Inland Waters Branch, Environment Canada. Inst. Ocean Sciences, Fisheries and Oceans Canada. Sidney, B.C. Unpublished.
- Henry, R.F., Storm Surges, Technical Report No. 19, Beaufort Sea Project, Depart. of the Environment, December 1975.
- Henry, R.F., Heaps, N.S. 1976. Storm surges in the southern Beaufort Sea. J. Fish. Res. Board of Canada, 33., pp. 2362-2376.
- Hodgins, D.O., Dal-Santo, R. 1981. A preliminary analysis of extreme wave conditions in the Beaufort Sea based on observed sea states for Esso Resources Canada Ltd. Seaconsult. Unpublished.
- Hodgins, D.O., LeBlond, P.H., Brink-Kjaer, O. 1981. A hindcast study of extreme water levels in the Beaufort Sea for Esso Resources Canada Ltd. Seaconsult and Danish Hydraulic Institute. Unpublished.
- Hodgins, D.O., Harry, K.F. 1982. On the occurrence of extreme storms and wind-wave fetch conditions in the southeastern Beaufort Sea for Esso Resources Canada Ltd. Seaconsult. Unpublished.
- Houmb, O.G., Overvik, T. 1976. Parameterization of wave spectra and long term joint distribution of wave height and period. BOSS76. Proc. Conf. Behaviour of Offshore Structures. The Norwegian Inst. of Technology.

Houmb, O.G., Overvik, T. 1977. On the statistical properties of 115 wave records from the Norwegian continental shelf. Div. Port and Harbour Engg. U. of Trondheim.

H.R.S. 1982. Private communication concerning parameterization of JONSWAP. Unpublished report of the Hydraulic Research Station, Wallingford.

Kamphuis, J.W., Readshaw, J.S. 1978. A model study of alongshore sediment transport rate. 16th Coastal Engineering Conference, Hamburg, A.S.C.E.

Kiewit, Peter and Sons Co. Ltd. King Point nearshore survey and samples. Unpublished data.

Kitaigorodskii, S.A., Krasitskii, V.P., Zaslavskii, M.M. 1975. On Phillips' theory of equilibrium range in the spectra of wind-generated gravity waves. J. Phys. Geophys., 5., pp. 410-420.

Kolberg, T.O., Shah, Y.K. 1974. Shore erosion and protection study - Stage 2. Report No. 41. Marine Directorate. Department of Public Works H.Q. Ottawa, Canada. Unpublished.

Lalonde, M.E., McCulloch, J.A.W. 1975. Ratios of wind over water to that over land for the Beaufort Sea. Atmospheric Environment Service.

LeBlond, P.H., Calisal, S.M., Isaacson, M. 1982. Wave spectra in Canadian waters. Canadian Contractor Report of Hydrography and Ocean Sciences No. 6 MEDS, Dept. of Fisheries and Oceans Canada.

LeMehaute, B., Wang, J.D. 1982. Wave spectrum changes on sloped beach. J. Waterways, Harbours, Coastal and Ocean Div., A.S.C.E., 108, (WW1), pp. 33-47.

Longuet-Higgins, M.S. 1970. Longshore currents generated by obliquely incident sea waves, 1. J. Geophys. Res., 75, pp. 6778-6789.

Lowey, E. et al. 1976. Data collection and analysis for coastal projects. Proc. 15th Coastal Engineering Conference, Hawaii, A.S.C.E.

Markham, W.E. 1973. Ice climatology of the Beaufort Sea. Beaufort Sea Tech. Rep. No. 26, Institute of Ocean Sciences, Sidney, B.C.

McDonald, B.C., Lewis, C.P. 1973. Geomorphic and sedimentological processes of rivers and coast, Yukon coastal plain. Terrain Sciences Div. Geol. Survey of Canada, EMR, Environmental - Social Program, Northern Pipelines Task Force on Northern Oil Development. Rept. No. 73-39.

- MEP 1983. Sensitivity of wave hindcast to storm selection procedure based on Beaufort climatology. For Esso Resources Canada Limited. Meteorological and Environmental Planning Limited. Unpublished.
- Muir Wood, A.M., Fleming, C.A. 1981. Coastal hydraulics. Macmillan Press, 2nd Ed.
- Munk, W.H., Arthur, R.S. 1952. Wave intensity along a refracted ray. U.S. National Bureau of Stds. Circ. No. 521: Gravity Waves.
- Nielsen, P., Svendsen, I.A., Staub, C. 1978. Onshore-offshore sediment movement on a beach. Proc. 16th Coastal Engineering Conference, II, pp. 1475-1492.
- Nielsen, P. (1979). Some basic concepts of wave sediment transport. Institute of Hydrodynamics and Hydraulic Engineering, Technical University of Denmark, Series paper No. 20.
- Niwinski, C.T., Hodgins, D.O. 1984. Extreme wave conditions at Tuktoyaktuk. For Institute of Ocean Sciences, Fisheries and Oceans Canada, Sidney, B.C. Seaconsult Marine Research Ltd. Unpublished.
- Ostendorf, D.W., Madson, O.S. An analysis of longshore currents and associated sediment transport in the surf zone. Ralph M. Parsons Lab., M.I.T. Report No. 241.
- Owen, M.W., Thom, M.F.C. 1980. Effect of waves on sand transport by currents. Proc. 16th Coastal Engineering Conference, Hamburg, West Germany.
- Owens, E.H., Harper, J.R. 1977. Frost table and thaw depths in the littoral zone near Peard Bay, Alaska. Arctic. Sept. 1977. 30:30, pp. 155-168.
- Owens, E.H., Harper, J.R., Nummedal, D. 1980. Sediment transport processes and coastal variability on the Alaskan North Slope. Proc. 17th Intl. Coastal Eng. Conference. A.S.C.E. Sydney, Australia. pp. 1344-1363.
- Owens, E.H., Harper, J.R. 1983. Arctic coastal processes: a state of knowledge review. Proc. Canadian Coastal Conference. ACROSES. National Research Council of Canada, pp. 3-18.
- Philpott, K.L. 1979. Wave, surge and sediment conditions for proposed dredging at Tuktoyaktuk and McKinley Bay. A.P.D. Consultants for Conmar. Unpublished.
- Philpott, K.L. 1984. Comparison of cohesive coasts and beach coasts. Proc. Seminar on Coastal Engineering. Queen's University, Kingston, Canada.

Pelnard-Considere, R. 1956. Essai de theorie de l'evolution des formes de rivages en plages de sables et de galets. IVieme journees de l'Hydraulique, Question III.

Pinchin, B.M., Fleming, C.A., Skafel, M.G., Aubrey, D.G. 1985. Comparison of measured with computed wave heights using offshore to onshore transformations of directional wave spectra at Pointe-Sapin, New Brunswick. Proc. Canadian Coastal Conference. ACROSES. National Research Council of Canada.

Poole, L.R. 1975. Comparison of techniques for approximating ocean bottom topography in a wave refraction computer model. NASA Report No. NASA, TND-8050.

Readshaw, J.S. 1982. Preliminary coastal engineering study for a supply base at McKinley Bay, N.W.T. For Gulf Canada Resources Inc. Calgary, Canada. Baird Assoc. Unpublished.

Readshaw, J.S. 1983. Coastal engineering investigations for a supply base marine facility at Stokes Point, N.W.T. For Gulf Canada Resources Inc. Beaufort Drilling System. Baird Assoc. Unpublished.

Resio, D.T. 1978. Estimation of longshore drift rates from numerical models. Proc. A.S.C.E., Specialty Conference Coastal zone '78, San Francisco, U.S.A.

Sayao, O.F.S.J., Kamphuis, J.W. 1982. Littoral sand transport: review of the state of the art. Dept. of Civil Eng., Queen's University, Kingston. C.E. Res. Rept. No. 78., p. 62.

Sayao, O.F.S.J., Nairn, R.B. 1985. Dimensional analysis of littoral transport. Canadian Coastal Engineering Conference, St. John's, Newfoundland.

Seymour, R.J., Castel D. 1985. Episodicity in longshore sediment transport. Journal of Waterway, Part, Coastal and Ocean Engineering, Vol. III, No. 3, May 1985 p 542-555.

Seymour, R.J., Higgins, A.L. 1978. Continuous estimations of longshore sand transport. A.S.C.E. Specialty Conference, Coastal Zone '78, San Francisco, U.S.A.

Skafel, M.G. 1983 Offshore wind and wave data, Pointe Sapin, New Brunswick CCIW wave direction buoy Canadian Coastal Sediment Study. Report prepared for National Research Council of Canada by National Water Research Institute.

Swart, D.H. 1976a. Coastal sediment transport: computation of longshore transport. Delft Hydraulics Laboratory Report R968.

Swart, D.H. 1976b. Predictive equations regarding coastal transport. 15th Coastal Engineering Conference. A.S.C.E., Hawaii.

Swart, D.H. 1978. Offshore sediment transport and equilibrium beach profiles. Delft Hydraulics Laboratory Publication No. 131.

Swart, D.H., Fleming, C.A. 1980. Longshore water and sediment movement. Proc. 18th Coastal Engineering Conference. A.S.C.E., Sydney.

Swart, D.H., Lenhoff, L. 1980. Wave induced incipient motion of bed material. CSIR Report. NR10, Stellenbosch, S. Africa.

Thornton, E.B., Wu, C.S. 1984. Breaking wave design criteria. Proc. of the 19th Coastal Engineering Conference, Houston, U.S.A.

Van de Graaf, J., van Overeem, J. 1979. Evaluation of sediment transport formulae in coastal engineering practice. Coastal Engineering, Vol. 3, pp. 1-32.

Wang, S.Y., Shen, H.W. 1985. Incipient sediment motion and riprap design. Journal of Hydraulic Engineering ASCE, Vol. III, No. 3.

Willis, D.H. 1978. Sediment load under waves and currents. Proc. 16th Coastal Engineering Conference, Hamburg, West Germany.

BEAUFORT SEA COASTAL SEDIMENT STUDY

APPENDIX A

HINDCAST CALIBRATION RESULTS

KEITH PHILPOTT CONSULTING LTD
P.O. BOX 938
THORNHILL
ONTARIO L3T 4A5

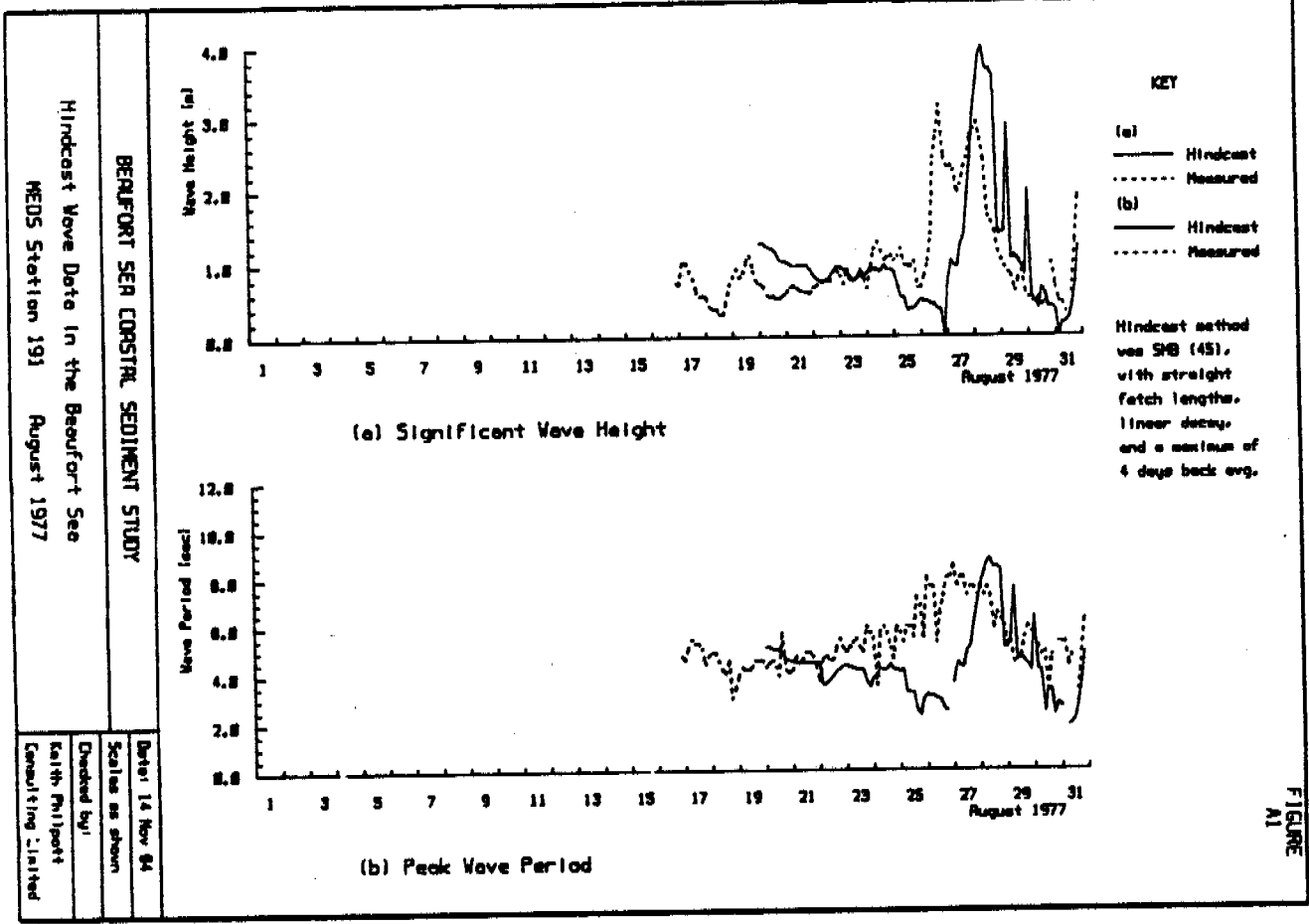


FIGURE A1

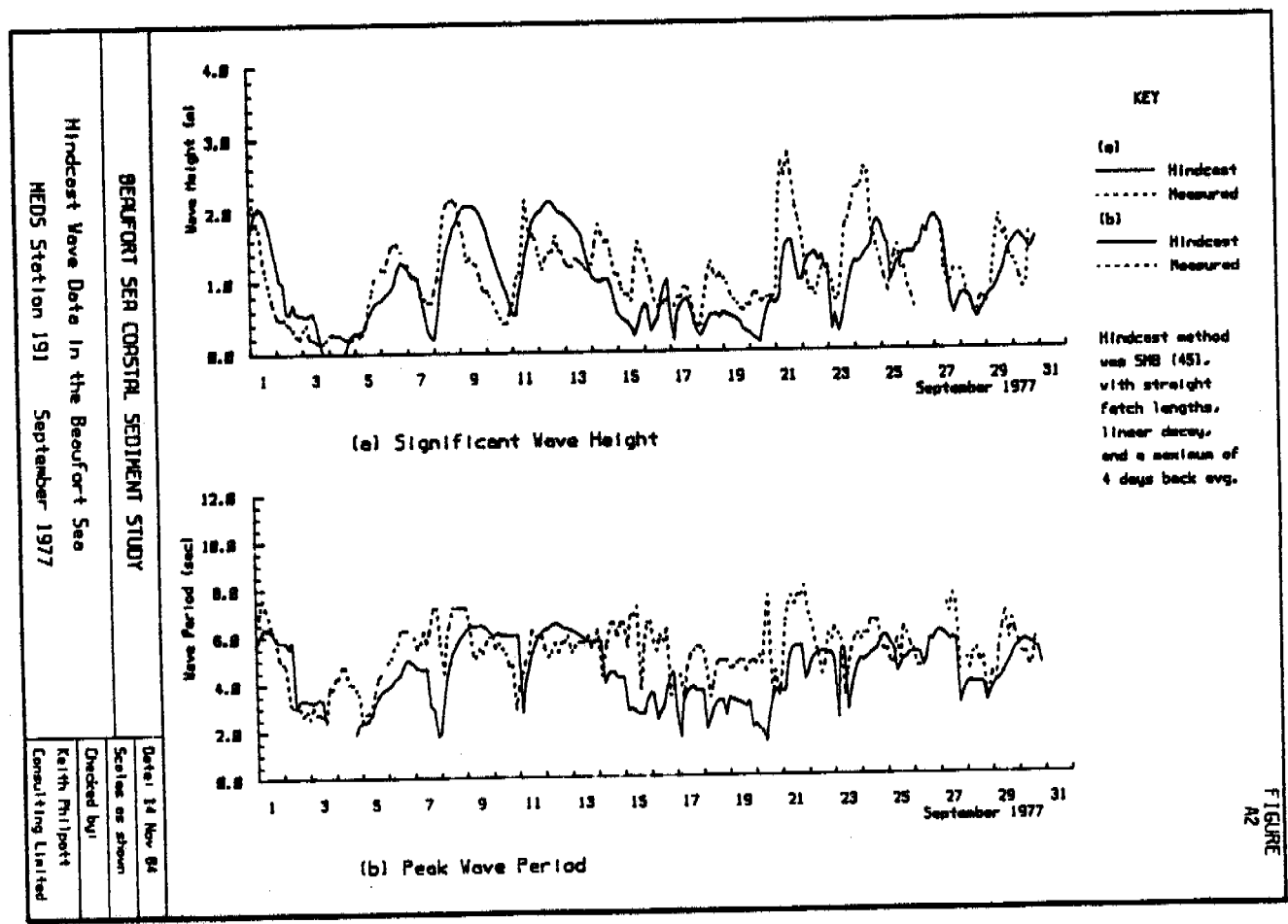
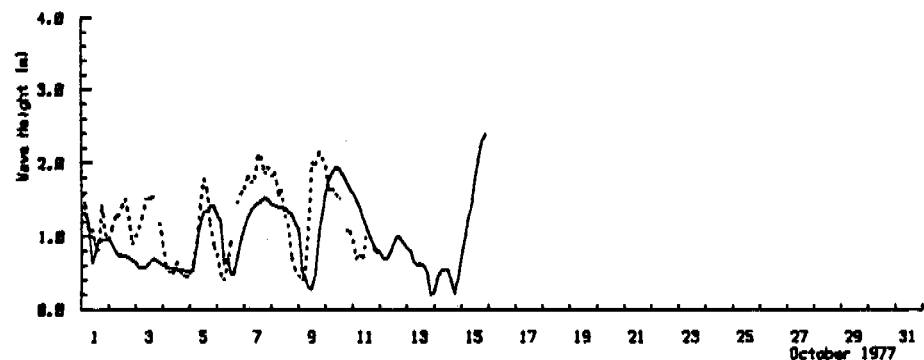


FIGURE A2

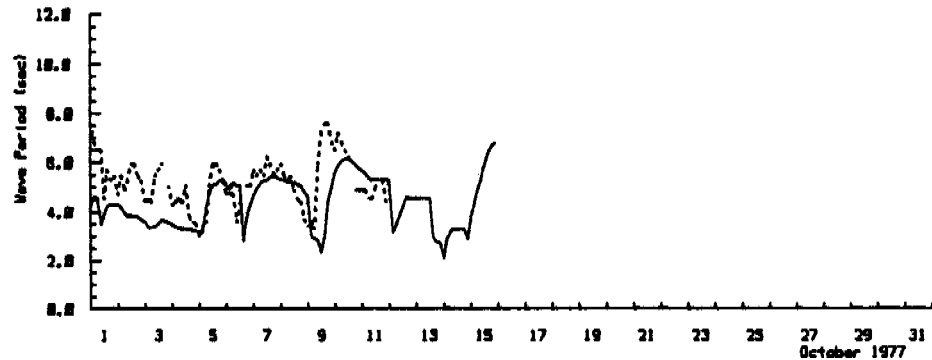
Hindcast Wave Data in the Beaufort Sea
 NEOS Station 191 October 1977

BEAUFORT SEA COASTAL SEDIMENT STUDY

Date: 14 Nov 84
 Scales as shown
 Checked by:
 Keith Phillips
 Consulting Limited



(a) Significant Wave Height



(b) Peak Wave Period

KEY
 (a) — Hindcast
 Measured
 (b) — Hindcast
 Measured

Hindcast method was SMB (45), with straight fetch lengths, linear decay, and a maximum of 4 days back avg.

FIGURE
 A3

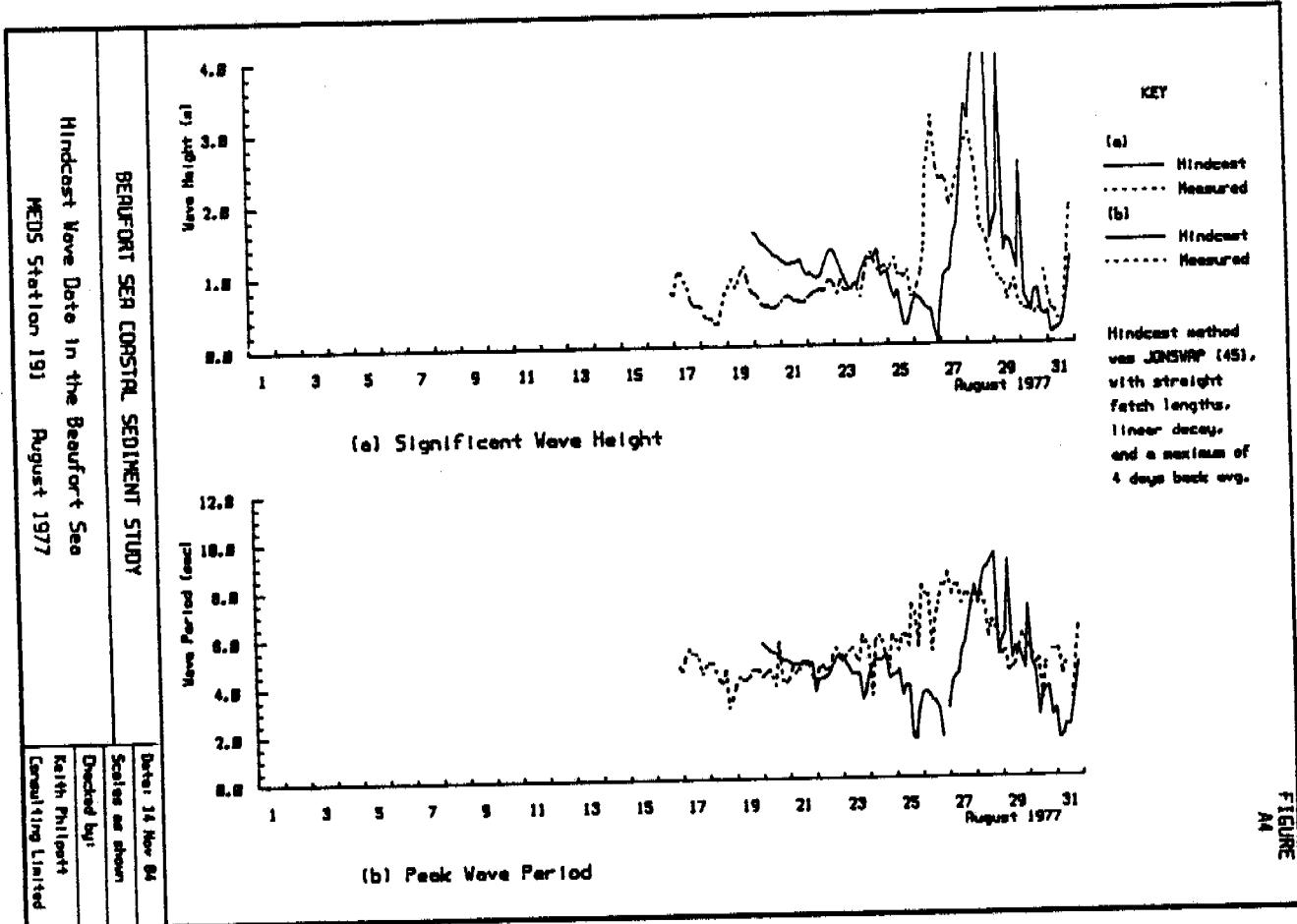


FIGURE A4

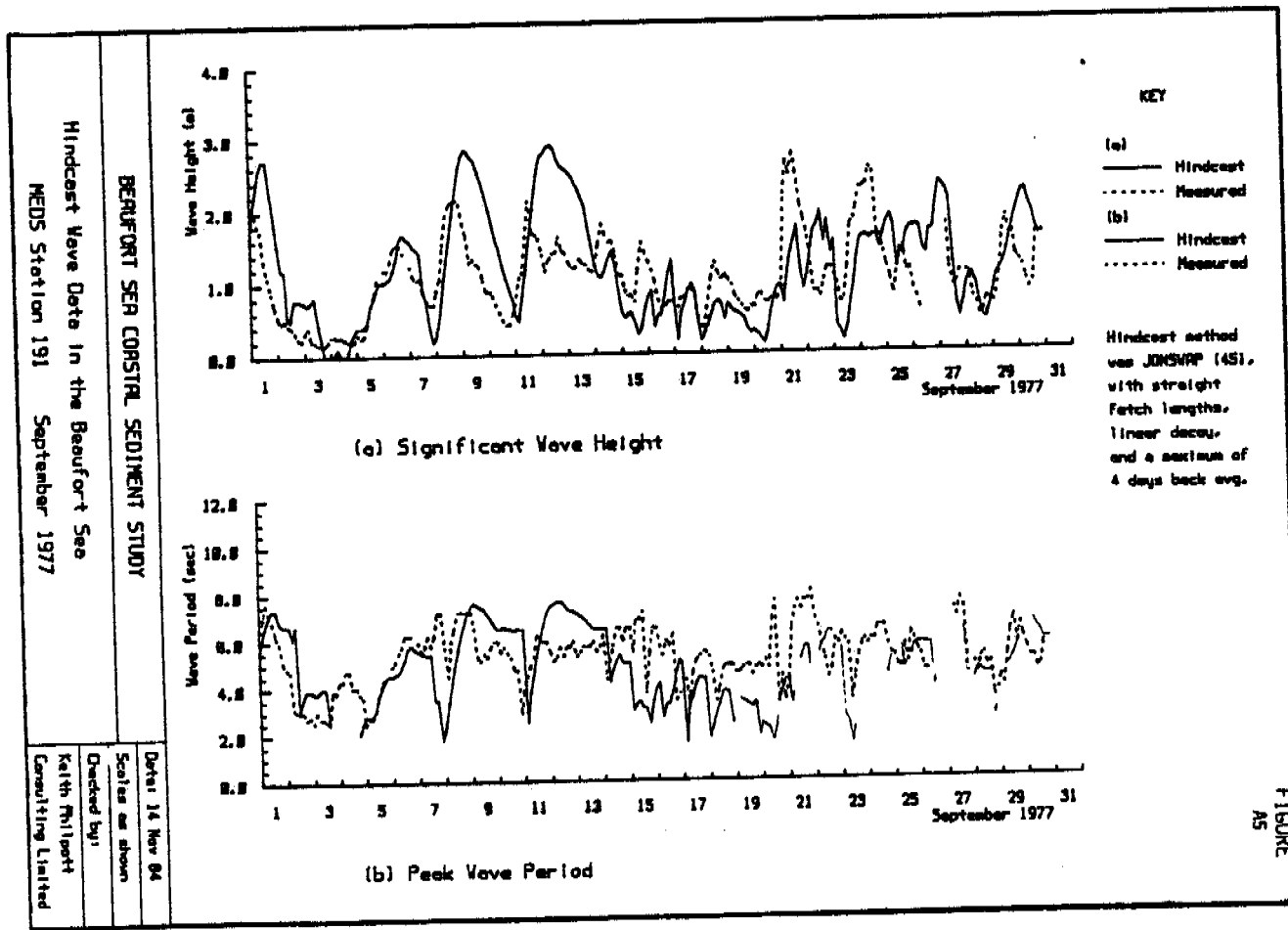
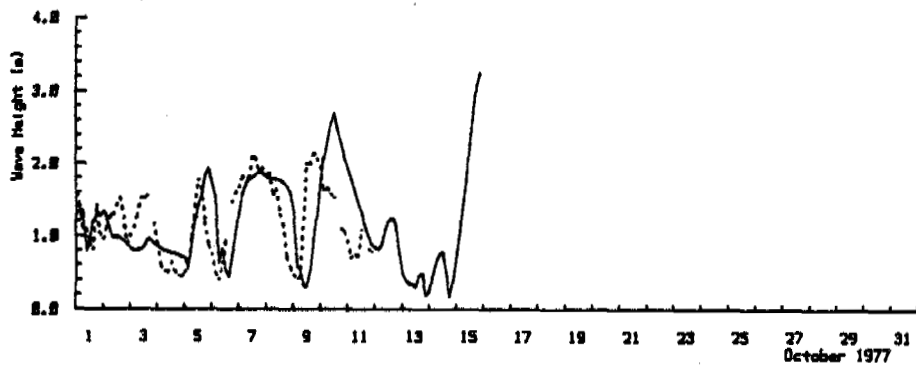


FIGURE A5



(a) Significant Wave Height



(b) Peak Wave Period

KEY

(a)
 — Hindcast
 Measured

(b)
 — Hindcast
 Measured

Hindcast method
 uses JONSWAP (4S),
 with straight
 fetch lengths,
 linear decay,
 and a maximum of
 4 days back avg.

FIGURE
 No

BEAUFORT SEA COASTAL SEDIMENT STUDY

Hindcast Wave Data in the Beaufort Sea

NEUS Station 191 October 1977

Date: 14 Nov 84
 Scales as shown
 Checked by:
 Keith Phillips
 Consulting Limited

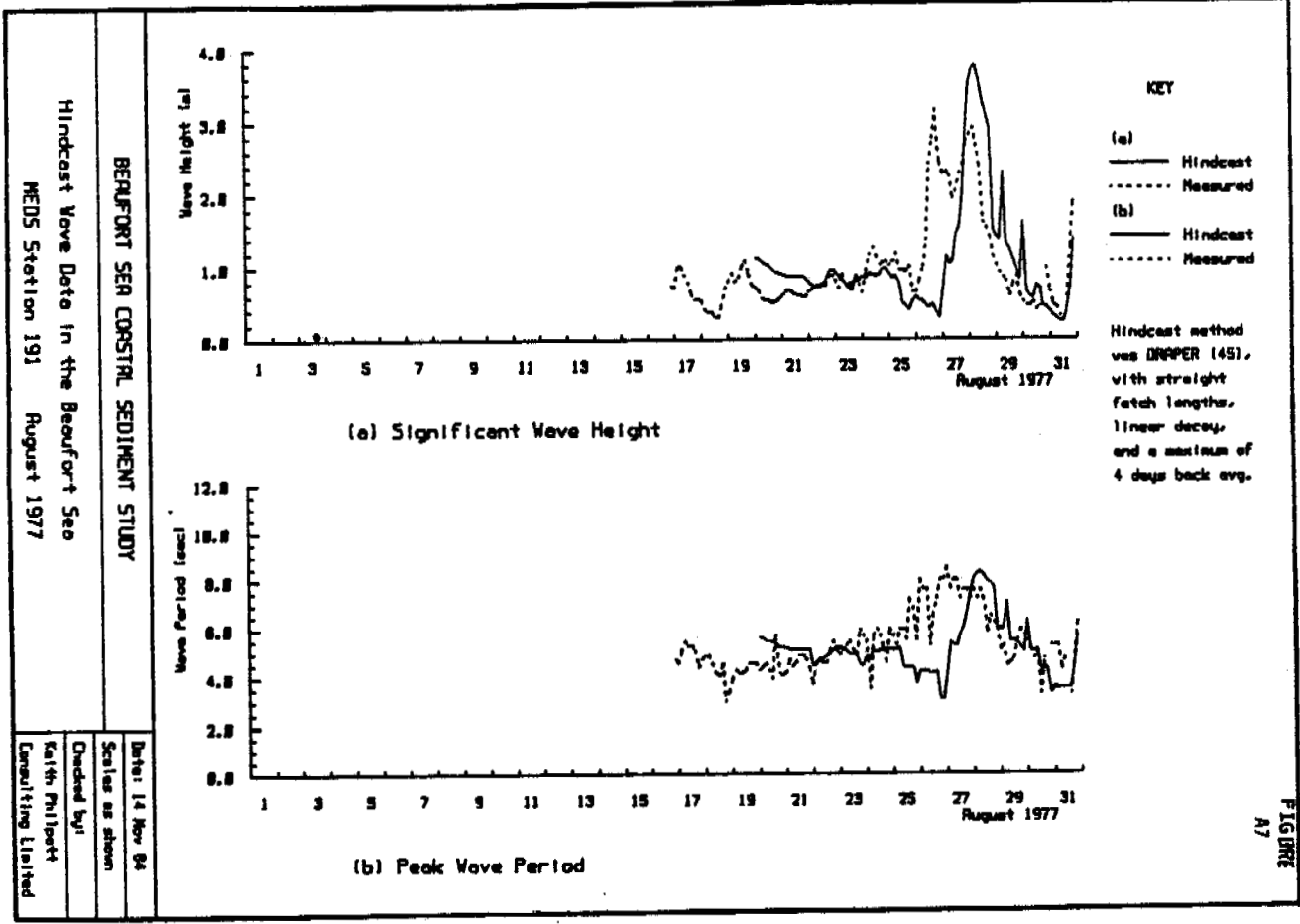


FIGURE A7

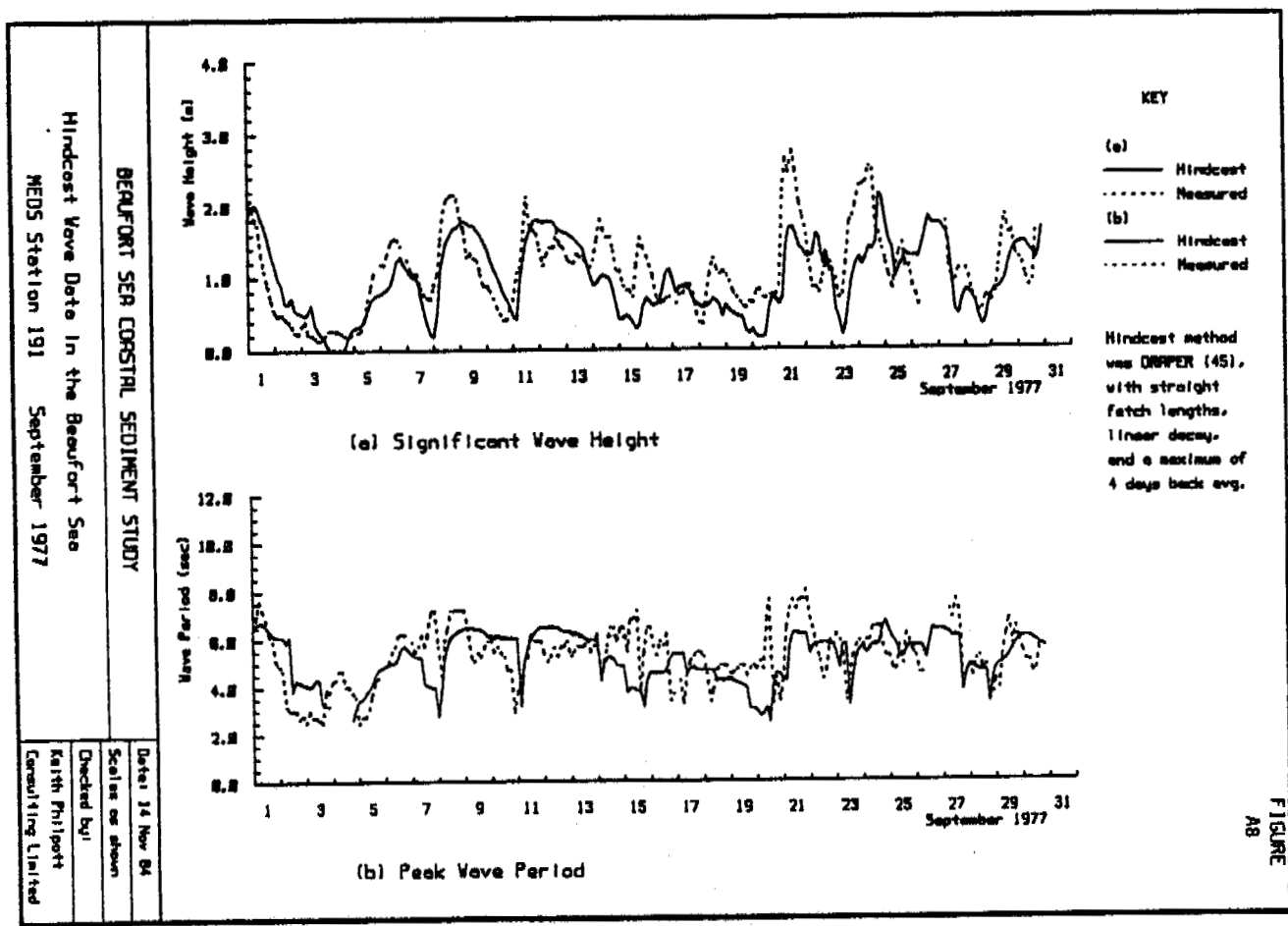
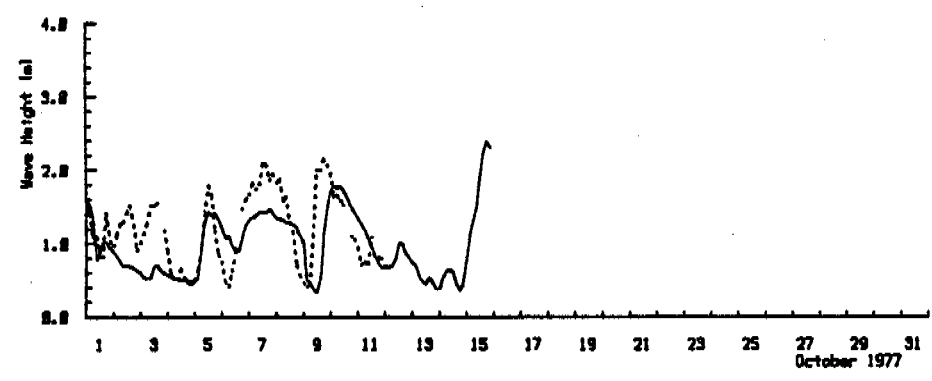


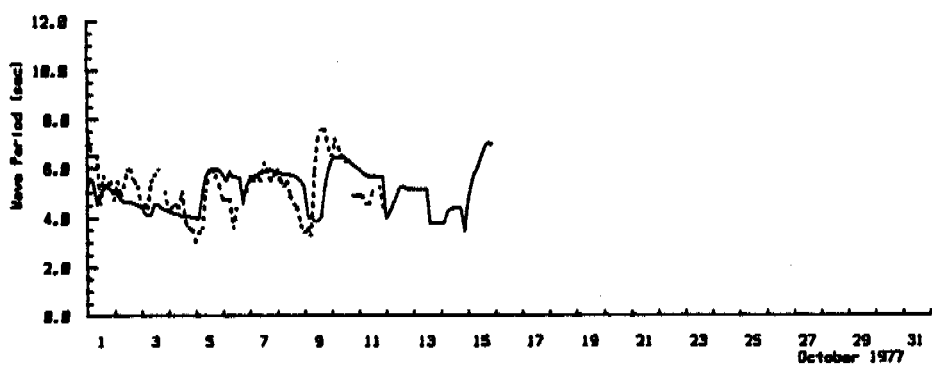
FIGURE A8

Hindcast Wave Data in the Beaufort Sea
 NEBS Station 191 October 1977

BEAUFORT SEA COASTAL SEDIMENT STUDY



(a) Significant Wave Height



(b) Peak Wave Period

KEY
 (a) — Hindcast
 - - - Measured
 (b) — Hindcast
 - - - Measured

Hindcast method was DRAPER (45), with straight fetch lengths, linear decay, and a maximum of 4 days back avg.

FIGURE
 A9

Date: 14 Nov 84
 Scale: as shown
 Checked by:
 Keith Pittman
 Consulting Limited

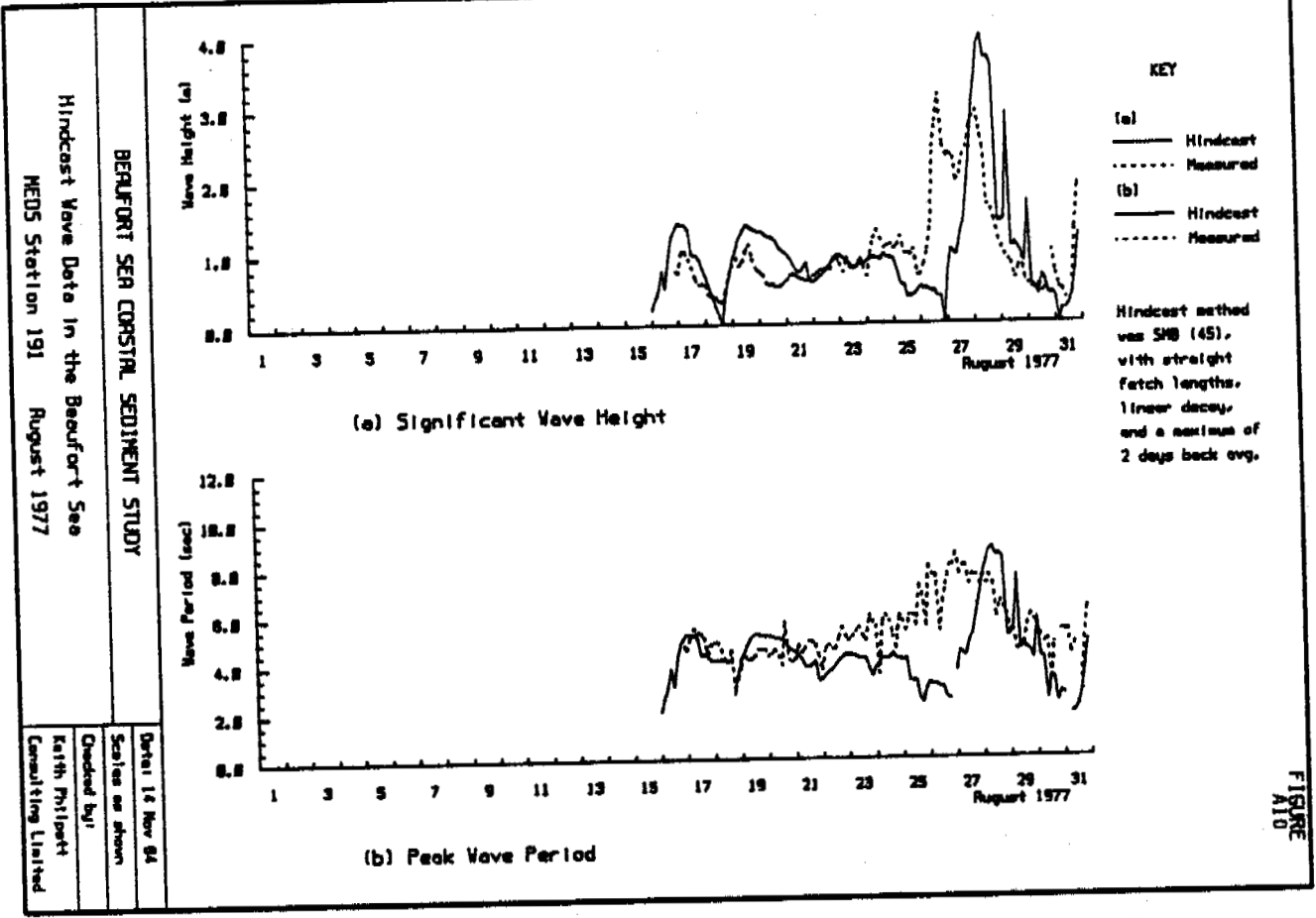


FIGURE A10

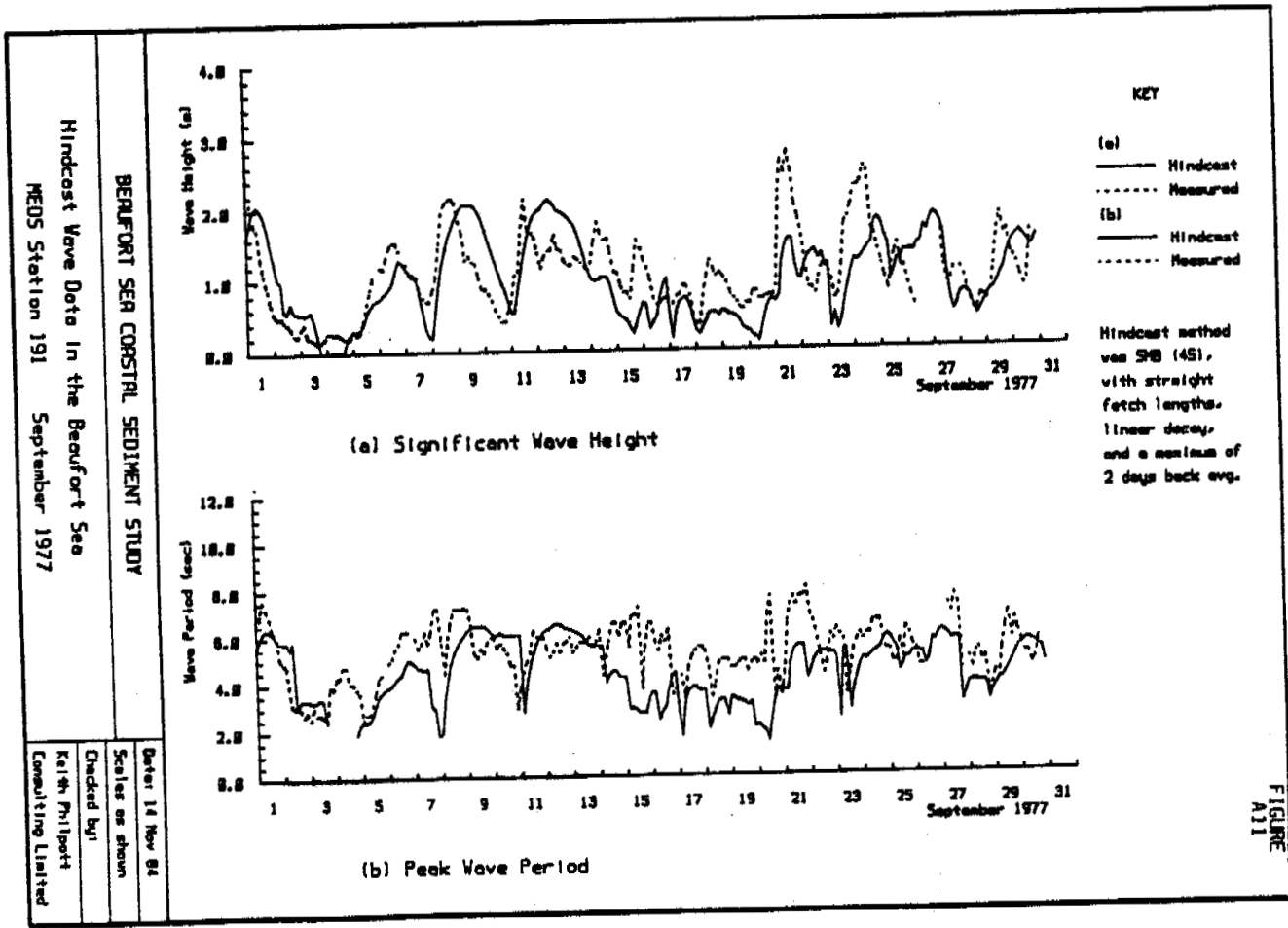
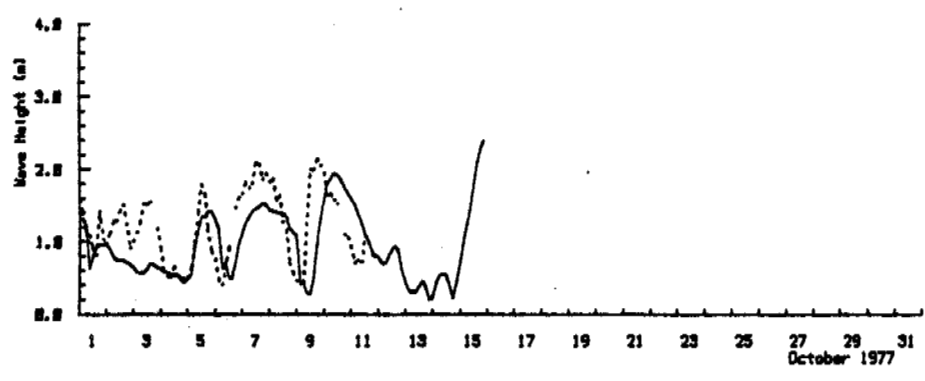


FIGURE A11

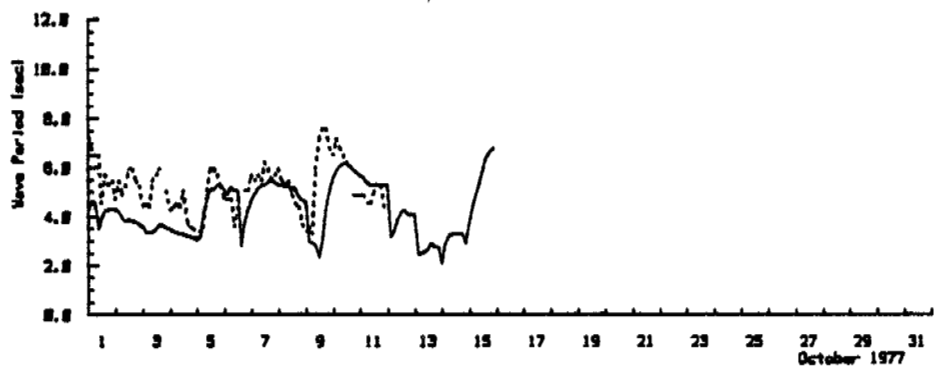
BEAUFORT SEA COASTAL SEDIMENT STUDY

Hindcast Wave Data in the Beaufort Sea
 NEOS Station 191 October 1977

Date: 16 Nov 84
 Scale: as shown
 Checked by:
 Keith Phillips
 Consulting Limited



(a) Significant Wave Height



(b) Peak Wave Period

KEY

(a) — Hindcast
 Measured

(b) — Hindcast
 Measured

Hindcast method
 via SHB (45),
 with straight
 fetch lengths,
 linear decay,
 and a maximum of
 2 days back avg.

FIGURE
 A12

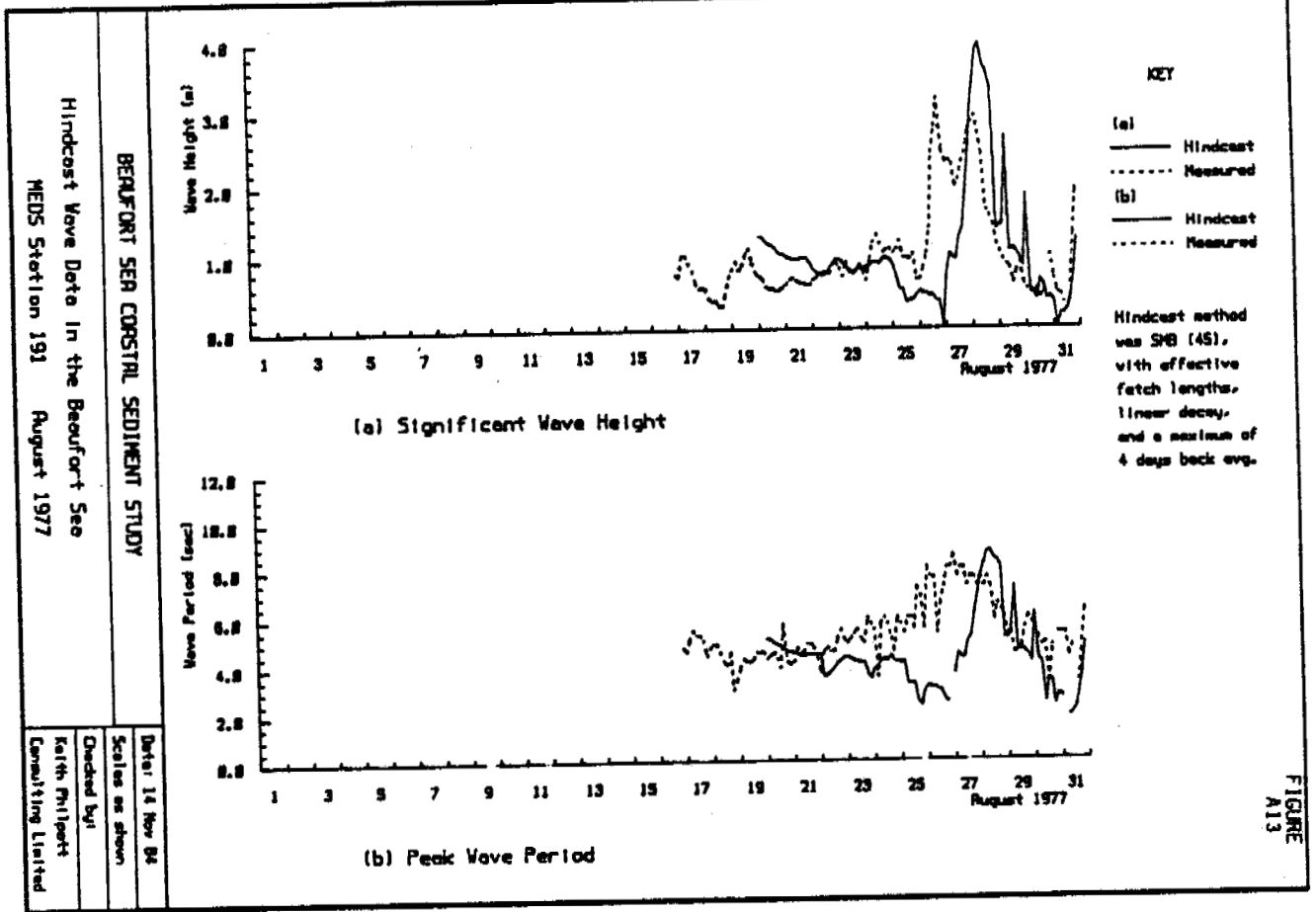


FIGURE A13

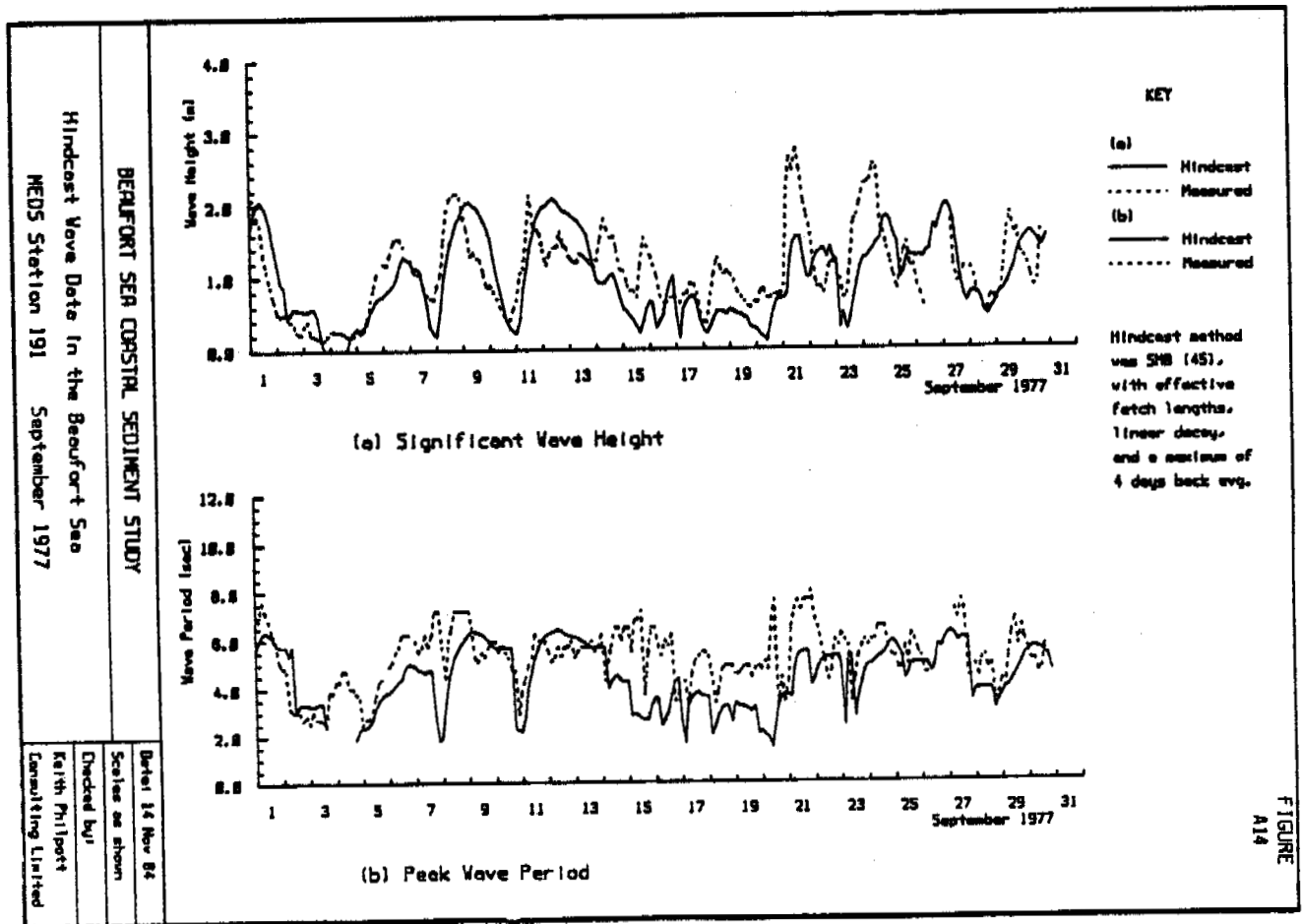
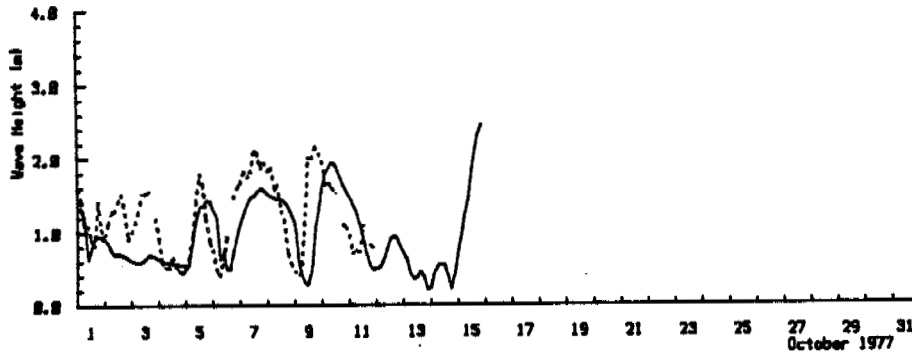


FIGURE A14

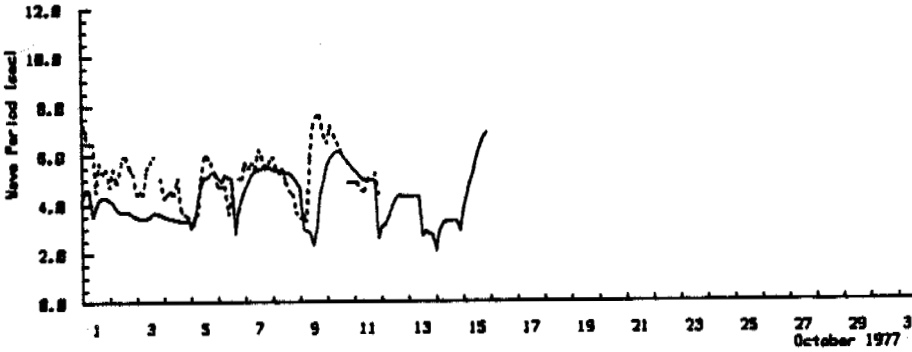
Hindcast Wave Data in the Beaufort Sea
NEOS Station 191 October 1977

BEAUFORT SEA COASTAL SEDIMENT STUDY

Date: 14 Nov 84
Scales as shown
Checked by:
Keith Philpott
Consulting Limited



(a) Significant Wave Height



(b) Peak Wave Period

KEY
(a) — Hindcast
 Measured
(b) — Hindcast
 Measured

Hindcast method was SHB (45), with effective fetch lengths, linear decay, and a maximum of 4 days back avg.

FIGURE
A15

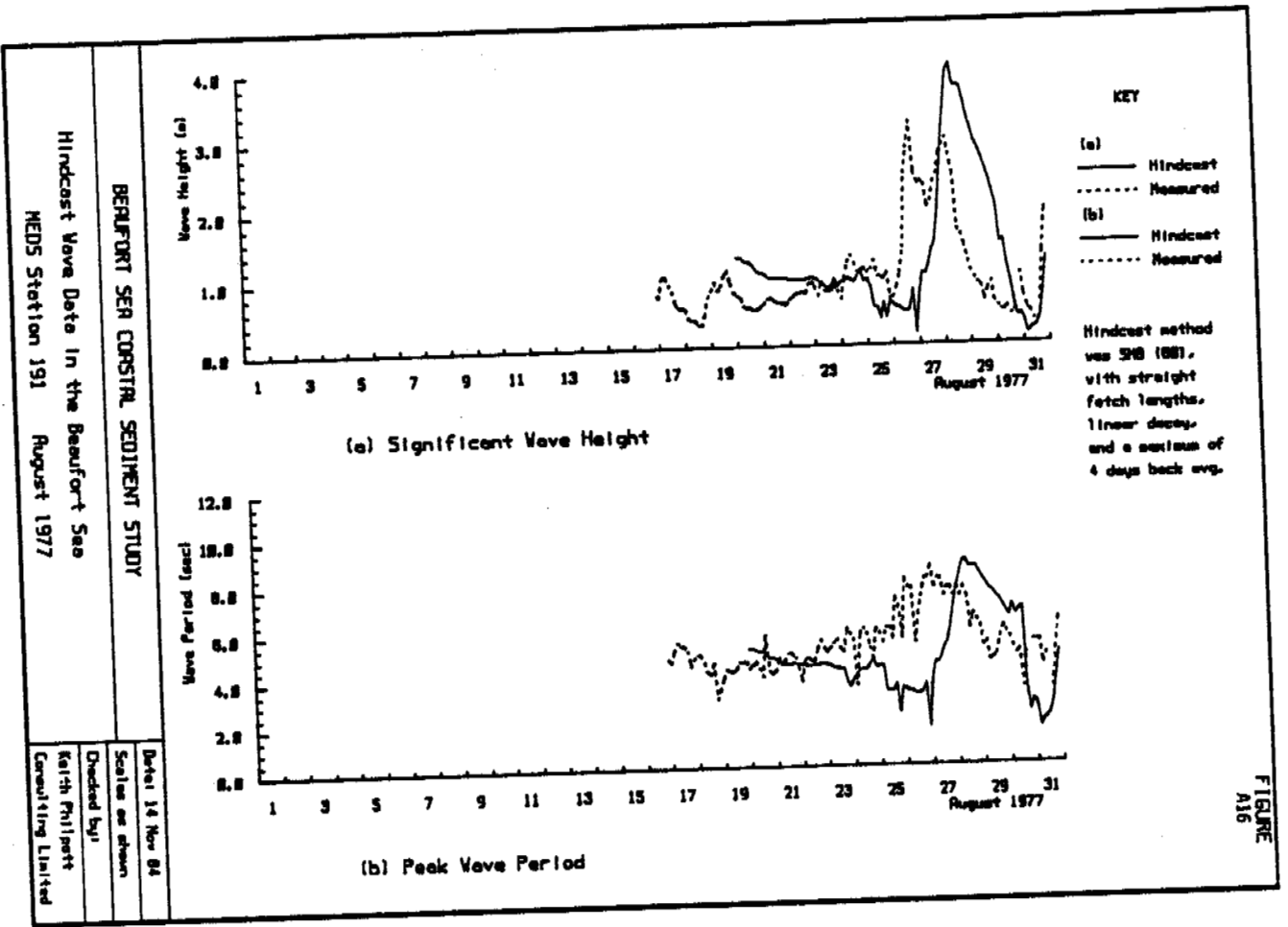


FIGURE A16

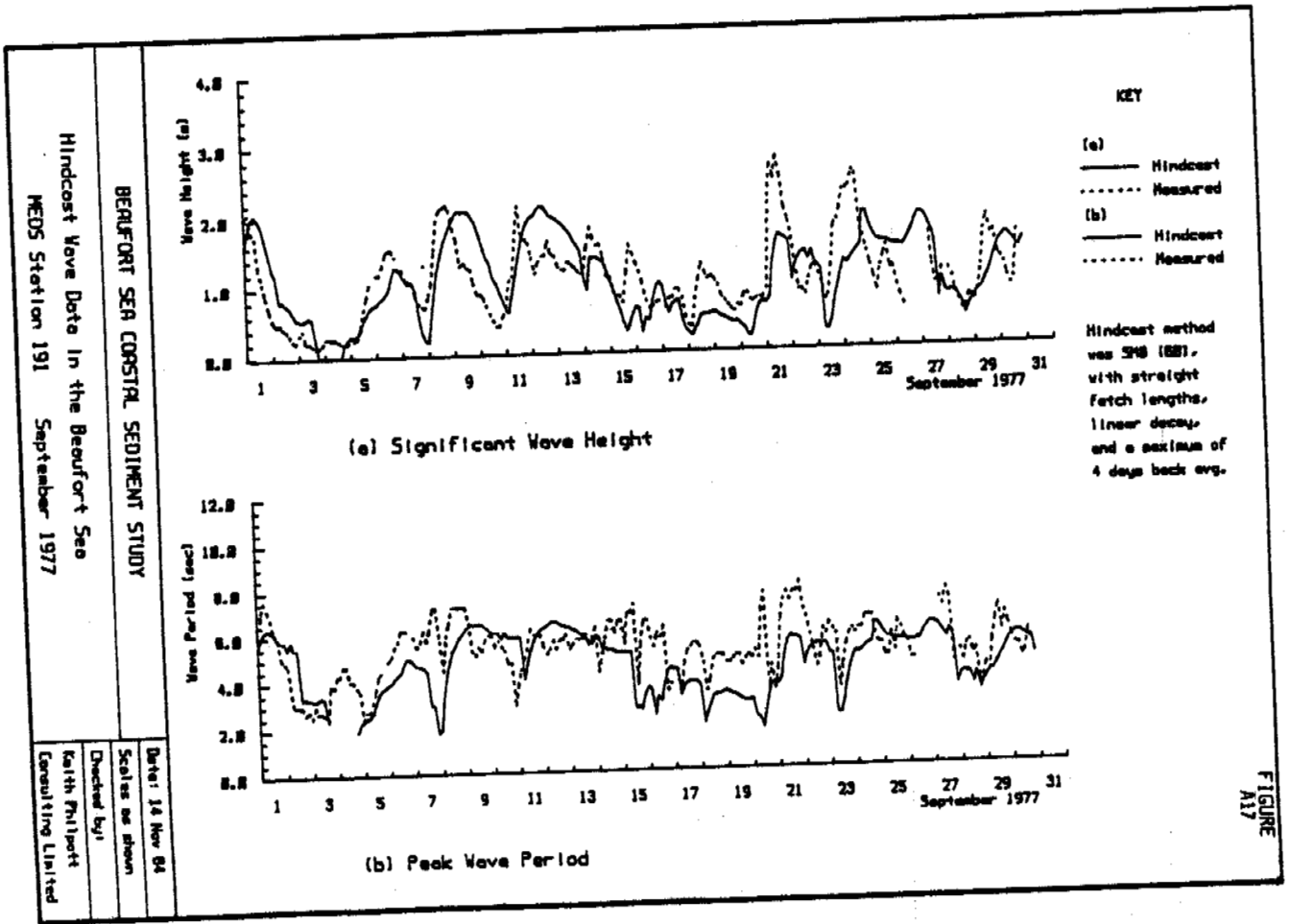
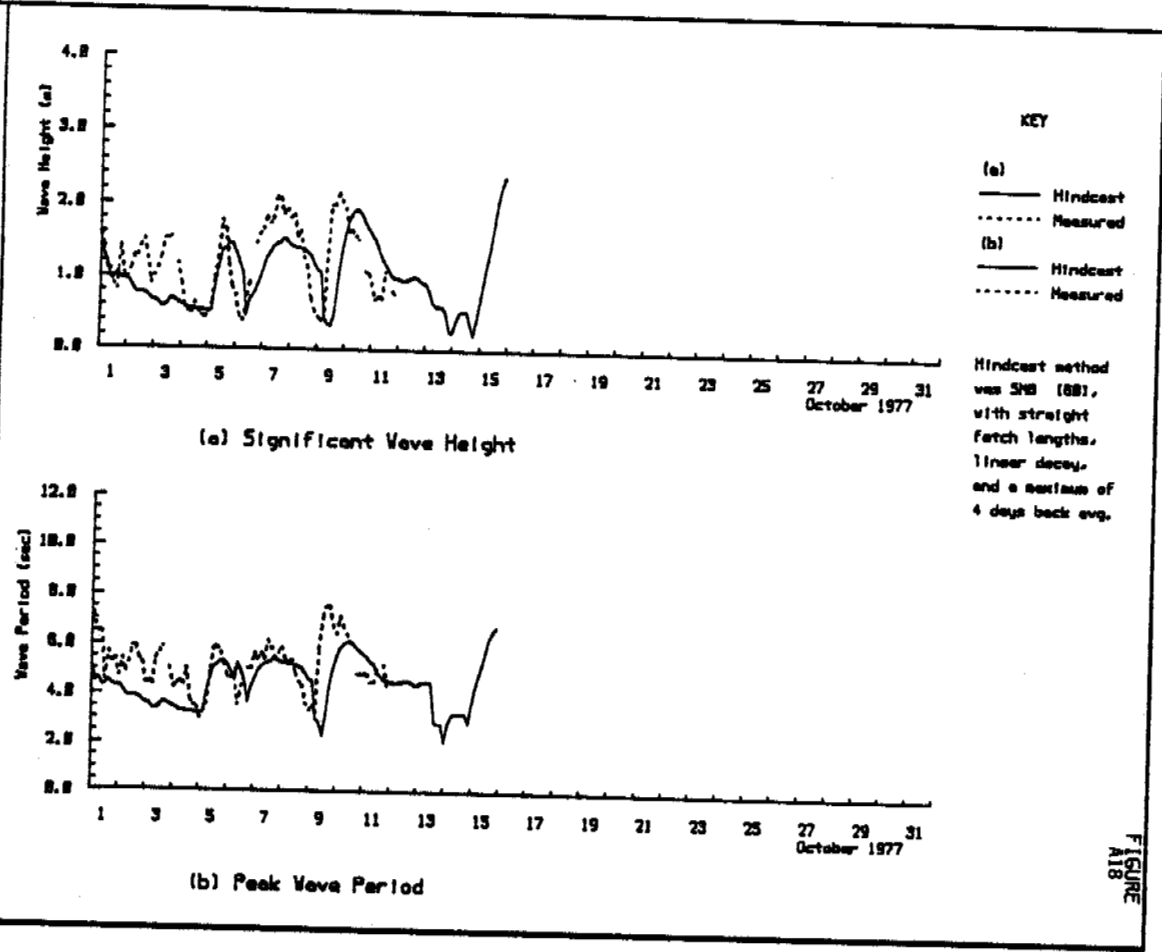


FIGURE A17

BEAUFORT SEA COASTAL SEDIMENT STUDY

Hindcast Wave Data in the Beaufort Sea
NEOS Station 191 October 1977

Date: 14 Nov 82
Scale: as shown
Checked by: Keith Phillips
Consulting Limited



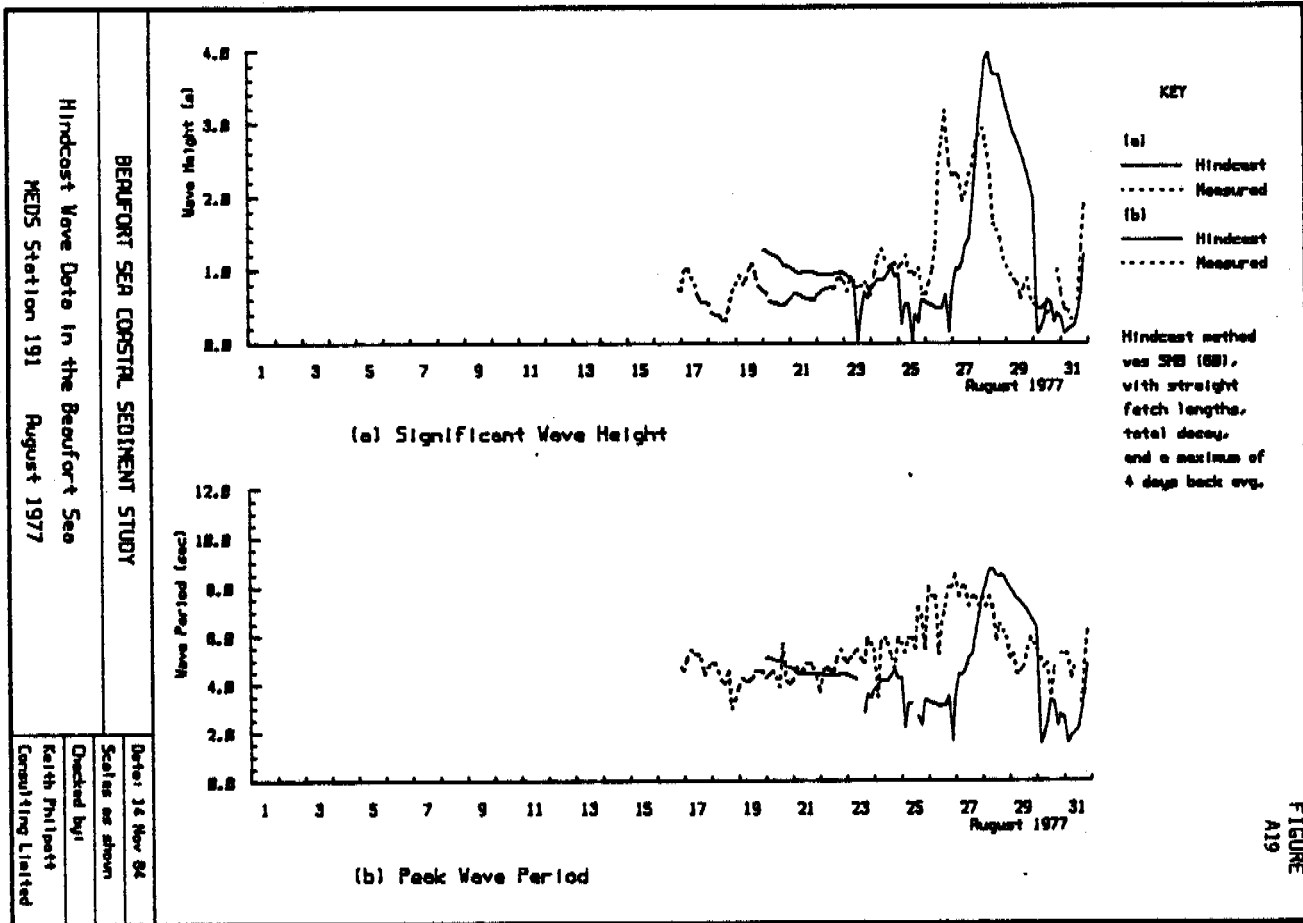


FIGURE A19

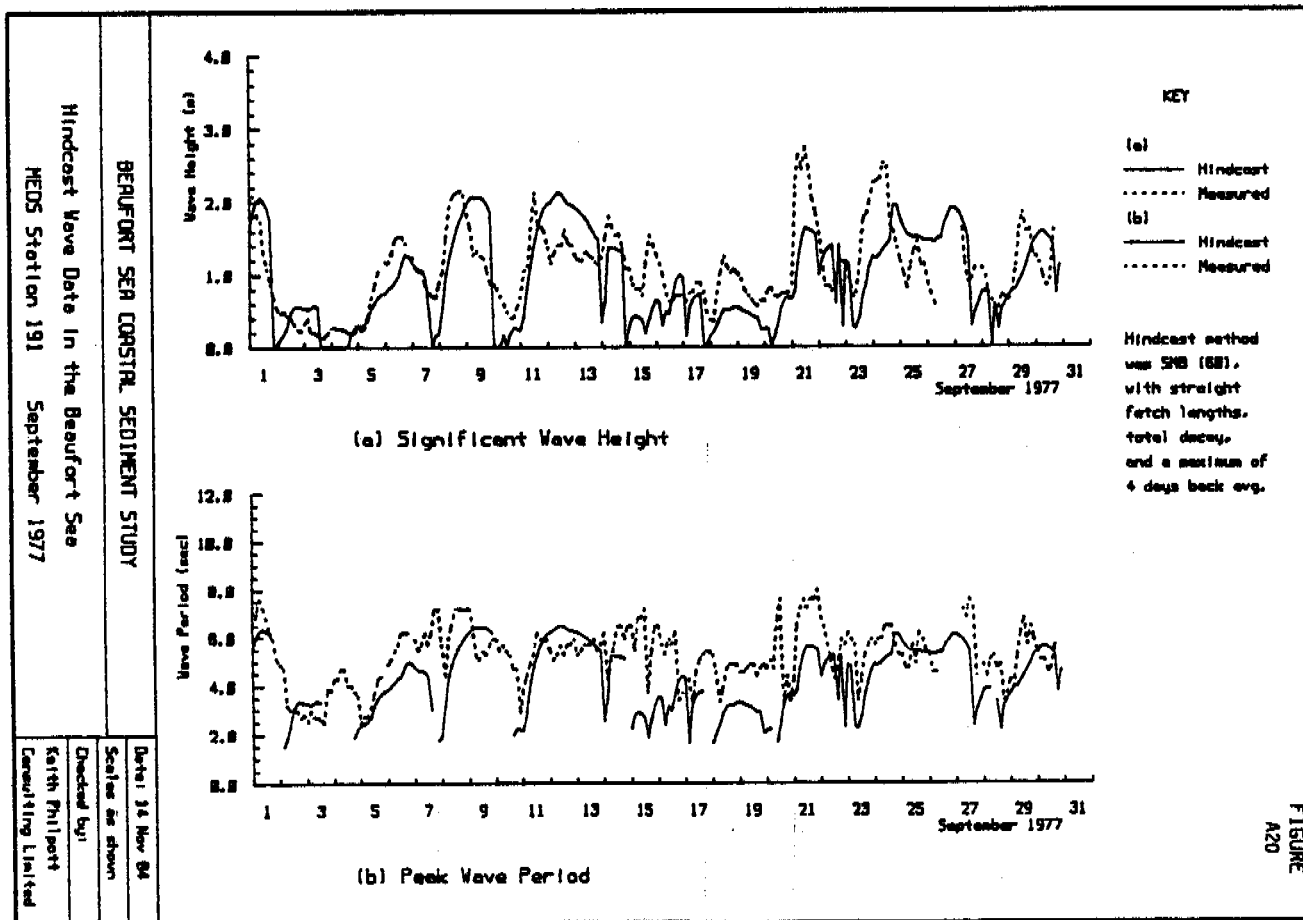
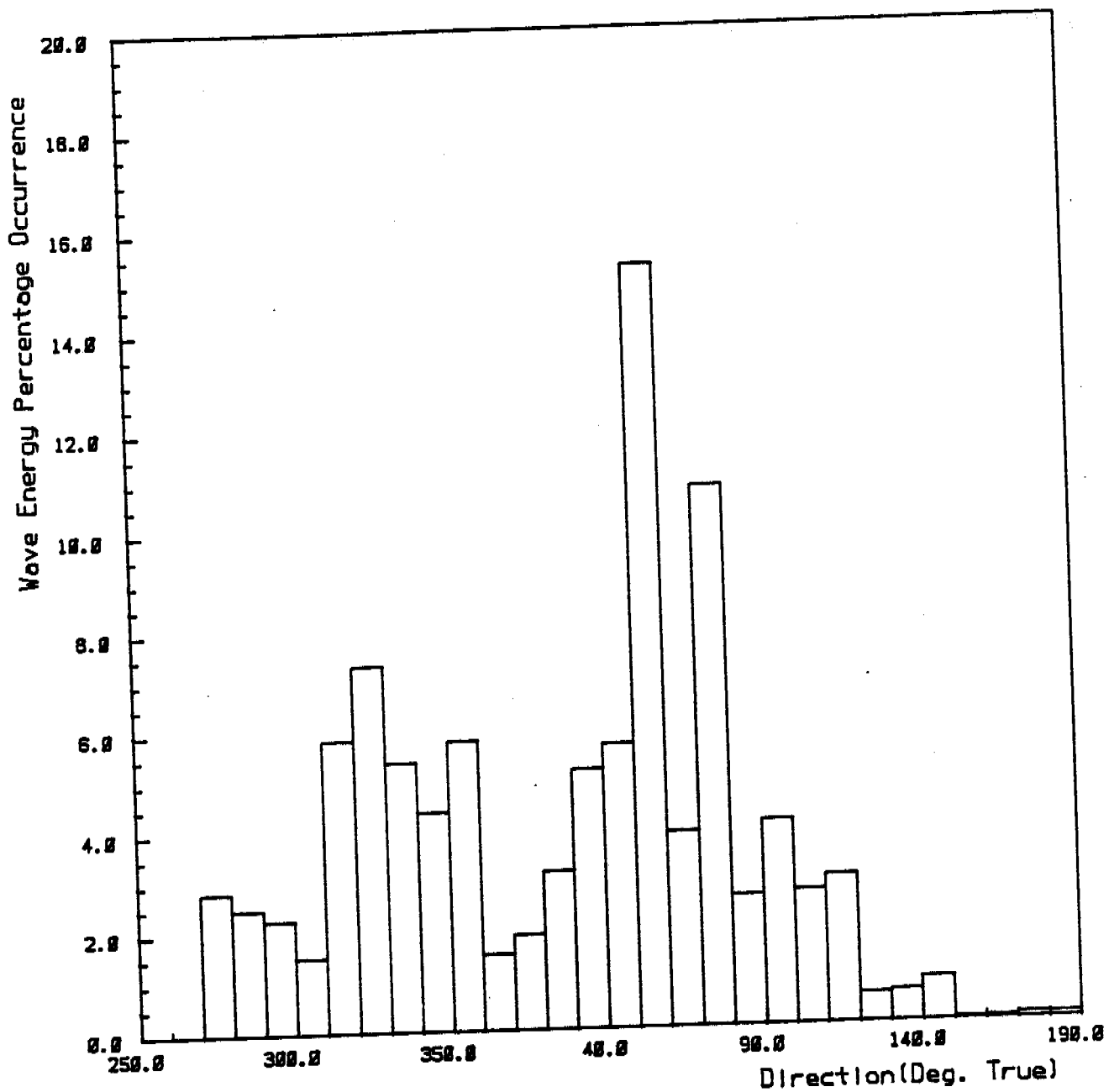


FIGURE A20



Direction Limits: 270.0 TO 190.0

Calms: 19.4 %

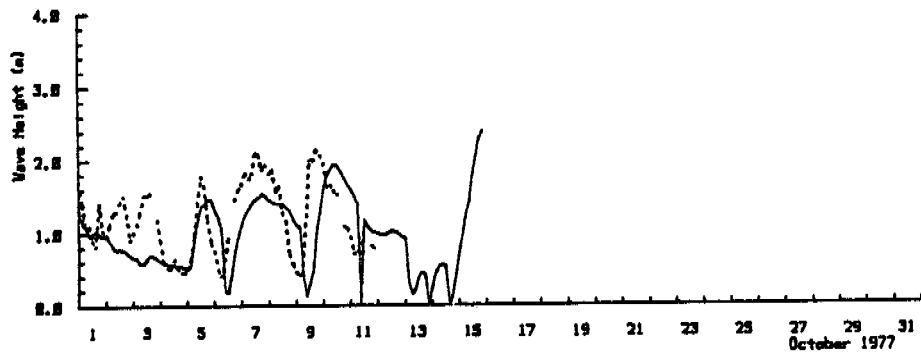
Dates: 2/7/78 to 7/9/83

Season: Summer, Fall

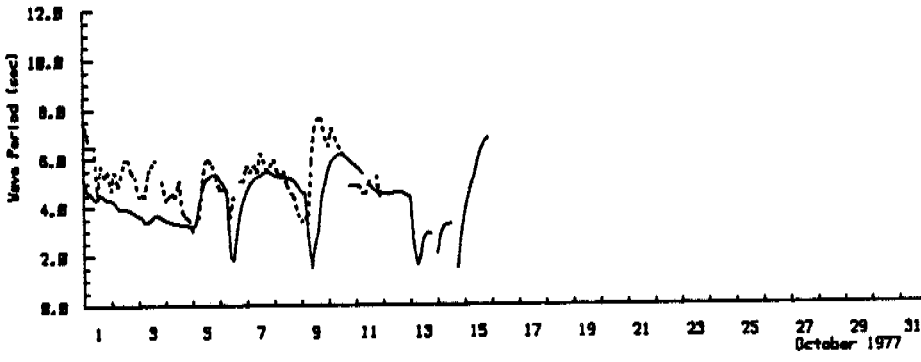
Total No. of Records: 34865

Waves Hindcast Using Wind Data from Tuktoyaktuk N.W.T.

BEAUFORT SEA COASTAL SEDIMENT STUDY	Date: 17 Feb 85
	Scales as shown
King Point: Deep Water Wave Energy Distribution 1978 - 1983	Checked by:
	Keith Philpott
	Consulting Limited



(a) Significant Wave Height



(b) Peak Wave Period

KEY
 (a) — Hindcast
 Measured
 (b) — Hindcast
 Measured

Hindcast method was SIM (681), with straight fetch lengths, total decay, and a maximum of 4 days back avg.

FIGURE
 A21

BERFORD SEA COASTAL SEDIMENT STUDY

Hindcast Wave Data in the Baurfort Sea
 NEBS Station 191 October 1977

Date: 14 Nov 84
 Scale: as shown
 Checked by:
 Keith Phillips
 Consulting Limited

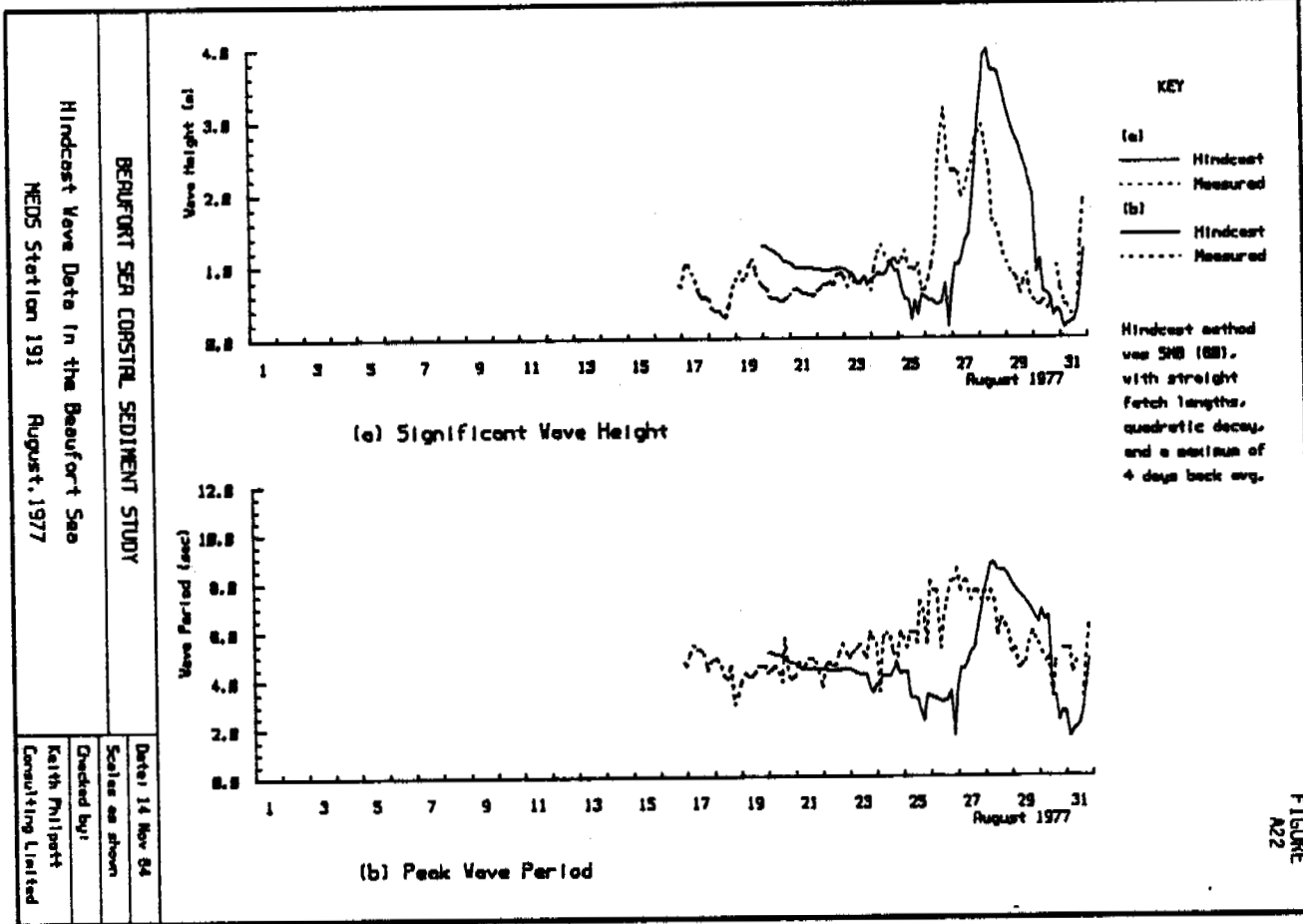


FIGURE A22

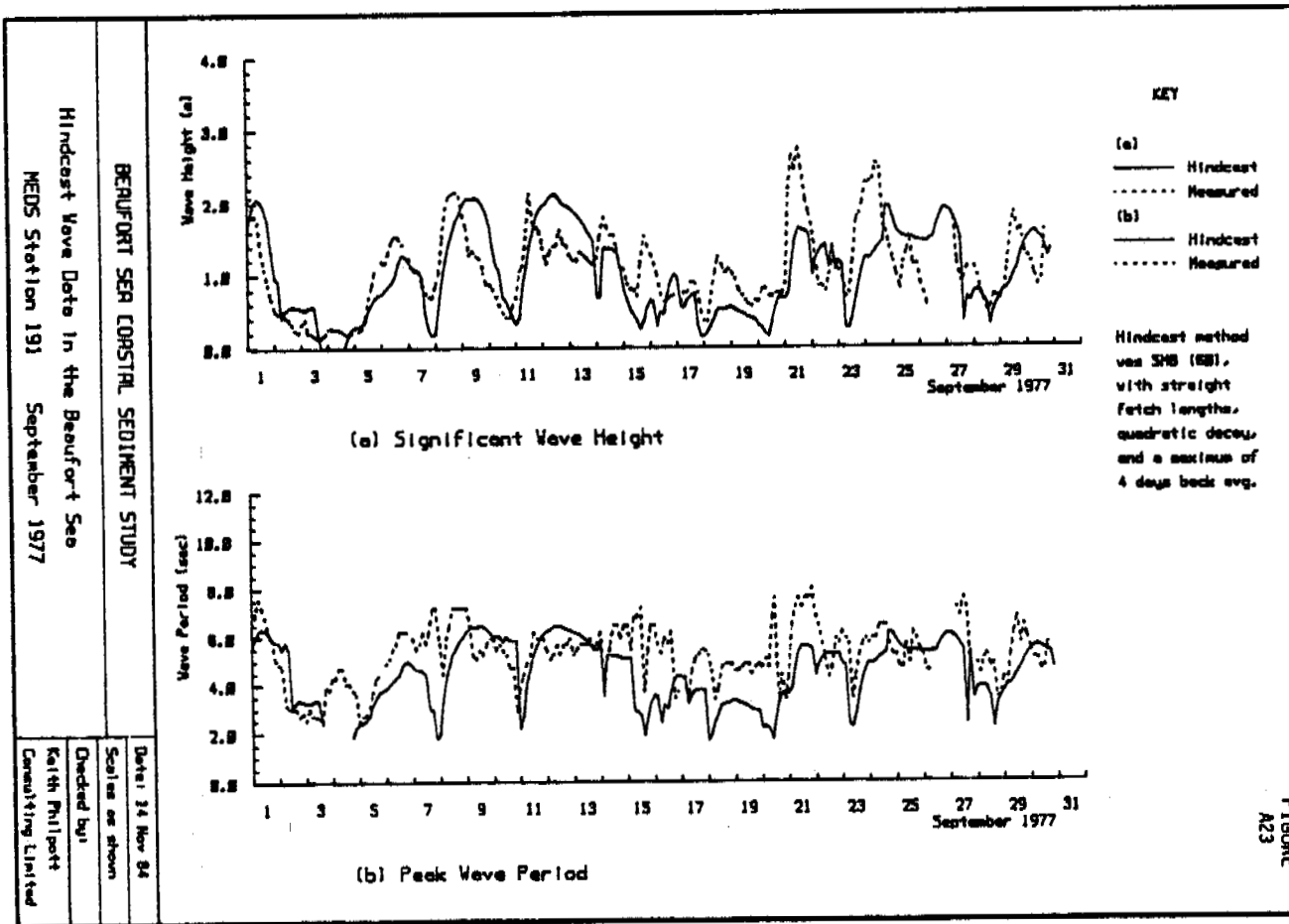
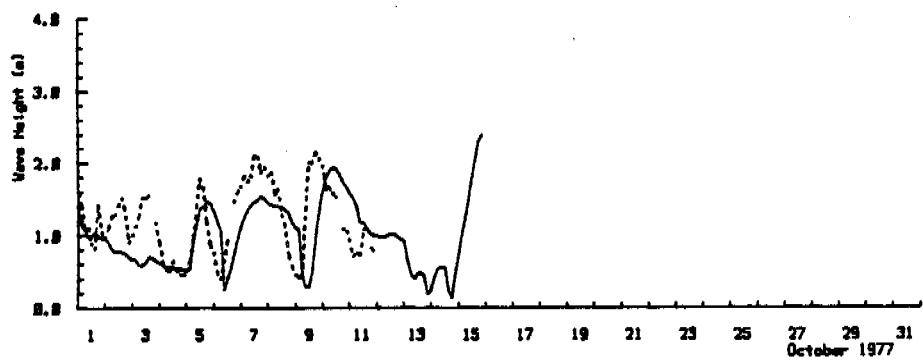


FIGURE A23

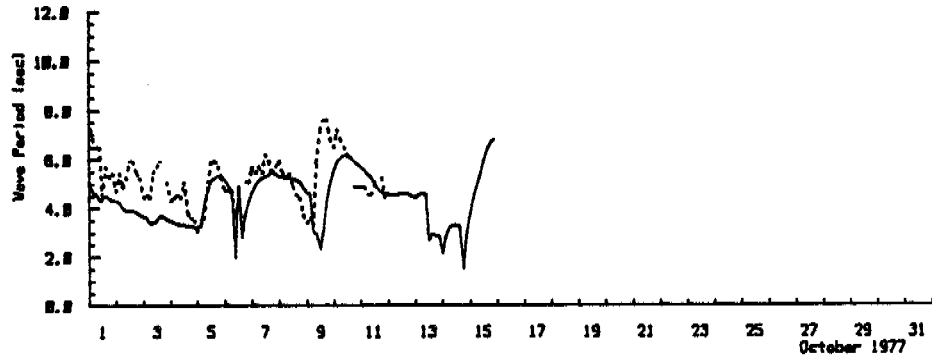
Hindcast Wave Data in the Beaufort Sea
 NEOS Station 191 October 1977

BEAUFORT SEA COASTAL SEDIMENT STUDY

Date: 14 Nov 84
 Scaled as shown
 Checked by:
 Keith Philpott
 Consulting Limited



(a) Significant Wave Height



(b) Peak Wave Period

KEY
 (a) — Hindcast
 Measured
 (b) — Hindcast
 Measured

Hindcast method was SHB (88), with straight fetch lengths, quadratic decay, and a maximum of 4 days back avg.

FIGURE
 A24

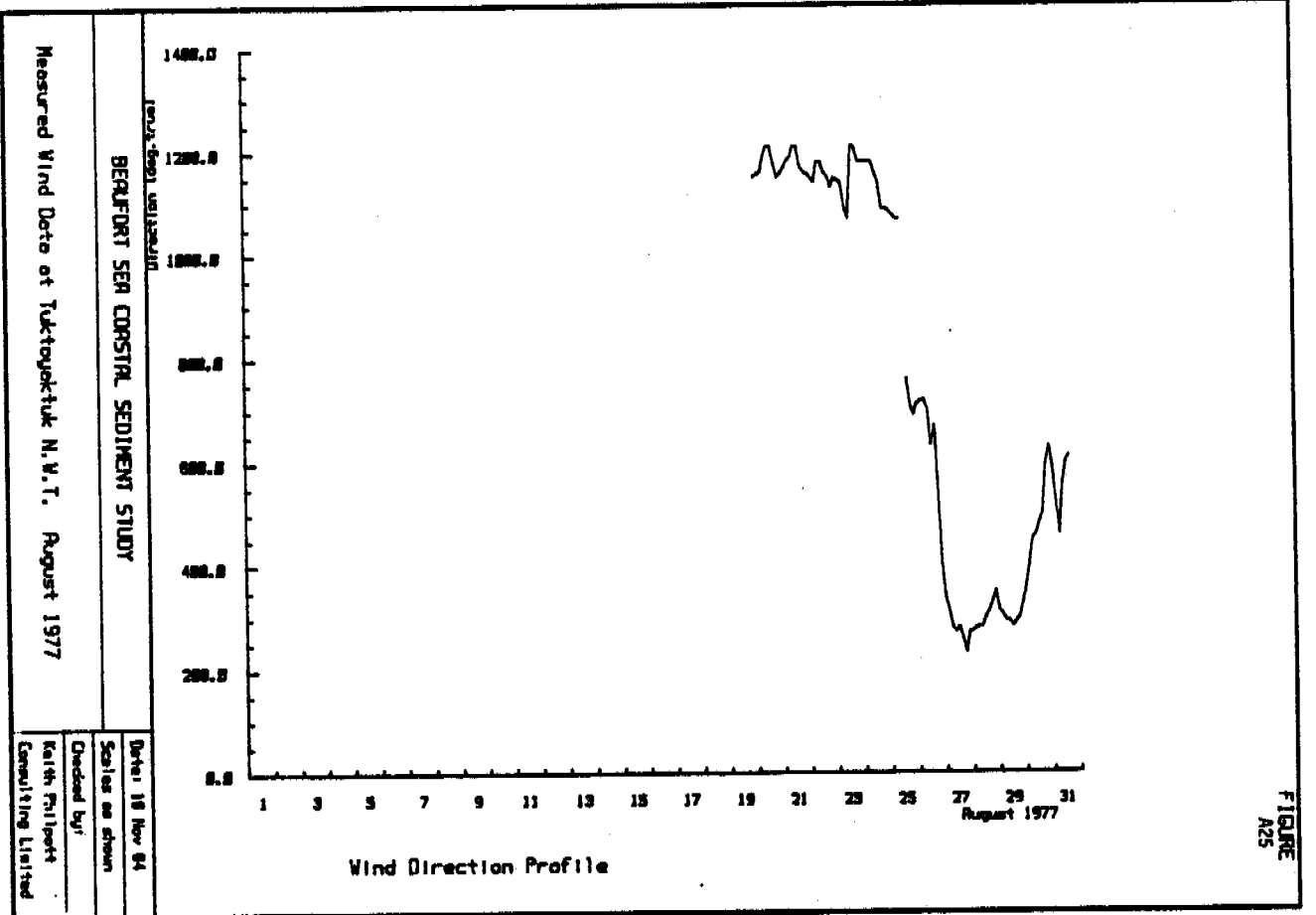


FIGURE A25

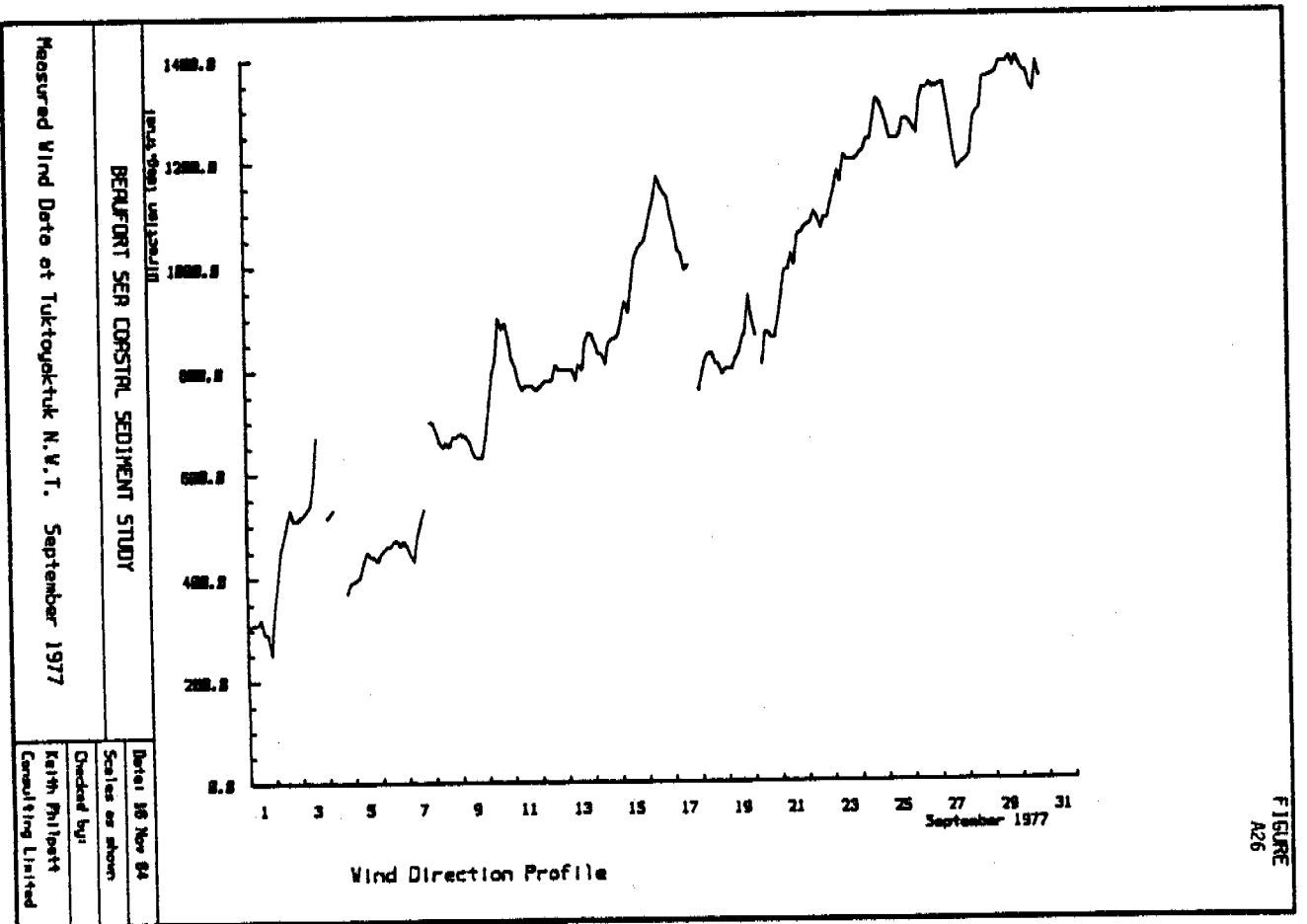
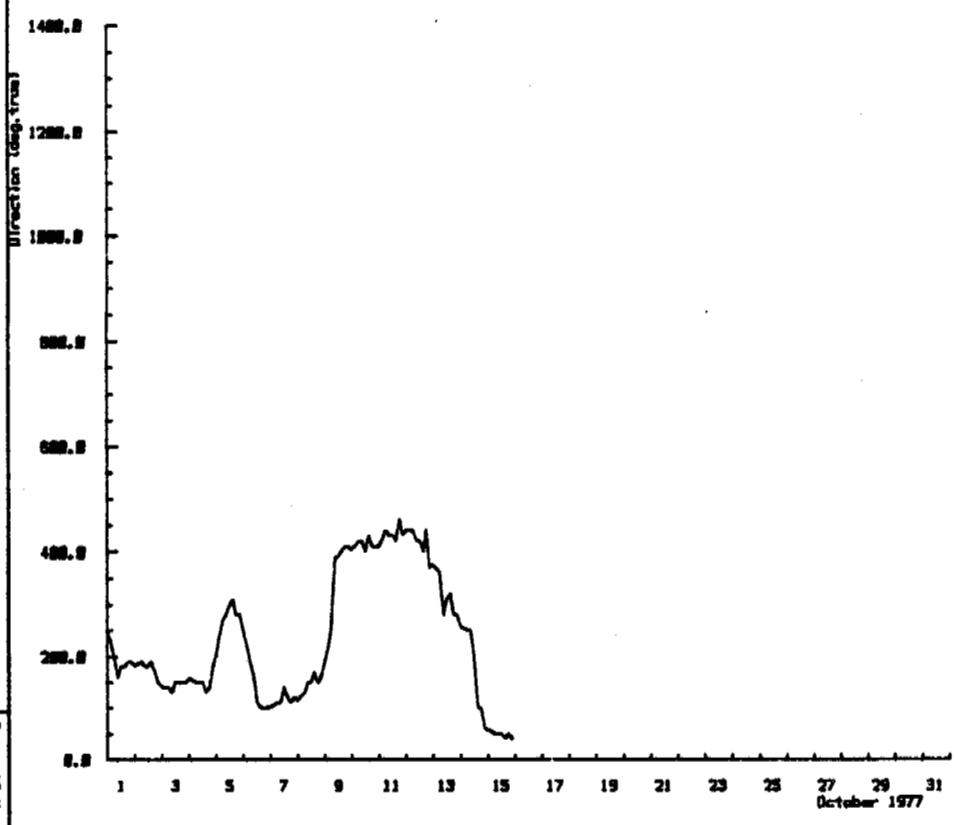


FIGURE A26



Wind Direction Profile

FIGURE A27

Measured Wind Data at Tuktoyaktuk N.W.T. October 1977

BEAUFORT SEA COASTAL SEDIMENT STUDY

Date: 18 Nov 84
 Scale: as shown
 Checked by:
 Catch: Fullport
 Consulting: Listed

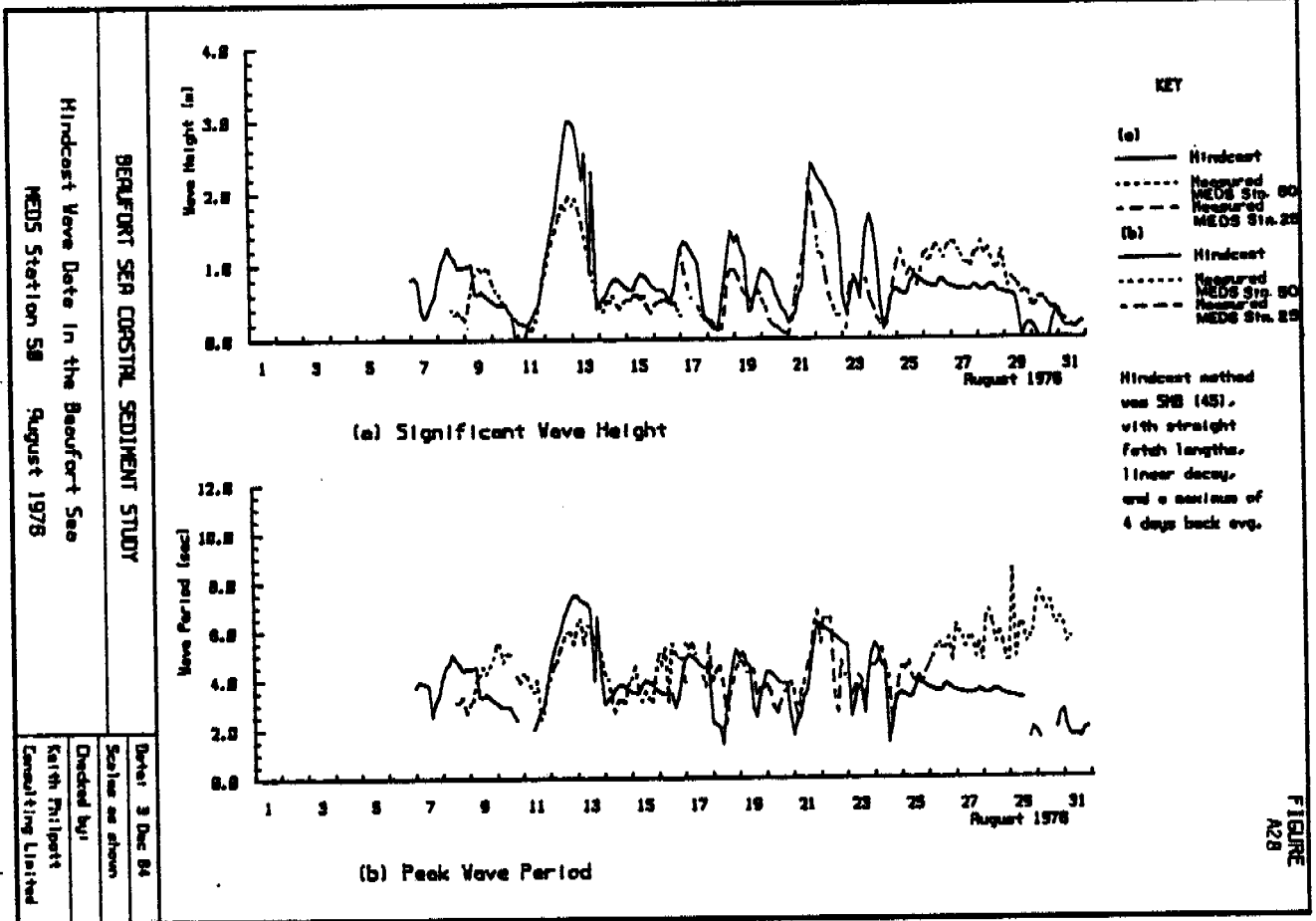


FIGURE A28

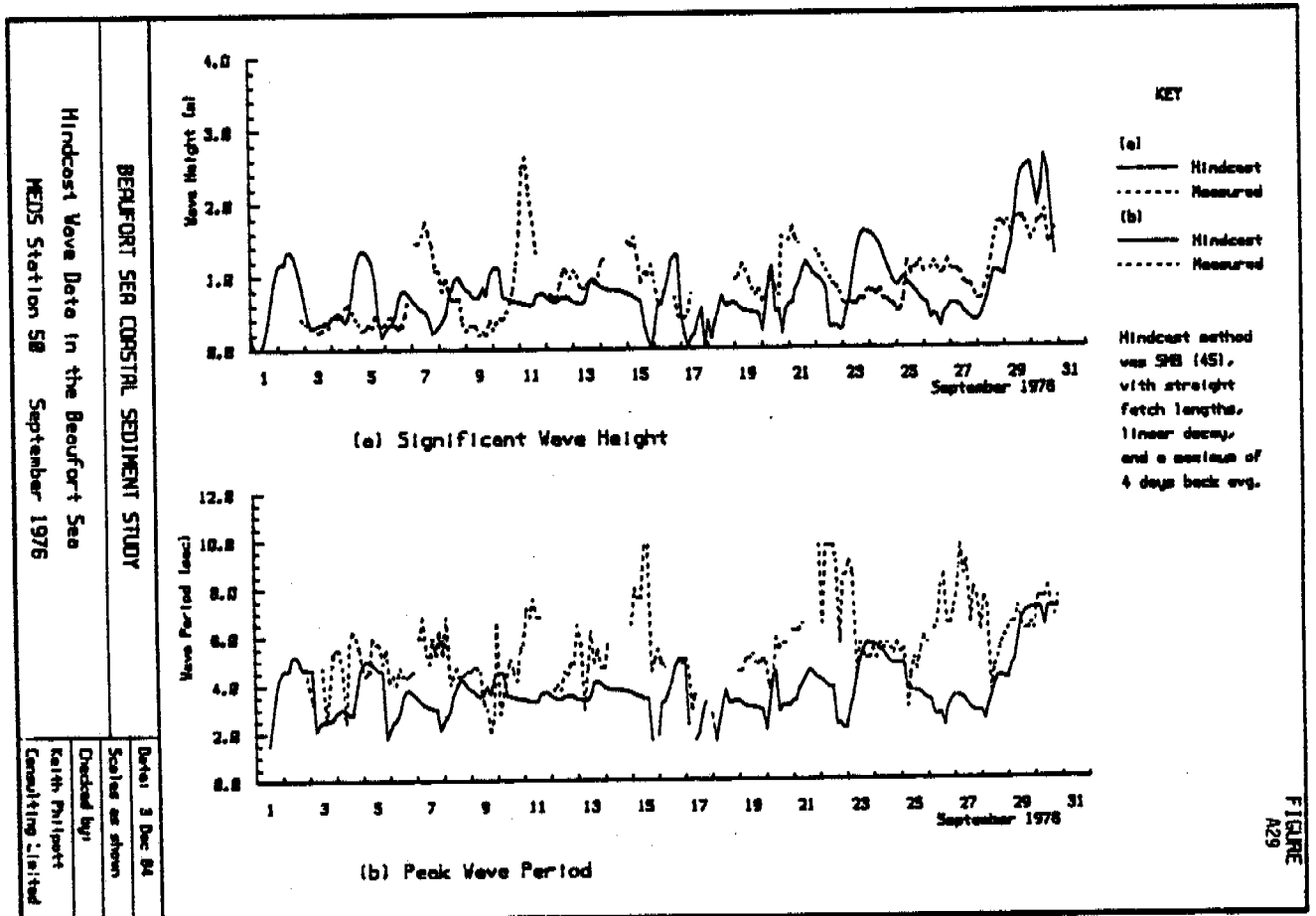
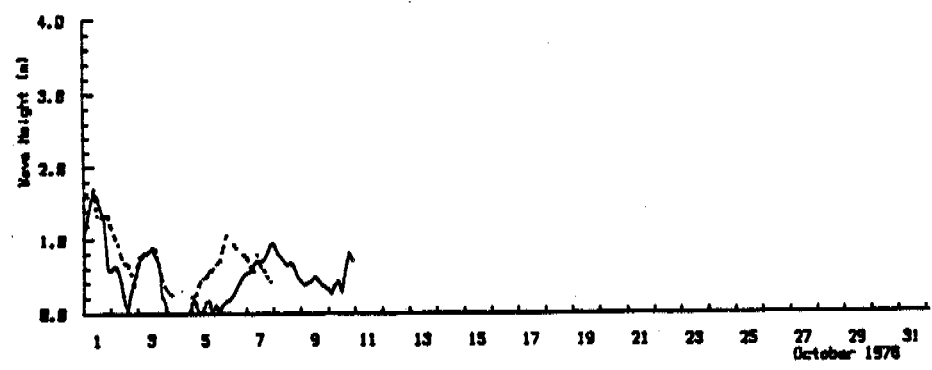


FIGURE A29

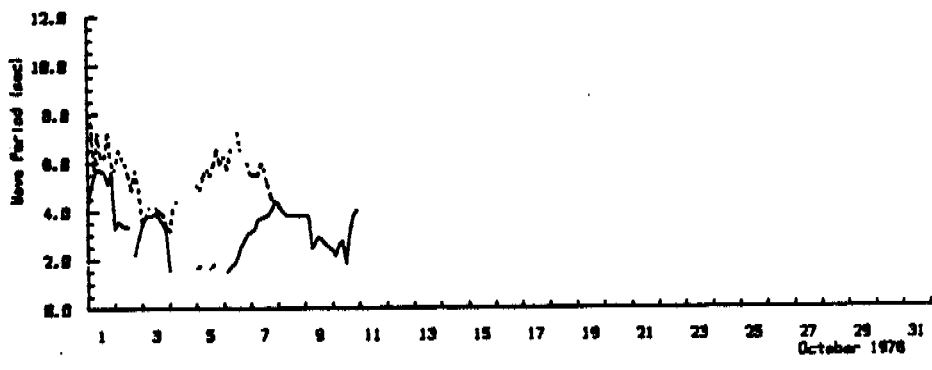
Hindcast Wave Data in the Beaufort Sea
 WEDS Station 58 October 1976

BEAUFORT SEA COASTAL SEDIMENT STUDY

Date: 9 Dec 84
 Scale: as shown
 Checked by:
 Keith Phillips
 Consulting Limited



(a) Significant Wave Height



(b) Peak Wave Period

KEY
 (a) — Hindcast
 - - - Measured
 (b) — Hindcast
 - - - Measured

Hindcast method was SMB (45), with straight fetch lengths, linear decay, and a minimum of 4 days back avg.

FIGURE
 A30

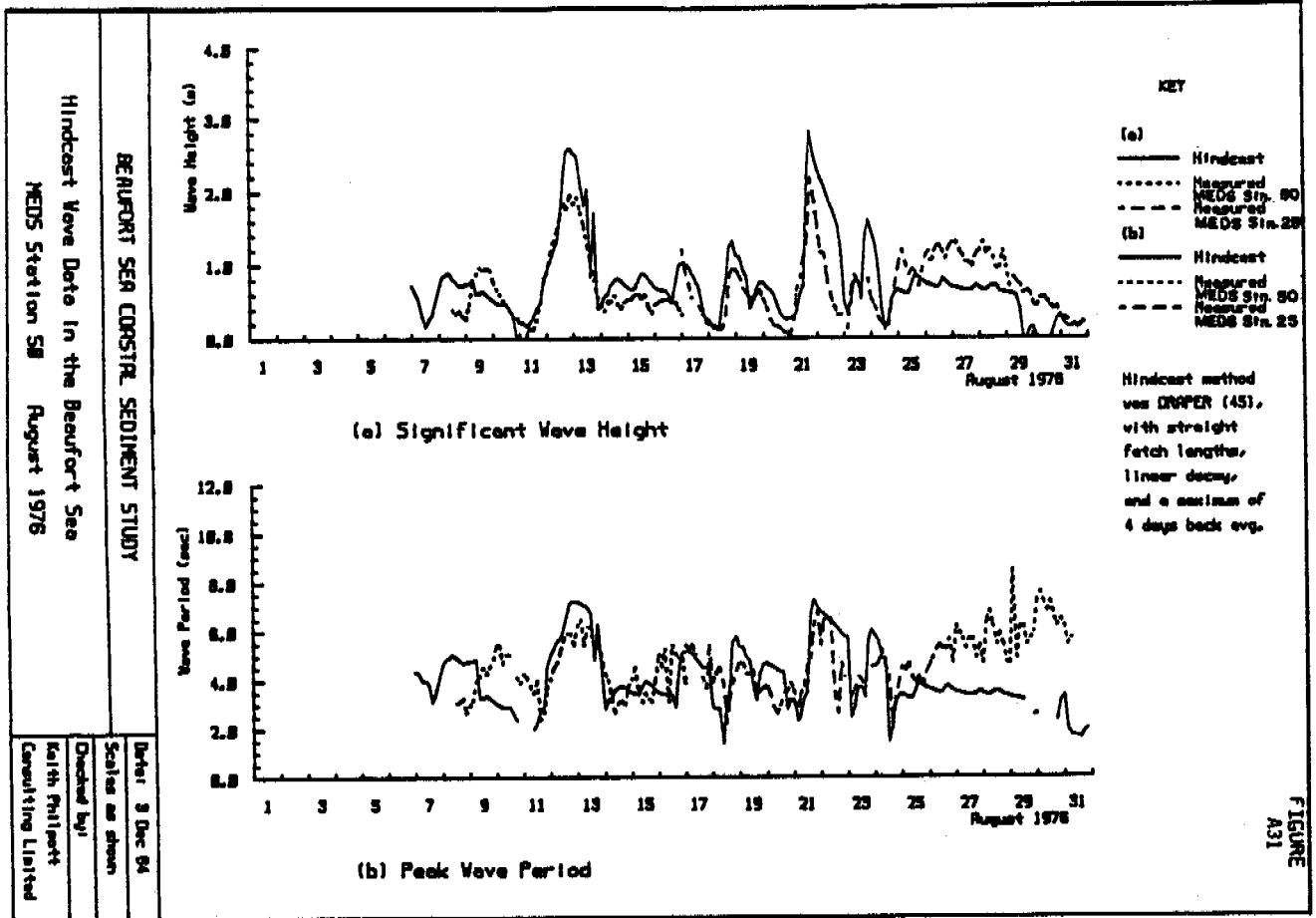


FIGURE A31

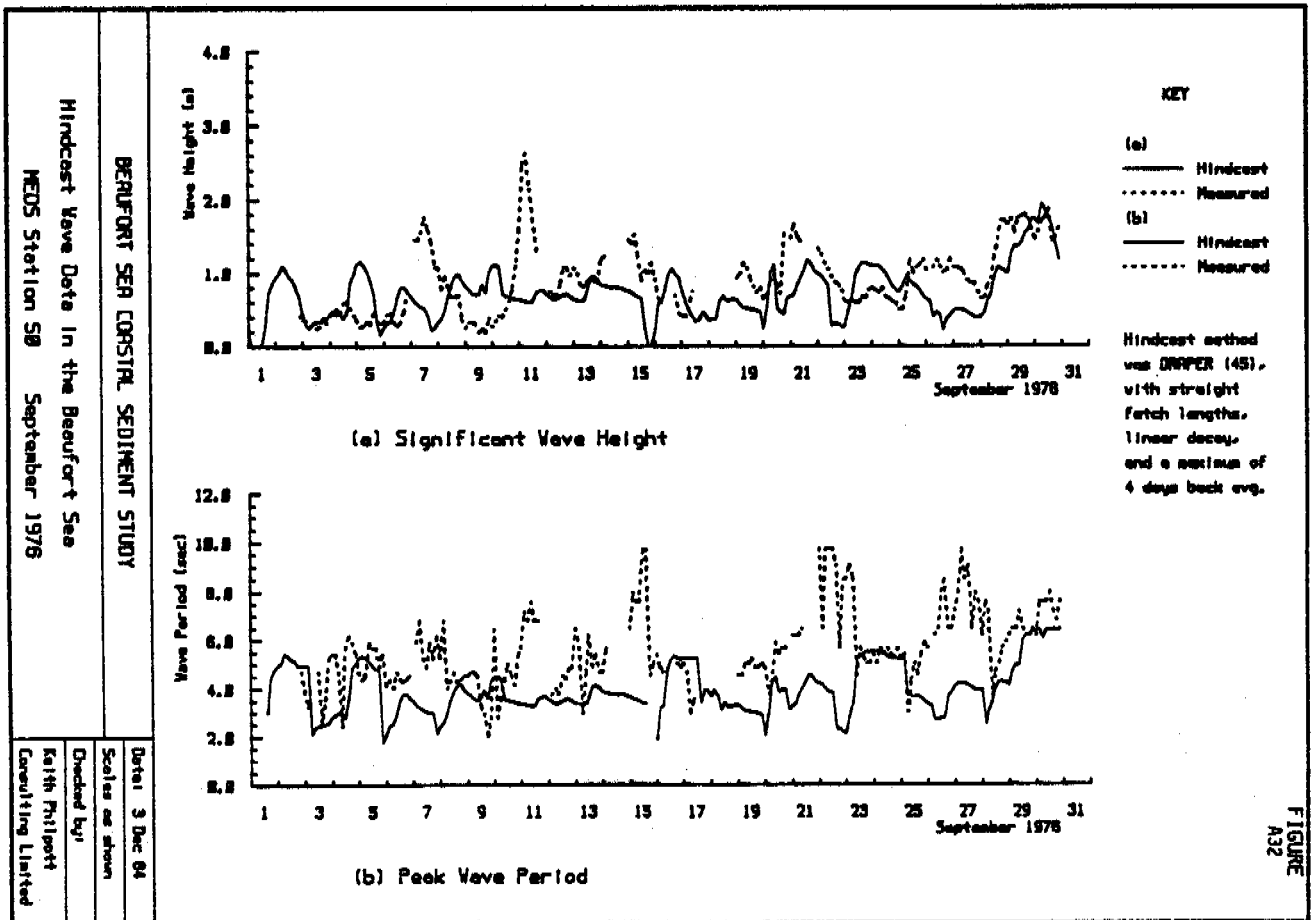


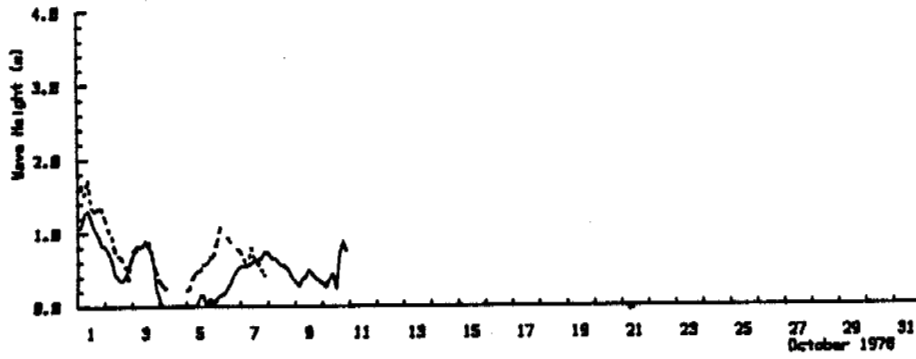
FIGURE A32

Hindcast Wave Data in the Beaufort Sea
 NEOS Station 58 October 1978

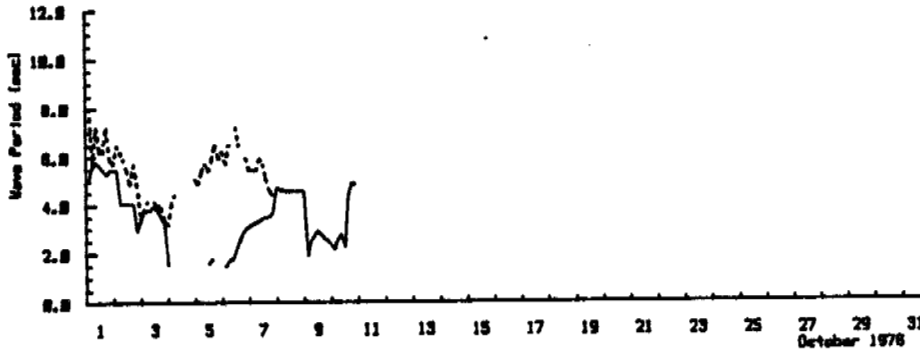
BEAUFORT SEA COASTAL SEDIMENT STUDY

Checked by:
 Keith Phillips
 Consulting Analyst

Date: 9 Dec 84
 Scale as shown



(a) Significant Wave Height



(b) Peak Wave Period

KEY
 (a) — Hindcast
 Measured
 (b) — Hindcast
 Measured

Hindcast method was CRAPER (45), with straight fetch lengths, linear decay, and a maximum of 4 days back avg.

FIGURE
 A33

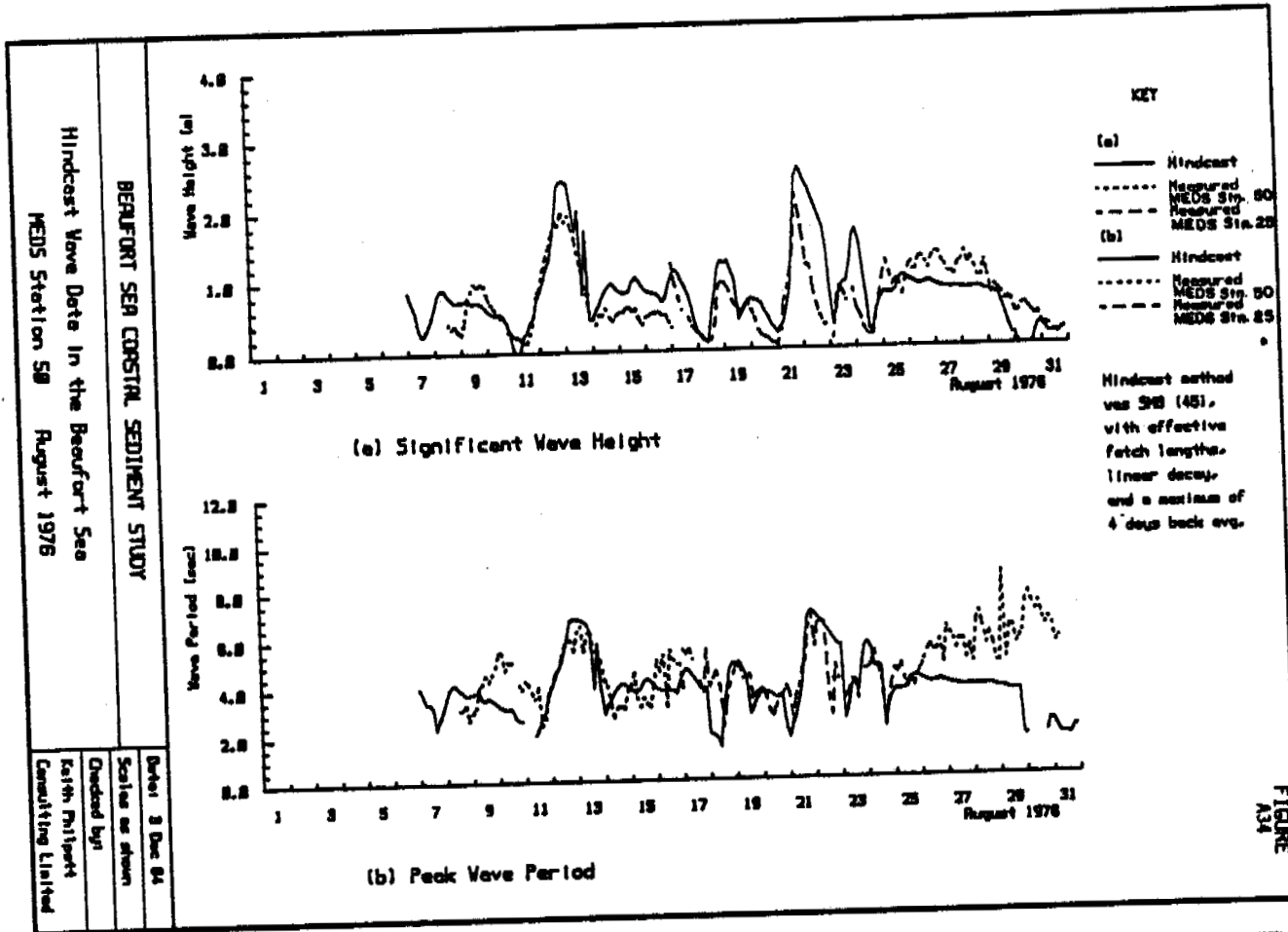


FIGURE A34

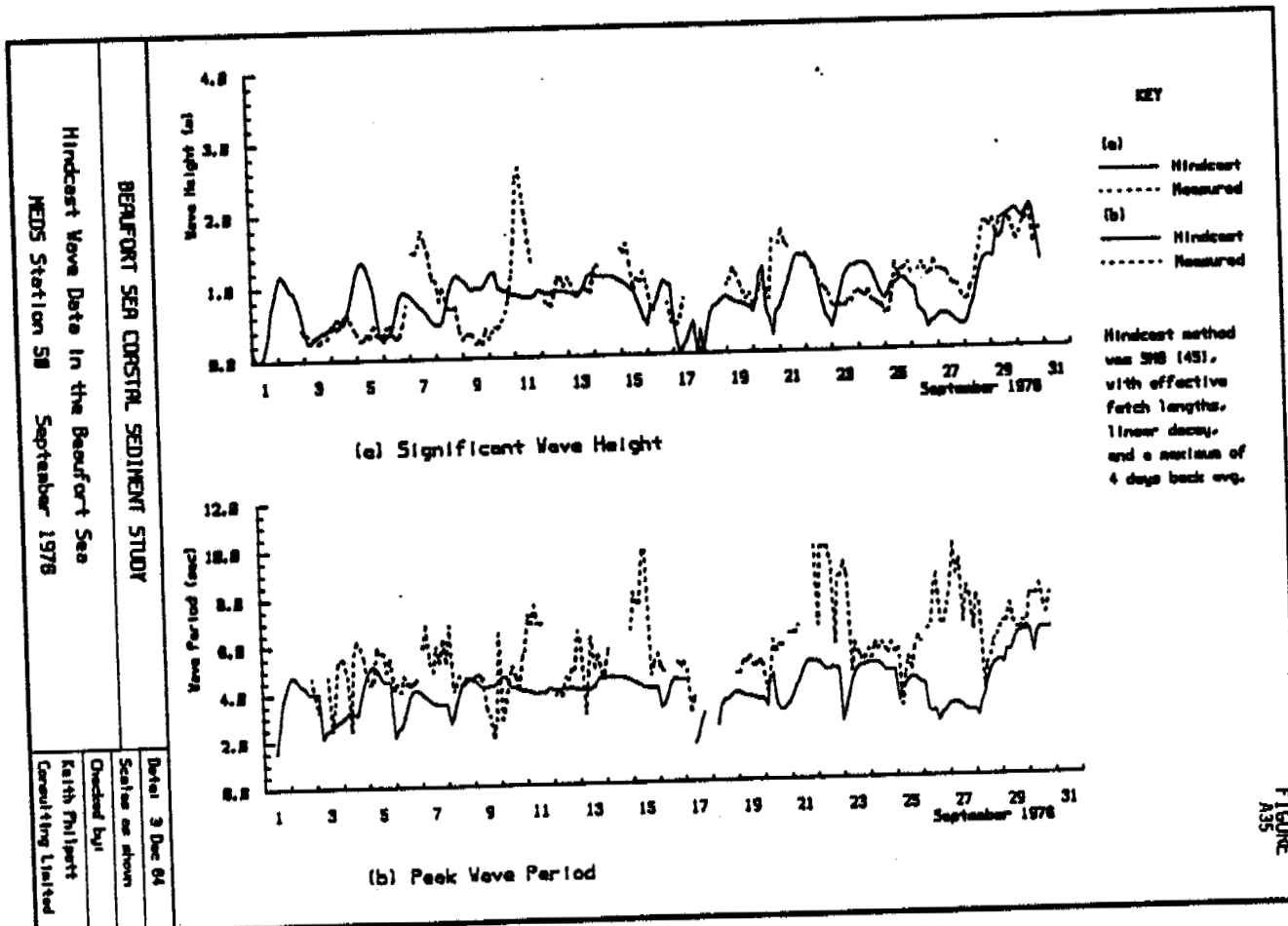


FIGURE A35

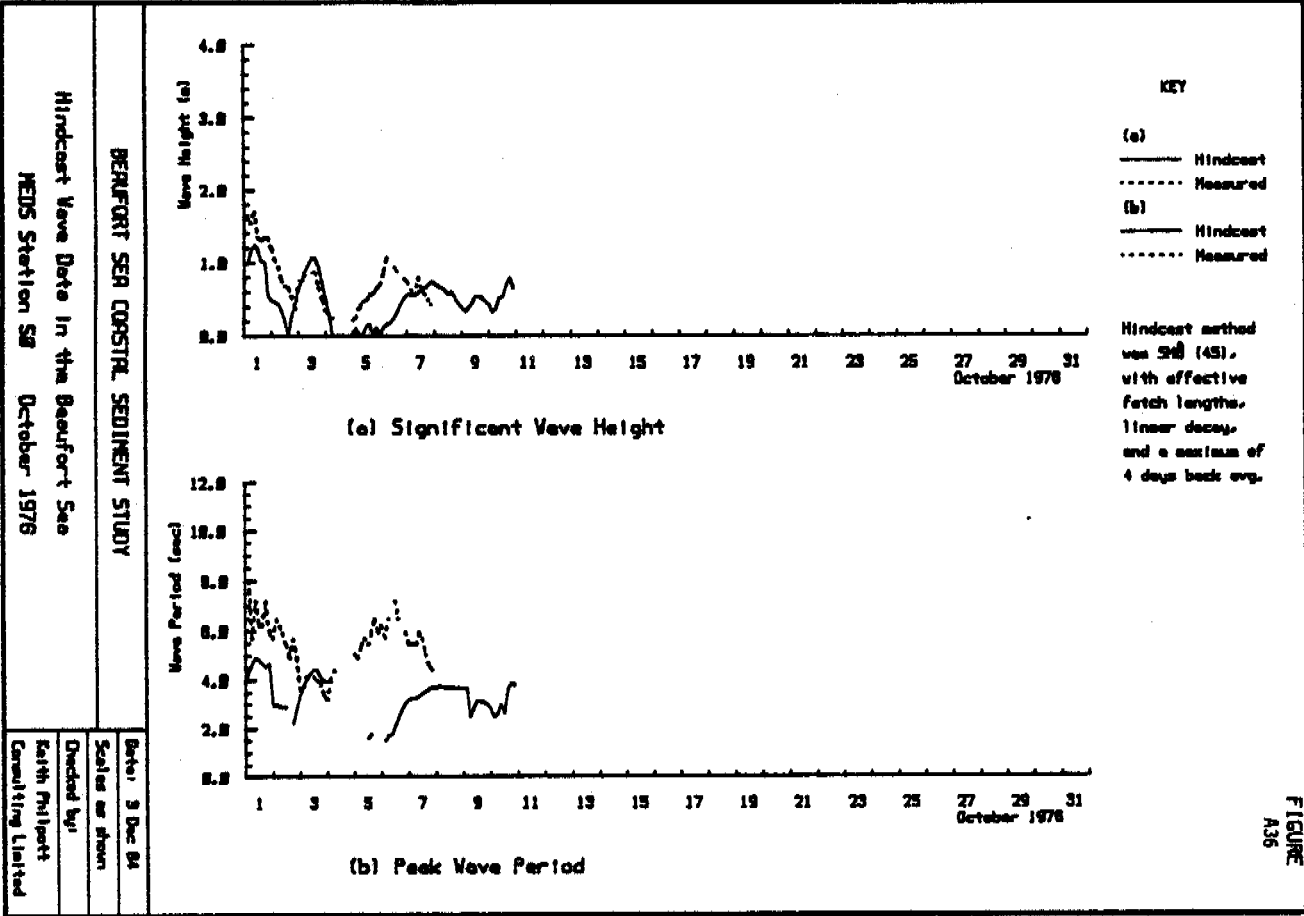


FIGURE
 A36

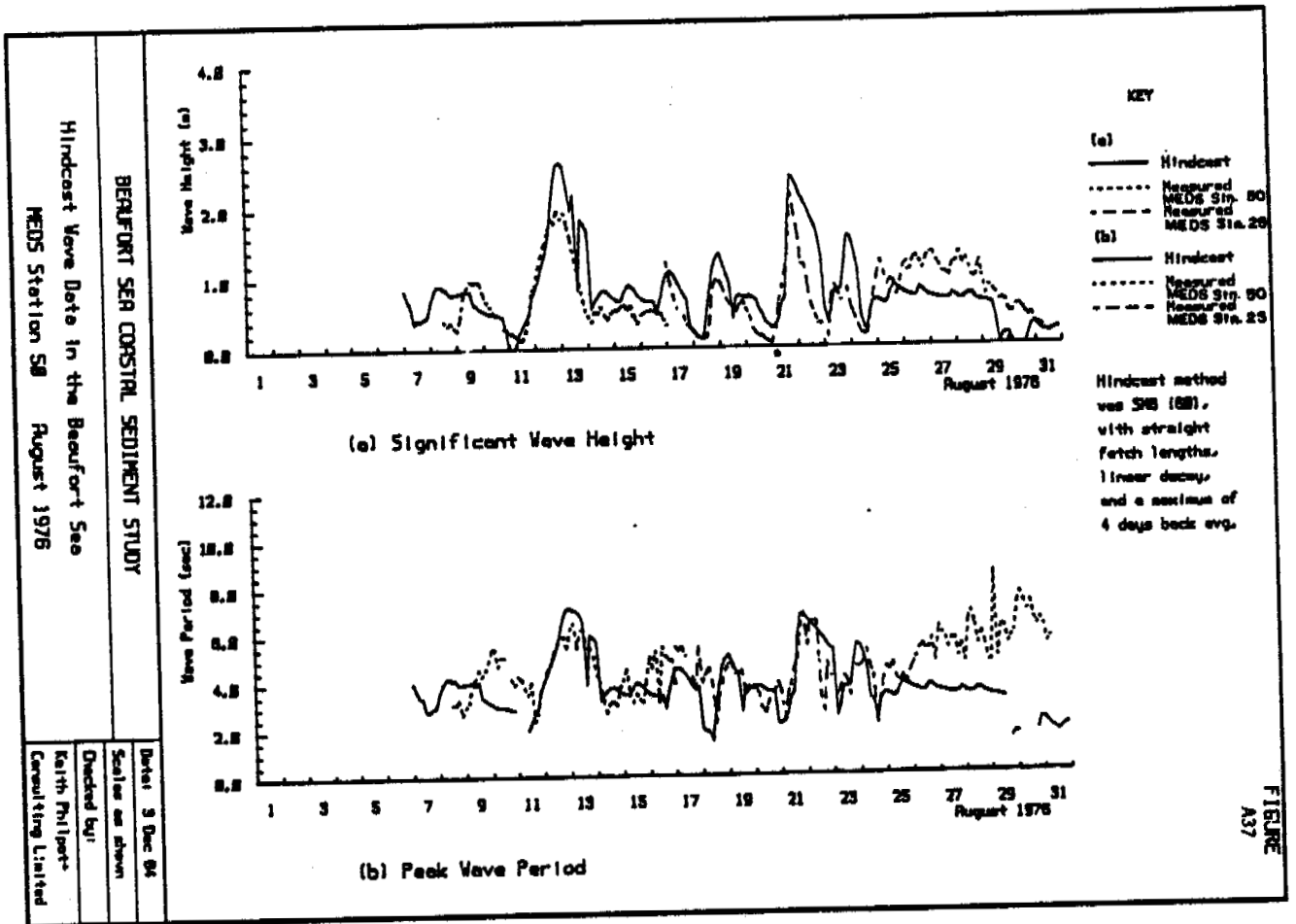


FIGURE A37

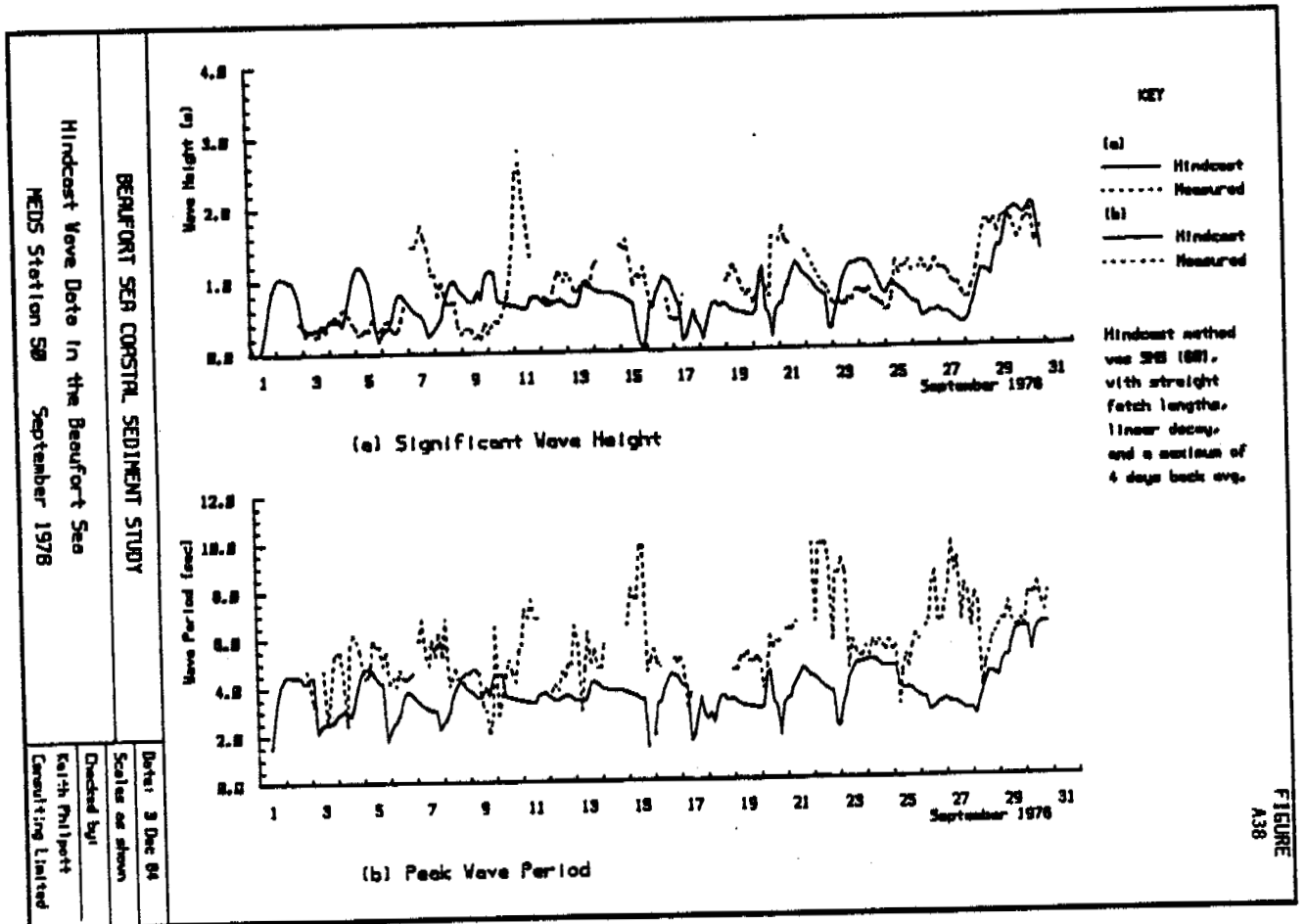
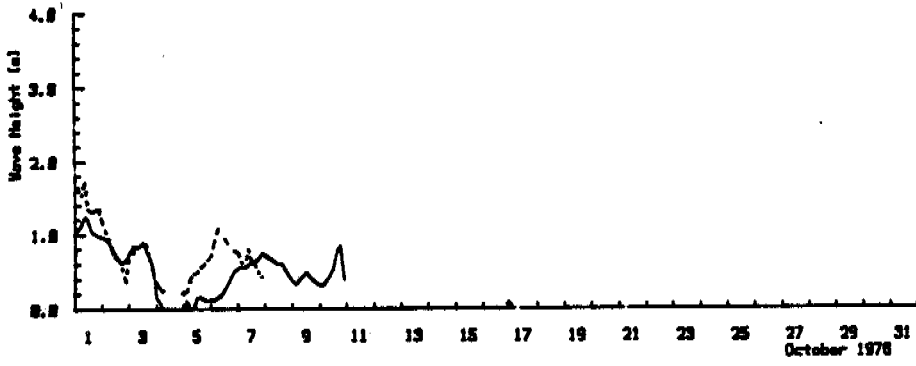
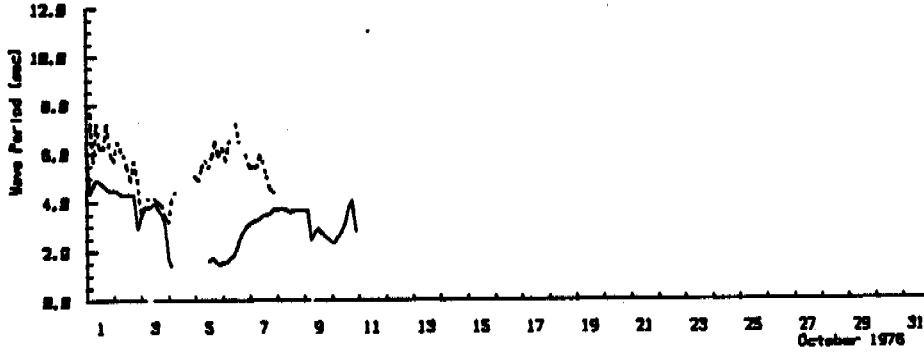


FIGURE A38



(a) Significant Wave Height



(b) Peak Wave Period

KEY
 (a) — Hindcast
 - - - Measured
 (b) — Hindcast
 - - - Measured

Hindcast method was SHB (88), with straight fetch lengths, linear decay, and a maximum of 4 days back avg.

FIGURE
 A39

BEAUFORT SEA COASTAL SEDIMENT STUDY

Hindcast Wave Data in the Beaufort Sea

NEUS Station 58 October, 1978

Date: 3 Dec 84
 Scale as shown
 Checked by:
 Keith Philbett
 Consulting Limited

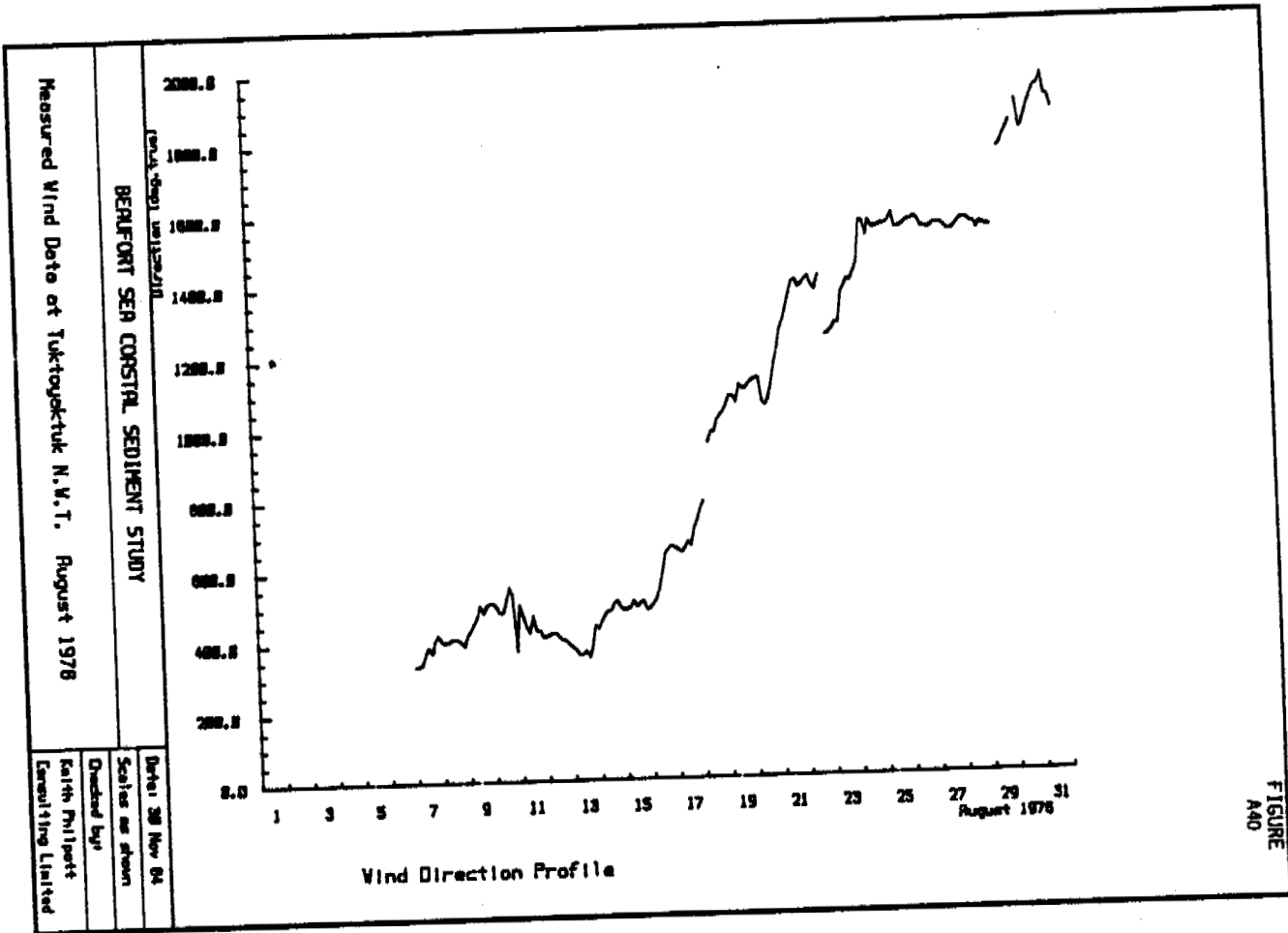


FIGURE A40

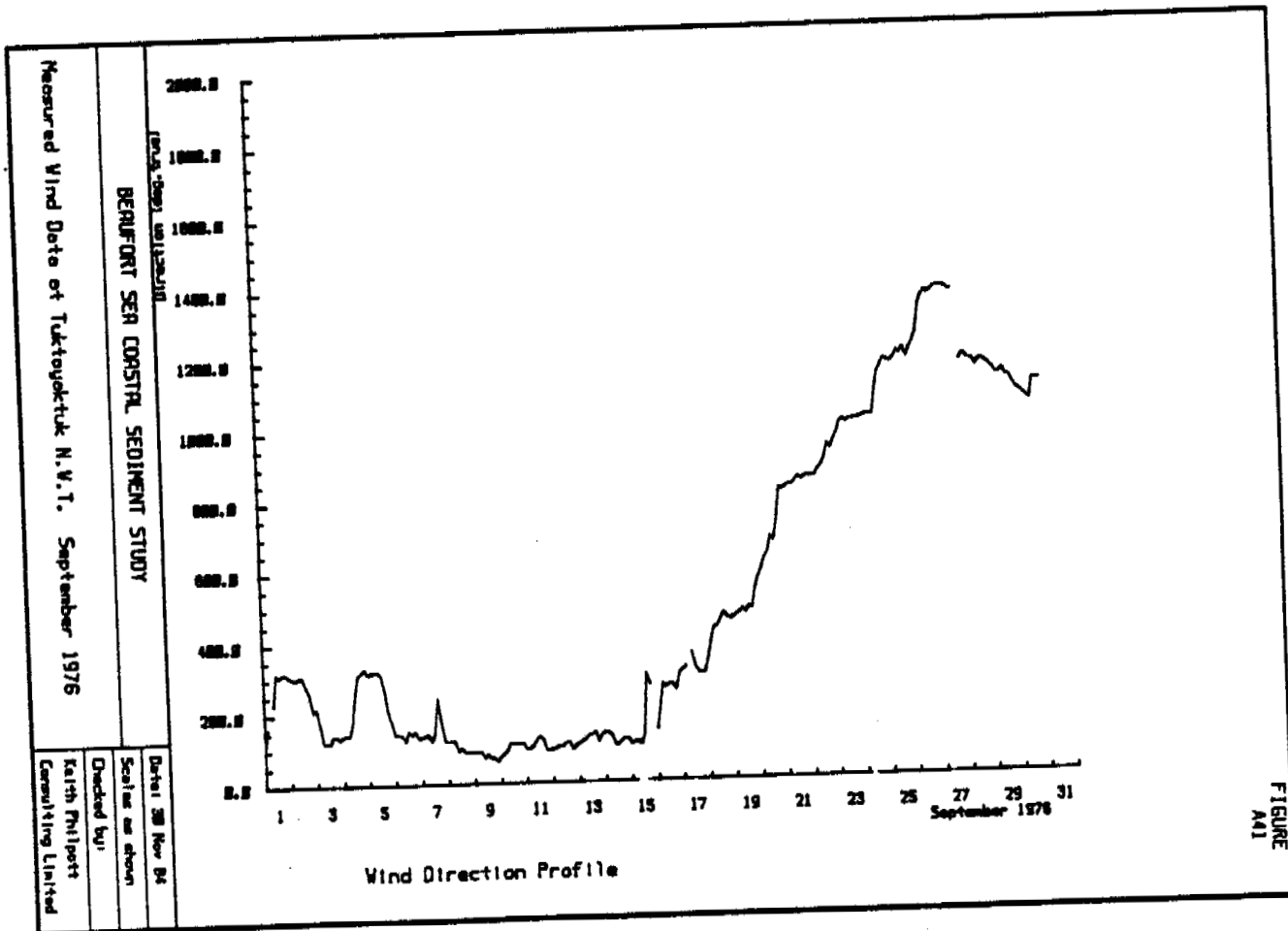


FIGURE A41

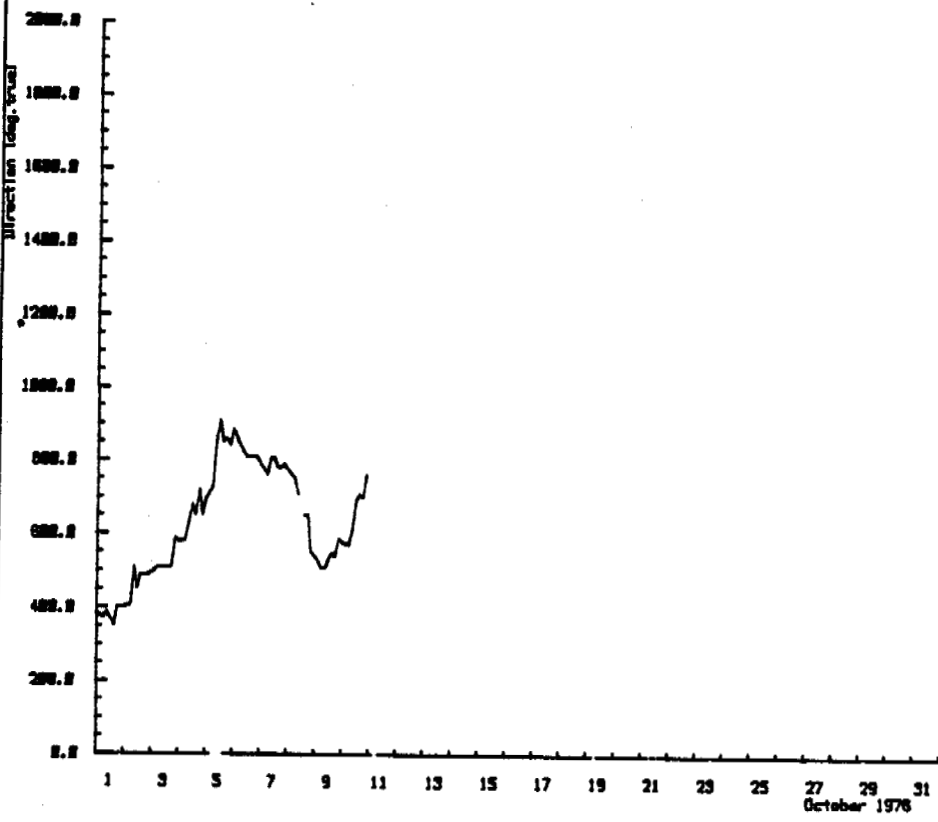


FIGURE
AA2

BENFORT SEA COASTAL SEDIMENT STUDY

Measured Wind Data at Tuktoyaktuk, N.W.T. October 1976

Dated: 30 Nov 84
 Scales as shown
 Checked by:
 Keith Philpott
 Consulting Limited

BEAUFORT SEA COASTAL SEDIMENT STUDY

APPENDIX B

PREDICTIVE EQUATIONS REGARDING COASTAL TRANSPORTS

by

D.H. Swart

Substitution of equation (2.10) above into equation (2.7) yields an expression for f_c :

$$f_c = 1 - \exp(-X_b t) \quad \dots (2.11)$$

where $K_{ei} = \frac{W_e \delta_e}{\delta_{1i}(X_b^{-1} X_i - 1)} \quad \dots (2.12)$

$$K_{ci} = \frac{W_c \delta_c}{\delta_{2i}(X_b^{-1} X_i - 1)} \quad \dots (2.13)$$

$$X_b = \frac{s_e}{\delta_e} = \frac{s_c}{\delta_c} \quad \dots (2.14)$$

$$X_i = \frac{\delta_{1i} s_{yi}}{\delta_{2i}} \quad \dots (2.15)$$

(7) The theory is valid, not only for perpendicular waves, but also for oblique wave attack. In the latter case the transport coefficients s_{yi} and s_{ym} are increased, to allow for the effect of the increase in shear stress at the bed, due to the presence of nearshore currents, generated by the oblique waves. The data used to derive the relationship for the increase in s_{yi} and s_{ym} , as presented in [14] and [13], was derived from model tests in which a strong rip-current formation was found. A subsequent study into the effect of the rip-currents on the increase in offshore transport, showed that the increase in transport, which is due to the presence of longshore currents alone, can best be written in terms of the increase (due to longshore currents) of the sediment mobility F (refer to [17] and [1]).

$$\frac{(s_{yi})_{wc}}{(s_{yi})_w} = \frac{(F_i)_{wc}}{(F_i)_w} \quad \dots (2.16)$$

(see Figure 6)

where F_i is the sediment mobility at location i and the subscripts wc and w refer to *combined wave and current action* and *wave action only* respectively.

In order to comply with step (5) above, the mean value of equation (2.16) over the whole area of profile development will be applied to all transport coefficients.

$$\frac{(s_{yi})_{wc}}{(s_{yi})_w} = \left\{ \frac{(F_i)_{wc}}{(F_i)_w} \right\} \quad \dots (2.17)$$

Keeping in mind the normal uncertainty factor in the evaluation of sediment transport data, it can be stated that the validity of equations (2.16) and (2.17) is proved by the data in Figure 6.

2.3. Representative wave height

The theory described above was derived and verified for regular wave attack. In order to make it generally applicable to prototype conditions, the effect of irregular waves on the theory must be known. The irregular waves will affect not the underlying principles, but the empirical predictive equations which will be described in section 2.4 below.

Observations showed that the higher waves in the wave spectrum will define the profile limits described in section 2.2, step (1) above. The lower limits of the D-profile and transition area respectively are both found by using the significant wave height in the empirical formulae derived for regular wave attack, whereas the upper limit of the D-profile is found from the regular-wave formula by using a wave with a height twice that of the significant wave height

If it is assumed that the transport-formulae are still applicable in the transport zones defined by these representative wave heights, the single representative wave height which will yield the same resultant transport as the spectrum, can be computed (the wave heights are assumed to be Raleigh-distributed).

The formulae for irregular wave attack, derived in this manner, and those for regular wave attack, will be given in section 2.4.

2.4 Predictive equations

The various equations needed for the application of the theory in section 2.2, will be summarized below for the sake of convenience.

2.4.1 Limits of profile development (refer to Figure 1)

The upper limit of the backshore is chosen at the highest level from which sediment can be eroded indirectly by wave action.

h_e is chosen

upper limit D-profile :

$$h_o = 7650 D_{50} \left[1 - \exp \left(-0.000143 \frac{H_{mo}^{0.488} T^{0.93}}{0.786} \right) \right] \quad \dots (2.18)$$

where H_{mo} = maximum wave height in the spectrum = $2(H_o)_{sign}$; T is the wave period and D_{50} is the median particle diameter. For regular wave attack, such as in small-scale hydraulic models, $H_{mo} = H_o$.

Lower limit D-profile

$$h_m = 0.0063 \lambda_o \exp \left(4.347 \frac{(H_o)_{sign}^{0.473}}{T^{0.894} D_{50}^{0.093}} \right) \quad \dots (2.19)$$

where λ_o is the deepwater wave length. For regular wave attack $(H_o)_{sign} = H_o$.

Lower limit transition area

The maximum orbital velocity at the bed at the location where initiation of sediment movement takes place (u_{SEGAR}), is found from the following formula, which represents the weighted mean of a number of different initiation of movement-Formulae. [12], [16].

$$u_{SEGAR} = 4.58 D_{50}^{0.38} T^{0.043} \quad \dots (2.20)$$

The depth at which this velocity occurs is h_c . The corresponding wave length is λ_c . The first order wave representation of the orbital velocity can now be used to obtain a value for h_c/λ_c , whereafter it follows that :

$$h_c = \lambda_o \left(\frac{h_c}{\lambda_c} \right) \tanh \left(2\pi \left(\frac{h_c}{\lambda_c} \right) \right) \quad \dots (2.21)$$

In the case of irregular wave attack the significant wave height should be used for the computation of (h_c/λ_c) . Finally, with the aid of equations (2.18), (2.19) and (2.21), it follows that :

$$\delta_e = h_e - h_o \quad \dots (2.22)$$

$$\delta = h_o - h_m \quad \dots (2.23)$$

$$\delta_c = h_c - h_m \quad \dots (2.24)$$

(see Figure 1).

2.4.2 Equilibrium profile characteristics (refer to [14] and [13])

The computation of the equilibrium length W_i is subdivided into two parts, viz. :

- (1) the computation of a reference value W_r ($=W_i$ at the still-water level), and
- (2) the computation at all other locations in the D-profile of the ratio W_i/W_r .

in (1)

$$m_r = \frac{1.51 \times 10^3 D_{50}^{1.06} H_o^{0.39}}{\lambda_o^{0.71}} + 0.11 \times 10^{-3} \left(\frac{\lambda_o}{H_o} \right) \quad \dots (2.25)$$

$$W_r = \frac{\delta}{2m_r} \quad \dots (2.26)$$

In the case of irregular wave attack, equation (2.25) is rewritten as :

$$m_r = \frac{1.21 \times 10^3 D_{50}^{1.06} (H_o)^{0.39} \text{sign}}{\lambda_o^{0.71}} + 0.22 \times 10^{-3} \frac{\lambda_o}{(H_o)^{\text{sign}}} \quad \dots (2.27)$$

re (2)

For any location i in the D-profile the ratio W_i/W_r is given by :

$$W_i/W_r = 0.7\Delta_r + 1 + 3.97 \times 10^7 b D_{50}^2 \Delta_r^{1.36} \times 10^4 D_{50} \quad \dots (2.28)$$

where
$$\Delta_r = \frac{\delta_{1i} - h_o}{\delta} = \frac{h_m - \delta_{2i}}{\delta} \quad \dots (2.29)$$

and
$$b = \begin{cases} 0 & ; \Delta_r < 0 \\ 1 & ; \Delta_r > 0 \end{cases} \quad \dots (2.30)$$

With the aid of equations (2.25) - (2.30) above the form of the equilibrium D-profile, measured relative to the position in the profile where $\delta_{1i} = 0$ (see Figure 1), can be written as :

$$Y_{i\infty} = W_r [2.1 z^2 - (1.4 + 2Q) z + P (1 - 2z)(h_r - z)^E - EP (z^2 - z) (h_r - z)^{E-1} + (2Q - 0.7)] \quad \dots (2.31)$$

where $h_r = h_m/\delta \quad \dots (2.32)$

$z = \delta_{2i}/\delta \quad \dots (2.33)$

$Q = 0.7 h_r + 1 \quad \dots (2.34)$

$P = 3.97 \times 10^7 b D_{50}^2 \quad \dots (2.35)$

$E = 1.36 \times 10^4 D_{50} \quad \dots (2.36)$

The equilibrium slope $\alpha_{t\infty}$ of the deposited material in the transition area can be found from the equation of Eagleson et al [6] :

$$\alpha_{t\infty} = \frac{\Delta Z_t}{\Delta L_t} \quad \dots (2.37)$$

$$\Delta L_t = 42.73 \frac{J}{K} \lambda_o \left[\ln \left(0.01335 - 0.0161 \frac{d}{\lambda_o} \right) + 0.7271 \left(\frac{d}{\lambda_o} \right)^2 + 1.206 \left(\frac{d}{\lambda_o} \right) - 1.50 \right] \left| \frac{h_m/\lambda_o}{(h_m + \Delta Z_t)/\lambda_o} \right. \quad \dots (2.38)$$

where ΔZ_t is a depth increment and ΔL_t is the horizontal distance in the equilibrium depositional profile between the depths bracketing ΔZ_t .

The values of the schematized recession of the backshore (W_b) and the schematized growth of the transition area (W_t) can be found by drawing up equations for :

- (1) the conservation of mass (re Figure 7a)
- (2) the geometrical form of the equilibrium profile (re (Figure 7b), and
- (3) the distribution of the sediment in the transition area at equilibrium (re Figure 7b). The

reason why three equations are necessary to solve for the two unknowns W_e and W_c , is that δ_{tr} (see Figure 7a) is also an unknown.

2.4.3 Coastal constants (see [17])

At the elevation where $\delta_{1i} = 0.5\delta$, the value of s_{yi} approximates s_{ym} very closely. s_{ym} is given by :

$$s_{ym} = \frac{D_{50}}{T} \exp \left[10.7 - 28.9 \left\{ (H_o)_{50}^{0.78} \lambda_o^{0.9} D_{50}^{-1.29} \left(\frac{(H_o)_{sign}}{h_m} \right)^{2.66} \right\}^{-0.079} \right] \quad \dots (2.39)$$

where $(H_o)_{50}$ is the median deepwater wave height and $(H_o)_{sign}$ is the significant deepwater wave height. In the case of regular wave attack, both $(H_o)_{50}$ and $(H_o)_{sign}$ are replaced by H_o . With the aid of section 2.2, step (5), it follows that :

$$x_b = \left(\frac{s_e}{\delta_e} \right) = \left(\frac{s_c}{\delta_c} \right) = \left\{ \frac{(y_2 - y_1)_{io}}{W_{bi} + (y_2 - y_1)_{io}} \right\} x_i \quad \dots (2.40)$$

with as a result

$$\frac{s_{yi}}{s_{ym}} = \frac{4\delta_{1i} \delta_{2i}}{\delta^2} \left[\frac{(y_2 - y_1)_{mo}}{W_{bm} + (y_2 - y_1)_{mo}} \right] \left[\frac{W_{bi} + (y_2 - y_1)_{io}}{(y_2 - y_1)_{io}} \right] \quad \dots (2.41)$$

where

$$W_{bi} = \left(\frac{\delta_a}{\delta_{1i}} \right) W_e + \left(\frac{\delta_c}{\delta_{2i}} \right) W_c \quad \dots (2.42)$$

$$(y_2 - y_1)_{io} = W_i - (L_2 - L_1)_{io} \quad \dots (2.43)$$

Subscript m refers to middepth ($\delta_{1i} = 0.5\delta$) and subscript o refers to time $t = 0$.

The characteristic quantities K_{ei} and K_{ci} can now be found from equations (2.12) and (2.13) respectively.

2.4.4 Mobility number

(for a more detailed description of the mobility number and the following equations, reference should be made to [15] and [17]).

$$(F_i)_{vc} = \left\{ \frac{v I_{vc}^n}{C_D^{1-n} C_h^n (\Delta_s D_{35})^{\frac{1}{2}}} \right\}_i \quad \dots (2.44)$$

$$(F_i)_w = \left\{ \frac{2^{-n} f_w^{n/2} u_o}{C_D^{1-n} C_h^n (\Delta_s D_{35})^{\frac{1}{2}}} \right\}_i \quad \dots (2.45)$$

where

$$I_{vc} = \left\{ 1 + \frac{1}{2} \left(\frac{\xi_J u_o}{v} \right)^2 \right\}_i^{\frac{1}{2}} \quad \dots (2.46)$$

$$\xi_{Ji} = \left\{ C_h \left(\frac{f_w}{2g} \right)^{\frac{1}{2}} \right\}_i \quad \dots (2.47)$$

$$C_{hi} = \left\{ 18 \log \left(\frac{12d}{r} \right) \right\}_i \quad \dots (2.48)$$

$$C_{Di} = \left\{ 18 \log \left(\frac{10d}{D_{35}} \right) \right\}_i \quad \dots (2.49)$$

$$f_{wi} = \left\{ \exp \left(-5.977 + 5.213 \left(\frac{s_o}{r} \right)^{-0.194} \right) \right\}_i \quad \dots (2.50)$$

(if $f_{wi} > 0.3$; $f_{wi} = 0.3$)

$$r = \text{hydraulic bed roughness} \quad \dots (2.51)$$

$$= 25 \Delta_r \left(\frac{\Delta_r}{\lambda_r} \right) \quad \dots (2.51)$$

(See Figure 8)

s_o is the orbital excursion at the bed, Δ_r is the ripple height and λ_r is the ripple length.

$$n = 1 - 0.2432 \ln(D_{gr}) \quad (\text{with } 0 < n < 1) \quad \dots (2.52)$$

$$D_{gr} = \left(\frac{g \Delta_s}{v^2} \right)^{1/3} D_{35} \quad \dots (2.53)$$

D_{35} = particle diameter which is exceeded in size by 65% (in weight) of the total sample.

In the case of irregular wave attack the median wave height $(H_o)_{50}$ should be used in the equations (2.44) - (2.50).

2.5 Computational Method

The computation of *time-dependent profile changes* (Y_{it}) and *onshore-offshore sediment transport rates* S_{yit} , as well as of *integrated onshore-offshore transport rates* $(\int_0^t S_{yit} dt)$ up to any time t , can all be performed by using the following simple procedure :

- 1) compute the *equilibrium condition*,
- 2) compute the value of the *fraction f_t* as a function of time with the aid of section 2.4,
- 3) combine 1) and 2) to *predict time-dependent conditions*.

In the case of *profile-prediction*, the *location of the equilibrium profile* can be predicted, because the *initial profile* is given and the *equilibrium profile form* as well as the values W_o and W_t can be computed from section 2.4. The position Y_{it} of the profile at elevation Z_i and time t is then given by:

$$Y_{it} = Y_{i\infty} + f_t (Y_{i0} - Y_{i\infty}) \quad \dots (2.54)$$

(see Figure 9)

In the case of *transported-volume prediction* the total volume of transported material up to time $t = \infty$ ($V_{yi\infty}$) can be computed from equation (2.10) by putting $t = \infty$, whereafter V_{yit} , the total volume of sediment transported past the location in the profile with elevation Z_i , can be computed from :

$$V_{yit} = f_t V_{yi\infty} \quad \dots (2.55)$$

The *onshore-offshore sediment transport rate* at location i can also be found in terms of $V_{yi\infty}$ and f_t :

$$S_{yit} = V_{yi\infty} X_b (1 - f_t) \quad \dots (2.56)$$

3. LONGSHORE SEDIMENT TRANSPORT

3.1 General

Longshore sediment-transport computations can be used, either to gain an insight into the *overall sediment budget* of an area, or to study *detail problems* (such as deposition of sediment in an entrance channel to a harbour). The *total sediment load at various locations* will be needed in the first case, whereas the *vertical distribution of sediment load* (and specifically the division between bed and total load) will also be needed in the second case.

The available formulae for the prediction of longshore sediment transport rates can be classified into two groups, viz. :

- (1) *overall predictors*, such as the *SPM-formula* and the *Galvin-formula*, and
- (2) *detail predictors*, such as the *Bijker-formula* and the analogous *SWANBY-method*.

When a prediction of longshore sediment transport rates has to be made, it is useful to perform the computations with two or more of the available formulae, and to *base the final prediction on the outcome of all the results* obtained. In this chapter a detail-predictor method (SWANBY) will be described in detail, as well as a *modified version* of the SPM-predictor, which is used to back up the detail-predictor results.

3.2 Overall predictors

Although the overall predictors are by definition only applicable in areas with negligible longshore gradients, and cannot be used to obtain reliable estimates of the longshore transport rates in areas with strong longshore tidal flow, they can be useful in assessing the overall longshore sediment budget in an area. As such they can be used in conjunction with the detail predictors.

The SPM-formula, which relates the overall longshore transport rate S_{xtot} to a quantity resembling the longshore component of the wave-energy flux, is the best-known overall predictor available. This SPM-relationship can be rewritten to read :

$$S_{xtot} = K_o (T (H_o)_{rms}^2 K_r^2 \sin \theta_b \cos \theta_b) \quad \dots (3.1)$$

(see [19])

where K_r is the refraction coefficient, θ_b is the angle between the wave crest and the shoreline at wave breaking, and K_o is a coefficient which is assumed to be constant.

However, as lighter material will be transported more readily than heavier materials under the same wave conditions, it is to be expected that K_o will be a function of the grain size of the bed material. A re-evaluation of the data given in [19] and [3] yielded Figure 10, from which a clear tendency can be seen for K_o to vary with grain size. Although a steeper curve is to be expected intuitively, the data suggests K_o to vary as :

$$K_o = 365 \times 10^4 \log \left(\frac{0.00146}{D_{50}} \right) \text{ for } 0.1 \times 10^{-3} < D_{50} < 1.0 \times 10^{-3} \quad \dots (3.2)$$

Equations (3.1) and (3.2) are normally used to back up computations performed with the detail predictor, which will be described in section 3.3.

3.3 Detail predictors

3.3.1 Underlying principles

In 1966 Bijker [2] published a method for the computation of the longshore sediment transport at any specific location in the coastal environment, which constituted a major breakthrough in Coastal Engineering. Bijker assumed that it will be possible to use, in the coastal environment, a sediment transport formula which had been developed for uniform flow conditions, provided that the shear stress terms in the chosen formula are adapted to incorporate the effect of the wave action. He chose as basis for this adaptation the formula of Frijlink, which was at the time a much-used formula in river-flow problems in the Netherlands. Although the resulting Bijker-Frijlink equation sometimes yielded unrealistic results, it has been used since then with a reasonable amount of success in numerous applications in the coastal environment. However, the insight into the fundamentals of sediment transportation under wave action has increased over the past decade. Furthermore, various evaluations of the available predictor methods revealed recently ([5], [7], [18], [20]) that there are more reliable methods for the computation of sediment transport under uniform flow conditions than the Frijlink-equation, which can also be used over a wider range of boundary conditions. Therefore, a new pre-

dictor method was developed by Swart [15] under the auspices of the Coastal Sediment Group of the Dutch Applied Coastal-Research Programme, for application in the coastal environment. The basic differences between the new technique (called the SWANBY-method) and the old Bijker-Frijlink approach will be discussed below.

(1) The Frijlink-formula, used in the original approach, is a bed load formula. The total load was computed from the bed load by adding the suspended load, as computed with the aid of the Rouse/Einstein description of the vertical distribution of suspended sediment. The thickness of the bed layer is in such an approach an important parameter in the determination of the total load. Due to the uncertainty in the definition of the layer in which the bed load takes place, it will be more convenient to choose a total load formula as basis for computations in the coastal environment. If necessary, a definition can then be made of a bed layer thickness, and the amount of sediment transported in that layer can be computed.

(2) Various comparative investigations [5], [7], [18], [20], showed that the two most reliable total load formulae available for uniform flow conditions, are those of Engelund-Hansen and Ackers-White. Both these formulae give comparable results over a wide range of boundary conditions, the only exception being cases where the sediment transport rate was low (near initiation of motion). In such cases the Engelund-Hansen method over-predicted the transport rates, where Ackers-White showed a good comparison. Engelund-Hansen will thus not yield proper scale relationships, that can be used for the scaling of three-dimensional small-scale models. For the above-mentioned reasons the Ackers-White approach was chosen as the basic theory, which was to be adapted for use in the coastal environment.

(3) When evaluating the shear stress at the bed due to combined wave and current action, Bijker assumed the orbital velocity u_z , at the edge of the viscous sublayer to be :

$$u_z = p_B u_o \sin \left(\frac{2\pi z}{T} \right) \quad \dots (3.3)$$

where $p_B = \text{constant} = 0.45$ (see [2])

It is, however, to be expected that the effect of the wave motion on the shear stress will vary with a variation in the flow regime at the bed. Jonsson [9] defined the flow regime at the bed in terms of the ratio a_o/r where r is the hydraulic bed roughness and a_o the maximum wave particle excursion at the bed. Using Jonsson's work, it can be shown that

$$u_z = p_J u_o \sin \left(\frac{2\pi z}{T} \right) \quad \dots (3.4)$$

where $p_J = \left(\frac{f_w}{2g} \right)^{1/2} C_h^2 \quad \dots (3.5)$

C_h is the Chezy-roughness value and f_w is the wave friction factor. In the SWANBY-approach equation (3.4) was used instead of equation (3.3).

(4) In the Bijker-Frijlink approach the hydraulic bed roughness was taken equal to one-half the ripple height. A subsequent study [15] has shown the relative roughness (r/Δ_r) to vary with the ripple steepness Δ_r/λ_r (see Figure 8). This was used in the SWANBY-theory. It was shown in [15] that the thickness of the layer near the bed in which vortices (filled with sediment) are formed and diffused, is of the same order of magnitude as the hydraulic bed roughness r . The thickness of the layer in which bed load takes place was thereafter also assumed to be equal to the hydraulic bed roughness r .

(5) A comparative study of the various methods for the computation of the vertical distribution of suspended sediment (\bar{c}_z/\bar{c}_r) in the coastal environment [15] showed that there is little difference

between the prediction of \bar{c}_z/\bar{c}_r by various theories. The *best correlation* with data covering a wide range of boundary conditions in the coastal environment was, however, obtained with a theory in which the *diffusion coefficient* for solids c was assumed to *vary linearly* over the depth. The corresponding variation in \bar{c}_z/\bar{c}_r is :

$$\frac{\bar{c}_z}{\bar{c}_r} = \left(\frac{z}{r}\right)^{-b_1} \quad \dots (3.6)$$

where b_1 is a constant for each specific suspended sediment distribution over the depth.

With the assumption of a logarithmic variation in velocity over the depth, equation (3.6) yields an expression for the amount of suspended sediment which is transported, which is *easier to apply than any of the other* approaches tested. Due to these reasons it was decided to use equation (3.6) in the SWANBY-method instead of the Rouse/Einstein approach.

In Figure 11 longshore sediment transport rates, measured in a small-scale model, are compared with predicted transport rates, as given by the Bijker-Frijlink and SWANBY (Adapted Ackers-White) formulae. It is obvious that the SWANBY-method shows the better comparison with the data.

3.3.2 Predictive equations

The equations needed for the application of the SWANBY-method for the computation of the longshore sediment transport, will be given below.

total load

The total longshore sediment transport S_{xt} (bed plus suspended load) at any specific location is given by :

$$S_{xt} = \left(\frac{1}{1-p}\right) D_{35} v \left(\frac{C_h}{s}\right)^n I_{wc}^{-n} \frac{C}{A^m} (F_{wc} - A)^m \quad \dots (3.7)$$

where $\left(\frac{1}{1-p}\right)$ = determined by the porosity of the bed, normally taken = 1.45 and v = uniform current velocity in the longshore direction. The values of C_h , I_{wc} , F_{wc} and n are defined in section 2.4.4 (equation (2.44), (2.46) - (2.53)). Furthermore

$$m = \frac{9.66}{D_{gr}} + 1.34 \quad \dots (3.8)$$

$$A = \frac{0.23}{D_{gr}} = 0.14 \quad \dots (3.9)$$

$$C = \exp \{ 2.86 \ln(D_{gr}) - 0.4343 (\ln(D_{gr}))^2 - 8.128 \} \quad \dots (3.10)$$

The hydraulic bed roughness r is related to the ripple dimensions as given in equation (2.51). The ripple dimensions can either be known from observations or be computed from one of the available methods (for instance [11] and [15]).

bed load

The bed load can be computed from equation (3.7) and points (4) and (5) in section 3.3.1 above, viz. :

$$S_{xb} = \left(\frac{K_b}{K_b + K_s}\right) S_{xt} \quad \dots (3.11)$$

where $K_b = \ln\left(\frac{er}{\Delta_s}\right)$ for $b_1 = 1$

and $K_b = \left(\frac{1}{1-b_1}\right) \left(1 - b_1 \left(\frac{\Delta_s}{r}\right)^{1-b_1}\right)$ for $b_1 \neq 1$... (3.12)

$$K_s = 0.205 \ln \left(\frac{912d}{r} \right) \ln \left(\frac{d}{r} \right) \quad \text{for } b_1 = 1$$

and

$$K_s = 0.41 (1-b_1)^{-2} \left[(1-b_1) \left\{ \left(\frac{d}{r} \right)^{1-b_1} \ln \left(\frac{30.2d}{r} \right) - 3.4 \right\} + \left\{ 1 - \left(\frac{d}{r} \right)^{1-b_1} \right\} \right] \quad \text{for } b_1 \neq 1 \quad \dots (3.13)$$

b_1 was found empirically to be [15] :

$$b_1 = 1.05 \left(\frac{v}{\kappa v_{*c}} \right)^{0.96} \left(\frac{r}{d} \right)^{0.013} \left(\frac{v}{\kappa v_{*c}} \right) \quad \dots (3.14)$$

3.4 Representative wave height

The *single representative wave*, which will yield the same resultant longshore sediment transport as the *complete wave spectrum* in the case of irregular wave attack, will again be a function of the boundary conditions. By assuming (1) a Rayleigh-distributed wave height spectrum, and (2) the superposition of the transports generated by the individual waves in the spectrum, a *representative wave height* H_r was computed for the SWANBY-detail predictor in the same manner as in Chapter 2.

A design curve is presented in Figure 12, whereby it becomes possible to determine the *representative wave height* H_r in terms of the rms - wave conditions. The representative height varies between the median wave height (H_{50}) and the significant wave height (H_{sign}), with a tendency towards H_{sign} at the lower transport rates. Seeing that the lower waves in the spectrum will not transport sediment as readily in cases near the initiation of motion, this tendency is to be expected.

The single representative wave height for the SPM-overall predictor is by definition the rms wave height.

4. APPLICATION

4.1 General

Normally the losses from an area which had been replenished by a beachfill, can be estimated by using methods which are based on the *grain size distribution* of the borrow and native material only. The three most-used formulae in this category are those of *Krumbein-James* [10], which is suggested for use in the Shore Protection Manual [19], *Dean* [4] and *James* [8].

The Krumbein-James and Dean methods predict an *overflow ratio*, i.e. the ratio between the *volume of sediment* that has to be placed in order to retain the design volume and the *required design volume* of sediment in the fill. The Krumbein-James method assumes some portion of the borrow material (which has the same grain size distribution as the native material) to be absolutely stable and to stay on the beach indefinitely, whereas the rest of the borrow material will be lost. The Dean-method, on the other hand, assumes that the borrow material which is coarser than the native material will *not be lost*.

James assumes that no material is absolutely stable, and that fine material is less stable than coarse material. He then computes a *relative retreat rate*, which is basically the ratio between the *loss rate* of the borrow material in the fill and that of the native material in the original beach profile.

In order to allow the comparison of the losses, as predicted by the techniques described in this paper, and those given by the above-mentioned three beachfill methods [10], [4], [8], the following two definitions were made :

$$\text{Overfill Ratio (SEGAR)} = \frac{(\Delta S_y)_{\text{borrow}} + (\Delta S_x)_{\text{borrow}}}{V_{\text{fill}}} \quad \dots (4.1)$$

and

$$\text{Relative Retreat Rate (SEGAR)} = \frac{(\Delta S_y)_{\text{borrow}} + (\Delta S_x)_{\text{borrow}}}{(\Delta S_y)_{\text{native}} + (\Delta S_x)_{\text{native}}} \quad \dots (4.2)$$

where (ΔS_y) and (ΔS_x) are the losses in the offshore and longshore directions respectively, and V_{fill} is the volume of sediment placed in the beachfill. When computing (ΔS_y) it should be kept in mind that the dimensions of the transport rates S_y in chapter 2 are $\text{m}^3/\text{m}/\text{s}$, while those in chapter 3 (S_x) are m^3/s . In equations (4.1) and (4.2) sediment is considered lost when it moves out of the area in which it was placed, i.e. that volume of sediment which has to be replaced in, for instance, an *annually recurring replenishment*. Due to the fact that the sediment moved in the offshore direction will eventually build a new equilibrium condition, which will conform to the borrow material and the wave climate, the annual losses, i.e. the required recurring replenishment, as characterized by equations (4.1) and (4.2), will gradually diminish with time. The present calculations only show the losses during the first replenishment period. The longshore losses were computed by both the SWANBY-detail predictor method and the SPM-overall predictor, whereafter a representative loss was computed from these two figures.

Due to the fact that both the *overfill ratio (SEGAR)* and the *relative retreat rate (SEGAR)* are time-dependent, a time-duration of 10 days was chosen as basis for the comparison, during which time one wave condition took place. When doing an actual beachfill design, the wave conditions in an average year should be applied *consecutively* to the gradually developing profile.

4.2 Beachfill characteristics

A typical beach profile for Natal (situated on the South African east coast) was taken as the initial profile for the computations. The geometry of the initial profile and the two beachfills, as well as the grain size characteristics, are given in Figure 13. As can be seen, six different cases result, viz. $\alpha_{\text{borrow}} = 1/10$ and $1/5$, each with $D_{50} = 200 \times 10^{-6}$, 500×10^{-6} and 1000×10^{-6} m. It was assumed that the beachfill has a longshore length $l_x = 1000$ m, and is situated in an area with no updrift supply of sediment. No gradients initiated by the placing of the fill itself, will be considered, i.e. edge effects at the longshore extremities of the fill will be neglected.

The wave condition in the area was taken to be :

$$(H_o)_{\text{sign}} = 2 \text{ m} ; T = 10 \text{ s} ; \theta_b = 5^\circ .$$

4.3 Discussion of results

The computed losses, as given by the various methods, are represented graphically in Figure 14. The following general observations regarding the results are relevant :

(1) The beachfill methods of Krumbein-James, Dean and James are all independent of the profile geometry, whereas the Krumbein-James and Dean methods are also independent of the wave climate. In the James-method the wave climate can perhaps be included via the choice of the measure of selectivity of the sorting process Δ (as defined by James [8]). Both the wave climate and the profile geometry do, however, influence the losses. Consequently, the above-mentioned three methods can only be used to obtain comparative results for various possible borrow materials.

(2) If all the consecutive wave conditions in an average year are taken into account, the resultant

losses will be lower than those given by the higher waves only, due to the fact that the lower waves will initiate an *onshore* sediment movement.

(3) Both the relative retreat rate (as given by James) and the overfill ratio (as given by Krumbein-James and Dean) are equal to unity in the case of a borrow material which is *identical* to the native material. The method presented in this paper (called the SEGAR-method) yields higher values of both the relative retreat rate and the overfill ratio (of approximately 2) in the case where the native and borrow materials are identical. This higher loss rate seems logical, seeing that the initial profile with fill is steeper than the initial profile alone (see Figure 13). Offshore losses will thus increase (re chapter 2).

(4) The relative retreat rates predicted by the James-method are appreciably smaller than those predicted by the SEGAR-method, for all values of D_{50} except $D_{50} = 200 \times 10^{-6}$ m. A study of the original paper by James reveals that if $\Delta = 1.0$ as suggested in [8], the relative retreat rate is actually < 1 for 330×10^{-6} m $< (D_{50})_{\text{borrow}} < 1000 \times 10^{-6}$ m, which is unfeasible from a physical viewpoint. For $(D_{50})_{\text{borrow}} < 200 \times 10^{-6}$ m, on the other hand, the relative retreat rate R_b increases drastically to completely unrealistic values (for instance, for $D_{50} = 100 \times 10^{-6}$ m; $M_{\phi_b} = 3.23$, $\sigma_{\phi_b} = 1.08$:- $R_b = 6.8 \times 10^3$ if $\Delta = .6$ and $R_b = 9.2 \times 10^4$ if $\Delta = 1.0$). As was already pointed out by James [8], the relative retreat rate is very dependent on the value of Δ . As Δ is mostly unknown, this represents a serious restriction in the applicability of the theory.

(5) The overfill ratios predicted by Dean and especially by Krumbein-James for values of $D_{50} < 500 \times 10^{-6}$ m (in the present illustration), are exceedingly high. The Dean-method seems to have the soundest physical background of the two methods.

(6) The SEGAR-method described in the present paper can, if necessary, be used to obtain the relative losses in the offshore and longshore directions respectively, as the transports in both these directions are already computed. This is not possible for the Krumbein-James [10], Dean [4] and James [8] methods.

4.4 Concluding remarks

Although the SEGAR-method, which takes into account the local wave climate and the geometry of the beachfill, is more complicated to apply than the other three beachfill methods [10], [4] and [8], it yields results which seem to be more comparable with the known prototype behaviour of a beachfill area, than the results given by [10], [4] and [8]. It is accordingly suggested that the SEGAR-method is used for beachfill design. *Back-up computations, yielding comparative results only*, of both the relative retreat rate and the overfill ratio, can be made by using the James-method (provided that an appropriate choice of Δ can be made) and the Dean-method respectively. The Krumbein-James method generally over-predicts the overfill ratio, and is not recommended for use.

5. SUMMARY

Predictor techniques have been presented, whereby it is possible to compute *onshore-offshore* and *longshore sediment transports* respectively. These respective techniques can be used in combination to compute sediment losses in numerous applications. One such application, viz. to a beachfill problem, was described in detail. The results were shown to be realistic.

A comparison of computed results with actual field measurements at a beachfill location will be the logical next step in the testing of the techniques.

LIST OF REFERENCES

1. ACKERS, P. and WHITE, W.R. Sediment transport : New approach and analysis; Proc. ASCE Journal of the Hydraulics Division, HY 11, November 1973.
2. BIJKER, E.W. Some considerations about scales for coastal models with movable bed; Delft Hydraulics Laboratory, Publication No. 50 142 pp, November 1967.
3. DAS, M.M. Suspended sediment and longshore sediment transport data review; Proc. 13th Coastal Engineering Conference, Vancouver, Volume II, 1972.
4. DEAN, R.G. Compatibility of borrow material for beach fills, Proc. 14th Coastal Engineering Conference, Copenhagen, Volume II, 1974.
5. DE HAAN, Evaluatie zandtransporten bij eenparige stroming ("Evaluation of sediment transport for uniform flow"); Delft University of Technology, graduation thesis, to be published in 1976.
6. EAGLESON, P.S., GLENNE, B. and DRACUP, J.A. Equilibrium characteristics of sand beaches; Proceedings, ASCE, Journal of the Hydraulics Div., 89, Paper No. 3387, pp 35-57, January 1963.
7. COLE, C.V., TARAPORE, Z.S. and DIXIT, J.G. Applicability of sediment transport formulae to natural streams; Proc. 15th Congress IAHR Istanbul, September 1973.
8. JAMES, W.R. Beach fill stability and borrow material texture; Proc. 14th Coastal Engineering Conference, Copenhagen, Volume II, 1974.
9. JONSSON, I.C. Wave boundary layers and friction factors; Proc. 10th Conference on Coastal Engineering, Tokyo, Volume I, Chapter 10, pp 127-148, 1966.
10. KRUMBEIN, W.C. and JAMES, W.R. A lognormal size distribution model for estimating stability of beach fill material; T.M.-16, U S Army, Corps of Engineers, Coastal Engineering Research Center, Washington, D.C., November 1965.
11. MOGRIDGE, C.R. and KAMPHUIS, J.W. Experiments on bed form generation by wave action; Proc. 13th Coastal Engineering Conference, Vancouver, Vol. 2, pp 1123-1142, 1972.
12. SILVESTER, R. Coastal Engineering, 2; Developments in Geotechnical Engineering, Vol. 4B; Elsevier Scientific Publishing Company, Amsterdam, 1974.
13. SWART, D.H. A schematization of onshore-offshore transport; Proc. 14th Coastal Engineering Conference, Copenhagen, June 1974.
14. SWART, D.H. Offshore transport and equilibrium beach profiles; Delft Hydraulics Laboratory, Publication No. 131, December 1974.
15. SWART, D.H. and DELFT HYDRAULICS LABORATORY. Coastal sediment transport : computation of longshore transport; Delft Hydraulics Laboratory Report R968, November 1975.
16. SWART, D.H. Weighted value of depth of initiation of movement; Unpublished note, June 1976.
17. SWART, D.H. Sediment transportation in the coastal environment; Lecture notes for post-graduate ECOR-course in Coastal Engineering, Port Elizabeth, South Africa, June 1976.
18. TASK COMMITTEE FOR PREPARATION OF SEDIMENT MANUAL. Sediment transportation mechanics : H. Sediment discharge formulae; Proc. ASCE, Journal of the Hydraulics Division, Vol 97, HY 4, April 1971.
19. U.S. ARMY COASTAL ENGINEERING RESEARCH CENTER. Shore Protection Manual, Vol. 1 - 3; U.S. Government Printing Office, 1973.
20. WHITE, W.R., MILLI, H. and CRABBE, A.D. Sediment transport : an appraisal of available methods, Volumes 1 and 2; Hydraulics Research Station, Wallingford, Report INT 119, November 1973.

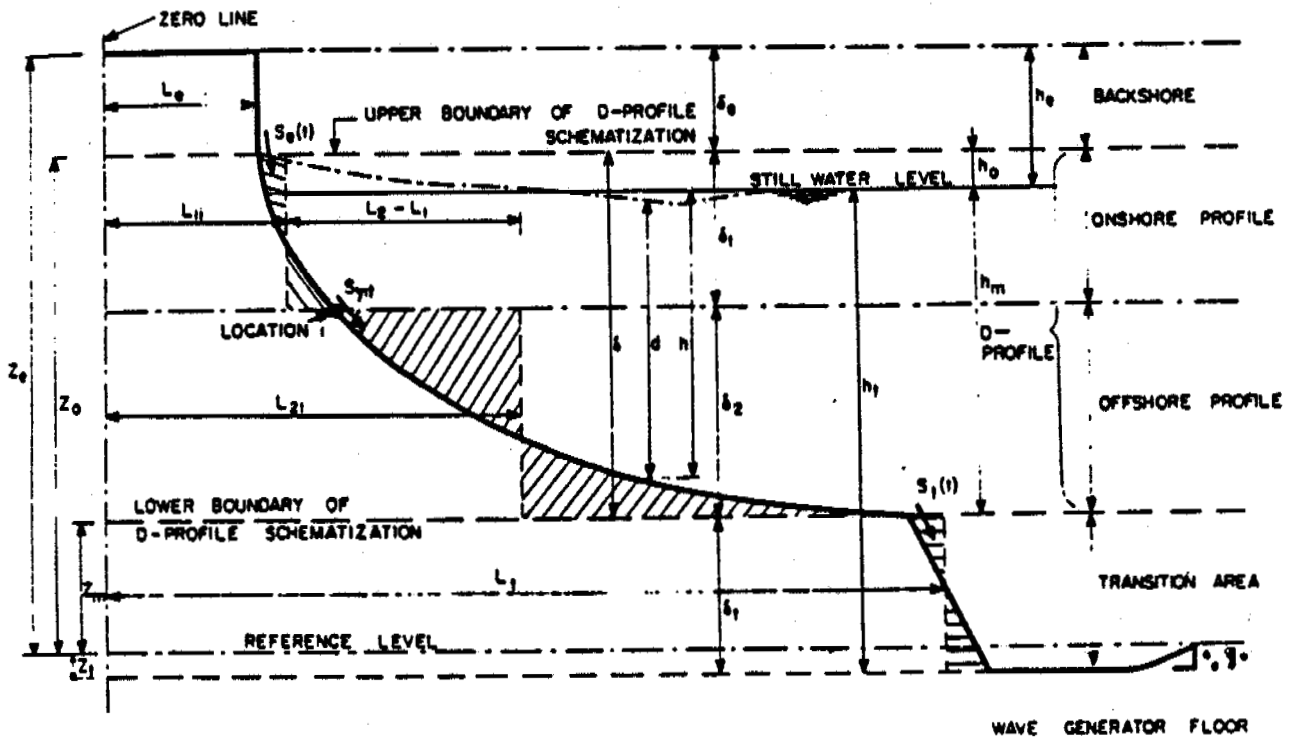
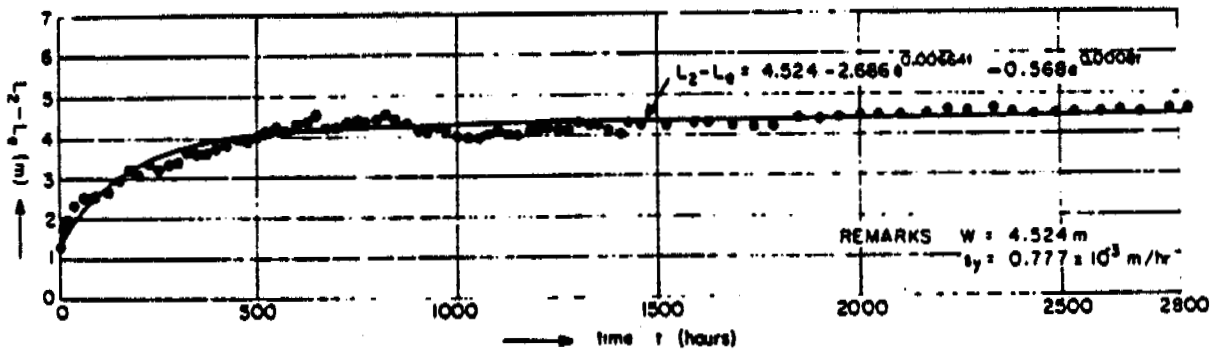


Figure 1 : Schematization of beach profile at time t



$$\delta_1 = \delta_0 = 0.22 \text{ m}; \delta_2 = \delta = 0.25 \text{ m}$$

Figure 2 : Schematized time-variation of sediment in D-profile

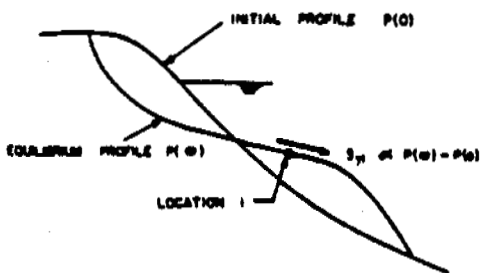


Figure 3 : Relationship between transport S_{yi} and profile form

REMARKS

$D_{50} = 220 \times 10^{-6} \text{ m}$

$H_0 = 0.07 \text{ m}$

$T = 1.04 \text{ s}$

\bar{x} : AVERAGE f_1 -VALUE OF f_1 AT 10 EQUALLY-SPACED LOCATIONS IN PROFILE

MEASURED FRACTION f_1 OF TOTAL TRANSPORT

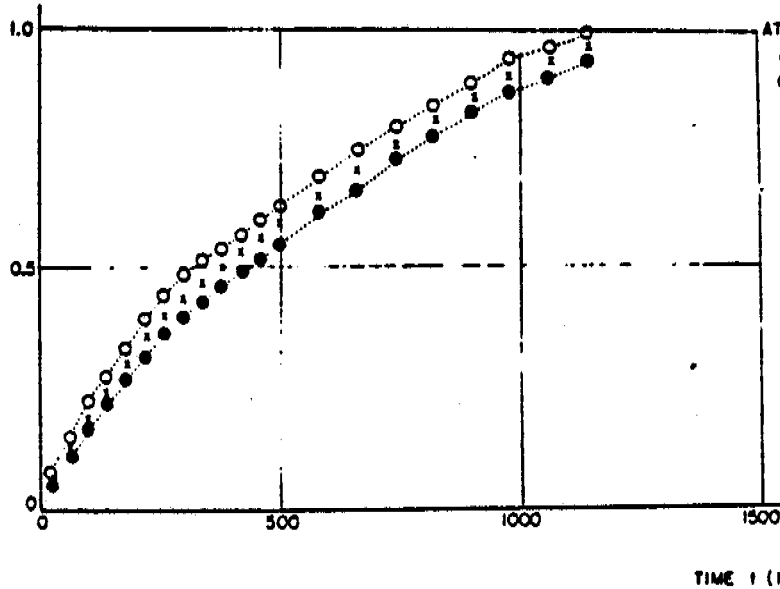


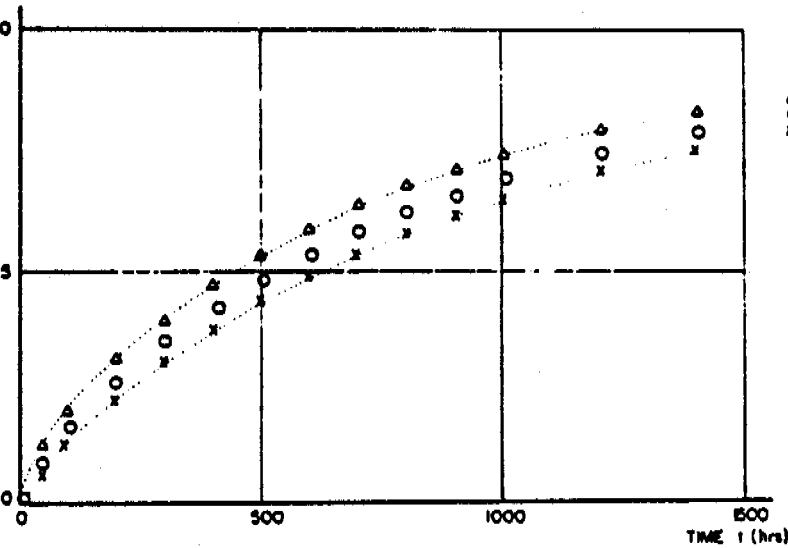
Figure 4 : Time- and depth-variation of measured fractions f_1

$D_{50} = 160 \times 10^{-6} \text{ m}$

$H_0 = 0.07 \text{ m}$

$T = 1.04 \text{ s}$

SMOOTHED FRACTION f_1 OF TOTAL TRANSPORT



- AVERAGE OF THE f_1 VALUES AT 10 EQUALLY-SPACED LOCATIONS IN PROFILE (DERIVED FROM SMOOTHED CURVES)
- △---△ UPPER 95% CONFIDENCE LIMIT
- x---x LOWER 95% CONFIDENCE LIMIT

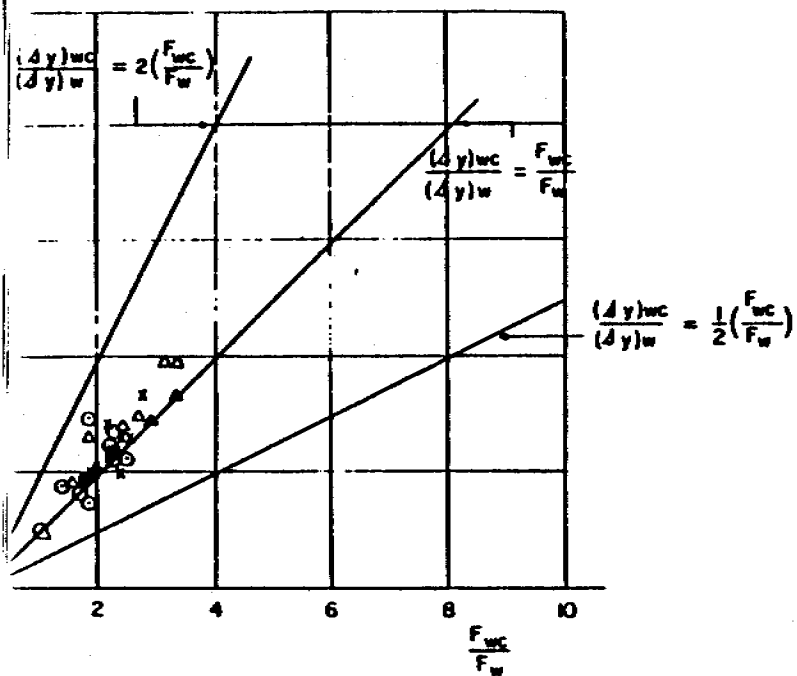


Figure 6 : Increase in coastal constant S_{yi}

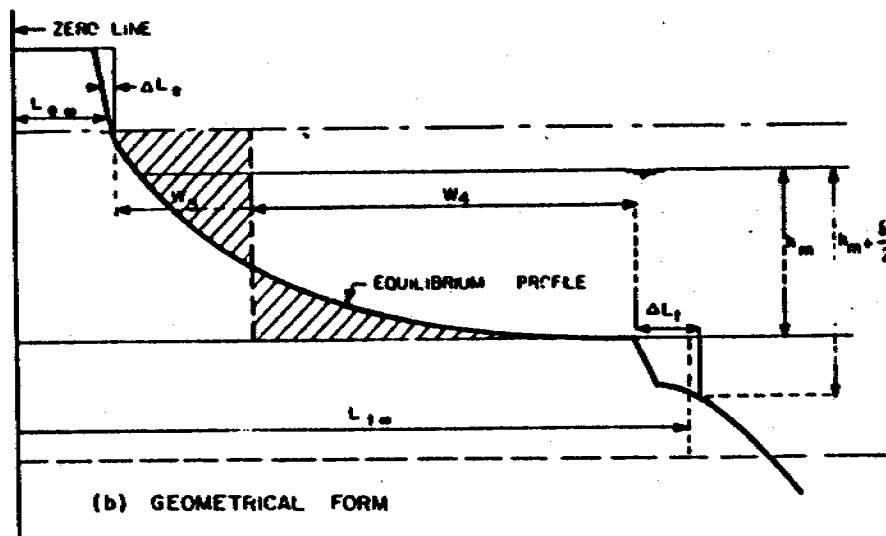
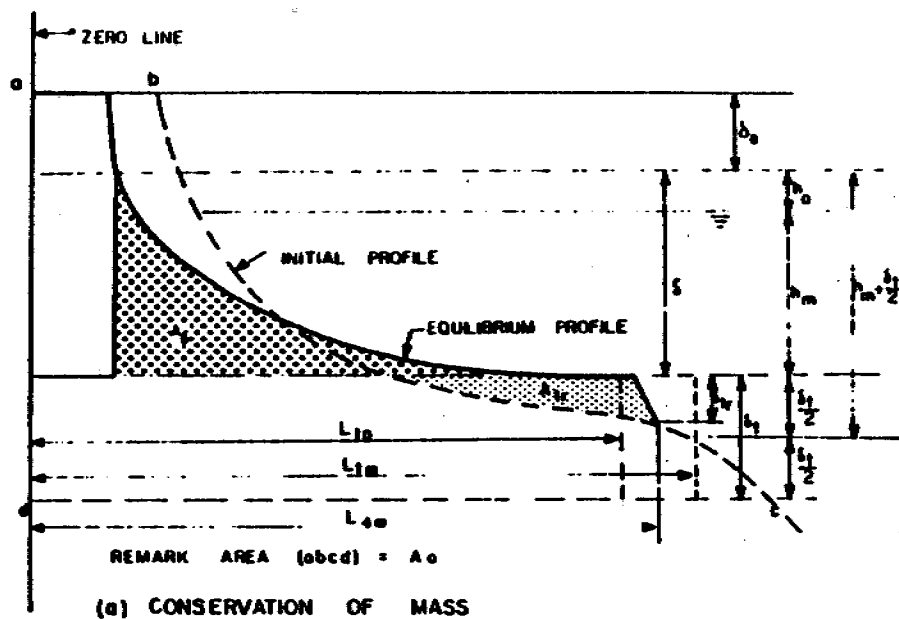


Figure 7 : Definition sketch: computation of W_e , W_t and δ_{tr}

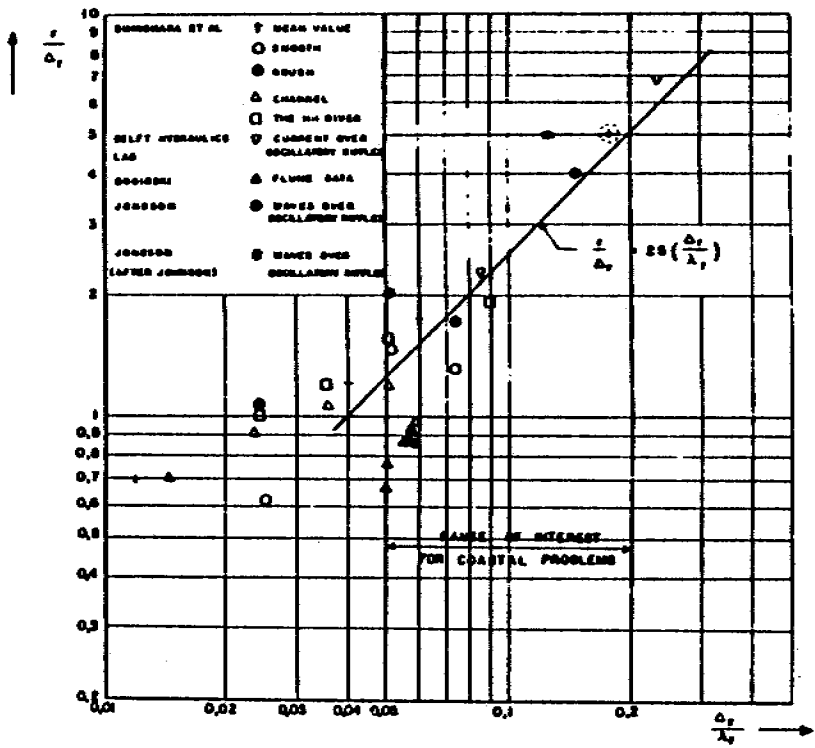


Figure 8 : Computation of relative roughness

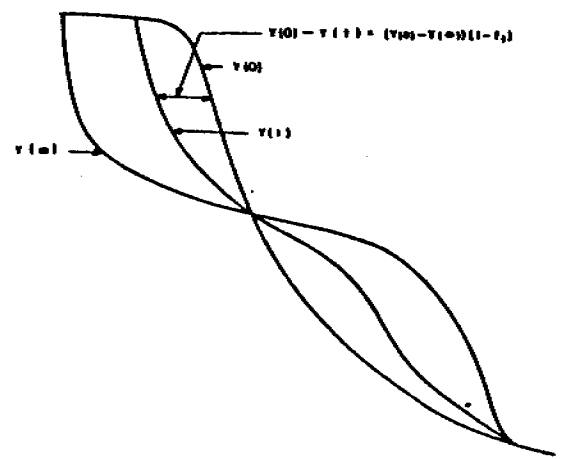


Figure 9 : Computation of time-dependent profiles

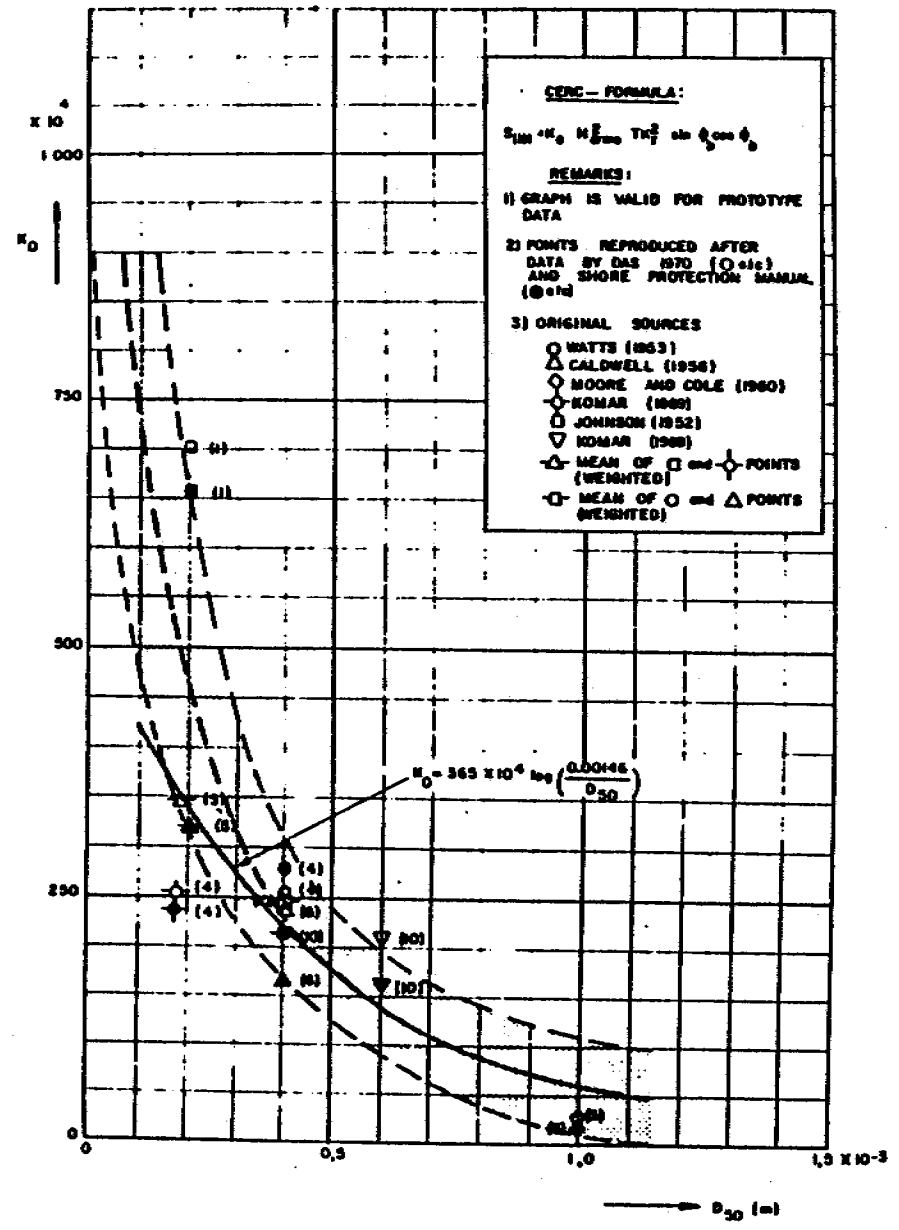


Figure 10 : Grain-size dependence of K_0

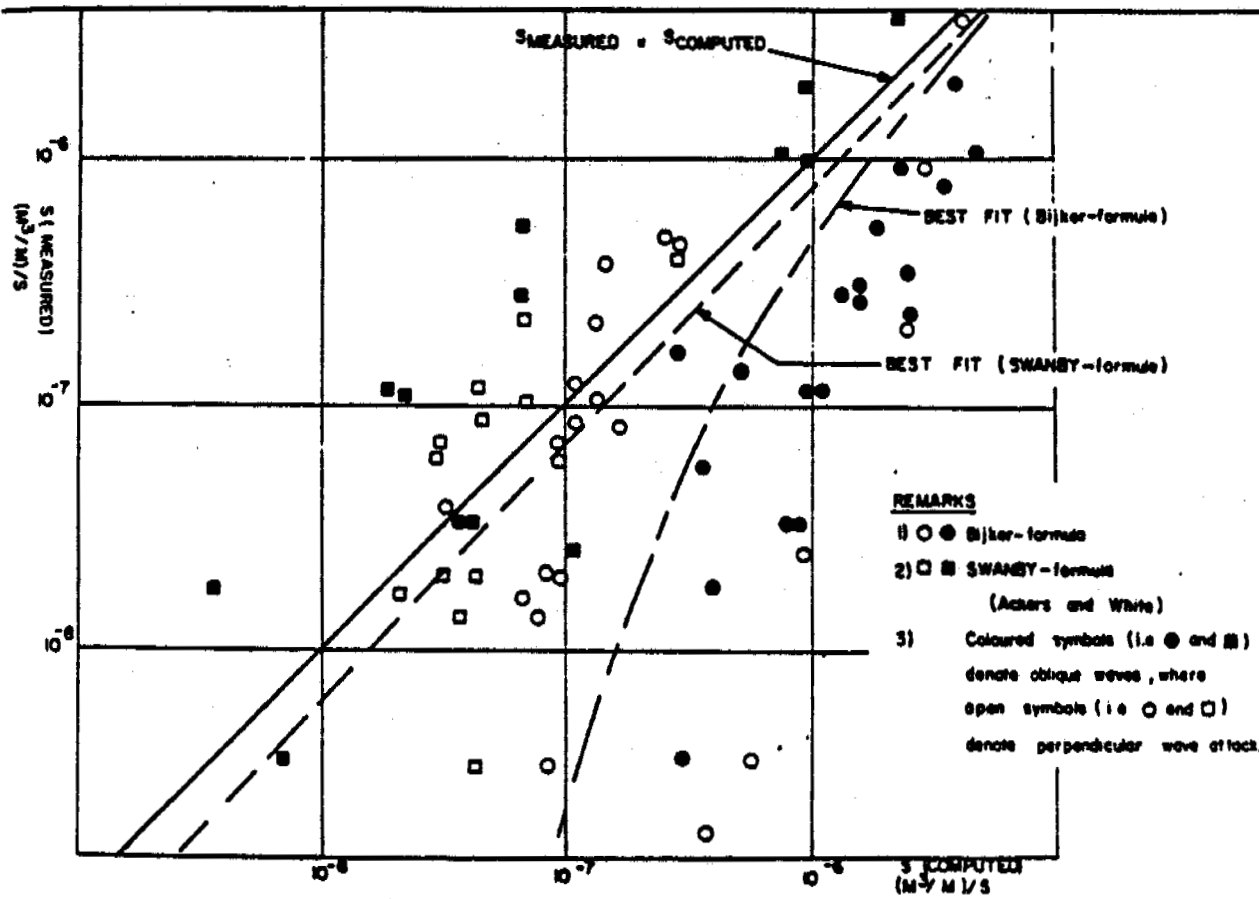


Figure 11 : Comparison between measured and computed longshore transport rates

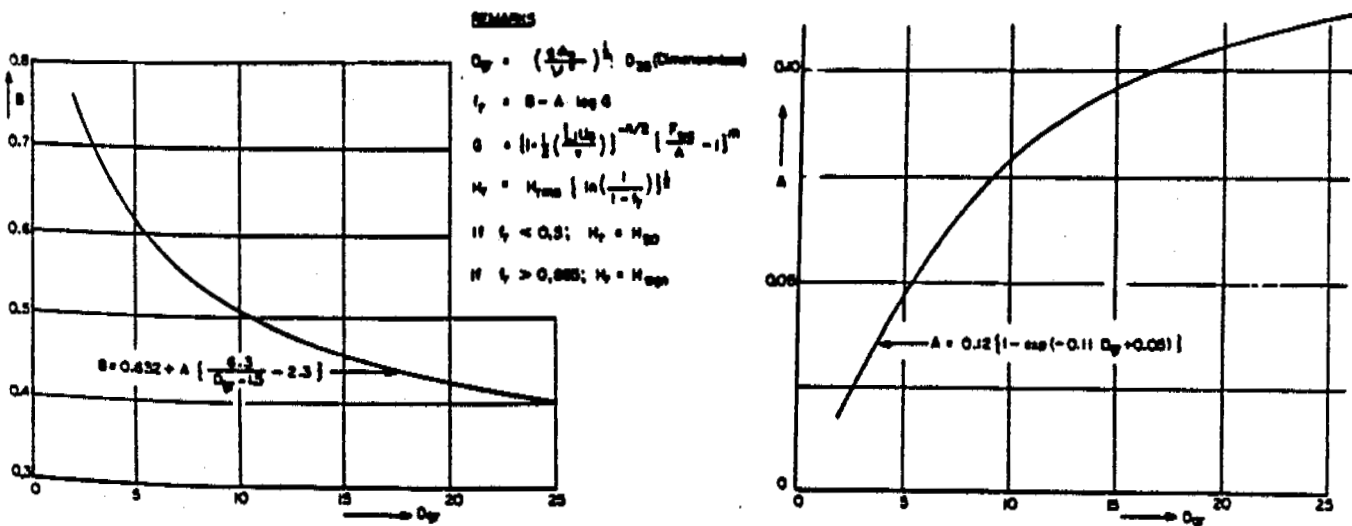


Figure 12 : Computation of representative wave height H_r

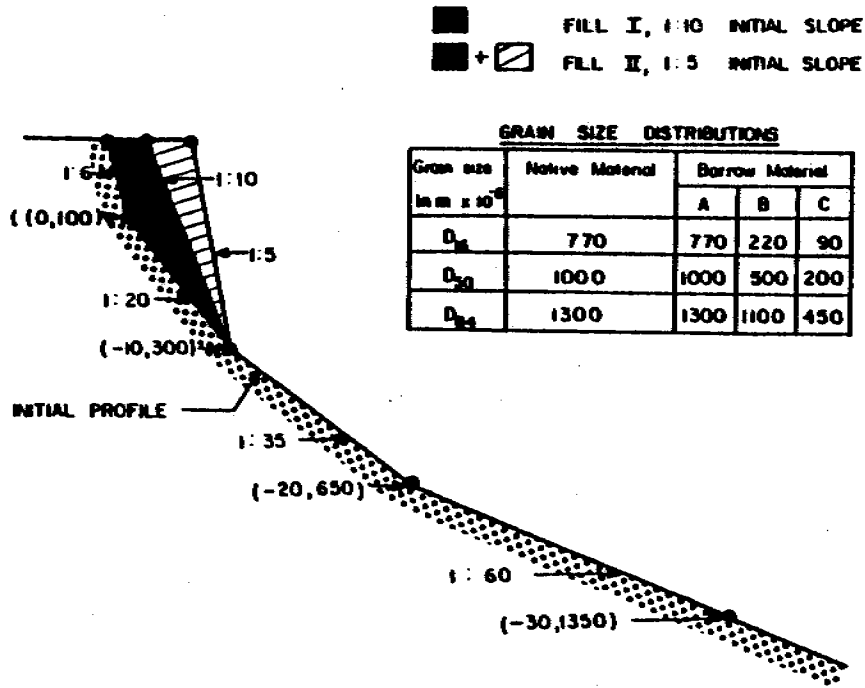


Figure 13 : Characteristics of beachfill

FILL I, 1:10 INITIAL SLOPE
 FILL II, 1:5 INITIAL SLOPE

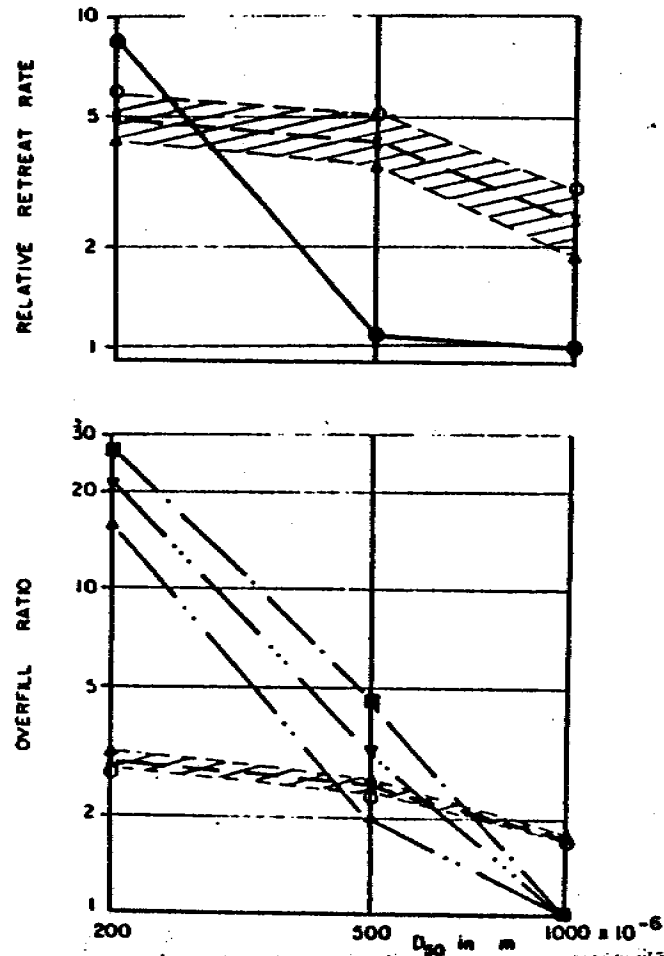
GRAIN SIZE DISTRIBUTIONS

Grain size in mm x 10 ⁻³	Native Material	Borrow Material		
		A	B	C
D ₁₅	770	770	220	90
D ₅₀	1000	1000	500	200
D ₈₅	1300	1300	1100	450

Figure 14 : Beachfill-stability results

REMARKS

- PRESENT PAPER $\alpha_{\text{borrow}} = \frac{1}{5}$
- △ PRESENT PAPER $\alpha_{\text{borrow}} = \frac{1}{10}$
- x PRESENT PAPER (AVERAGE OF $\alpha_{\text{borrow}} = \frac{1}{10}, \frac{1}{5}$)
- JAMES ($\Delta = 0.6$)
- KRUMBEIN - JAMES
- ▲ DEAN
- ▼ AVERAGE OF KRUMBEIN - JAMES AND DEAN (■, ▲)



PREDICTIVE EQUATIONS REGARDING COASTAL TRANSPORTS

by

D. H. SWART*

1. INTRODUCTION

Morphological changes are the result of gradients in longshore and onshore-offshore sediment transport. The coastal engineer is continually faced with engineering problems in which a quantitative knowledge of these morphological changes is required. For this purpose predictive equations have been developed for both longshore and onshore-offshore sediment transport, which are being used in practical applications. In this paper a few of these predictive techniques, as well as one of their typical applications, viz. to a beachfill problem, will be discussed.

2. ONSHORE-OFFSHORE SEDIMENT TRANSPORT

2.1 General

The basics of Swart's *onshore-offshore sediment-transport theory* were described in detail in [14]. A paper about this subject was presented at the 1974 Coastal Engineering Conference in Copenhagen [13]. Subsequently it had become clear that the computational method described in [14] is too complicated for normal use, and that it could be modified to simplify the computations, without affecting the results significantly. In the present paper a summary will be given of the basic principles underlying the theory, as well as of the modified computational approach used at present. In Chapter 4 the method will be applied to a *beachfill problem*, to illustrate one of its typical applications.

2.2 Underlying principles

(1) The development in a normal beach profile is characterized into three *definite zones*, (Figure 1), each with its own transport mechanism, viz.

- (a) the *backshore*, i.e. the area above the wave run-up limit in which "*dry*" transport takes place,
- (b) a *developing profile* (D-profile) where a combination of *bed load- and suspended load-transport* takes place, and
- (c) a *transition area*, seawards of the D-profile, and landwards of the point where sediment motion by wave action is initiated, where normally only *bed load* transport takes place.

(2) The most basic assumption in the schematization of onshore-offshore sediment transport is that the developing profile (D-profile) will eventually reach a *stable situation* under persistent wave attack. This stable situation implies both an *equilibrium form* and an *equilibrium position* of the beach profile. This last concept is illustrated in Figure 2, where the *schematized volume* of sediment in the D-profile is plotted as a function of time. Similar variations are found for the different locations in the D-profile, thus also confirming the equilibrium form concept.

(3) The sediment transport rates into (or out of) the D-profile from (or to) the backshore and the transition area ($S_b(t)$ and $S_c(t)$ respectively) form the boundary conditions for the computation of profile changes in the D-profile. These transport rates were found in [14] to be given by :

*Coastal Engineering and Hydraulics Division
National Research Institute for Oceanology, South Africa

$$S_b(t) = s_b W_b \exp\left(\frac{-s_b t}{\sigma_b}\right) \quad \dots (2.1)$$

and

$$S_c(t) = s_c W_c \exp\left(\frac{-s_c t}{\sigma_c}\right) \quad \dots (2.2)$$

where s_b and s_c are the backshore- and transition area-coastal constants and

$$W_b = L_b(t=0) - L_b(t=\infty) \quad \dots (2.3)$$

$$W_c = L_c(t=\infty) - L_c(T=0)$$

$$t = \text{time}$$

The other variables are defined in Figure 1.

(4) With the aid of the assumption in step (2) above, the rate of onshore-offshore sediment transport S_{yit} at a specific location i in the profile at any time t can be shown to be a function of the difference between the values of a profile characteristic P at time t ($P(t)$) and time $t = \infty$ ($P(\infty)$).

$$S_{yit} \propto P(\infty) - P(t) \quad \dots (2.4)$$

(see Figure 3)

Experiments showed that the best description of the transport is found if the profile characteristic is taken to be a horizontal length in the profile $(L_2 - L_1)_{it}$.

$$S_{yit} = s_{ym} \left(\frac{s_{yi}}{s_{ym}}\right) (W_i - (L_2 - L_1)_{it}) \quad \dots (2.5)$$

where s_{ym} and s_{yi} are transport coefficients and

$$(L_2 - L_1)_{it} \xrightarrow{t \rightarrow \infty} W_i \quad \dots (2.6)$$

The meaning of $(L_2 - L_1)_{it}$ and the geometry of the beach profile at time t is defined in Figure 1. Relationships are presented in [13], whereby s_{ym} , (s_{yi}/s_{ym}) and W_i , as well as the limits of the D-profile (i.e. the area in which equation (2.5) is valid) can be found in terms of the boundary conditions.

(5) A subsequent study of the given relationships indicated that the computation of time-dependent profile development can be significantly improved and simplified if it can be assumed that at each location i in the developing profile the same fraction f_{it} of the total transport $(\int_0^{\infty} S_{yit} dt)$ of sediment passing that location until time $t = \infty$, will have occurred at any given time t , i.e.

$$f_{it} = \left\{ \frac{\int_0^t S_{yit} dt}{\int_0^{\infty} S_{yit} dt} \right\} = f_t = \text{constant for all locations } i \text{ in the developing profile at time } t. \quad \dots (2.7)$$

The results of morphological tests with durations in excess of 1 000 hours, given in Figures 4 and 5, show that the above-mentioned assumption (equation (2.7)) is a *good engineering approximation*.

(6) With the principle of continuity of mass, and by using steps (1) - (5) above, it is possible to derive analytical expressions for the time variation of the length $(L_2 - L_1)_{it}$ and the sediment transport, viz. :

$$(L_2 - L_1)_{it} = W_i - (K_{ei} + K_{ci}) \exp(-X_b t) \quad \dots (2.8)$$

$$S_{yit} = s_{yi} (K_{ei} + K_{ci}) \exp(-X_b t) \quad \dots (2.9)$$

$$V_{yit} = \int_0^t S_{yit} dt = s_{yi} (K_{ei} + K_{ci}) X_b^{-1} (1 - \exp(-X_b t)) \quad \dots (2.10)$$